

MR-guided radiotherapy for patients with lymph node oligometastases

Anita Werensteijn-Honingh



**MR-guided radiotherapy for patients
with lymph node oligometastases**

Anita Werensteijn-Honingh



MR-guided radiotherapy for patients with lymph node oligometastases

PhD thesis, Utrecht University, The Netherlands: Anita Werensteijn-Honingh, 2022

The research described in this thesis was performed at the Department of Radiotherapy of the University Medical Center Utrecht.

Printed by Ipskamp Printing | proefschriften.net

Layout and (cover) design: Harma Makken, persoonlijkproefschrift.nl

ISBN: 978-94-6421-675-2

Copyright 2022 © Anita Werensteijn-Honingh

The Netherlands. All rights reserved. No part of this thesis may be reproduced, stored in a retrieval system or transmitted in any form or by any means without permission in writing from the author.

Publication of this thesis was financially supported by the UMC Utrecht Department of Radiotherapy and Elekta BV. The research described in this thesis was supported by the Dutch Cancer Society (KWF 2015-0848).

MR-guided radiotherapy for patients with lymph node oligometastases

**MRI-gestuurde radiotherapie voor patiënten
met lymfeklier oligometastasen**

(met een samenvatting in het Nederlands)

Proefschrift

ter verkrijging van de graad van doctor aan de Universiteit Utrecht
op gezag van de rector magnificus, prof. dr. H.R.B.M. Kummeling,
ingevolge het besluit van het college voor promoties
in het openbaar te verdedigen op

dinsdag 24 mei 2022 des middags te 2.15 uur

door

Anita Marijke Honingh

geboren op 14 oktober 1990
te Goirle

Promotor:

Prof. dr. B.W. Raaymakers

Copromotoren:

Dr. I.M. Jürgenliemk-Schulz

Dr. ir. P.S. Kroon

Contents

Chapter 1.	General introduction	7
------------	----------------------	---

Part I: Online adaptive MR-guided lymph node SBRT

Chapter 2.	Feasibility of stereotactic radiotherapy using a 1.5 T MR-linac: Multi-fraction treatment of pelvic lymph node oligometastases	19
Chapter 3.	Individual lymph nodes: “See it and Zap it”	33
Chapter 4.	Impact of a vacuum cushion on intrafraction motion during online adaptive MR-guided SBRT for pelvic and para-aortic lymph node oligometastases	53
Chapter 5.	Target coverage and dose criteria based evaluation of the first clinical 1.5T MR-linac SBRT treatments of lymph node oligometastases compared with conventional CBCT-linac treatment	79
Chapter 6.	Impact of MR-guided versus conventional radiotherapy workflows on organ at risk doses in SBRT for lymph node oligometastases	99

Part II: Treatment outcomes and patient selection

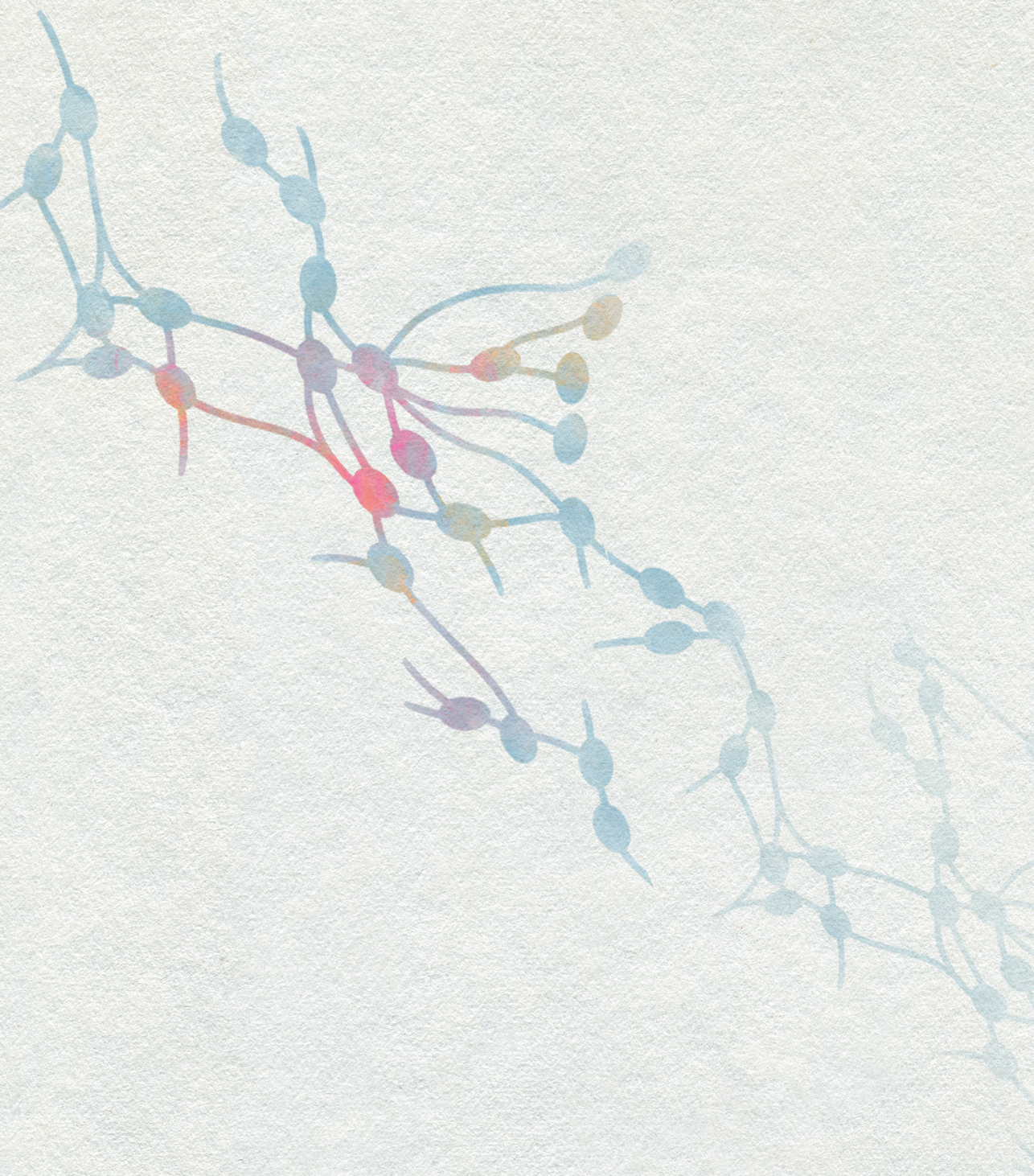
Chapter 7.	Progression-free survival in patients with 68 Ga-PSMA-PET- directed SBRT for lymph node oligometastases	125
------------	--	-----

Summary and discussion

Chapter 8.	Summary	157
Chapter 9.	General discussion	163
Chapter 10.	Dutch summary	183

Appendices

Review committee	192
List of publications	194
Dankwoord	196
Curriculum vitae	199



Chapter 1

General introduction

The role of image guidance in radiotherapy

Radiotherapy constitutes an important part of oncological treatment; it contributes to the treatment of an estimated 50% of patients with cancer [1]. Radiotherapy uses ionizing radiation to cause cell death in tumor cells, but it also kills healthy cells near the tumor. The challenge is therefore to maximize the dose to the tumor cells whilst minimizing the dose to the healthy surrounding tissues, which are referred to as 'organs at risk' (OAR). With increasing survival rates due to improvements in cancer diagnosis, treatment and supportive care, the focus is shifting to also include improving the quality of life (QoL) of cancer survivors and minimizing the side effects from radiotherapy [2]. Two relatively recent technological advancements have contributed to this clinical aim through improved sparing of the surrounding healthy tissues: improved shaping of the treatment field and daily target visualization on the treatment machine. The first example, improved shaping of the treatment field, has been accomplished by modulation of the radiation beams using intensity-modulated radiotherapy (IMRT) or volumetric-modulated arc therapy (VMAT). Treatment delivery using either IMRT or VMAT results in improved conformity of the treatment field to the target volumes, which reduces the volume of healthy surrounding tissue that is exposed to radiation [2]. The second major technological advancement is image guided radiotherapy (IGRT), in which daily target visualization on the treatment machine is used to improve treatment accuracy. Radiotherapy is usually delivered in a fractionated manner, with multiple treatment sessions over the course of 1-6 weeks. Treatment margins around the gross tumor volume (GTV) or the clinical target volume (CTV) are used to create a planning target volume (PTV), to which the radiation dose is prescribed for the initial treatment plan. The treatment margins are used to compensate for motion of the GTV and for geometric uncertainties related to the treatment machine [3]. Target motion occurs between the treatment sessions (interfraction motion) and during a treatment session (intrafraction motion). IGRT minimizes the uncertainty related to target interfraction motion, and thus allows the use of smaller treatment margins. Most treatment machines now facilitate daily target visualization using cone beam CT (CBCT) imaging, with a system that uses divergent (cone shaped) X-ray imaging, rotating around the treatment table [4]. CBCT-based target position verification has improved patient positioning accuracy [5]. Other examples of IGRT include treatment systems that use oblique radiographic images, such as the CyberKnife system (Accuray Inc., Sunnyvale, USA), and MR-guided delivery systems, which will be discussed below [6]. These two technological advancements paved the way for another recent development in radiotherapy: stereotactic body radiotherapy (SBRT). SBRT consists of radiotherapy treatment in only a few treatment sessions, generally five or less, with relatively high radiation doses per session (6 - 30 Gy) [7]. Small margins are used around the target volume and the treatment plan is created using a steep dose gradient, which allows for a high radiation dose within the target

volume without exceeding the tolerated doses for healthy surrounding organs. SBRT relies heavily on IGRT-based delivery, with target position verification directly before radiation delivery at each treatment session. Additionally, immobilization devices such as vacuum cushions and corsets are often used for consistent daily set-up and for minimization of target intrafraction motion [8]. However, relatively poor visualization of soft tissues is obtained using CBCT imaging [9]. Better soft tissue visualization could improve IGRT, both for mitigation of inter- and intrafraction motion of the target and even OAR. MRI has been shown to offer this improved soft tissue visualization compared with (CB)CT imaging, so integrating MRI with the treatment device could be a solution to improve IGRT [9].

MR-guided SBRT delivery

Integration of onboard MRI with a radiation delivery treatment device was a major technical challenge [10,11]. The 1.5 T MRI-linear accelerator (MR-linac) was developed largely in Utrecht, in collaboration with Elekta (Elekta AB, Stockholm, Sweden) and with Philips (Philips Medical Systems, Best, The Netherlands). It is a treatment system combining 1.5 T MRI with a linear accelerator. The first patients were treated in a research setting using a 1.5 T MR-linac in 2017, during which the geometric precision of both radiation delivery and MRI was confirmed [12]. Daily online treatment plans are created based on MRI scans acquired before each treatment session, with soft tissue contrast comparable to diagnostic MRI. This allows adaptation of the treatment plan to the anatomy of the day, incorporating the updated contours of both the target and the nearby OAR. MRI scans can be acquired before, during and after each treatment session, including diffusion weighted imaging for treatment response monitoring [13]. These developments resulted in the Unity system by Elekta. This thesis focusses on exploring the 1.5 T MR-linac, but there is a similar machine from another vendor: the 0.35 T MR-linac, also referred to as the MRIdian system, by Viewray (ViewRay Inc., Oakwood, USA), with patient treatments since 2014 [14].

For the 1.5 T MRI linac, a dedicated framework has been developed for systematic clinical evaluation of new technologies such as MR-guided radiotherapy [15]. In this R-IDEAL framework, different stages are employed in which 'in silico' studies form the first step of evaluation. An example of such an R-IDEAL stage 0 study is a comparison of treatment plans for lymph node SBRT from our research group in 2018, which showed that delivery with daily plan adaptation on an MR-linac gives a dosimetric benefit compared with simulated CBCT-linac delivery [16]. Important aspects of the following R-IDEAL stages are randomization early in the process of evaluation of the new technology and adequate follow-up for evaluation of early and late toxicity [15]. For the 1.5 T MR-linac, an international observational study has been set up to gather clinical and technical data

from MR-linac treatments, to facilitate evidence-based implementation (the MOMENTUM study: Multi-OutcoMe EvaluationN of radiation Therapy Using the MR-linac) [17].

Lymph node oligometastases

Lymph node oligometastases was the first tumor site for which MR-guided radiotherapy delivery using the CE-certified 1.5 T MR-linac, i.e. the Elekta Unity system, was started. It comprises a patient category that is treated with a long-term palliative intent, relying on the existence of an 'oligometastatic state'. Hellman and Weichselbaum postulated the concept of an oligometastatic state in 1995 by describing a new paradigm of metastatic spread [18]. Their paradigm was an adaptation on the 'contiguous hypothesis' by Halsted, which stated that cancer always spreads in an orderly, contiguous fashion from the primary tumor to the regional lymph nodes and then to other parts of the body. In the contiguous hypothesis, systemic metastases are considered to always be extensive and widespread, even when only a single metastasis could be observed. Hellman and Weichselbaum stated that metastatic spread is a multi-step process, in which tumor cells need to acquire a 'facility for metastatic growth'. They described the oligometastatic state as one or a small number of metastases in a single or a limited number of organs, in which the tumor has not yet fully developed the facility for metastatic growth. In 2019, Welch and Hurst have specified this facility for metastatic growth by defining four 'hallmarks of metastasis': motility and invasion, ability to modulate the secondary site or local microenvironments, plasticity, and ability to colonize secondary tissues [19]. Hellman and Weichselbaum referred to reports of favorable outcomes following resection of pulmonary and hepatic metastases for selected types of cancers, such as colorectal cancer, soft tissue sarcomas and osteosarcomas. Since then, surgical resection became more generally accepted as the standard treatment for patients with liver and lung oligometastases, and other local therapies were introduced as well, such as radiofrequency ablation (RFA) and SBRT [20]. Interest in the oligometastatic disease paradigm grew and SBRT was also applied to patients with oligometastatic disease in other organs, such as lymph nodes, adrenal glands and bones [21].

Hellman and Weichselbaum already described that the effectiveness of local treatments for oligometastatic disease would depend on the sensitivity and accuracy of tumor imaging [18]. Some years later, technological advancements in positron emission tomography (PET) imaging allowed for improved diagnosis of (oligo)metastatic disease [22]. PET imaging has been shown to be more sensitive in the detection of lymph node metastases compared with conventional imaging techniques such as computed tomography (CT) and magnetic resonance imaging (MRI) [23]. More recently, the sensitivity of PET imaging for prostate cancer metastases was further improved with the introduction of prostate-specific membrane antigen (PSMA)-labelled radiotracers, allowing lymph node metastases to be

diagnosed earlier and at lower prostate specific antigen (PSA) levels [24]. The increasing influence of PET in the field of radiotherapy even led to the development of a dedicated treatment system that facilitates PET/biology-guided radiotherapy treatments (Reflexion X1 system, Reflexion Medical, Hayward, USA) which could be applied to a wide range of patients with oligometastatic or even polymetastatic disease, especially when combined with some form of systemic therapy [25].

The treatment intent for patients with oligometastatic disease is often to obtain local control. Obtaining local control may prevent complications from tumor growth such as obstruction of an ureter or obstruction of the lymphatic vessels [26]. Furthermore, it may help to postpone the application of systemic therapies, which are often associated with substantial side effects [27]. For patients with prostate cancer oligometastases, metastasis-directed therapy (MDT) has been shown to improve the androgen deprivation therapy (ADT)-free survival compared with surveillance alone, with a median ADT-free survival of 13 months with surveillance compared with 21 months for the MDT-group [28]. In another phase II randomized clinical trial for patients with oligometastatic prostate cancer, SBRT reduced the onset of number of patients with disease progression at 6 months from 61% with surveillance to 19% after SBRT [29].

OLYMPOS cohort study

In October 2016, SBRT treatment for patients with lymph node oligometastases was initiated at our department. We have monitored the patients using an observational cohort study, the OLYMPOS study: Oligo LYMPH nOde metastasis. Later on the study name was changed to Oligo LYMPH nOde and other soft tissue metastasis, when other soft tissue oligometastases were also taken into account, such as liver and adrenal metastases. The OLYMPOS study has been registered at the Netherlands trial register as NL9252: <https://www.trialregister.nl/trial/9252>). With this study, patients could give informed consent for the use of their data for research purposes and to participate in QoL questionnaires to capture general QoL, fatigue and serious adverse events. In total 263 patients have been included in the OLYMPOS study, the study has ended in August 2021.

The main objectives and research questions for the OLYMPOS study were to investigate clinical outcomes after SBRT for soft tissue oligometastases, with a focus on patient reported outcomes and on future patient selection. Furthermore, the OLYMPOS study was set up to evaluate different aspects of MR-linac treatment for patients with soft tissue oligometastases, such as evaluation of technical feasibility, clinical safety and efficacy and quantification of the dosimetric benefits of MR-guided treatment for this specific patient category. The OLYMPOS study had been initiated before the international MOMENTUM registry and in the OLYMPOS study also patients who received SBRT on a CBCT-linac were included.

Thesis outline

Several aspects of SBRT delivery using a 1.5 T MR-linac have been investigated as part of this thesis, from establishing its feasibility to an evaluation of dosimetric improvements of clinical 1.5 T MR-linac treatments compared with CBCT-linac, both in terms of target coverage and OAR sparing. It will also give an overview of current treatment outcomes and aims to contribute towards better patient selection. This thesis has been split into two parts, the first part describes the research work related to 1.5 T MR-linac treatment delivery and the second part focuses on treatment outcomes and patient selection.

Part I: Online adaptive MR-guided lymph node SBRT

In **chapter 2**, feasibility of 1.5 T MR-linac treatments for patients with lymph node oligometastases will be discussed. The first-ever clinical treatments using the CE-certified 1.5 T MR-linac, i.e. the Elekta Unity system, were performed at our center; this paper describes the workflow that was used and technological outcomes from the first five treatments.

In **chapter 3**, the adequacy of treatment margins for MR-linac SBRT delivery will be reported on. Intrafraction motion on an MR-linac time scale will be taken into account together with the spatial and geometrical accuracies related to radiation delivery and MR imaging of the 1.5 T MR-linac. Furthermore, target coverage will be evaluated for two strategies that can be used for daily online plan adaptation on the 1.5 T MR-linac.

In **chapter 4**, the necessity of using a vacuum cushion for patient immobilization during SBRT delivery on an MR-linac will be explored. With the potential of the MR-linac to correct for inter- and intrafraction changes in patient anatomy, it may not be necessary to use vacuum cushion immobilization when delivering SBRT with an MR-linac.

In **chapters 5 and 6**, the dosimetrical advantages of SBRT delivery on an MR-linac compared with an CBCT-linac will be looked into, based on patient data from 1.5 T MR-linac treatments. In **chapter 5**, the target coverage will be compared between clinical 1.5 T MR-linac treatments and simulated CBCT-linac delivery. In **chapter 6**, the dose to the OAR will be compared between clinical 1.5 T MR-linac treatments and simulated CBCT-linac delivery.

Part II: Treatment outcomes and patient selection

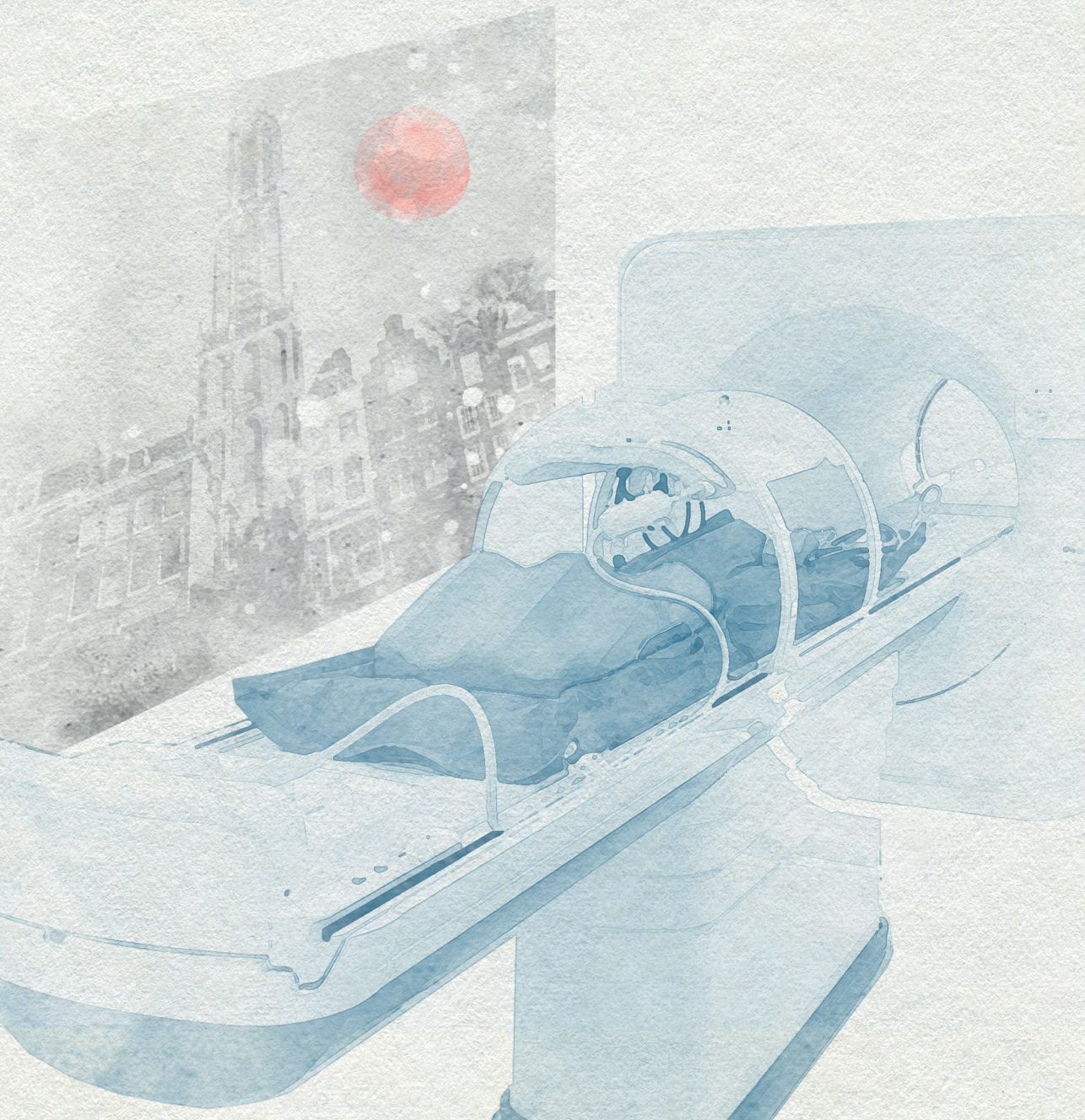
In **chapter 7**, clinical outcomes will be reported for the largest group of patients in the OLYMPOS cohort: patients with prostate cancer oligorecurrences. Prostate cancer is the most frequently occurring primary tumor within the OLYMPOS cohort and therefore this has been the first patient group for which we have investigated the clinical outcomes. Clinical outcomes including progression-free survival and ADT-free survival will be reported and a preliminary prediction model for progression-free survival will be presented, which could contribute towards better patient selection in the future.

In **chapters 8 and 9**, a summary of this thesis and a general discussion will be provided, with a summary in Dutch in **chapter 10**.

References

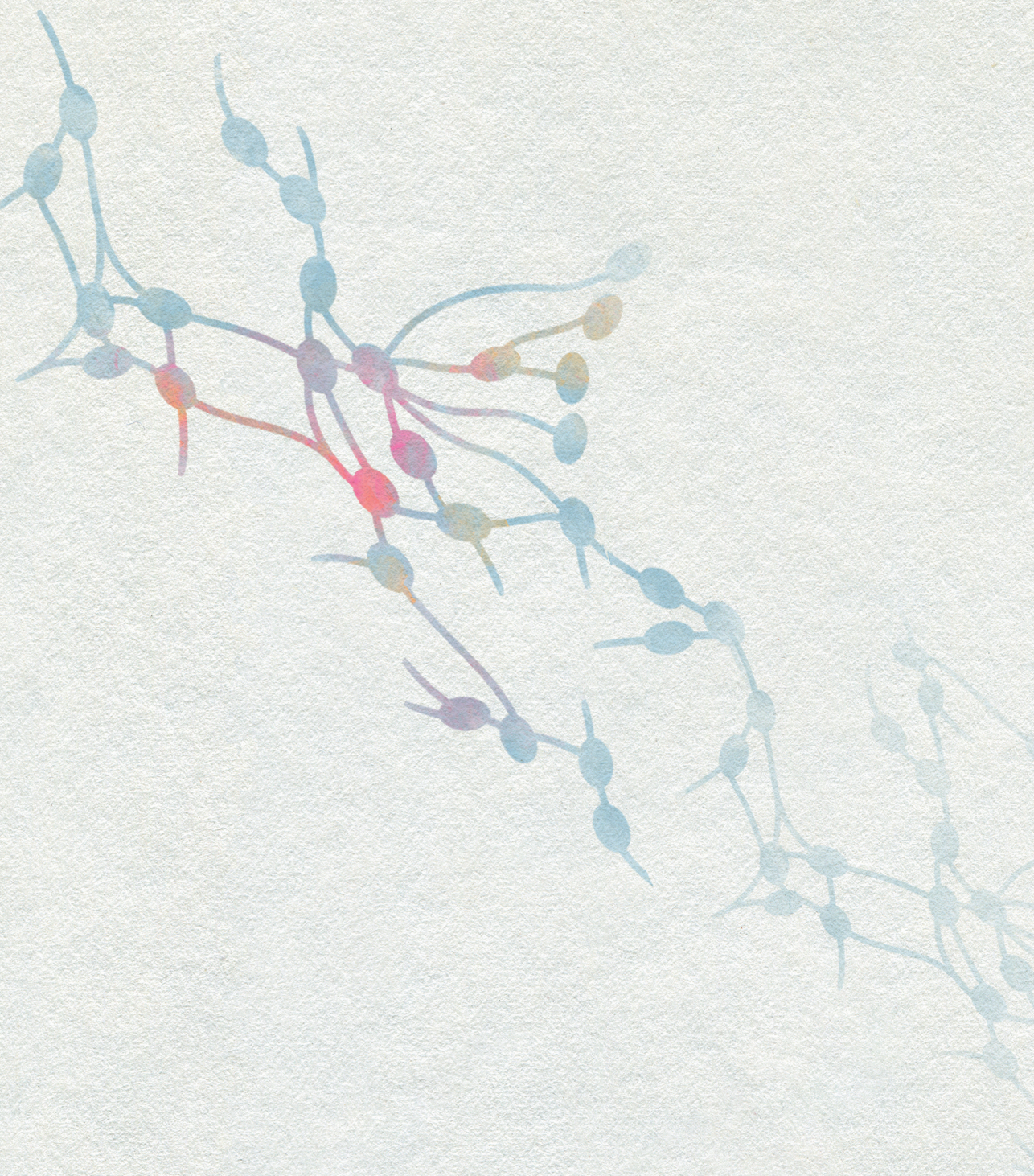
1. Delaney G, Jacob S, Featherstone C, Barton M. The role of radiotherapy in cancer treatment: estimating optimal utilization from a review of evidence-based clinical guidelines. *Cancer* 2005;104:1129-37. <https://doi.org/10.1002/cncr.21324>.
2. Citrin DE. Recent Developments in Radiotherapy. *N Engl J Med* 2017;377:1065-75. <https://doi.org/10.1056/NEJMra1608986>.
3. International Commission on Radiation Units and Measurements. ICRU Report 62, Prescribing, Recording and Reporting Photon Beam Therapy (Supplement to ICRU 50). Bethesda, USA: ICRU, 1999.
4. Sharpe MB, Moseley DJ, Purdie TG, Islam M, Siewerdsen JH, Jaffray DA. The stability of mechanical calibration for a kV cone beam computed tomography system integrated with linear accelerator. *Med Phys* 2006;33:136-44. <https://doi.org/10.1118/1.2143141>.
5. Purdie TG, Bissonnette JP, Franks K, Bezjak A, Payne D, Sie F, et al. Cone-beam computed tomography for on-line image guidance of lung stereotactic radiotherapy: localization, verification, and intrafraction tumor position. *Int J Radiat Oncol Biol Phys* 2007;68:243-52. <https://doi.org/10.1016/j.ijrobp.2006.12.022>.
6. Jaffray DA. Image-guided radiotherapy: from current concept to future perspectives. *Nat Rev Clin Oncol* 2012;9:688-99. <https://doi.org/10.1038/nrclinonc.2012.194>.
7. Chang BK, Timmerman RD. Stereotactic body radiation therapy: a comprehensive review. *Am J Clin Oncol* 2007;30:637-44. <https://doi.org/10.1097/COC.0b013e3180ca7cb1>.
8. Heerkens HD, Reerink O, Intven MPW, Hiensch RR, van den Berg CAT, Crijns SPM, et al. Pancreatic tumor motion reduction by use of a custom abdominal corset. *Phys Imaging Radiat Oncol* 2017;2:7-10. <https://doi.org/10.1016/j.phro.2017.02.003.9>.
9. Noel CE, Parikh PJ, Spencer CR, Green OL, Hu Y, Mutic S, et al. Comparison of onboard low-field magnetic resonance imaging versus onboard computed tomography for anatomy visualization in radiotherapy. *Acta Oncol* 2015;54:1474-82. <https://doi.org/10.3109/0284186X.2015.1062541>.
10. Raaymakers BW, Lagendijk JJ, Overweg J, Kok JG, Raaijmakers AJ, Kerkhof EM, et al. Integrating a 1.5 T MRI scanner with a 6 MV accelerator: proof of concept. *Phys Med Biol* 2009;54:N229-37. <https://doi.org/10.1088/0031-9155/54/12/N01>.
11. Lagendijk JJ, van Vulpen M, Raaymakers BW. The development of the MRI linac system for online MRI-guided radiotherapy: a clinical update. *J Intern Med* 2016;280:203-8. <https://doi.org/10.1111/joim.12516>.
12. Raaymakers BW, Jürgenliemk-Schulz IM, Bol GH, Glitzner M, Kotte ANTJ, van Asselen B, et al. First patients treated with a 1.5 T MRI-Linac: clinical proof of concept of a high-precision, high-field MRI guided radiotherapy treatment. *Phys Med Biol* 2017;62:L41-50. <https://doi.org/10.1088/1361-6560/aa9517>.
13. Kooreman ES, van Houdt PJ, Keesman R, Pos FJ, van Pelt VWJ, Nowee ME, et al. ADC measurements on the Unity MR-linac - A recommendation on behalf of the Elekta Unity MR-linac consortium. *Radiother Oncol* 2020;153:106-13. <https://doi.org/10.1016/j.radonc.2020.09.046>.
14. Mutic S, Dempsey JF. The ViewRay system: magnetic resonance-guided and controlled radiotherapy. *Semin Radiat Oncol* 2014;24:196-9. <https://doi.org/10.1016/j.semradonc.2014.02.008>.
15. Verkooijen HM, Kerkmeijer LGW, Fuller CD, Huddart R, Faivre-Finn C, Verheij M, et al. R-IDEAL: A Framework for Systematic Clinical Evaluation of Technical Innovations in Radiation Oncology. *Front Oncol* 2017;7:59. <https://doi.org/10.3389/fonc.2017.00059>.

16. Winkel D, Kroon PS, Werensteijn-Honingh AM, Bol GH, Raaymakers BW, Jürgenliemk-Schulz IM. Simulated dosimetric impact of online re-planning for stereotactic body radiation therapy of lymph node oligometastases on the 1.5T MR-linac. *Acta Oncol* 2018;3:1–8. <https://doi.org/10.1080/0284186X.2018.1512152>.
17. de Mol van Otterloo SR, Christodouleas JP, Blezer ELA, Akhlat H, Brown K, Choudhury A, et al. The MOMENTUM Study: An International Registry for the Evidence-Based Introduction of MR-Guided Adaptive Therapy. *Front Oncol* 2020;10:1328. <https://doi.org/10.3389/fonc.2020.01328>.
18. Hellman S, Weichselbaum RR. Oligometastases. *J Clin Oncol* 1995;13:8-10. <https://doi.org/10.1200/JCO.1995.13.1.8>.
19. Welch DR, Hurst DR. Defining the Hallmarks of Metastasis. *Cancer Res* 2019;79:3011-27. <https://doi.org/10.1158/0008-5472.CAN-19-0458>.
20. Timmerman RD, Bizekis CS, Pass HI, Fong Y, Dupuy DE, Dawson LA, et al. Local surgical, ablative, and radiation treatment of metastases. *CA Cancer J Clin* 2009;59:145-70. <https://doi.org/10.3322/caac.20013>.
21. Tree AC, Khoo VS, Eeles RA, Ahmed M, Dearnaley DP, Hawkins MA, et al. Stereotactic body radiotherapy for oligometastases. *Lancet Oncol* 2013;14:e28-37. [https://doi.org/10.1016/S1470-2045\(12\)70510-7](https://doi.org/10.1016/S1470-2045(12)70510-7).
22. Jones T, Townsend D. History and future technical innovation in positron emission tomography. *J Med Imaging (Bellingham)* 2017;4:011013. <https://doi.org/10.1117/1.JMI.4.1.011013>.
23. Liu B, Gao S, Li S. A Comprehensive Comparison of CT, MRI, Positron Emission Tomography or Positron Emission Tomography/CT, and Diffusion Weighted Imaging-MRI for Detecting the Lymph Nodes Metastases in Patients with Cervical Cancer: A Meta-Analysis Based on 67 Studies. *Gynecol Obstet Invest* 2017;82:209-22. <https://doi.org/10.1159/000456006>.
24. Moghul M, Somani B, Lane T, Vasdev N, Chaplin B, Peedell C, et al. Detection rates of recurrent prostate cancer: 68 Gallium (Ga)-labelled prostate-specific membrane antigen versus choline PET/CT scans. A systematic review. *Ther Adv Urol* 2019;11:1756287218815793. <https://doi.org/10.1177/1756287218815793>.
25. Shirvani SM, Huntzinger CJ, Melcher T, Olcott PD, Voronenko Y, Bartlett-Roberto J, et al. Biology-guided radiotherapy: redefining the role of radiotherapy in metastatic cancer. *Br J Radiol* 2021;94:20200873. <https://doi.org/10.1259/bjr.20200873>.
26. Wang Z, Wang J, Zhuang H, Wang P, Yuan Z. Stereotactic body radiation therapy induces fast tumor control and symptom relief in patients with iliac lymph node metastasis. *Sci Rep* 2016;6:37987. <https://doi.org/10.1038/srep37987>.
27. Nguyen PL, Alibhai SMH, Basaria S, D'Amico AV, Kantoff PW, Keating NL, et al. Adverse effects of androgen deprivation therapy and strategies to mitigate them. *Eur Urol* 2015;67:825-36. <https://doi.org/10.1016/j.eururo.2014.07.010>.
28. Ost P, Reynders D, Decaestecker K, Fonteyne V, Lumen N, De Bruycker A, et al. Surveillance or metastasis-directed therapy for oligometastatic prostate cancer recurrence: a prospective, randomized, multicenter phase II trial. *J Clin Oncol* 2018;36:446–53. <https://doi.org/10.1200/JCO.2017.75.4853>.
29. Phillips R, Shi WY, Deek M, Radwan N, Lim SJ, Antonarakis ES, et al. Outcomes of Observation vs Stereotactic Ablative Radiation for Oligometastatic Prostate Cancer: The ORIOLE Phase 2 Randomized Clinical Trial. *JAMA Oncol* 2020;6:650-9. <https://doi.org/10.1001/jamaoncol.2020.0147>.



Part I

**Online adaptive MR-guided
lymph node SBRT**



Chapter 2

Feasibility of stereotactic radiotherapy using a 1.5 T MR-linac: Multi-fraction treatment of pelvic lymph node oligometastases

Anita M. Werensteijn-Honingh, Petra S. Kroon, Dennis Winkel, Ellart M. Aalbers, Bram van Asselen, Gijsbert H. Bol, Kevin J. Brown, Wietse S.C. Eppinga, Corine A. van Es, Markus Glitzner, Eline N. de Groot-van Breugel, Sara L. Hackett, Martijn Intven, Jan G.M. Kok, Charis Kontaxis, Alexis N. Kotte, Jan J.W. Lagendijk, Mariëlle E.P. Philippens, Rob H.N. Tijssen, Jochem W.H. Wolthaus, Simon J. Woodings, Bas W. Raaymakers, Ina M. Jürgenliemk-Schulz.

Radiother Oncol 2019;134:50–4.

<https://doi.org/10.1016/j.radonc.2019.01.024>.

Summary

Online adaptive radiotherapy using the 1.5 Tesla MR-linac is feasible for SBRT (5x7 Gy) of pelvic lymph node oligometastases. The workflow allows full online planning based on daily anatomy. Session duration is less than 60 minutes. Quality assurance tests, including independent 3D dose calculations and film measurements were passed.

Introduction

Daily magnetic resonance imaging (MRI) directly before each treatment session enables online adaptive external beam radiotherapy based on excellent soft tissue contrast [1]. This may allow for planning target volume (PTV) margin reduction, improved sparing of organs at risk (OAR), dose escalation and hypofractionation [2-4]. Recently, the 1.5 Tesla (T) MR-linac system has become clinically available [5-8]. This system is composed of a 1.5 T MRI scanner and a ring-based gantry that contains a 7 MV standing wave linear accelerator.

In August 2018, routine clinical use of the MR-linac was started at our department with treatment of patients with pelvic lymph node oligometastases. Treatment aim for these patients is local control of the affected nodes and delay of potentially more toxic systemic therapy [9]. Based on institutional experience, we hypothesized that online MRI will yield improved lymph node visibility compared with cone beam computed tomography (CBCT). With treatment for pelvic lymph node oligometastases on the MR-linac, clinical experience is gained of multi-fraction, stereotactic radiotherapy (SBRT) treatment of soft tissue lesions, thereby expanding the knowledge from the 'first in mankind' trial [7].

Clinical treatment with the 1.5 T MR-linac using the vendor-provided commercially-available clinical workflow software has not been described before. Our aim was to report on the feasibility of SBRT on the 1.5 T MR-linac for lymph node oligometastases, based on our first clinical experiences.

Materials and Methods

Patients

Five patients have undergone clinical treatment on the 1.5 T MR-linac (Unity, Elekta AB, Stockholm, Sweden) at our institute between August and October 2018. They have provided written informed consent for use of their data as part of an ethics review board approved observational study. All patients had single pelvic lymph node metastases originating from prostate cancer, median 64 months (range 19 - 129) after initial diagnosis of the primary tumor. Diagnosis of the metastatic lymph nodes was based on Gallium-68 prostate-specific membrane antigen positron emission tomography (PSMA PET) scans. The metastatic lymph nodes were situated in obturator or external iliac regions and had a median diameter of 7 mm (range 5 - 8).

Feasibility criteria

Criteria for feasibility evaluation in this report were:

- Treatment delivery using the MR-linac, with full online planning based on daily anatomy;
- Maximum session time of 60 minutes;
- Passed all quality assurance (QA) tests, including independent 3D dose calculations and film measurements.

Clinical workflow

The clinical workflow is illustrated in Figure 1.

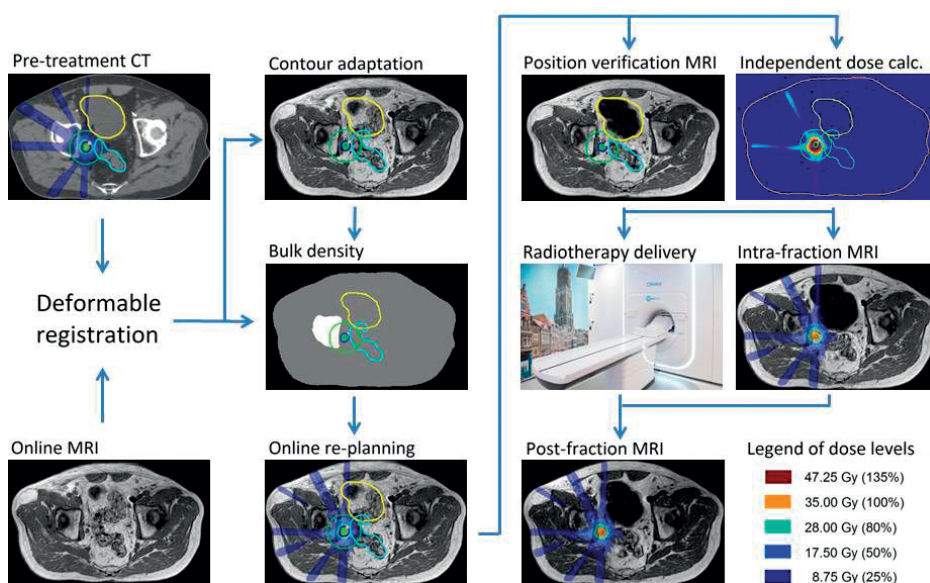


Figure 1. Flow chart of online MR-linac workflow

Anatomical contours: yellow: bladder; light blue: sigmoid; pink: ureter; light green: GTV; dark blue: PTV; green oval: PTV + 2 cm. Images are shown for the first fraction of the second patient.

Pre-treatment imaging, planning and QA

Pre-treatment imaging included CT and MRI. The radiation oncologist contoured the gross tumor volume (GTV) on a multi-sequence MRI scan acquired on a 1.5 T Philips Ingenia MRI scanner (Philips Medical Systems, Best, NL), which was registered to the PSMA-PET and CT scans (Brilliance CT big bore, Philips Medical Systems, Best, NL). Nearby OAR (rectum, sigmoid, bladder, bowel bag, ureter, sacral plexus) were contoured on the CT scan. A special table overlay was used for CT scan acquisition, to enable patient set-up using specific couch index points. A vacuum mattress (BlueBAG, Elekta AB, Stockholm, Sweden) was used for immobilization.

A 3 mm PTV margin was applied [7,8,10]. For each patient, a pre-treatment step-and-shoot intensity-modulated radiotherapy (IMRT) plan was created in Monaco, to serve as a patient-specific template for online treatment planning. Calculation grid size was 2 mm. Monaco takes into account the 1.5 T magnetic field along the direction of the scanner bore ($-Y_{IEC1217}$). Seven non-uniformly spaced beam angles were used, avoiding the couch at beam angles of 115 - 135° and 225 - 245° and the cryostat connection pipe at 8 - 18°. Similar to our current clinical practice, 35 Gy in five fractions (2-3 fractions per week) was prescribed to 95% of the PTV. OAR dose constraints (Supplementary material: Table 1) were prioritized above PTV coverage.

Offline QA for the pre-treatment plan included an independent 3D dose check with 50% dose threshold in Oncentra version 4.5.2 (Elekta AB, Stockholm, Sweden) which was compared to the Monaco plan via Gamma analysis [11]. The dose recalculation in Oncentra is intended as a fast check of the dose calculation from Monaco, using an independent beam model and algorithm. Oncentra is based on a collapsed cone algorithm that does not account for effects of the magnetic field, but was shown to be feasible for voxel-to-voxel comparisons in the target volume for different target sites [11]. Further, GafChromic absolute dose EBT3 film measurement was performed with a 10% low dose threshold, which took into account doses ranging from 10% of D_{max} up until D_{max} (Ashland ISP Advanced Materials, NJ, USA) [7,11]. Pass criterion was 90% with a Gamma index of ≤ 1 , with 3%/3 mm for independent dose check pass criterion and with 5%/2 mm for film measurement. In case of a 90-95% Gamma pass rate a visual inspection would be performed by the attending physicist.

Online patient set-up

Patients were positioned on the MR-linac couch using specific couch index points, which were intended to ensure that the position of the patient along the length of the couch is known and reproducible between the CT scan and each treatment session. Lasers were also used for patient positioning, these were institutionally added to the MR-linac. An MRI scan for online treatment planning was acquired: a transverse 3D T1-weighted FFE scan, for patients 1-2 the acquisition time was 5 minutes (TR 11 ms, TE 4.6 ms, acquired voxel size 1.2x1.2x2.0 mm³, FOV 400x447x300 mm³), for patients 3-5 the acquisition time was reduced to 2 minutes (TR 11 ms, TE 4.6 ms, acquired voxel size 1.5x1.5x2.0 mm³, FOV 400x400x300 mm³). Contours were propagated from pre-treatment CT using a rigid and deformable registration in Monaco, version 5.4 build 19 (Elekta AB, Stockholm, Sweden). Electron density was based on assignment to structures: bones were assigned the average bone density from pre-treatment CT, all other tissues were assigned a relative electron density of 1. If necessary, contours of GTV and OAR within 20 mm of the (propagated) pre-treatment PTV were manually adapted by the radiation oncologist, to limit contouring time.

Online planning

Multiple online planning options are available in Monaco for the 1.5 T MR-linac. We used the ‘adapt to shape’ workflow to perform full online planning with the ‘optimize weights and shapes from fluence’ option [12]. As for the pre-treatment plan, calculation grid size was 2 mm and OAR dose constraints (Supplementary material: Table 1) were prioritized above PTV coverage. Beam angles were identical to the pre-treatment plan.

Online position verification and QA

During plan optimization, a position verification MRI scan was acquired, with the same parameters as the online planning MRI scan (5-minute sequence for patients 1-2, 2-minute sequence for patients 3-5). An overlay of anatomical contours from the online MRI scan was used to exclude significant motion of the target before radiotherapy delivery.

Online QA for the optimized plan was performed by comparing the number of monitor units and segments of the optimized treatment plan to the pre-treatment plan and by performing an independent 3D dose calculation in Oncentra, as described for pre-treatment QA.

Radiotherapy delivery

Radiotherapy was delivered using 7 MV FFF IMRT. An intra-fraction MRI scan (5-minute sequence) was acquired during dose delivery and a post-fraction MRI scan (2-minute sequence) directly after treatment, with the same parameters as the online planning MRI scans. Both scans were used for offline assessment of intra-fraction motion by recalculating GTV coverage on the actual anatomy.

Post-treatment QA

For all patients, post-treatment film measurement was performed for the online treatment plan of at least the first session, as described for pre-treatment QA.

Results

All five patients completed the full course treatment on the MR-linac. Contour adaptation of the GTV and/or nearby OAR was performed and new online treatment plans were created for each treatment session. Figure 2 gives two examples of inter-fraction anatomical differences of OAR positions and shapes, with the corresponding dose distributions after online planning.

All treatment plans from online planning were clinically accepted and used for treatment. For patients 1-4, the predefined coverage and OAR constraints were met by the online treatment plans for all treatment sessions. For patient 5, the PTV coverage planning aim was not met

for the pre-treatment and two online plans (respectively 90.5, 92.8 and 93.9%, aim >95%), the sacral plexus was situated very close to the target lymph node for this patient.

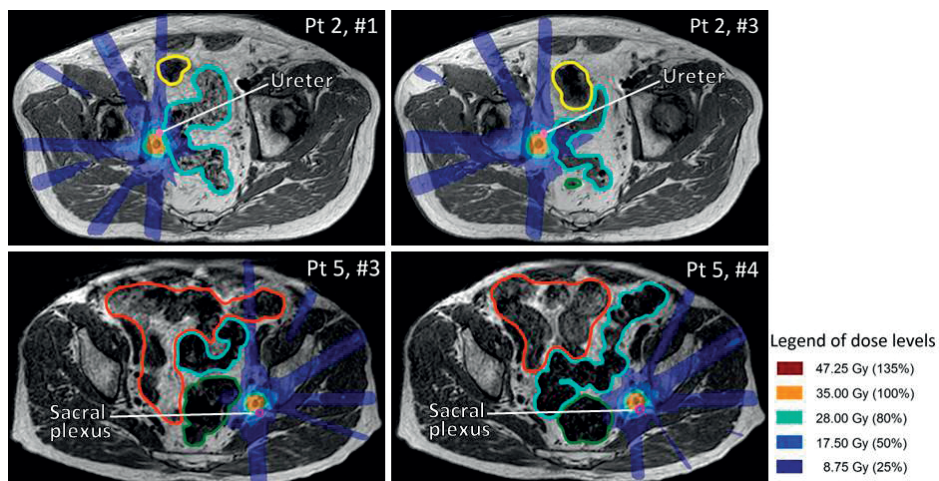


Figure 2. Illustration of inter-fraction anatomical differences in OAR location with corresponding online treatment plans.

Online MRI scans with OAR contours (contoured offline) and corresponding online treatment plans for illustrative treatment sessions (#). Anatomical contours: yellow: bladder; light blue: sigmoid; pink: ureter (denoted); green: rectum; purple: sacral plexus (denoted); red: bowel bag.

All treatment sessions were completed within 60 minutes, shown in Supplementary material: Figure S1 with time to completion results for each of the workflow items. For patients 1-2, the average online session duration was 44 minutes (range 39-49), including an average of 36 minutes on couch time (range 32-39). After the introduction of shorter MRI scans for planning and position verification, starting with the third patient, average online session duration was 39 minutes (range 33-58) for patients 3-5, with 32 minutes on couch time (range 27-51). For one session, the Monaco software crashed during planning, which prompted a restart of the treatment session (visible in Supplementary material: Figure S1 with a longer maximum session duration for patient 4).

QA for the pre-treatment plans yielded an average Gamma pass rate of 97.1% (range 94.7-98.8%) for the independent dose check and a Gamma pass rate of 99.9% (range 99.7-100%) for film measurements. The online independent dose calculations in Oncentra resulted in an average Gamma pass rate of 97.8% (range 90.4-99.3%). Post-treatment film measurements of online treatment plans resulted in an average Gamma pass rate of 99.9% (range 99.4-100%). All treatment plans with Gamma pass rates 90-95% were accepted by the attending physicist after visual inspection.

Discussion

To our knowledge, this is the first report on the clinical use of the commercially available 1.5 T MR-linac including the associated clinical workflow. In this report feasibility for SBRT treatment of pelvic lymph node oligometastases was evaluated using three criteria (treatment delivery using the MR-linac, with full online planning; maximum session time of 60 minutes; passed all QA tests).

All 25 treatment fractions were delivered as scheduled using the 1.5 T MR-linac. For each treatment session, online planning was used to generate new treatment plans based on daily anatomy. All treatment plans were clinically accepted and used for treatment. For patient 5, the pre-treatment and two online plans did not satisfy the PTV planning aim due to the proximity of the sacral plexus to the target lymph node. All patients could also have been treated with SBRT using a CBCT-linac, but for patient 1 a larger PTV margin of 8 mm would have been used because of poor target visibility on CBCT. In a preliminary investigation, the daily target coverage seemed to be slightly improved with MR-linac treatment compared with simulated CBCT-linac treatment [13].

All treatment sessions were completed within 60 minutes, even with a software problem in Monaco that resulted in a session restart for one session. To reduce the online session time, a shorter MRI scan was used for planning and position verification starting with the third patient (acquisition time 2 minutes instead of 5). This contributed to a 5-minute decrease in average online session duration (from 44 minutes for patients 1-2 to 39 minutes for patients 3-5). Timing results varied between patients, mainly depending on the amount of contour adaptation performed for lymph nodes and OAR. Further reductions of online session duration could be achieved by ongoing optimization of the online planning parameters and by improving the deformable image registration. Other options for reducing session duration include faster data transfer between the different applications using a different treatment session manager [7] or the use of other treatment planning software that is currently being developed [14].

Finally, all QA tests were passed, which encompassed independent 3D dose calculations and film measurements. Therefore, all three feasibility criteria being evaluated in this report have been satisfied.

With clinical feasibility having been established for multi-fraction stereotactic radiotherapy using the MR-linac, we are currently implementing MR-linac treatment for multiple lymph node oligometastases in pelvic or low para-aortic regions. Future treatment of abdominal lymph node metastases will likely require breathing motion management, such as the use of

an abdominal compression device [15], an internal target volume (ITV) or future tracking and gating functionality of the treatment machine [16].

Conclusions

Clinical use of the 1.5 T MR-linac (Unity, Elekta AB, Stockholm, Sweden) was feasible for multi-fraction stereotactic radiotherapy, applied for pelvic lymph node oligometastases. All sessions were delivered using the MR-linac, new treatment plans were generated based on daily anatomy, all treatment sessions were completed within 60 minutes and all quality assurance tests were passed including independent 3D dose calculations and film measurements.

Acknowledgements

The authors wish to thank the Dutch Cancer Society for their financial support (grant 2015-0848).

The authors are grateful for the contributions to patient treatment on the MR-linac of J. Hes, N.G.P. Vissers, R. Bouwmans, M.M.C. Schoenmakers, L.M. Wijkhuizen, R.H.A. Rutgers, A. Scheeren, I.H. Kiekebosch, G.G. Sikkens, E. van Aert and J.H.W. de Vries.

Conflict of interest

The University Medical Center Utrecht MR-linac scientific project, including employment of multiple authors, has been partly funded by Elekta AB (Stockholm, Sweden) and Philips Medical Systems (Best, The Netherlands).

K.J. Brown is an employee of Elekta AB (Stockholm, Sweden).

R.H.N. Tijssen receives research support from Philips Medical Systems (Best, The Netherlands).

The other authors declared that there is no other conflict of interest.

References

1. Noel CE, Parikh PJ, Spencer CR, Green OL, Hu Y, Mutic S, et al. Comparison of onboard low-field magnetic resonance imaging versus onboard computed tomography for anatomy visualization in radiotherapy. *Acta Oncol* 2015;54:1474-82. <https://doi.org/10.3109/0284186X.2015.1062541>.
2. Henke L, Kashani R, Yang D, Zhao T, Green O, Olsen L, et al. Simulated Online Adaptive Magnetic Resonance-Guided Stereotactic Body Radiation Therapy for the Treatment of Oligometastatic Disease of the Abdomen and Central Thorax: Characterization of Potential Advantages. *Int J Radiat Oncol Biol Phys* 2016;96:1078-86. <https://doi.org/10.1016/j.ijrobp.2016.08.036>.
3. van Herk M, McWilliam A, Dubec M, Faivre-Finn C, Choudhury A. Magnetic Resonance Imaging-Guided Radiation Therapy: A Short Strengths, Weaknesses, Opportunities, and Threats Analysis. *Int J Radiat Oncol Biol Phys* 2018;101:1057-60. <https://doi.org/10.1016/j.ijrobp.2017.11.009>.
4. Winkel D, Kroon PS, Werensteijn-Honingh AM, Bol GH, Raaymakers BW, Jürgenliemk-Schulz IM. Simulated dosimetric impact of online re-planning for stereotactic body radiation therapy of lymph node oligometastases on the 1.5T MR-linac. *Acta Oncol* 2018;3:1-8. <https://doi.org/10.1080/0284186X.2018.1512152>.
5. Raaymakers BW, Lagendijk JJ, Overweg J, Kok JG, Raaijmakers AJ, Kerkhof EM, et al. Integrating a 1.5 T MRI scanner with a 6 MV accelerator: proof of concept. *Phys Med Biol* 2009;54:N229-37. <https://doi.org/10.1088/0031-9155/54/12/N01>.
6. Lagendijk JJ, van Vulpen M, Raaymakers BW. The development of the MRI linac system for online MRI-guided radiotherapy: a clinical update. *J Intern Med* 2016;280:203-8. <https://doi.org/10.1111/joim.12516>.
7. Raaymakers BW, Jürgenliemk-Schulz IM, Bol GH, Glitzner M, Kotte ANTJ, van Asselen B, et al. First patients treated with a 1.5 T MRI-Linac: clinical proof of concept of a high-precision, high-field MRI guided radiotherapy treatment. *Phys Med Biol* 2017;62:L41-50. <https://doi.org/10.1088/1361-6560/aa9517>.
8. Goodburn RJ, Tijssen RHN, Philippens MEP. Comparison of Spatial-Distortion Maps for MRSim Versus MR-Linac in the Brain and Pelvis at 1.5T. *Radiother Oncol* 2018;127:S1184-5 (conference abstract). [https://doi.org/10.1016/S0167-8140\(18\)32456-3](https://doi.org/10.1016/S0167-8140(18)32456-3).
9. Ost P, Reynders D, Decaestecker K, Fonteyne V, Lumen N, De Bruycker A, et al. Surveillance or Metastasis-Directed Therapy for Oligometastatic Prostate Cancer Recurrence: A Prospective, Randomized, Multicenter Phase II Trial. *J Clin Oncol* 2018;36:446-53. <https://doi.org/10.1200/JCO.2017.75.4853>.
10. Wiersema L, Borst G, Nakhaee S, Peulen H, Wiersma T, Kwint M, et al. First IGRT results for SBRT bone and lymph node oligometastases within the pelvic region. *Radiother Oncol* 2017;123:S1006 (conference abstract). [https://doi.org/10.1016/S0167-8140\(17\)32273-9](https://doi.org/10.1016/S0167-8140(17)32273-9).
11. Hackett S, van Asselen B, Feist G, Pencea S, Akhiat H, Wolthaus J, et al. A Collapsed Cone Algorithm Can Be Used for Quality Assurance for Monaco Treatment Plans for the MR-Linac. *Med Phys* 2016;43:3441 (conference abstract). <https://doi.org/10.1118/1.4956056>.
12. Winkel D, Bol GH, Kiekebosch IH, Van Asselen B, Kroon PS, Jürgenliemk-Schulz IM, et al. Evaluation of Online Plan Adaptation Strategies for the 1.5T MR-linac Based on "First-In-Man" Treatments. *Cureus* 2018;10:e2431. <https://doi.org/10.7759/cureus.2431>.

13. Winkel D, Bol GH, Werensteijn-Honingh AM, Intven MPW, Eppinga WSC, Van Asselen B, et al. Dosimetric benefit of the first clinical SBRT of lymph node oligometastases on the 1.5T MR-linac. (conference abstract, accepted for e-poster ESTRO 38, abstract number E38-1622).
14. Kontaxis C, Bol GH, Lagendijk JJ, Raaymakers BW. A new methodology for inter- and intra-fraction plan adaptation for the MR-linac. *Phys Med Biol* 2015;60:7485-97. <https://doi.org/10.1088/0031-9155/60/19/7485>.
15. Heerkens HD, Reerink O, Intven MPW, Hiensch RR, van den Berg CAT, Crijns SPM, et al. Pancreatic tumor motion reduction by use of a custom abdominal corset. *Phys Imaging Radiat Oncol* 2017;2:7-10. <https://doi.org/10.1016/j.phro.2017.02.003>.
16. van Sörnsen de Koste JR, Palacios MA, Bruynzeel AME, Slotman BJ, Senan S, Lagerwaard FJ. MR-guided Gated Stereotactic Radiation Therapy Delivery for Lung, Adrenal, and Pancreatic Tumors: A Geometric Analysis. *Int J Radiat Oncol Biol Phys* 2018;102:858-66. <https://doi.org/10.1016/j.ijrobp.2018.05.048>.

Supplementary material

Table S1

Clinical dose criteria

Structure	Offline constraints (pre-treatment plan)	Online constraints
Planning target volume	$V_{35 \text{ Gy}} > 95\%$ $D_{0.1 \text{ cm}^3} < 47.25 \text{ Gy}$	$V_{35 \text{ Gy}} > 95\%$ $D_{0.1 \text{ cm}^3} < 47.25 \text{ Gy}$
Bladder	$V_{38 \text{ Gy}} < 0.5 \text{ cm}^3$ $V_{18.3 \text{ Gy}} < 15 \text{ cm}^3$	$V_{38 \text{ Gy}} < 0.5 \text{ cm}^3$
Bowel bag	$V_{32 \text{ Gy}} < 0.5 \text{ cm}^3$ $V_{25 \text{ Gy}} < 10 \text{ cm}^3$	$V_{32 \text{ Gy}} < 0.5 \text{ cm}^3$
Rectum + sigmoid	$D_{\text{max}} < 40 \text{ Gy}$ $V_{32 \text{ Gy}} < 0.5 \text{ cm}^3$	$V_{32 \text{ Gy}} < 0.5 \text{ cm}^3$
Ureter	$D_{\text{max}} < 40 \text{ Gy}$	$D_{\text{max}} < 40 \text{ Gy}$
Sacral plexus	$D_{0.1 \text{ cm}^3} < 32 \text{ Gy}$	$D_{0.1 \text{ cm}^3} < 32 \text{ Gy}$

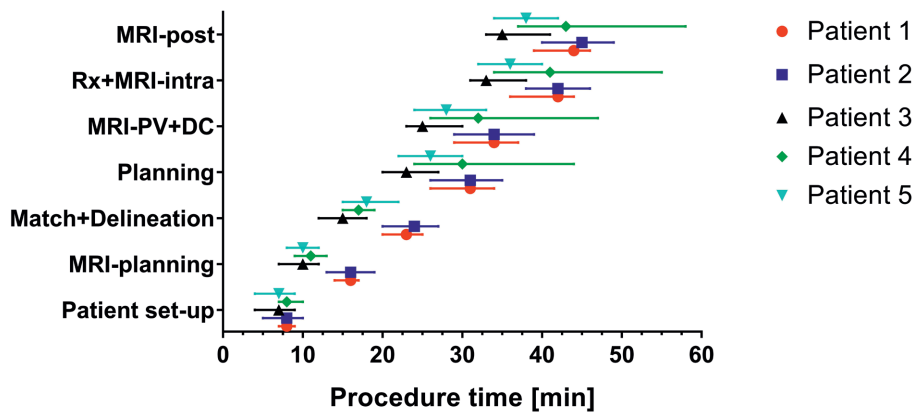
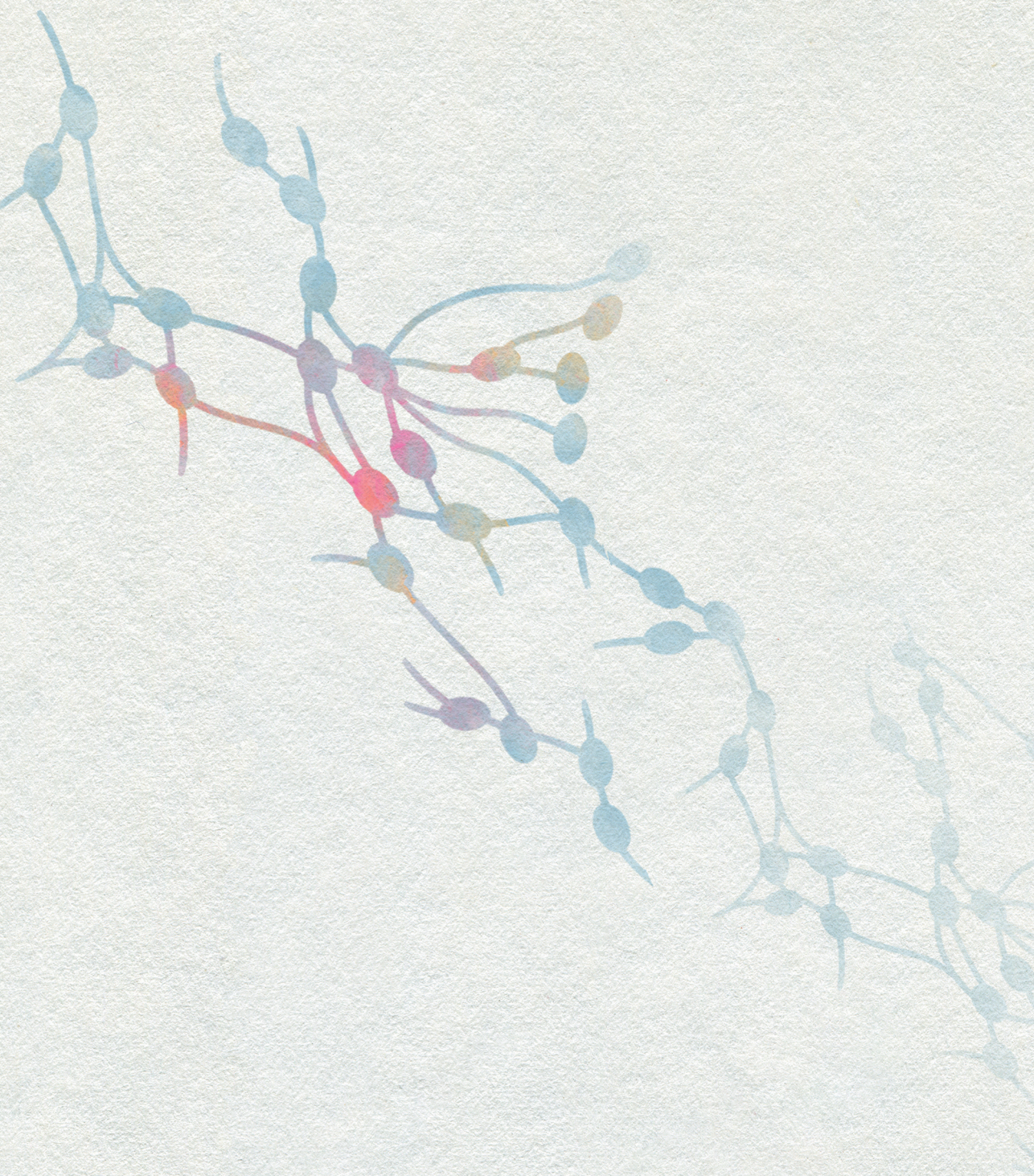


Figure S1. Visualization of online session duration

Average and range of time to completion (from session start) for the different workflow items.

Rx: radiotherapy delivery; PV: position verification; DC: independent dose check.



Chapter 3

Individual lymph nodes: “See it and Zap it”

Dennis Winkel*, Anita M. Werensteijn-Honingh*, Petra S. Kroon, Wietse S.C. Eppinga, Gijsbert H. Bol, Martijn P.W. Intven, Hans C.J. de Boer, Louk M.W. Snoeren, Jochem Hes, Bas W. Raaymakers, Ina M. Jürgenliemk-Schulz.

* Contributed equally to this manuscript

Clin Transl Radiat Oncol 2019;18:46–53.
<https://doi.org/10.1016/j.ctro.2019.03.004>.

Abstract

Background and purpose: With magnetic resonance imaging (MRI)-guided radiotherapy systems such as the 1.5T MR-linac the daily anatomy can be visualized before, during and after radiation delivery. With these treatment systems, seeing metastatic nodes with MRI and zapping them with stereotactic body radiotherapy (SBRT) comes into reach. The purpose of this study is to investigate different online treatment planning strategies and to determine the planning target volume (PTV) margin needed for adequate target coverage when treating lymph node oligometastases with SBRT on the 1.5T MR-linac.

Materials and methods: Ten patients were treated for single pelvic or para-aortic lymph node metastases on the 1.5T MR-linac with a prescribed dose of 5x7Gy with a 3 mm isotropic GTV- PTV margin. Based on the daily MRI and actual contours, a completely new treatment plan was generated for each session (adapt to shape, ATS). These were compared with plans optimized on pre-treatment CT contours after correcting for the online target position (adapt to position, ATP). At the end of each treatment session, a post-radiation delivery MRI was acquired on which the GTV was delineated to evaluate the GTV coverage and PTV margins.

Results: The median PTV V35Gy was 99.9% [90.7–100%] for the clinically delivered ATS plans compared to 93.6% [76.3–99.7%] when using ATP. The median GTV V35Gy during radiotherapy delivery was 100% [98–100%] on the online planning and post-delivery MRIs for ATS and 100% [93.9–100%] for ATP, respectively. The applied 3 mm isotropic PTV margin is considered adequate.

Conclusion: For pelvic and para-aortic metastatic lymph nodes, online MRI-guided adaptive treatment planning results in adequate PTV and GTV coverage when taking the actual patient anatomy into account (ATS). Generally, GTV coverage remained adequate throughout the treatment session for both adaptive planning strategies. “Seeing and zapping” metastatic lymph nodes comes within reach for MRI-guided SBRT.

Introduction

In recent years, stereotactic body radiotherapy (SBRT) has developed into standard clinical care for patients with oligometastases in many centers [1–3]. Based on the oligometastatic disease paradigm [4], treatment of individual metastatic lesions is being used to treat patients with limited metastatic disease to postpone the start of systemic therapies and ideally improve the progression-free survival or overall survival without compromising the quality of life [1,5–7].

Experience with minimally invasive therapies such as stereotactic body radiotherapy (SBRT) as alternative to surgery has mainly been gained for inoperable patients with liver and lung oligometastases [8–13]. However, SBRT has since been incorporated in standard clinical care for lymph node and bone oligometastases [6,14,15] and is also being used for oligometastases located in adrenal glands [16,17]. The minimally invasive nature of SBRT can be an advantage compared with surgical resection [1,8], especially for small target structures such as metastatic lymph nodes.

With prostate specific membrane antigen positron emission tomography (PSMA-PET) small metastatic nodes can be detected in a very early stage with less than 10 mm and even less than 5 mm short axis diameter [18]. In the majority of patients treated with SBRT for oligometastatic lymph nodes, the affected nodes originate from prostate cancer and like the primary tumors, have a low alpha/beta ratio [19]. This is considered one of the reasons for responding very well to SBRT, with local control being achieved in 98.1% of patients in a pooled analysis [20]. For oligometastases from other origins, a biological effective dose >100 Gy is also thought to be beneficial for achieving local control [1], but this will require a higher dose per fraction. In general, toxicity for SBRT of lymph node oligometastases is reported being mild, with on average 3% acute grade 2, 1% late grade 2, 0.3% acute grade 3 and 0.4% late grade 3 toxicity [2]. For prostate cancer oligometastases, SBRT can delay the start of androgen deprivation therapy (ADT) with approximately 8–13 months [5,6], thereby hopefully maintaining the patient’s quality of life and avoiding the side effects of ADT such as sexual dysfunction [21].

SBRT for oligometastases has mainly been applied with cone beam computed tomography (CBCT) linear accelerators (linacs) or CyberKnife, with fractionation schedules ranging from 5 x 5–10 Gy to 1 x 12–24 Gy [20]. Single fraction SBRT has been used in some centers, in several cases aided by fiducial marker implantation [22–26]. To our knowledge, peer reviewed reports on the accuracy of lymph node targeting with CBCT are lacking. However, in our own clinical routine about 30% of metastatic lymph node (as detected by diagnostic PET-CT and MRI) are poorly visible on CBCT [27]. Compared to CBCT, magnetic resonance

imaging (MRI) provides superior visualization of soft tissue targets with metastatic lymph nodes being one example [28].

The combination of online MRI for target and organ at risk (OAR) delineation, full online treatment planning and MRI for position verification is realized in the 1.5T MR-linac (combined 1.5TMR scanner and linear accelerator, Unity, Elekta AB, Stockholm, Sweden) [29,30]. New treatment plans based on the actual anatomy as depicted on MRI can be generated for every treatment fraction and online position verification is based on MRI information. The anatomy can be visualized during radiotherapy delivery (beam-on MRI) and after radiation delivery. With these facilities on board seeing the metastatic nodes with MRI and zapping them with SBRT comes into reach, as does high dose single fraction SBRT without fiducial markers. Furthermore, the daily anatomy of nearby OAR can easily be taken into account for daily treatment planning [30], which may decrease treatment related toxicity and increase the number of patients eligible for single fraction treatments [27,31,32].

However, despite the expected gain there are still uncertainties with regard to 1.5T MR-linac treatments in general and for lymph node metastases SBRT in particular. The clinically used PTV margin is still based on experiences at CBCT-linac, intra-fraction analyses using diagnostic MRIs and MR-linac commissioning data. In addition, the quality of inter-fraction correction with the 1.5T MR-linac with the two distinct online planning workflows: ‘adapt to position’ (ATP) and ‘adapt to shape’ (ATS) has not been investigated based on clinical data. The dosimetric effects of these different planning strategies may significantly affect the treatment benefit of online MRI guidance.

The objective of this manuscript is to demonstrate how close we are to “See it and Zap it” when treating lymph node oligometastases in the pelvis and para-aortic region with SBRT on the 1.5T MR-linac. Focus will be on 1) the suitability of ATS and ATP for correcting for inter-fraction motion and 2) the feasibility of delivering the dose adequately with ATS and ATP with a pre-defined PTV margin of 3 mm.

Material and methods

Patient characteristics

Ten patients were treated for single pelvic lymph node oligometastases on the 1.5T MR-linac (Unity, Elekta AB, Stockholm, Sweden) at our institute between August 2018 and February 2019. The metastatic lymph nodes were located in the pelvic region for seven patients, the other three patients had para-aortic lymph nodes (at the levels of L2-Th12 vertebral bodies). The patients with para-aortic lymph nodes received a 4D CT to assess

whether the breathing induced target motion amplitude was within limits. For eight patients, the metastatic nodes originated from prostate cancer and were detected using Gallium-68 PSMA PET scans. The primary tumor was rectal or esophageal cancer for two patients, diagnosis of these lymph nodes was based on 2-deoxy-2-fluorine-18-fluoro-D-glucose PET ((18)FDG-PET). The metastatic lymph nodes were diagnosed within median 49 months [range 18–159] after initial diagnosis of the primary tumor. All patients have provided written informed consent for using their data as part of an ethics review board approved observational study. The median short-axis diameter of the metastatic lymph nodes was 7.5 mm [5.3–21.3 mm].

Clinical treatment

Pre-treatment preparation consisted of MR imaging followed by CT-based treatment planning using the anatomical information of the registered MRI. For pre-treatment CT scan acquisition a special table overlay was used to enable patient set-up using specific couch index points. By doing so the position of the patient along the length of the couch is known and reproducible between the CT scan and each MRI based treatment session [30]. To reduce eventual motion, patients with lymph node metastases in the pelvic region were immobilized using a vacuum mattress (BlueBAG, Elekta AB, Stockholm, Sweden) with both hands on the chest and the elbows along the body. The patients with affected nodes in the para-aortic region were treated whilst wearing an abdominal corset [33] with the arms along the body.

Nodal targets were treated with a GTV-PTV margin of 3 mm. For each patient, a seven-beam IMRT pre-treatment plan [34] was created using Monaco TPS (Elekta AB, Stockholm, Sweden), taking into account the presence of the 1.5T magnetic field. For patients treated with the arms along the body, beam angles were selected such that the beams would not traverse the arms. OAR dose was lowered as much as possible, while maintaining a sufficient PTV coverage of $V_{35\text{Gy}} > 95\%$ and a D_{max} between 120 and 135%. Clinical dose criteria for the OARs were based on the UK SABR consortium guidelines (2016) (Table 1).

With online MR imaging as provided in the 1.5T MRI-linac, the pre-treatment plan can be adapted by either 1) taking the new target position into account (adapt to position, ATP) and optimizing on the pre-treatment CT and contours after a rigid registration and translation or 2) using the new patient anatomy (adapt to shape, ATS) and optimizing on the daily image and adapted contours (Figure 1). For our clinical treatments plan adaptation was performed using the ATS workflow. During each treatment session, a daily MRI was acquired. Contours were automatically deformed. If necessary, the contours of the target lymph node(s) and OARs within 2 cm of the PTV(s) were manually adapted by a radiation oncologist [30]. Based on the daily MRI and the adapted contours, a completely new

treatment plan was generated using segment shape and weight optimization based on a newly optimized fluence [35]. Radiation delivery according to the new plan was performed after MRI based position verification.

Table 1

Clinical dose criteria

Structure	Offline constraints (pre-treatment plan)	Online constraints
Planning target volume	$V_{35\text{Gy}} > 95\%$ $D_{0.1\text{ cm}^3} < 47.25\text{ Gy}$	$V_{35\text{ Gy}} > 95\%$ $D_{0.1\text{ cm}^3} < 47.25\text{ Gy}$
Aorta	$V_{53\text{Gy}} < 0.5\text{ cm}^3$	$V_{53\text{Gy}} < 0.5\text{ cm}^3$
Bladder	$V_{38\text{Gy}} < 0.5\text{ cm}^3$ $V_{18.3\text{Gy}} < 15\text{ cm}^3$	$V_{38\text{Gy}} < 0.5\text{ cm}^3$
Bowel bag + colon	$V_{32\text{Gy}} < 0.5\text{ cm}^3$ $V_{25\text{Gy}} < 10\text{ cm}^3$	$V_{32\text{Gy}} < 0.5\text{ cm}^3$
Duodenum + stomach	$V_{35\text{Gy}} < 0.5\text{ cm}^3$ $V_{25\text{Gy}} < 10\text{ cm}^3$	$V_{35\text{Gy}} < 0.5\text{ cm}^3$
Esophagus	$V_{34\text{Gy}} < 0.5\text{ cm}^3$ $V_{27.5\text{Gy}} < 5\text{ cm}^3$	$V_{34\text{Gy}} < 0.5\text{ cm}^3$
Kidney	$V_{16.8\text{Gy}} < 67\%$	$V_{16.8\text{Gy}} < 67\%$
Nerve root + sacral plexus	$V_{32\text{Gy}} < 0.1\text{ cm}^3$	$V_{32\text{Gy}} < 0.1\text{ cm}^3$
Rectum + sigmoid	$D_{\text{max}} < 40\text{ Gy}$ $V_{32\text{Gy}} < 0.5\text{ cm}^3$	$V_{32\text{Gy}} < 0.5\text{ cm}^3$
Spinal cord	$D_{\text{max}} < 28\text{ Gy}$	$D_{\text{max}} < 28\text{ Gy}$
Ureter	$D_{\text{max}} < 40\text{ Gy}$	$D_{\text{max}} < 40\text{ Gy}$

After each treatment session offline assessment of the intrafraction motion was performed by recalculating the GTV coverage on the actual anatomy as seen on the post-delivery MRI, which was acquired on average $31:03 \pm 3:40$ min after the online planning MRI. Contouring of the GTV on the post-delivery MRI was performed by a single observer. Inter-observer contouring variation is considered negligible for these small and well visible lesions.

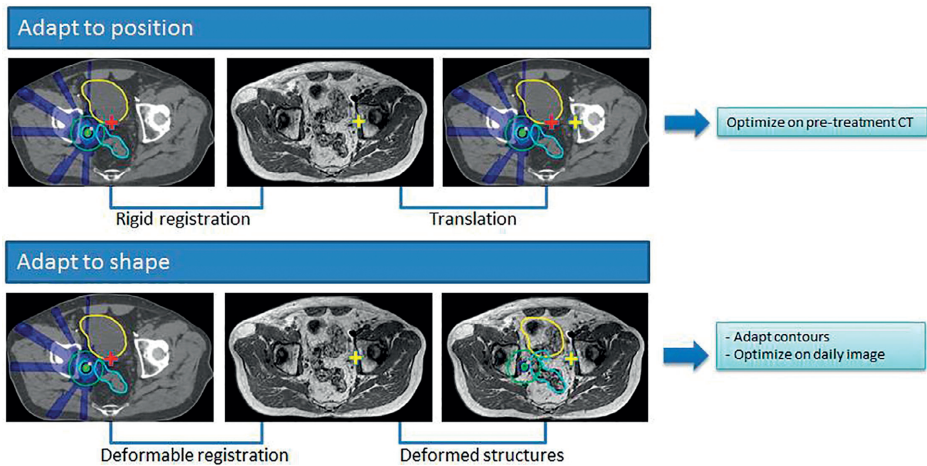


Figure 1. Schematic overview of the differences between the MR-linac Unity “adapt to shape” method in which online plan adaptation is performed on the new patient anatomy and optimized on the daily MRI and adapted contours, and the “adapt to position” method in which online plan adaptation is performed based on the new patient position and optimized on the pre-treatment CT and contours. Using the “adapt to position” method, rigid registration can be performed on the entire image sets, or using a clipbox around a region of interest [36].

Retrospective analyses

ATS versus ATP based plan adaptation

To investigate the suitability for correcting for inter-fraction motion the dosimetric impact of plan adaptation based on the new patient position (ATP) versus plan adaptation using the daily anatomic information and contours (ATS) was evaluated. An additional plan was retrospectively created for each treatment fraction using the ATP workflow with segment shape and weight optimization. Because the resulting dose-volume histogram parameters for an ATP plan are based on the pre-treatment CT contours and may essentially give a false representation of the actual situation, these plans have additionally been calculated on the daily MRI and contours. The GTV and PTV coverage was then compared for each of these 3 plans; the clinically delivered ATS plans, the ATP plans and the ATP plans calculated on the daily anatomy.

GTV target coverage analysis

To determine whether dose coverage was sufficient during treatment and if PTV margins were adequate, the GTV coverage for the clinically delivered (ATS) plans and the ATP plans was evaluated. This was done by evaluating the dose on both the online planning MRI, acquired at the start of the treatment fraction, as well as the post-delivery MRI, acquired after dose delivery.

PTV margin determination

The PTV margin was re-evaluated using data of these first 10 patients with single lymph node metastases treated on the MR-linac. The margin M_{PTV} required to ensure a minimum dose to the GTV of 35 Gy for 90% of the patients was calculated using the Van Herk recipe [37] given by

$$M_{PTV} = \alpha\Sigma + \beta\sigma - \beta\sigma_p$$

with $\alpha = 2.5$, $\beta = 0.84$ and $\sigma_p = 3.2$ mm. A β value of 0.84 was used assuming a stereotactic treatment with a plateau-prescription dose ratio of 1.25 and maximum short axis diameter of the GTV $> \sigma_p$. σ_p defines the standard deviation that describes the width of an idealized Gaussian penumbra for the total dose distribution in water, which was approximately valid because electron densities were assessed to electron density of water except for the bones [30].

$\sigma = \sqrt{\sigma_{intra}^2 + \sigma_p^2}$ defines the total random error and $\Sigma = \sqrt{\Sigma_{intra}^2 + \Sigma_{MV-MRI}^2 + \Sigma_{MRI}^2}$ the total systematic error. This recipe is still adequate for hypo-fractionated treatments when $\sigma_{intra} \ll \sigma_p$ [38] and the effective systematic and random errors are used [39]. Delineations errors were not taken into account assuming that the physician includes the GTV generously as had been decided by forehand. The different error sources were also assumed to be statistically independent and normally distributed.

Both Σ_{MV-MRI} and Σ_{MRI} were based on 3D vector measurements in our clinic. The contributions to the systematic errors were assumed isotrope. $\Sigma_{MV-MRI} = 0.3/\sqrt{3}$ mm was obtained from Raaymakers et al. [29] which defines the global error between the machine and MRI coordinate system. $\Sigma_{MRI} = 0.84/\sqrt{3}$ mm was determined during commissioning and describes the maximum residual geometric errors after gradient non-linearity correction within a 200 mm diameter spherical volume (DSV). This was measured on a large geometric fidelity phantom as described in Tijssen et al [40]. To obtain the systematic (Σ_{intra}) and random (σ_{intra}) group error due to intra-fraction motion, the distance in center of gravity of both GTV delineations, on the online MRI and post treatment MRI, was calculated for all five fractions of each patient. The intra-fraction deviations were then defined as the distance in center of gravity divided by two. The methodology given in Stroom and Heijmen. [41] was used to determine the group mean M (mean-of-means), systematic group error (defined as the standard deviation of the means) and random group error (defined as the root-mean-square of the standard deviations). The effective systematic error and effective random error were equal to the derived systematic and random error because the errors due to intrafraction motion were already based on only 5 fractions. In case the group mean M significantly differed from zero, M was added to margin M_{PTV} .

Results

ATS versus ATP plan adaptation

The clinically delivered ATS plans show the highest PTV coverage with a median $V_{35\text{Gy}}$ of 99.9% [90.7–100%] and GTV coverage with a median $V_{35\text{Gy}}$ of 100% [99.7–100%]. For 9 fractions, PTV coverage was reduced during online planning to meet OAR constraints. The ATP plans, evaluated on the pre-treatment CT, also show sufficient target coverage with a median PTV $V_{35\text{Gy}}$ of 98.5% [91.0–99.9%] and GTV $V_{35\text{Gy}}$ of 100% for all fractions. However, after calculating the ATP plans on the new MRI based anatomy and contours, the PTV coverage is significantly lower (p-value < 0.01, Wilcoxon matched-pairs signed rank test) with a median PTV $V_{35\text{Gy}}$ of 93.6% [76.3–99.7%] and a median GTV $V_{35\text{Gy}}$ of 100% [93.9–100%]. Additionally, a larger variance between target coverage is observed (Figure 2). If an OAR dose constraint violation occurred, the violation was with a maximum of 2 Gy or 0.2 cc for both methods.

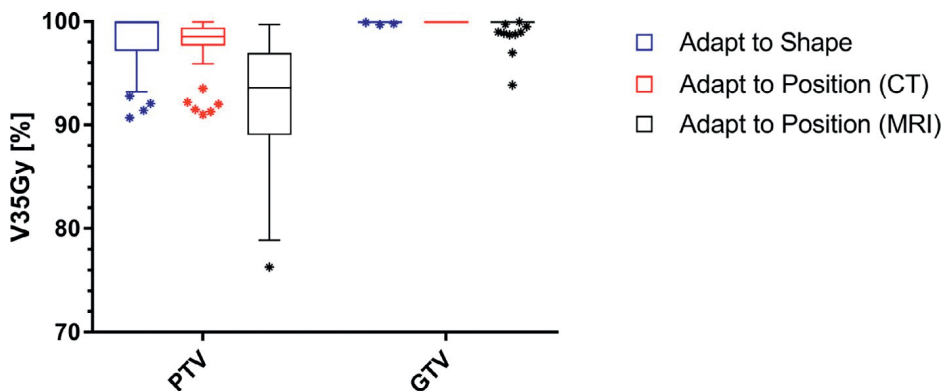


Figure 2. Boxplot of the target dose coverage (N = 50 fractions) described as planning target volume (PTV) and gross target volume (GTV) $V_{35\text{Gy}}$ in % for the adapted treatment plans. The bars show the upper and lower quartiles. The whiskers show the minimum and maximum values, excluding outliers (1.5 times the interquartile range) which are denoted with an asterisk. The target coverage for the adapt to shape plans is evaluated on the daily MRI. The target coverage for the adapt to position (CT) plans is evaluated on the pre-treatment CT and the target coverage for the adapt to shape (MRI) plans is evaluated on the daily MRI.

GTV target coverage analysis

For the clinically delivered ATS plans the median GTV $V_{35\text{Gy}}$ was 100% [99.7–100%] and the median GTV D_{mean} was 42.3 Gy [37.6–44.7 Gy] on the online planning MRI. On the post-radiation delivery MRI the median GTV $V_{35\text{Gy}}$ was 100% [98.0–100%] and the median GTV D_{mean} was 42.2 Gy [37.9–44.7 Gy] (Figure 3). For 45 of the 50 fractions (90%) the GTV $V_{35\text{Gy}}$ on the post-delivery MRI remained 100%. For one patient, a slight reduction of the GTV coverage was necessary during online treatment planning for 3 fractions due to the dose

constraint for the sacral plexus in the vicinity of the target. For the ATP plans the median GTV $V_{35\text{Gy}}$ was 100% [93.9–100%] and the median GTV D_{mean} was 41.6 Gy [39.0–43.6 Gy] on the online planning MRI. On the post-radiation delivery MRI the median GTV $V_{35\text{Gy}}$ was 100% [93.4–100%] and the median GTV D_{mean} was 41.5 Gy [38.9–43.7 Gy]. For 35 of the 50 fractions (70%) the GTV $V_{35\text{Gy}}$ was 100% on the post-delivery MRI. Figure 4 shows a visual example.

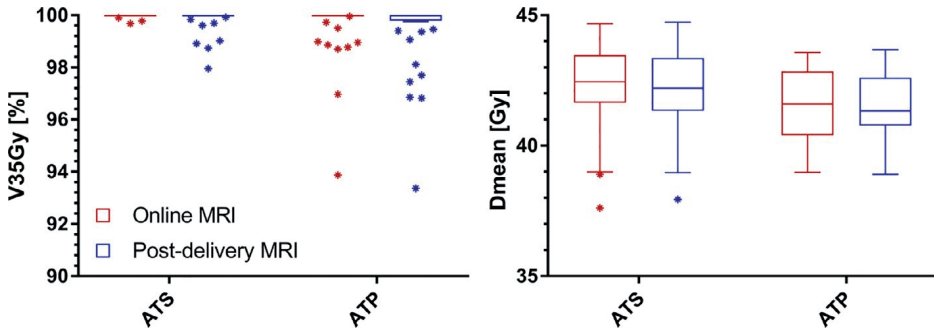


Figure 3. Boxplot graph of the GTV coverage ($N = 50$) described as $V_{35\text{Gy}}$ in % and D_{mean} in Gy for the clinically delivered (ATS) plans and the ATP plans. The bars show the upper and lower quartiles. The whiskers show the minimum and maximum values, excluding outliers (1.5 times the interquartile range) which are denoted with an asterisk. The coverage is evaluated on the daily MRI.

PTV margin analyses

The systematic and random intra-fraction displacement errors were respectively 0.31 and 0.27 mm in AP-direction, 0.54 and 0.23 mm in CC-direction and 0.22 and 0.33 mm in LR-direction. Only in AP-direction the group mean M (mean-of-mean) was significantly different from zero. The targets moved systematic in posterior direction during the individual MR-linac treatments. The group mean M was 0.33 mm in AP-direction, -0.07 mm in CC direction and 0.04 mm in LR-direction. The required PTV margin was estimated being 1.5 mm in LR-direction, 1.8 in AP-direction and 1.9 in CC-direction, respectively. Figure 5 shows two examples of intra-fraction motion.

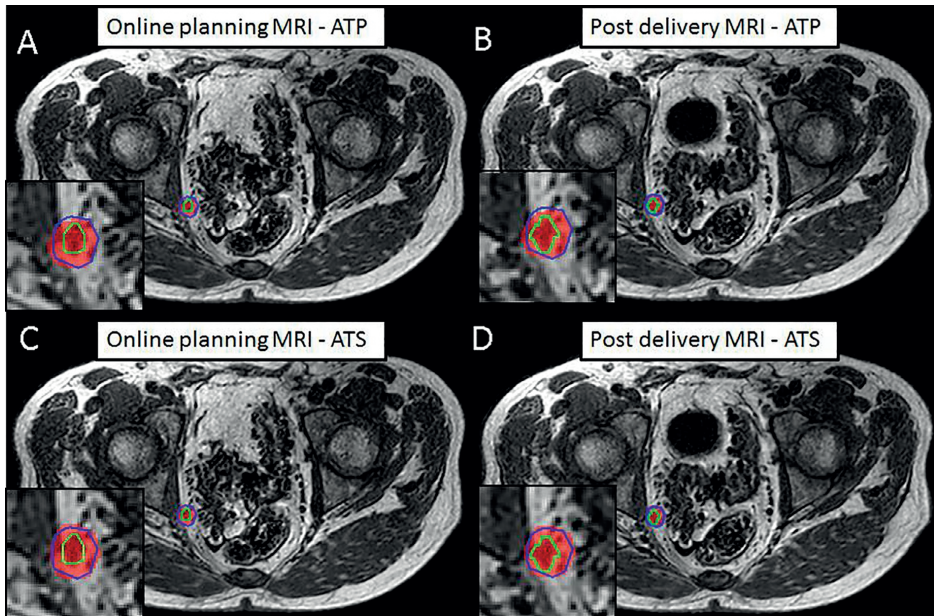


Figure 4. Sample case with intra-fraction expansion of the bladder due to increased filling. Visible are the 35 Gy dose level (red), the PTV (blue) and the actual location of the GTV (green) for the ATP plan on the online planning MRI (A) and the post-delivery MRI (B) and the ATS plan on the online planning MRI (C) and the post-delivery MRI (D). The GTV $V_{35\text{Gy}}$ remained 100% for the clinically delivered (ATS) plan. For this particular case the increasing bladder filling and GTV shift resulted in a small reduction of GTV $V_{35\text{Gy}}$ from 100% to 97.5% with the ATP plan.

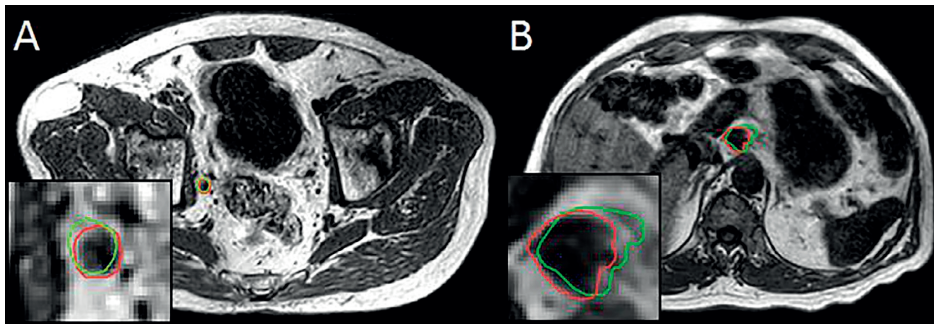


Figure 5. Example cases intra-fraction target motion of lymph node oligometastases in the pelvic (A) and para-aortic (B) region. Visible are the post-delivery MRIs with the online planning GTV (green) and the GTV as observed on the post-delivery MRI (red).

Discussion

MRI guided radiotherapy has been established during the last two decades. Broad clinical implementation has been realized for brachytherapy indications, mainly cervix and prostate [42–44]. Clinical gain of MRI guided brachytherapy in terms of local control and survival, not to the cost of treatment related morbidity, has been demonstrated for all stages of advanced cervical [45,46] and for prostate cancer [47]. In parallel, MRI guidance has become clinically available for external beam radiotherapy (EBRT) in 2014 with the combination of a 0.3 T MRI and 60 Cobalt radiotherapy device as realized in MRidian [48]. Since 2017 the combination of a 1.5T MRI and 7MV linear accelerator is available, bringing new opportunities for MRI guided high accuracy radiotherapy [29]. Since July 2018 this radiotherapy system is increasingly available for clinical routine treatments, starting in Europe and North-America with potential for global spread.

In our institute first clinical treatments on the 1.5T MR-linac were performed for patients with single oligometastatic lymph nodes in pelvis and para-aortic region. All nodes were well visible on the MRIs taken for treatment planning and position verification. The nodes were treated with SBRT (5 x 7 Gy) and the ATS online planning option, which allows to correct for inter-fraction motion by full online treatment planning based on the actual anatomy. All treatment planning aims were met for 40 out of 50 fractions. For 10 fractions the PTV coverage had to be sacrificed slightly in order to meet the hard constraints for OAR adjacent to the nodes and in 3 of these fractions the GTV coverage of the online plan was slightly less than intended (minimum 99.7%). In case the ATP workflow had been used online optimization would have been performed on the pre-treatment patient anatomy. In this case our treatment planning aims would have been met for only 19 out of 50 fractions and the GTV $V_{35\text{Gy}}$ was reduced to 93.9% in the worst case. These clinical results show the additional dosimetric benefit of adaptive MRI-guided radiotherapy with online treatment planning based on the actual patient anatomy. In case of (hypo)- fractionated treatment approaches eventual inter-fraction anatomical changes can be accounted for. Because the ATS workflow is relatively labour-intensive compared to ATP, future studies will aim at predicting for which patients ATS would be most beneficial, and for whom ATP would also provide sufficient target coverage.

When evaluating the dose distributions of the online treatment plan on the anatomy of the post-treatment anatomy the chosen isotropic PTV margin of 3 mm turned out being adequate for treating single lymph nodes in the pelvis and para-aortic region on the MR-linac with the ATS treatment planning option. A limitation of this method is that potential system errors (e.g. MV-MR misalignments) are not accounted for. The PTV margin has to account for system errors as well as intra-fraction target motions and was therefore re-

evaluated. Based on the Van Herk recipe [37] an isotropic PTV margin of 2 mm would have been adequate in all three directions in our series. However, noting the limitations of the recipe for SBRT treatments, very small tumors and higher density structures [38,49] we will still use a PTV margin of 3 mm for this particular indication in further treatments.

Within the group of oligometastatic nodal disease gain in terms of PTV margin reduction and less dose to the surrounding is especially expected for multiple metastatic lesions. In this situation daily treatment planning according to the daily anatomy might attenuate the effect of relative position shifts of the individual nodes relative to each other due to the changes of surrounding organs. Position shifts of pelvic lymph nodes are caused by movements and volume changes of the surrounding organs [50] and are not comparable to the intra-fraction motions of thoracic and abdominal lymph nodes, which are mainly affected by breathing [51,52]. Dosimetric gain of 1.5T MR-linac treatments is also expected in other tumor sites with potentially large inter and intra-fraction motion and substantial deformations such as prostate [53], cervix [54], and rectum [55].

A factor with potential impact on the PTV-margin is the time needed for an entire MR-linac treatment procedure. On-couch time for single lymph node SBRT is currently between 30 and 45 min in our clinical routine. The majority of this time is occupied by treatment planning and radiation delivery with IMRT, which is considerably longer than the few minutes being needed to deliver a VMAT plan as available for CBCT machines. However, when comparing the CBCT-linac single plan option for all treatment fractions with the daily treatment plan option of the 1.5T MR-linac we see dosimetric gain for target and/or OARs [36]. Further PTV margin reduction and dosimetric gain of MR-linac treatments is to be expected with intended machine and software updates. Less time consuming MRI protocols and treatment planning algorithms, VMAT instead of IMRT, tumor tracking during irradiation are among the options currently being developed.

Gain for our patients will include improved comfort through further hypo-fractionation with single fraction treatments on the MR-linac being aimed at as final goal. Due to the excellent soft tissue contrast of MRI treatment margins can be small, fiducial marker implantation as applied by others for position verification purposes can be avoided [22,23]. Clinical gain in terms of tumor related outcome such as local control, prolonged survival, later onset of systemic treatment as well as morbidity and quality of life is yet to be established.

Our study is limited by the relatively low number of cases available for the retrospective evaluation of ATS and ATP planning approaches and the margin analysis. The nodes, which are mainly originating from prostate cancer were detected by PSMA-PET, reflect

small volume targets and essential volume reductions during the course of treatment are not expected [56]. Regardless of these limitations, the here presented findings correspond to earlier reported pre-clinical investigations [27,35] and validate our current treatment approach.

In conclusion, metastatic lymph nodes in the pelvis and para-aortic region can be treated on the 1.5T MR-linac within an acceptable time frame for the whole treatment procedure. We can effectively perform MRI based online treatment planning taking into account the actual patient anatomy and deliver the intended dose to the targets using small but adequate treatment margins. We feel that we are close to “See it and Zap it” with single fraction treatments including MRI based tumor tracking as final goal.

Acknowledgements

The authors wish to thank the Dutch Cancer Society for their financial support (grant 2015-0848).

Conflict of interest statement

The University Medical Center Utrecht MR-linac scientific project, including employment of multiple authors, has been partly funded by Elekta AB (Stockholm, Sweden) and Philips Medical Systems (Best, The Netherlands).

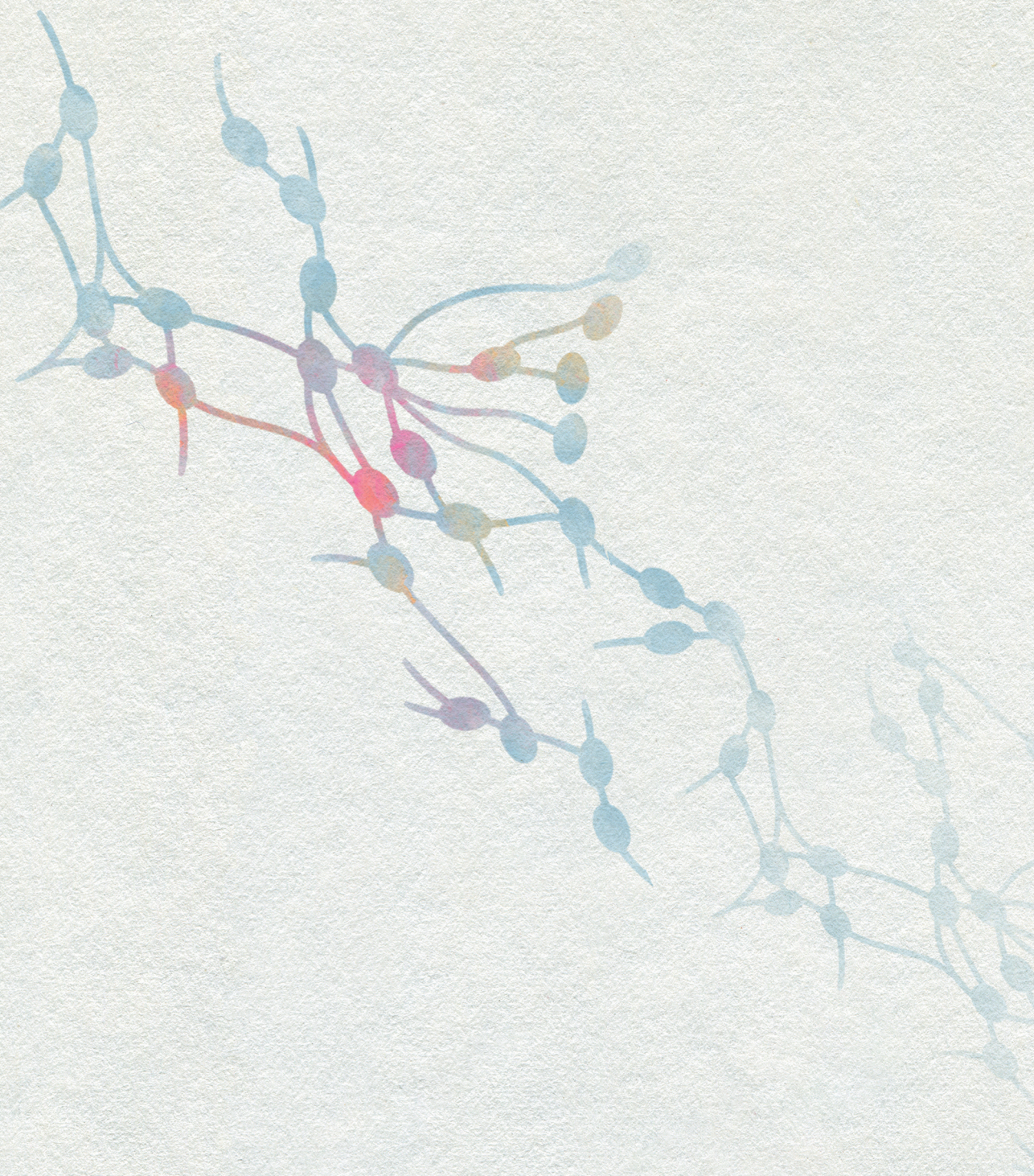
References

1. Tree AC, Khoo VS, Eeles RA, Ahmed M, Dearnaley DP, Hawkins MA, et al. Stereotactic body radiotherapy for oligometastases. *Lancet Oncol* 2013;1: e28–37. [https://doi.org/10.1016/S1470-2045\(12\)70510-7](https://doi.org/10.1016/S1470-2045(12)70510-7).
2. De Bleser E, Tran PT, Ost P. Radiotherapy as metastasis-directed therapy for oligometastatic prostate cancer. *Curr Opin Urol* 2017;27:587–95. <https://doi.org/10.1097/MOU.0000000000000441>.
3. Otake S, Goto T. Stereotactic Radiotherapy for Oligometastasis. *Cancers (Basel)* 2019;11:E133. <https://doi.org/10.3390/cancers11020133>.
4. Hellman S, Weichselbaum RR. Importance of local control in an era of systemic therapy. *Nat Clin Pract Oncol* 2005;2:60–1. <https://doi.org/10.1038/ncponc0075>.
5. Bouman-Wammes EW, van Dodewaard-De Jong JM, Dahele M, Cysouw MCF, Hoekstra OS, van Moorselaar RJA, et al. Benefits of using stereotactic body radiotherapy in patients with metachronous oligometastases of hormone-sensitive prostate cancer detected by [18F]fluoromethylcholine PET/CT. *Clin Genitourin Cancer* 2017;15:e773–82. <https://doi.org/10.1016/j.clgc.2017.03.009>.
6. Ost P, Reynders D, Decaestecker K, Fonteyne V, Lumen N, De Bruycker A, et al. Surveillance or metastasis-directed therapy for oligometastatic prostate cancer recurrence: a prospective, randomized, multicenter phase II trial. *J Clin Oncol* 2018;36:446–53. <https://doi.org/10.1200/JCO.2017.75.4853>.
7. Steuber T, Jilg C, Tennstedt P, De Bruycker A, Tilki D, Decaestecker K, Zilli T, Jereczek-Fossa BA, Wetterauer U, Grosu AL, Schultze-Seemann W, Heinzer H, Graefen M, Morlacco A, Karnes RJ, Ost P. Standard of care versus metastasis-directed therapy for PET-detected nodal oligorecurrent prostate cancer following multimodality treatment: a multi-institutional case-control study. *Eur Urol Focus* 2018. <https://doi.org/10.1016/j.euf.2018.02.015> (Epub ahead of print).
8. Timmerman RD, Bizakis CS, Pass HI, Fong Y, Dupuy DE, Dawson LA, et al. Local surgical, ablative, and radiation treatment of metastases. *CA Cancer J Clin* 2009;59:145–70. <https://doi.org/10.3322/caac.20013>.
9. Aitken KL, Hawkins MA. Stereotactic body radiotherapy for liver metastases. *Clin Oncol (R Coll Radiol)* 2015;27:307–15. <https://doi.org/10.1016/j.clon.2015.01.032>.
10. Shultz DB, Filippi AR, Thariat J, Mornex F, Loo Jr BW, Ricardi U. Stereotactic ablative radiotherapy for pulmonary oligometastases and oligometastatic lung cancer. *J Thorac Oncol* 2014;9:1426–33. <https://doi.org/10.1097/JTO.0000000000000317>.
11. Comito T, Cozzi L, Clerici E, Campisi MC, Liardo RL, Navarria P, et al. Stereotactic Ablative Radiotherapy (SABR) in inoperable oligometastatic disease from colorectal cancer: a safe and effective approach. *BMC Cancer* 2014;14:619. <https://doi.org/10.1186/1471-2407-14-619>.
12. Andratschke N, Alheid H, Allgäuer M, Becker G, Blanck O, Boda-Heggemann J, et al. The SBRT database initiative of the German Society for Radiation Oncology (DEGRO): patterns of care and outcome analysis of stereotactic body radiotherapy (SBRT) for liver oligometastases in 474 patients with 623 metastases. *BMC Cancer* 2018;18:283. <https://doi.org/10.1186/s12885-018-4191-2>.
13. Scorsetti M, Comito T, Clerici E, Franzese C, Tozzi A, Iftode C, et al. Phase II trial on SBRT for unresectable liver metastases: long-term outcome and prognostic factors of survival after 5 years of follow-up. *Radiat Oncol* 2018;13:234. <https://doi.org/10.1186/s13014-018-1185-9>.
14. Lancia A, Zilli T, Achard V, Dirix P, Everaerts W, Gomez-Iturriaga A, et al. Oligometastatic prostate cancer: the game is afoot. *Cancer Treat Rev* 2019;73:84–90. <https://doi.org/10.1016/j.ctrv.2019.01.005>.

15. Palacios-Eito A, Béjar-Luque A, Rodríguez-Liñán M, García-Cabezas S. Oligometastases in prostate cancer: ablative treatment. *World J Clin Oncol* 2019;10:3-51. <https://doi.org/10.5306/wjco.v10.i2.38>.
16. Chance WW, Nguyen QN, Mehran R, Welsh JW, Gomez DR, Balter P, et al. Stereotactic ablative radiotherapy for adrenal gland metastases: factors influencing outcomes, patterns of failure, and dosimetric thresholds for toxicity. *Pract Radiat Oncol* 2017;7:e195-203. <https://doi.org/10.1016/j.prro.2016.09.005>.
17. Ippolito E, D'Angelillo RM, Fiore M, Molfese E, Trodella L, Ramella S. SBRT: a viable option for treating adrenal gland metastases. *Rep Pract Oncol Radiother* 2015;20:484-90. <https://doi.org/10.1016/j.rpor.2015.05.009>.
18. Moghul M, Somani B, Lane T, Vasdev N, Chaplin B, Peedell C, et al. Detection rates of recurrent prostate cancer: 68Gallium (Ga)-labelled prostate-specific membrane antigen versus choline PET/CT scans. A systematic review. *Ther Adv Urol* 2019;11. <https://doi.org/10.1177/1756287218815793>.
19. Fowler J, Chappell R, Ritter M. Is alpha/beta for prostate tumors really low? *Int J Radiat Oncol Biol Phys* 2001;50:1021-31. [https://doi.org/10.1016/S0360-3016\(01\)01607-8](https://doi.org/10.1016/S0360-3016(01)01607-8).
20. Ponti E, Lancia A, Ost P, Trippa F, Triggiani L, Detti B, et al. Exploring all avenues for radiotherapy in oligorecurrent prostate cancer disease limited to lymph nodes: a systematic review of the role of stereotactic body radiotherapy. *Eur Urol Focus* 2017;3:538-44. <https://doi.org/10.1016/j.euf.2017.07.006>.
21. Taylor LG, Canfield SE, Du XL. Review of major adverse effects of androgen-deprivation therapy in men with prostate cancer. *Cancer* 2009;115:2388-99. <https://doi.org/10.1002/cncr.24283>.
22. Detti B, Bonomo P, Masi L, Doro R, Cipressi S, Iermano C, et al. Stereotactic radiotherapy for isolated nodal recurrence of prostate cancer. *World J Urol* 2015;33:1197-203. <https://doi.org/10.1007/s00345-014-1427-x>.
23. Muldermans JL, Romak LB, Kwon ED, Park SS, Olivier KR. Stereotactic body radiation therapy for oligometastatic prostate cancer. *Int J Radiat Oncol Biol Phys* 2016;95:696-702. <https://doi.org/10.1016/j.ijrobp.2016.01.032>.
24. Pasqualetti F, Panichi M, Sainato A, Matteucci F, Galli L, Cocuzza P, et al. [¹⁸F] Choline PET/CT and stereotactic body radiotherapy on treatment decision making of oligometastatic prostate cancer patients: preliminary results. *Radiat Oncol* 2016;11:9. <https://doi.org/10.1186/s13014-016-0586-x>.
25. Laliscia C, Fabrini MG, Delishaj D, Morganti R, Greco C, Cantarella M, et al. Clinical outcomes of stereotactic body radiotherapy in oligometastatic gynecological cancer. *Int J Gynecol Cancer* 2017;27:396-402. <https://doi.org/10.1097/IGC.0000000000000885>.
26. Siva S, Bressel M, Murphy DG, Shaw M, Chander S, Violet J, et al. Stereotactic ablative body radiotherapy (SABR) for oligometastatic prostate cancer: a prospective clinical trial. *Eur Urol* 2018;74:455-62. <https://doi.org/10.1016/j.eururo.2018.06.004>.
27. Winkel D, Kroon PS, Werensteijn-Honingh AM, Bol GH, Raaymakers BW, Jürgenliemk-Schulz IM. Simulated dosimetric impact of online replanning for stereotactic body radiation therapy of lymph node oligometastases on the 1.5T MR-linac. *Acta Oncol* 2018;3:1-8. <https://doi.org/10.1080/0284186X.2018.1512152>.
28. Noel CE, Parikh PJ, Spencer CR, Green OL, Hu Y, Mutic S, et al. Comparison of onboard low-field magnetic resonance imaging versus onboard computed tomography for anatomy visualization in radiotherapy. *Acta Oncol* 2015;54:1474-82. <https://doi.org/10.3109/0284186X.2015.1062541>.
29. Raaymakers BW, Jürgenliemk-Schulz IM, Bol GH, Glitzner M, Kotte ANTJ, van Asselen B, et al. First patients treated with a 1.5 T MRI-Linac: clinical proof of concept of a high-precision, high-field MRI guided radiotherapy treatment. *Phys Med Biol* 2017;62:L41-50. <https://doi.org/10.1088/1361-6560/aa9517>.

30. Werensteijn-Honingh AM, Kroon PS, Winkel D, Aalbers EM, Van Asselen B, Bol GH, et al. Feasibility of stereotactic radiotherapy using a 1.5 T MR-linac: multi-fraction treatment of pelvic lymph node oligometastases. *Radiother Oncol* 2019;134:50–4. <https://doi.org/10.1016/j.radonc.2019.01.024>.
31. Winkel D, Bol G, Werensteijn-Honingh A, Kiekebosch I, Hes J, Intven M, et al. Dose escalation and hypofractionation for SBRT of lymph node oligometastases on the 1.5T MRI-Linac. *Radiother Oncol* 2018;127:S443–4. [https://doi.org/10.1016/S0167-8140\(18\)31158-7](https://doi.org/10.1016/S0167-8140(18)31158-7) (conference abstract).
32. Henke L, Kashani R, Yang D, Zhao T, Green O, Olsen L, et al. Simulated online adaptive magnetic resonance-guided stereotactic body radiation therapy for the treatment of oligometastatic disease of the abdomen and central thorax: characterization of potential advantages. *Int J Radiat Oncol Biol Phys* 2016;96:1078–86. <https://doi.org/10.1016/j.ijrobp.2016.08.036>.
33. Heerkens HD, Reerink O, Intven MPW, Hiensch RR, van den Berg CAT, Crijns SPM, et al. Pancreatic tumor motion reduction by use of a custom abdominal corset. *Phys Imaging Radiat Oncol* 2017;2:7–10. <https://doi.org/10.1016/j.phro.2017.02.003>.
34. Winkel D, Kroon PS, Hes J, Bol GH, Raaymakers BW, Jürgenliemk-Schulz IM. Automated full-online replanning of SBRT lymph node oligometastases for the MR-linac. *Radiother Oncol* 2017;123:S904. [https://doi.org/10.1016/S0167-8140\(17\)32195-3](https://doi.org/10.1016/S0167-8140(17)32195-3) (conference abstract).
35. Winkel D, Bol G, Werensteijn-Honingh A, Kiekebosch I, Van Asselen B, Intven M, et al. Evaluation of plan adaptation strategies for stereotactic radiotherapy of lymph node oligometastases using online magnetic resonance image guidance. *Phys Imaging Radiat Oncol* 2019;9:58–64. <https://doi.org/10.1016/j.phro.2019.02.003>.
36. Winkel D, Bol G, Werensteijn-Honingh A, Intven M, Eppinga W, van Asselen B, et al. Dosimetric benefit of the first clinical SBRT of lymph node oligometastases on the 1.5T MR-linac. *ESTRO 2019* (conference abstract).
37. van Herk M, Remeijer P, Rasch C, Lebesque JV, et al. The probability of correct target dosage: dose-population histograms for deriving treatment margins in radiotherapy. *Int J Radiat Oncol Biol Phys* 2000;47:1121–35.
38. Gordon JJ, Siebers JV. Convolution method and CTV-to-PTV margins for finite fractions and small systematic errors. *Phys Med Biol* 2007;52:1967–90. <https://doi.org/10.1088/0031-9155/52/7/013>.
39. de Boer JJC, Heijmen BJM. A protocol for the reduction of systematic patient setup errors with minimal portal imaging workload. *Int J Radiat Oncol Biol Phys* 2001;50:1350–65.
40. Tijssen RHN, Philippens MEP, Saulson ES, Glitzner M, Chugh B, Wetscherek A, et al. MRI commissioning of 1.5T MR-linac systems – a multi-institutional study. *Radiother Oncol* 2019;132:114–20. <https://doi.org/10.1016/j.radonc.2018.12.011>.
41. Stroom JC, Heijmen BJ. Geometrical uncertainties, radiotherapy planning margins, and the ICRU-62 report. *Radiother Oncol* 2002;64:75–83.
42. Tanderup K, Viswanathan A, Kirisits C, Frank SJ. MRI-guided brachytherapy. *Semin Radiat Oncol* 2014;24:181–91. <https://doi.org/10.1016/j.semradonc.2014.02.007>.
43. Sturdza A, Pötter R, Fokdal LU, Haie-Meder C, Tan LT, Mazon R, et al. Image guided brachytherapy in locally advanced cervical cancer: improved pelvic control and survival in RetroEMBRACE, a multicenter cohort study. *Radiother Oncol* 2016;120:428–33. <https://doi.org/10.1016/j.radonc.2016.03.011>.

44. Pötter R, Tanderup K, Kirisits C, de Leeuw A, Kirchheiner K, Nout R, et al. The EMBRACE II study: the outcome and prospect of two decades of evolution within the GEC-ESTRO GYN working group and the EMBRACE studies. *Clin Transl Radiat Oncol* 2018;9:48–60. <https://doi.org/10.1016/j.ctro.2018.01.001>.
45. Rijkmans EC, Nout RA, Rutten IH, Ketelaars M, Neelis KJ, Laman MS, et al. Improved survival of patients with cervical cancer treated with image-guided brachytherapy compared with conventional brachytherapy. *Gynecol Oncol* 2014;135:231–8. <https://doi.org/10.1016/j.ygyno.2014.08.027>.
46. Tanderup K, Fokdal LU, Sturdza A, Haie-Meder C, Mazon R, van Limbergen E, et al. Effect of tumor dose, volume and overall treatment time on local control after radiochemotherapy including MRI guided brachytherapy of locally advanced cervical cancer. *Radiother Oncol* 2016;120:441–6. <https://doi.org/10.1016/j.radonc.2016.05.014>.
47. Nguyen PL, Chen MH, Zhang Y, Tempany CM, Cormack RA, Beard CJ, et al. Updated results of magnetic resonance imaging guided partial prostate brachytherapy for favorable risk prostate cancer: implications for focal therapy. *J Urol* 2012;188:1151–6. <https://doi.org/10.1016/j.juro.2012.06.010>.
48. Fischer-Valuck BW, Henke L, Green O, Kashani R, Acharya S, Bradley JD, et al. Two-and-a-half-year clinical experience with the world's first magnetic resonance image guided radiation therapy system. *Adv Radiat Oncol* 2017;2:485–93. <https://doi.org/10.1016/j.adro.2017.05.006>.
49. Witte MG, van der Geer J, Schneider C, Lebesque JV, van Herk M. The effects of target size and tissue density on the minimum margin required for random errors. *Med Phys* 2004;31:3068–79. <https://doi.org/10.1118/1.1809991>.
50. Wiersema L, Borst G, Nakhaee S, Peulen H, Wiersma T, Kwint M, et al. First IGRT results for SBRT bone and lymph node oligometastases within the pelvic region. *Radiother Oncol* 2017;123:S1006. [https://doi.org/10.1016/S0167-8140\(17\)32273-9](https://doi.org/10.1016/S0167-8140(17)32273-9) (conference abstract).
51. Pantarotto JR, Piet AH, Vincent A, van Sörnsen de Koste JR, Senan S. Motion analysis of 100 mediastinal lymph nodes: potential pitfalls in treatment planning and adaptive strategies. *Int J Radiat Oncol Biol Phys* 2009;74:1092–9. <https://doi.org/10.1016/j.ijrobp.2008.09.031>.
52. Yorke E, Xiong Y, Han Q, Zhang P, Mageras G, Lovelock M, et al. Kilovoltage imaging of implanted fiducials to monitor intrafraction motion with abdominal compression during stereotactic body radiation therapy for gastrointestinal tumors. *Int J Radiat Oncol Biol Phys* 2016;95:1042–9. <https://doi.org/10.1016/j.ijrobp.2015.11.018>.
53. McPartlin AJ, Li XA, Kershaw LE, Heide U, Kermeijer L, Lawton C, et al. MRI-guided prostate adaptive radiotherapy – a systematic review. *Radiother Oncol* 2016;119:371–80. <https://doi.org/10.1016/j.radonc.2016.04.014>.
54. Kerkhof EM, van der Put RW, Raaymakers BW, van der Heide UA, Jürgenliemk-Schulz IM, Lagendijk JJ. Intrafraction motion in patients with cervical cancer: the benefit of soft tissue registration using MRI. *Radiother Oncol* 2009;93:115–21. <https://doi.org/10.1016/j.radonc.2009.07.010>.
55. Nijkamp J, Swellengrebel M, Hollmann B, de Jong R, Marijnen C, van Vliet-Vroegindewij C, et al. Repeat CT assessed CTV variation and PTV margins for short- and long-course pre-operative RT of rectal cancer. *Radiother Oncol* 2012;102:399–405. <https://doi.org/10.1016/j.radonc.2011.11.011>.
56. Schippers MG, Bol GH, de Leeuw AA, van der Heide UA, Raaymakers BW, Verkooijen HM, et al. Position shifts and volume changes of pelvic and para-aortic nodes during IMRT for patients with cervical cancer. *Radiother Oncol* 2014;111:442–5. <https://doi.org/10.1016/j.radonc.2014.05.013>.



Chapter 4

Impact of a vacuum cushion on intrafraction motion during online adaptive MR-guided SBRT for pelvic and para-aortic lymph node oligometastases

Anita M. Werensteijn-Honingh, Ina M. Jürgenliemk-Schulz, Christa G. Gadellaa-Van Hooijdonk, Gonda G. Sikkes, Nicole G.P.M. Vissers, Dennis Winkel, Wietse S.C. Eppinga, Martijn Intven, Bas W. Raaymakers, Petra S. Kroon.

Radiother Oncol 2021;154:110-7.
<https://doi.org/10.1016/j.radonc.2020.09.021>.

Abstract

Background and Purpose: Vacuum cushion immobilization is commonly used during stereotactic body radiotherapy (SBRT) to reduce intrafraction motion. We investigated target and bony anatomy intrafraction motion (translations and rotations) during online adaptive SBRT on an MR-linac for pelvic/para-aortic lymph node metastases with and without vacuum cushion.

Materials and Methods: Thirty-nine patients underwent 5x7 Gy SBRT on a 1.5 T MR-linac, 19 patients were treated with vacuum cushion, 19 without and 1 patient sequentially with and without. Intrafraction motion was calculated for target lymph nodes (GTVs) and nearby bony anatomy, for three time intervals (pre-position verification (PV), pre-post, PV-post, relating to the online MRI scans) per treatment fraction.

Results: Vacuum cushion immobilization significantly reduced anterior-posterior translations for the pre-PV and pre-post intervals, for bony anatomy and pre-post interval for GTV ($p < 0.05$). Mean GTV intrafraction motion reduction in posterior direction was 0.7 mm (95% confidence interval 0.3-1.1 mm) for pre-post interval (mean time=32 min). Shifts in other directions were not significantly reduced. More motion occurred in pre-PV interval than in PV-post interval (mean time=16 min for both); vacuum cushion immobilization did not reduce intrafraction motion during the beam-on period.

Conclusion: A vacuum cushion reduces GTV and bony anatomy intrafraction motion in posterior direction during pelvic/para-aortic lymph node SBRT. This motion reduction was found for the first 16 minutes per session. For single targets this motion can be corrected for directly with an MR-linac. Intrafraction motion was not reduced during the second half of the session, the period of radiotherapy delivery on an MR-linac. Vacuum cushion immobilization may not be necessary for patients with single lymph node oligometastases undergoing SBRT on an MR-linac.

Introduction

Stereotactic body radiotherapy (SBRT) is characterized by precise delivery of high radiation doses per fraction [1]. Tightly conformal dose distributions are used with small safety margins around the gross tumor volume (GTV). Minimization of these margins is intended to minimize the volume of healthy tissue exposed to radiation, as SBRT fractionation schedules do not sufficiently allow healthy tissues to recover from the large ablative doses that are administered to the tumor volume [2,3]. On the other hand, the rapid dose fall-off outside the planning target volume (PTV) means that GTV coverage may be impacted if the PTV margins do not sufficiently correct for intrafraction motion and possible technical uncertainties during SBRT delivery [4,5].

Historically, a stereotactic body frame (SBF) that included a vacuum cushion was used for daily SBRT set-up. However, due to internal organ motion set-up errors of up to 10 mm remained present [6]. Patient positioning accuracy has been improved with the introduction of online cone beam CT (CBCT) image guidance [7]. Vacuum cushions are still widely used in SBRT for limiting intrafraction motion, especially for spinal targets [8-13]. Additional reasons for using a vacuum cushion can be patient comfort and reducing interfraction rotations for couches without rotational correction possibilities [14].

Serago *et al.* have compared prostate cancer intrafraction motion with and without immobilization [15]. Immobilization with vacuum body fixation (BodyFIX system) decreased prostate cancer intrafraction motion by 1.3 mm compared to no immobilization (3.4 ± 2.7 mm without immobilization, 2.1 ± 1.5 mm with vacuum device immobilization). The addition of the vacuum sheet as part of the vacuum body fixation, on top of the vacuum cushion, has been used for patients with large respiratory motion in pulmonary SBRT [16] and was shown to further reduce intrafraction motion for spine and pulmonary SBRT [9,17], but not for prostate [18]. Data from (simulated) thoracic spine SBRT showed a reduction in intrafraction motion with vacuum cushion compared to no immobilization [13].

However, SBRT is also applied without immobilization devices with good patient stability during the fractions [19-22]. This could be an attractive option, eliminating additional preparation time and storage of the cushion. Furthermore, a vacuum cushion may complicate treatments with online adaptive MR-guidance: even though combined MRI-linear accelerator (MR-linac) treatment systems have a wide bore (70 cm), the addition of a vacuum cushion causes some obese patients to not fit under the coil or in the bore. MR-linac safety evacuation procedures are more difficult as the vacuum cushion is attached to the treatment table with lock bars. MR-linacs have been developed to correct for intrafraction motion and technological developments currently focus on making real-time adaptive

radiotherapy possible [23,24]. Currently, an MR-linac allows for correction of intrafraction motion occurring until the acquisition of the position verification (PV) scan, after online contour adaptation and planning [25,26]. This is comparable to correction possibilities on a CBCT-linac, but the time interval between patient positioning and PV scan is longer for MR-linac [25]. The effect of vacuum cushion immobilization has not been evaluated for lumbar spine or pelvic/para-aortic lymph node metastases and neither for the longer time scales on an MR-linac. Therefore, it remains unknown whether a vacuum cushion needs to be used for pelvic/para-aortic lymph node SBRT, especially with treatment systems that can perform intrafraction motion correction.

In this study we investigated the impact of a vacuum cushion on intrafraction motion during online adaptive MR-guided SBRT for pelvic/para-aortic lymph node metastases. Intrafraction motion has been analyzed both for bony anatomy and for the target lymph nodes, testing the need for vacuum cushion immobilization in the context of online adaptive MRI guidance.

Materials and Methods

Patients and treatment

Thirty-nine patients with 1-3 pelvic and/or para-aortic lymph node oligometastases were included in this study. Patient characteristics are shown in Table 1; the anatomical locations of the GTVs are shown in Supplementary material: Figure S1. All patients gave written informed consent for the use of their data as part of an institutional review board approved observational study. All patients were treated with a prescribed dose of 5x 7 Gy to 95% of the PTV on a 1.5 T MR-linac (Unity, Elekta AB, Stockholm, Sweden) [25]. Employing a longitudinal cohort design, 19 patients were treated with a vacuum cushion (BlueBAG BodyFIX 14 Rectangular 700x1825 mm/50L, Elekta AB) according to our standard clinical practice, in order to minimize intrafraction motion. Subsequently 19 patients were treated without a vacuum cushion as part of a clinical pilot workflow. One patient received SBRT treatment with and without vacuum cushion for repeated oligometastases, 9 months apart, making the total number of treatments for both groups 20. This patient has been included in both groups, intrafraction motion results of these two treatments have been analyzed as independent measurements. Patients with high para-aortic lymph node metastases who were treated with a corset were excluded from this study.

For each treatment fraction, daily plan optimization was performed using adapt to shape as described in [25]. GTV position was checked on the PV scan that was acquired after contour adaptation and planning. If GTV motion between pre-treatment and PV scan exceeded the 3 mm PTV margin, the plan was adapted using an additional adapt to position procedure for patients with a single GTV: adapting the plan to the new target location [26]. In case

of multiple GTVs with movement relative to one another, an additional adapt to shape procedure was initiated: manually adapting the GTV contours and performing the online planning procedure again, followed by another PV scan. After each fraction, the GTV coverage was recalculated on the post-treatment scan using automatically deformed GTV contours ($GTV V_{35 Gy} = 100\%$) and if necessary PTV margins were adapted for subsequent fractions, as part of routine clinical care.

Table 1

Patient characteristics for patients treated with and without vacuum cushion.

		N with vacuum cushion	N without vacuum cushion
Number of treatments		20	20
Location	Pelvic	19	16
	Para-aortic	1	4
N GTVs	1	15	9
	2	3	5
	3	2	6
N PTVs	1	16	12
	2	4	5
	3	0	3
GTV in mL (mean (sd))		0.9 (1.0)	2.5 (4.6)
Primary tumor	Prostate	19	15
	Colorectal	0	3
	Esophageal	1	0
	Lung	0	1
	Melanoma	0	1
ECOG performance status	0	14	16
	1	6	4

Anatomical locations of the GTV(s) are specified as pelvic (caudal of aortic bifurcation) or para-aortic (cranial of aortic bifurcation), this is shown in more detail in Supplementary Material: Figure S1. ECOG: Eastern Cooperative Oncology Group.

MRI scans obtained on the MR-linac and used for this study included a transverse 3D T1-weighted FFE scan with an acquisition time of 2 min (TR 11 ms, TE 4.6 ms, acquired voxel size 1.5x1.5x2.0 mm³, FOV 400x400x300 mm³) and a transverse 3D T2-weighted

TSE scan with an acquisition time of 3 min 40 s (TR 1500 ms, TE 124 ms, acquired voxel size $1.3 \times 1.3 \times 2.0 \text{ mm}^3$, FOV $400 \times 400 \times 300 \text{ mm}^3$). For each patient the MRI sequence with the best target and organ at risk visualization was selected.

Session time was defined as time since acquisition of the pre-treatment scan.

GTV intrafraction motion analysis

GTV intrafraction motion was derived by rigid registration of PV and post-treatment scans to the pre-treatment scan using the ITK-based, open source image registration toolkit elastix (v 4.8) [27,28]. If multiple PV scans were acquired (after additional plan adaptation procedures), only the first PV scan was used for this study.

Rigid registration (translations and rotations) was performed on cropped scans with GTV masks, to obtain registration on the target lymph nodes. Pre-processing of scans was performed with MeVisLab software (v 3.2, MeVis Medical Solutions AG, Bremen, Germany) [29]. Scan cropping, GTV masks for both fixed and moving scans and an additional cost function on the overlap of centers of gravity for each GTV on both fixed and moving scan were used to guide the registration, as the target lymph node(s) were very small. Scans were cropped to a rectangular area that included all GTV contours on all three scans (pre, PV, post) for a single fraction, expanded with 1 cm in all directions. Clinical contours of the pre scans were used; PV and post scans were manually contoured (in total 3 observers for contouring). GTV masks were created by expanding the GTV contour(s) of a single scan with 0.5 cm in all directions. For patients with a single GTV, the center of rotation was placed on the GTV center of gravity. For patients with multiple GTVs, intrafraction motion of all GTVs was calculated in a single elastix registration with the center of rotation placed in the center of the GTV centers of gravity. Thus, 'common' translations and rotations for all GTVs of a patient were derived and analyzed.

Translations were calculated by elastix along three body axes: left-right (positive towards left), anterior-posterior (positive towards posterior) and cranial-caudal (positive towards cranial). Rotations were calculated by elastix around these axes (ZXY Tait-Bryan angles). Translations and rotations were calculated for three time intervals: 1) between pre-treatment and PV scan (pre-PV), 2) between pre- and post-treatment scan (pre-post) and 3) between PV and post-treatment scan (PV-post).

Bony anatomy intrafraction motion analysis

Elastix was also used to derive the bony anatomy intrafraction motion. The PV and post-treatment scans were rigidly registered to the pre-treatment scan, but scan cropping was different and a bone mask was used. Scans were cropped, in left-right direction limited to

the body contour without arms, in anterior-posterior direction limited by the treatment table and 28 cm above treatment table and in cranial-caudal direction limited to 2 cm above and below the PTV(s). The center of the cropped image was used as the center of rotations, and corresponded to the MR-linac isocenter: at the center of the treatment table in lateral (patient left-right) direction and at 14 cm above the treatment table in vertical (patient anterior-posterior) direction. The bone mask was generated by including 1 cm in each direction around a manually adapted bone contour. Registration in elastix was performed by sampling from the region of the pre-treatment scan (fixed scan) indicated by the bone mask and finding the corresponding voxels of the PV/post-treatment scan (moving scan). The parameter file used for elastix registration in this study is available as par0061 on http://elastix.bigr.nl/wiki/index.php/Parameter_file_database.

Statistics

The open source R software package (v 3.6.1) was used for statistical comparisons and to create figures (R Foundation for Statistical Computing, Vienna, Austria; <http://www.R-project.org>). To correct for repeated measures per patient, mean absolute translations per patient (three directions) were compared for patients with and without vacuum cushion. The Mann-Whitney U-test was used to test the differences as the absolute data were not normally distributed, two-sided $p < 0.05$ was considered significant. Mean translations and systematic and random errors were calculated according to the methodology described by Stroom and Heijmen [30]. Standard deviations of translations were calculated taking outcomes of individual fractions into account without correcting for repeated measures per patient. Correlation between GTV and bony anatomy intrafraction motion was calculated using repeated measures correlation [31] with the R-package rmcrr (v 0.3.0). This method assumes a linear relationship between the variables and then takes the repeated measurements (five SBRT fractions) per patient into account, whilst searching for the slope of a regression line that best fits the data of all patients. Regression slope, repeated measures correlation coefficient r and corresponding p -value were calculated without making a distinction regarding vacuum cushion use.

Results

Patients treated with a vacuum cushion had significantly smaller absolute translations in anterior-posterior direction for the pre-PV ($p = 0.02$) and pre-post ($p = 0.005$) intervals (Figure 1) for bony anatomy. The reduction for the pre-post interval was also significant for GTV ($p = 0.03$). Mean GTV translation in anterior-posterior direction (positive towards posterior) was 0.3 mm (SD 0.9) with cushion and 1.0 mm (SD 1.8) without cushion for the pre-post interval (mean time between pre and post scan was 31 min with cushion and 33 min without cushion). The 95% confidence interval of anterior-posterior GTV translation

reduction for pre-post interval was 0.3 - 1.1 mm. Patients with cushion also showed smaller systematic and random errors of the translations in anterior-posterior direction of both GTV and bony anatomy for the pre-PV and pre-post intervals (Table 2). The use of a vacuum cushion did not have an effect on bony anatomy or GTV rotations (Figure 2, Supplementary material: Table S1). Mean, systematic and random errors of GTV rotations were larger than for bony anatomy (Supplementary material: Table S1).

Table 2

Mean, systematic and random errors of GTV and bony anatomy intrafraction translations. Intrafraction motion analysis of patients treated with MR-linac SBRT for pelvic or para-aortic lymph node metastases. GTV and bony anatomy translations are shown in left-right (LR, + towards left), anterior-posterior (AP, + towards posterior) and cranial-caudal (CC, + towards cranial) directions for patients treated with (N=20) and without vacuum cushion (N=20), for the three time intervals (mean time per interval reported for patients with and without cushion).

Pre-PV scan		GTV translation (mm)			Bony translation (mm)		
		LR	AP	CC	LR	AP	CC
Vacuum cushion (mean t=15 min)	Mean	-0.1	0.3	0.0	0.0	0.2	-0.3
	Systematic	0.5	0.3	0.9	0.4	0.3	0.7
	Random	0.5	0.6	0.6	0.4	0.4	0.5
No cushion (mean t=17 min)	Mean	-0.3	0.7	0.0	-0.2	0.6	-0.4
	Systematic	0.8	1.0	0.5	0.7	0.7	0.5
	Random	0.6	1.0	0.7	0.6	0.5	0.4
Pre-post scan		GTV translation (mm)			Bony translation (mm)		
		LR	AP	CC	LR	AP	CC
Vacuum cushion (mean t=31 min)	Mean	0.0	0.3	-0.2	-0.1	0.3	-0.6
	Systematic	0.7	0.6	1.1	0.6	0.3	0.8
	Random	0.7	0.7	0.5	0.5	0.4	0.5
No cushion (mean t=33 min)	Mean	-0.4	1.0	0.0	-0.2	0.9	-0.5
	Systematic	1.1	1.3	0.9	1.0	0.9	0.7
	Random	0.8	1.2	0.9	0.8	0.5	0.7
PV-post scan		GTV translation (mm)			Bony translation (mm)		
		LR	AP	CC	LR	AP	CC
Vacuum cushion (mean t=16 min)	Mean	0.0	0.0	-0.2	-0.1	0.1	-0.3
	Systematic	0.4	0.5	0.4	0.3	0.3	0.2
	Random	0.5	0.7	0.5	0.4	0.4	0.5
No cushion (mean t=16 min)	Mean	-0.1	0.4	0.1	-0.1	0.3	-0.1
	Systematic	0.4	0.5	0.5	0.4	0.3	0.5
	Random	0.6	0.5	0.7	0.5	0.3	0.5

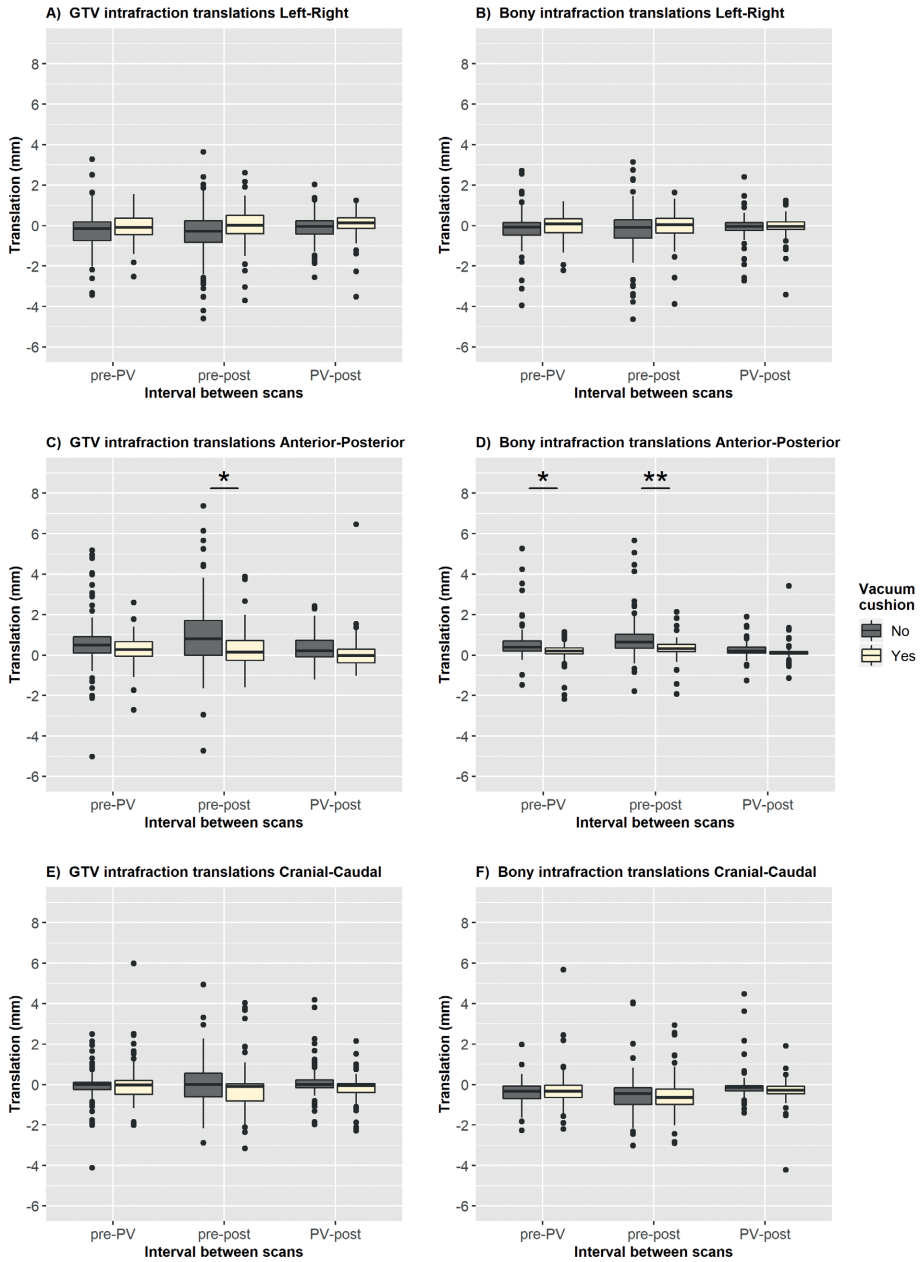


Figure 1. GTV and bony anatomy intrafraction translations with and without cushion, per time interval. Intrafraction motion analysis of patients treated with MR-linac SBRT for pelvic or para-aortic lymph node metastases. Translations for each fraction (five per patient) are shown in left-right (+ towards left), anterior-posterior (+ towards posterior) and cranial-caudal (+ towards cranial) directions, for patients treated with (N=20) and without vacuum cushion (N=20), for three time intervals (mean time interval for pre-PV 16 min, pre-post 32 min, PV-post 16 min). Center line indicates median, hinges depict 25th and 75th percentiles

Figure 1. (continued)

(inter-quartile range, IQR) and whiskers extend from the hinge to the largest/smallest value at maximally $1.5 \cdot \text{IQR}$. Outlying data points ($>1.5 \cdot \text{IQR}$ from hinge) are plotted individually. Asterisks depict significant differences in patient mean absolute translations between patients treated with and without cushion (Mann-Whitney U-test (two-sided), * $p < 0.05$, ** $p < 0.01$).

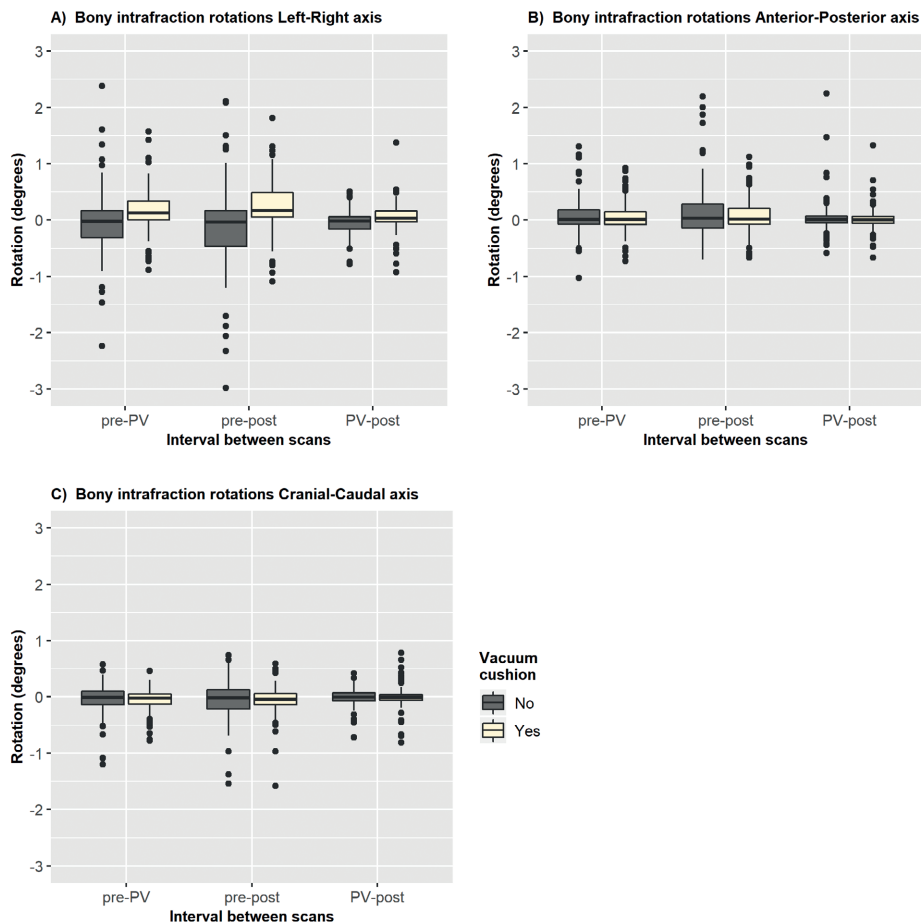


Figure 2. Bony anatomy intrafraction rotations with and without cushion, per time interval. Intrafraction motion analysis of patients treated with MR-linac SBRT for pelvic or para-aortic lymph node metastases. Rotations for each fraction (five per patient) are shown around the left-right, anterior-posterior and cranial-caudal axes, for patients treated with (N=20) and without vacuum cushion (N=20), for three time intervals (mean time interval for pre-PV 16 min, pre-post 32 min, PV-post 16 min). Center line indicates median, hinges depict 25th and 75th percentiles (inter-quartile range, IQR) and whiskers extend from the hinge to the largest/smallest value at maximally $1.5 \cdot \text{IQR}$. Outlying data points ($>1.5 \cdot \text{IQR}$ from hinge) are plotted individually. Mann-Whitney U-test (two-sided) did not reveal any significant differences between patients treated with and without cushion.

As shown in Figure 3, most intrafraction translations occurred during the pre-PV interval (mean time was 15 min with cushion and 17 min without cushion). After the PV scan, the average motion was comparable with and without vacuum cushion (mean time of PV-post interval was 16 min). Systematic/random errors of translations for PV-post interval were also similar for patients treated with or without vacuum cushion.

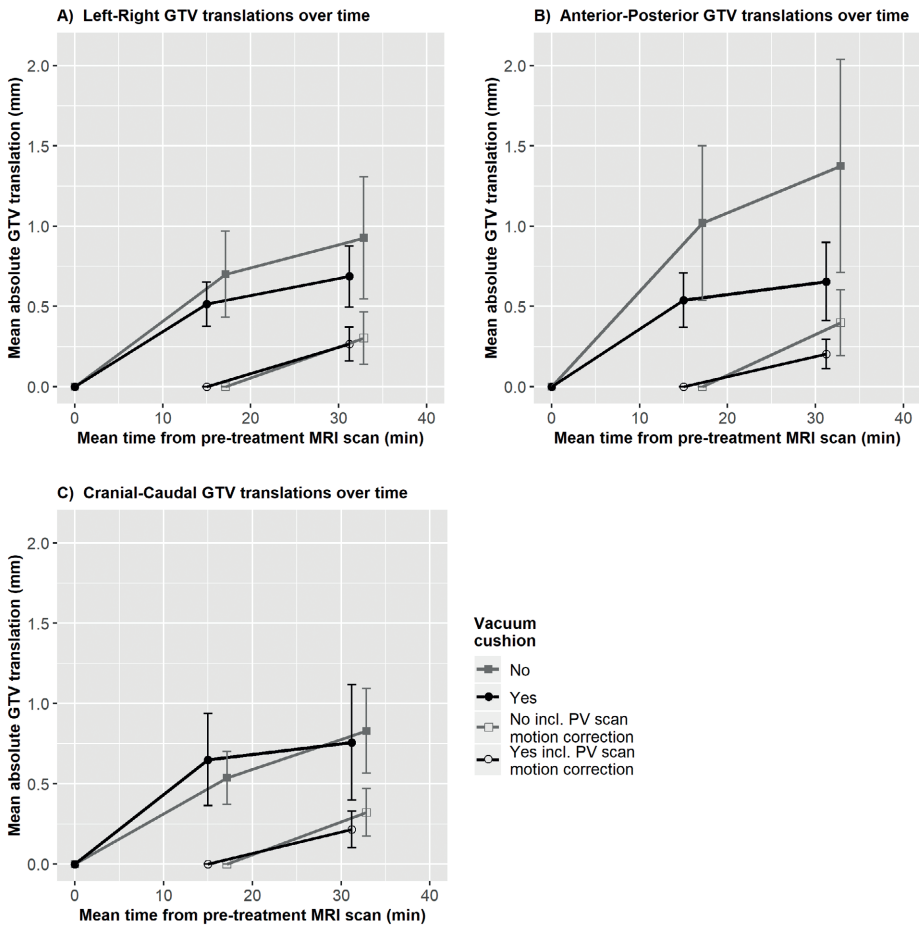


Figure 3. GTV intrafraction motion over time for patients with and without cushion. Intrafraction motion analysis of patients treated with MR-linac SBRT for pelvic or para-aortic lymph node metastases. Mean absolute GTV translations in three directions are shown at the group-average moments of PV and post scan, for patients treated with (N=20) and without vacuum cushion (N=20) as filled circles/squares. The data points are connected with straight lines and for each data point the 95% confidence interval is shown with error bars. The same results are also separately shown for the situation after PV scan motion correction, with data points indicated as open circles/squares.

For one patient (with a vacuum cushion) the PTV margin for fractions 3-5 was adapted based on relatively large intrafraction motion that was observed during the second fraction. When taking into account the clinically delivered treatments, the GTV moved outside the PTV on the post scan for 3/100 fractions with cushion and 9/100 fractions without cushion. For 95% and 99% of the fractions with cushion and 93% and 98% of the fractions without cushion, GTV motion during the PV-post interval was < 2 and < 3 mm, respectively.

The highest correlation between GTV translations and bony anatomy translations was found in left-right direction for all three time intervals, with a repeated measures correlation coefficient $r = 0.77$ for pre-post interval (Supplementary material: Figure S2). The correlation was lowest in anterior-posterior direction: $r = 0.44$ in anterior-posterior direction for the pre-post interval, $r^2 = 0.20$ indicating that only 20% of variance in GTV motion could be explained by bony anatomy motion.

Discussion

To the best of our knowledge, this is the first study which has investigated intrafraction motion with and without vacuum cushion immobilization during SBRT to pelvic and para-aortic lymph nodes. When treating single pelvic/para-aortic lymph node metastases on an MR-linac using a workflow composed of daily online contour adaptation and planning, position verification just before radiation delivery and, if necessary, additional plan adaptation, vacuum cushion immobilization could be omitted, as no motion reduction was seen for the second half of the treatment session (PV-post interval, approximately 16 minutes) in which radiation delivery takes place.

During the first approximately 16 minutes we found that a vacuum cushion can significantly reduce intrafraction motion in anterior-posterior direction, both for bony anatomy and for the target lymph nodes. With a cushion we found reductions in mean anterior-posterior translations of 0.4 mm for GTV and bony anatomy for pre-PV interval. As this time interval on MR-linac is most comparable to treatment duration on CBCT-linac, it is likely that vacuum cushion immobilization will also reduce intrafraction motion on a CBCT-linac.

In a comparable study, Gerlich *et al.* [13] showed a reduction in mean absolute translation of 1.1 mm in anterior-posterior and cranial-caudal directions and 0.6 mm in left-right direction for patients with cushion in (simulated) spine SBRT. Thoracic spine SBRT was simulated for patients that underwent lung SBRT without cushion, the intrafraction motion was compared to that of patients undergoing spine SBRT with cushion. Our results for intrafraction motion of bony anatomy for patients with vacuum cushion in anterior-posterior and cranial-caudal directions were comparable to the results from Gerlich *et al.*, but our mean absolute

translations in all directions were about two times smaller for patients treated without cushion compared to the data from Gerlich *et al.* [13]. Li *et al.* have shown that patients with Eastern Cooperative Oncology Group performance status of 1-2 showed more intrafraction motion than patients with performance status 0 [16]. The performance status of patients in the study from Gerlich *et al.* was not reported; in our patient population 75% of patients had a performance status of 0 (Table 1). Furthermore, the effect of vacuum cushion immobilization may have been different for thoracic spine versus pelvis/lumbar spine.

To be able to further compare our results with published literature, we performed a literature search for articles that reported bony anatomy intrafraction motion for treatments with or without vacuum cushion. Treatments with a vacuum cushion as part of stereotactic body frames or combined with dual vacuum compression (Bodyfix, Elekta AB) were also taken into account. We included studies that reported on bony anatomy motion, as GTV intrafraction motion is very dependent on clinical target type and location. Eleven other studies were included (Supplementary material: Table S2). Seven studies reported on treatments with vacuum cushion [8-13,32] and five on treatments without [13,19-23]. Time interval duration for which intrafraction motion was assessed varied greatly, from 5 to 30 minutes. Our own results show that motion during a treatment fraction does not develop linearly, which makes it difficult to compare results from the different studies. Based on this literature search, use of a vacuum cushion seems to reduce systematic errors in left-right and anterior-posterior directions with approximately 0.3 and 0.5 mm respectively, but data are very heterogeneous and difficult to congregate, especially in the absence of other directly comparative studies.

GTV translations derived in our study are in line with previously published GTV intrafraction motion of prostate cancer [33,34]. In our study, translations were largest in anterior-posterior direction, maximum absolute anterior-posterior translation for pre-PV interval (most comparable to the time interval of CBCT-linac treatments) was 5.2 mm. This coincides with the 95 percentile spread of prostate GTV intrafraction motion of approximately 5 mm in both the study of De Muinck Keizer *et al.* (both with fiducial-based tracking and with soft tissue registration using elastix) and the study of Lovelock *et al.* which were both derived for a time interval of 10 minutes [33,34]. Absolute left-right translations in our study were larger than in De Muinck Keizer *et al.* (up to 3.4 mm compared to approximately 2 mm) but comparable to results in Lovelock *et al.* and our absolute cranial-caudal translations (up to 6 mm) were comparable to the results from both other studies. Furthermore, the systematic drift in posterior direction of 0.7 mm for pre-PV interval without cushion in our study was also found in the prostate studies (1.0 mm in De Muinck Keizer *et al.*).

For online adaptive MR-guided SBRT, the possibility of correcting for motion observed on the PV scan changes the interpretation of the immobilizing effect of a vacuum cushion.

PTV margin calculation was not part of this study given the limited applicability of traditional margin recipes such as in Van Herk *et al.* [35] for SBRT treatments with very few fractions [36,37]. Nonetheless, with MR-linac plan adaptation based on the PV scan, only motion occurring after the PV scan would need to be taken into account for PTV margin calculation. Plan adaptation based on the PV scan is also possible on MRIdian treatment systems (ViewRay Inc., Oakwood, USA) [38]. In our study, we did not find a reduction in intrafraction motion using a vacuum cushion for the time interval between PV and post scan. Most motion had occurred in the first half of the session, as in the study of Li *et al.* [16]. This motion could be corrected for with fast additional plan adaptation (adapt to position) [26]. However, this simple plan adaptation strategy is only feasible for patients with single (lymph node) targets. Multiple target lymph nodes can move independently [39], which calls for more elaborate plan adaptation strategies (re-start adapt to shape workflow: again contour GTVs and perform online planning) to correct for motion observed on the PV scan [26, 38]. Thus, SBRT on an MR-linac without vacuum cushion immobilization seems feasible for patients with single targets; for patients with multiple targets larger, anisotropic PTV margins could be considered for SBRT without vacuum cushion immobilization [40].

Another reason for vacuum cushion immobilization may be to minimize interfraction rotations for CBCT-linac SBRT without a 6 degrees of freedom table. In our experience, most lymph node GTVs are spherical in shape, so rotations are not expected to affect GTV coverage for patients with single GTVs. In case of multiple GTVs, inter- and intrafraction rotations could affect the GTV coverage depending on distance between the GTVs and the volume of the GTVs [41]. In the study of Winkel *et al.*, correcting for up to 3° of interfraction rotations only partially improved GTV coverage for CBCT-linac treatment of multiple GTVs; independent translations remained [39]. Finally, increasing patient comfort has been named as a reason for vacuum cushion immobilization. In our clinic, we did not use vacuum cushions for this reason and patient comfort has not been investigated in this study.

In this study we analyzed both GTV and bony anatomy intrafraction motion, as bony anatomy motion is expected to represent the part of the GTV intrafraction motion that can be influenced by cushion immobilization. We found the highest correlation between bony anatomy and GTV translations for the left-right direction, consistent with previously published results from lung SBRT [19]. In anterior-posterior direction, only 20% of the variance in GTV motion could be explained by bony anatomy motion, so a large part of the GTV motion was likely caused by internal organ motion such as bladder and rectum filling. This was also observed for the patient who underwent two sequential SBRT treatments, respectively with and without vacuum cushion. Absolute GTV translations in anterior-posterior direction were reduced with 0.6 mm with cushion, whereas a 0.4 mm increase was observed with cushion for bony anatomy. This emphasizes the influence of internal

organ motion and target location on lymph node intrafraction motion, irrespective of vacuum cushion immobilization.

This study was set-up with a longitudinal cohorts-design, which means other factors such as the patient population may have changed in the meantime. We indeed saw that in the group of patients treated without cushion, more patients had multiple lymph node targets and more patients were treated for para-aortic lymph node metastases. The pre-PV interval took on average 2 minutes longer for patients without cushion, likely because of the increased number of patients with multiple GTVs with longer manual contour adaptation time online. Furthermore, this study was set up without a sample size calculation, because of the small patient population (about 50 patients per year at our center). The small number of patients also prevents us from performing further subgroup analyses, comparing pelvic and para-aortic lymph node locations and their intrafraction motion patterns. Furthermore, it would be interesting to investigate intrafraction motion reduction with vacuum cushion immobilization in patients who are treated with abdominal compression devices for high para-aortic lymph node metastases or other abdominal targets (liver, adrenal gland, pancreas) [42].

In conclusion, a vacuum cushion can reduce GTV and bony anatomy intrafraction motion in posterior direction during pelvic and para-aortic lymph node SBRT. However, most of the GTV motion occurs in the first half of the session time (measured from the daily MRI scan, about 30 minutes total session time) which can be corrected for with an MR-linac. No significant reduction of intrafraction motion with a vacuum cushion was found during the second half of the session time, which is the time interval of radiotherapy delivery on an MR-linac. Therefore, vacuum cushion immobilization may not be needed for patients with single lymph node targets undergoing SBRT on an MR-linac using a workflow composed of daily online re-contouring and -planning, position verification just before radiation delivery and, if necessary, additional plan adaptation.

Funding

This work was supported by the Dutch Cancer Society under Grant 2015-0848.

Disclosure of interest

The overarching University Medical Center Utrecht MR-linac scientific project, including employment of multiple authors, has been partly funded by Elekta AB (Stockholm, Sweden). Elekta did not have any part in the design, execution or analysis of this study. The authors declared that there is no other conflict of interest.

References

- [1] Chang BK, Timmerman RD. Stereotactic body radiation therapy: a comprehensive review. *Am J Clin Oncol* 2007;30:637-44. <https://doi.org/10.1097/COC.0b013e3180ca7cb1>.
- [2] Nishimura S, Takeda A, Sanuki N, Ishikura S, Oku Y, Aoki Y, et al. Toxicities of organs at risk in the mediastinal and hilar regions following stereotactic body radiotherapy for centrally located lung tumors. *J Thorac Oncol* 2014;9:1370-6. <https://doi.org/10.1097/JTO.0000000000000260>.
- [3] Pollom EL, Chin AL, Diehn M, Loo BW, Chang DT. Normal Tissue Constraints for Abdominal and Thoracic Stereotactic Body Radiotherapy. *Semin Radiat Oncol* 2017;27:197-208. <https://doi.org/10.1016/j.semradonc.2017.02.001>.
- [4] Henry J, Moreno C, Crownover RL, Baacke D, Papanikolaou N, Gutierrez AN. Dosimetric quantification of dose fall-off in liver SBRT planning using dual photon energy IMRT. *J Radiosurg SBRT* 2016;4:145-51.
- [5] Brito Delgado A, Cohen D, Eng TY, Stanley DN, Shi Z, Charlton M, et al. Modeling the target dose fall-off in IMRT and VMAT planning techniques for cervical SBRT. *Med Dosim* 2018;43:1-10. <https://doi.org/10.1016/j.meddos.2017.07.009>.
- [6] Lax I, Blomgren H, Näslund I, Svanström R. Stereotactic radiotherapy of malignancies in the abdomen. Methodological aspects. *Acta Oncol* 1994;33:677-83. <https://doi.org/10.3109/02841869409121782>.
- [7] Purdie TG, Bissonnette JP, Franks K, Bezjak A, Payne D, Sie F, et al. Cone-beam computed tomography for on-line image guidance of lung stereotactic radiotherapy: localization, verification, and intrafraction tumor position. *Int J Radiat Oncol Biol Phys* 2007;68:243-52. <https://doi.org/10.1016/j.ijrobp.2006.12.022>.
- [8] Worm ES, Hansen AT, Petersen JB, Muren LP, Præstegaard LH, Høyer M. Inter- and intra-fractional localisation errors in cone-beam CT guided stereotactic radiation therapy of tumours in the liver and lung. *Acta Oncol* 2010;49:1177-83. <https://doi.org/10.3109/0284186X.2010.498435>.
- [9] Li W, Sahgal A, Foote M, Millar BA, Jaffray DA, Letourneau D. Impact of immobilization on intrafraction motion for spine stereotactic body radiotherapy using cone beam computed tomography. *Int J Radiat Oncol Biol Phys* 2012;84:520-6. <https://doi.org/10.1016/j.ijrobp.2011.12.039>.
- [10] Foster R, Meyer J, Iyengar P, Pistenmaa D, Timmerman R, Choy H, et al. Localization accuracy and immobilization effectiveness of a stereotactic body frame for a variety of treatment sites. *Int J Radiat Oncol Biol Phys* 2013;87:911-6. <https://doi.org/10.1016/j.ijrobp.2013.09.020>.
- [11] Finnigan R, Lamprecht B, Barry T, Jones K, Boyd J, Pullar A, et al. Inter- and intra-fraction motion in stereotactic body radiotherapy for spinal and paraspinal tumours using cone-beam CT and positional correction in six degrees of freedom. *J Med Imaging Radiat Oncol* 2016;60:112-8. <https://doi.org/10.1111/1754-9485.12353>.
- [12] Han Z, Bondeson JC, Lewis JH, Mannarino EG, Friesen SA, Wagar MM, et al. Evaluation of initial setup accuracy and intrafraction motion for spine stereotactic body radiation therapy using stereotactic body frames. *Pract Radiat Oncol* 2016;6:e17-24. <https://doi.org/10.1016/j.prro.2015.08.00>.
- [13] Gerlich AS, van der Velden JM, Fanetti G, Zoetelief A, Eppinga WSC, Seravalli E. EP-1620: The immobilizing effect of the vacuum cushion in spinal SBRT and the impact of pain [conference abstract]. *Radiother Oncol* 2017;123:S876-7. [https://doi.org/10.1016/S0167-8140\(17\)32055-8](https://doi.org/10.1016/S0167-8140(17)32055-8).

- [14] Lui RJ, Yang SX, Nevlon J, Hall MD, Dandapani S, Vora N, et al. Residual Setup Errors in Cranial Stereotactic Radiosurgery Without Six Degree of Freedom Robotic Couch: Frameless Versus Rigid Immobilization Systems. *J Appl Clin Med Phys* 2020;21:87-93. <https://doi.org/10.1002/acm2.12828>.
- [15] Serago CF, Buskirk SJ, Igel TC, Gale AA, Serago NE, Earle JD. Comparison of daily megavoltage electronic portal imaging or kilovoltage imaging with marker seeds to ultrasound imaging or skin marks for prostate localization and treatment positioning in patients with prostate cancer. *Int J Radiat Oncol Biol Phys* 2006;65:1585-92. <https://doi.org/10.1016/j.ijrobp.2006.04.019>.
- [16] Li W, Purdie TG, Taremi M, Fung S, Brade A, Cho BC, et al. Effect of Immobilization and Performance Status on Intrafraction Motion for Stereotactic Lung Radiotherapy: Analysis of 133 Patients. *Int J Radiat Oncol Biol Phys* 2011;81:1568-75. <https://doi.org/10.1016/j.ijrobp.2010.09.035>.
- [17] Siva S, Devereux T, Kron T, Gill S, Macmanus M, Bressel M, et al. Vacuum immobilization reduces tumour excursion and minimises intrafraction error in a cohort study of stereotactic ablative body radiotherapy for pulmonary metastases. *J Med Imaging Radiat Oncol* 2014;58:244-52. <https://doi.org/10.1111/1754-9485.12112>.
- [18] Rosewall T, Chung P, Bayley A, Lockwood G, Alasti H, Bristow R, et al. A randomized comparison of interfraction and intrafraction prostate motion with and without abdominal compression. *Radiother Oncol* 2008;88:88-94. <https://doi.org/10.1016/j.radonc.2008.01.019>.
- [19] Sonke JJ, Rossi M, Wolthaus J, van Herk M, Damen E, Belderbos J. Frameless stereotactic body radiotherapy for lung cancer using four-dimensional cone beam CT guidance. *Int J Radiat Oncol Biol Phys* 2009;74:567-74. <https://doi.org/10.1016/j.ijrobp.2008.08.004>.
- [20] Dahele M, Verbakel W, Cuijpers J, Slotman B, Senan S. An analysis of patient positioning during stereotactic lung radiotherapy performed without rigid external immobilization. *Radiother Oncol* 2012;104:28-32. <https://doi.org/10.1016/j.radonc.2012.03.020>.
- [21] Dahele M, Slotman B, Verbakel W. Stereotactic body radiotherapy for spine and bony pelvis using flattening filter free volumetric modulated arc therapy, 6D cone-beam CT and simple positioning techniques: Treatment time and patient stability. *Acta Oncol* 2016;55:795-8. <https://doi.org/10.3109/0284186X.2015.1119885>.
- [22] Knybel L, Cvek J, Cermakova Z, Havelka J, Pomaki M, Resova K. Evaluation of spine structure stability at different locations during SBRT. *Biomed Pap Med Fac Univ Palacky Olomouc Czech Repub* 2019 [Epub ahead of print]. <https://doi.org/10.5507/bp.2019.027>.
- [23] Kontaxis C, Bol GH, Stemkens B, Glitzner M, Prins FM, Kerkmeijer LGW, et al. Towards fast online intrafraction replanning for free-breathing stereotactic body radiation therapy with the MR-linac. *Phys Med Biol* 2017;62:7233-48. <https://doi.org/10.1088/1361-6560/aa82ae>.
- [24] Kontaxis C, Bol GH, Lagendijk JJW, Raaymakers BW. DeepDose: towards a fast dose calculation engine for radiation therapy using deep learning. *Phys Med Biol* 2020 [Epub ahead of print]. <https://doi.org/10.1088/1361-6560/ab7630>.
- [25] Werensteijn-Honingh AM, Kroon PS, Winkel D, Aalbers EM, van Asselen B, Bol GH, et al. Feasibility of stereotactic radiotherapy using a 1.5 T MR-linac: Multi-fraction treatment of pelvic lymph node oligometastases. *Radiother Oncol* 2019;134:50-4. <https://doi.org/10.1016/j.radonc.2019.01.024>.

- [26] Winkel D, Bol GH, Kroon PS, van Asselen B, Hackett SS, Werensteijn-Honingh AM, et al. Adaptive radiotherapy: The Elekta Unity MR-linac concept. *Clin Transl Radiat Oncol* 2019;18:54-9. <https://doi.org/10.1016/j.ctro.2019.04.001>.
- [27] Klein S, Staring M, Murphy K, Viergever MA, Pluim JP. elastix: a toolbox for intensity-based medical image registration. *IEEE Trans Med Imaging* 2010;29:196-205. <https://doi.org/10.1109/TMI.2009.2035616>.
- [28] Shamonin DP, Bron EE, Lelieveldt BP, Smits M, Klein S, Staring M, et al. Fast parallel image registration on CPU and GPU for diagnostic classification of Alzheimer's disease. *Front Neuroinform* 2014;7:50. <https://doi.org/10.3389/fninf.2013.00050>.
- [29] Ritter F, Boskamp T, Homeyer A, Laue H, Schwier M, Link F, et al. Medical image analysis. *IEEE Pulse* 2011;2:60-70. <https://doi.org/10.1109/MPUL.2011.942929>.
- [30] Stroom JC, Heijmen BJ. Geometrical uncertainties, radiotherapy planning margins, and the ICRU-62 report. *Radiother Oncol* 2002;64:75-83. [https://doi.org/10.1016/s0167-8140\(02\)00140-8](https://doi.org/10.1016/s0167-8140(02)00140-8).
- [31] Bland JM, Altman DG. Calculating correlation coefficients with repeated observations: Part 1--Correlation within subjects. *BMJ* 1995;310:446. <https://doi.org/10.1136/bmj.310.6977.446>.
- [32] Guckenberger M, Meyer J, Wilbert J, Richter A, Baier K, Mueller G, et al. Intra-fractional uncertainties in cone-beam CT based image-guided radiotherapy (IGRT) of pulmonary tumors. *Radiother Oncol* 2007;83:57-64. <https://doi.org/10.1016/j.radonc.2007.01.012>.
- [33] De Muinck Keizer DM, Kerkmeijer LGW, Maspero M, Andreychenko A, Van der Voort van Zyp JRN, Van den Berg CAT, Raaymakers BW, Lagendijk JJW, De Boer JC. Soft-tissue Prostate Intrafraction Motion Tracking in 3D cine-MR for MR-guided Radiotherapy. *Phys Med Biol* 2019;64:235008. <https://doi.org/10.1088/1361-6560/ab5539>.
- [34] Lovelock DM, Messineo AP, Cox BW, Kollmeier MA, Zelefsky MJ. Continuous Monitoring and Intrafraction Target Position Correction During Treatment Improves Target Coverage for Patients Undergoing SBRT Prostate Therapy. *Int J Radiat Oncol Biol Phys* 2015;91:588-94. <https://doi.org/10.1016/j.ijrobp.2014.10.049>.
- [35] van Herk M, Remeijer P, Rasch C, Lebesque JV. The probability of correct target dosage: dose-population histograms for deriving treatment margins in radiotherapy. *Int J Radiat Oncol Biol Phys* 2000;47:1121-35. [https://doi.org/10.1016/s0360-3016\(00\)00518-6](https://doi.org/10.1016/s0360-3016(00)00518-6).
- [36] Gordon JJ, Siebers JV. Convolution method and CTV-to-PTV margins for finite fractions and small systematic errors. *Phys Med Biol* 2007;52:1967-90. <https://doi.org/10.1088/0031-9155/52/7/013>.
- [37] Herschtal A, Foroudi F, Silva L, Gill S, Kron T. Calculating geometrical margins for hypofractionated radiotherapy. *Phys Med Biol* 2013;58:319-33. <https://doi.org/10.1088/0031-9155/58/2/319>.
- [38] Tetar SU, Bruynzeel AME, Lagerwaard FJ, Slotman BJ, Bohoudi O, Palacios MA. Clinical implementation of magnetic resonance imaging guided adaptive radiotherapy for localized prostate cancer. *Phys Imaging Radiat Oncol* 2019;9:69-76. <https://doi.org/10.1016/j.phro.2019.02.002>.

- [39] Winkel D, Bol GH, Werensteijn-Honingh AM, Intven MPW, Eppinga WSC, Hes J, et al. Target coverage and dose criteria based evaluation of the first clinical 1.5T MR-linac SBRT treatments of lymph node oligometastases compared with conventional CBCT-linac treatment. *Radiother Oncol* 2020;146:118-25. <https://doi.org/10.1016/j.radonc.2020.02.011>.
- [40] Winkel D, Werensteijn-Honingh AM, Kroon PS, Eppinga WSC, Bol GH, Intven MPW, et al. Individual Lymph Nodes: "See It and Zap It". *Clin Transl Radiat Oncol* 2019;18:46-53. <https://doi.org/10.1016/j.ctro.2019.03.004>.
- [41] Roper J, Chanyavanich V, Betzel G, Switchenko J, Dhakaan A. Single-Isocenter Multiple-Target Stereotactic Radiosurgery: Risk of Compromised Coverage. *Int J Radiat Oncol Biol Phys* 2015;93:540-6. <https://doi.org/10.1016/j.ijrobp.2015.07.2262>.
- [42] Heerkens HD, Reerink O, Intven MPW, Hiensch RR, van den Berg CAT, Crijs SPM, et al. Pancreatic tumor motion reduction by use of a custom abdominal corset. *Phys Imaging Radiat Oncol* 2017;2:7-10. <https://doi.org/10.1016/j.phro.2017.02.003.9>.

Supplementary material

Table S1.

Mean, systematic and random errors of bony intrafraction rotations.

Bony intrafraction motion		Rotations (°)								
		Pre-PV scan (16 min.)			Pre-post scan (32 min.)			PV-post scan (16 min.)		
		LR-axis	AP-axis	CC-axis	LR-axis	AP-axis	CC-axis	LR-axis	AP-axis	CC-axis
Vacuum cushion	Mean	0.2	0.0	-0.1	0.2	0.1	-0.1	0.1	0.0	0.0
	Systematic	0.3	0.2	0.1	0.3	0.3	0.2	0.1	0.1	0.1
	Random	0.3	0.2	0.2	0.4	0.2	0.2	0.2	0.2	0.2
No cushion	Mean	0.0	0.1	0.0	-0.1	0.1	-0.1	-0.1	0.1	0.0
	Systematic	0.5	0.3	0.2	0.6	0.4	0.2	0.2	0.2	0.1
	Random	0.3	0.2	0.2	0.5	0.3	0.3	0.3	0.3	0.1

Intrafraction motion analysis of patients treated with MR-linac SBRT for pelvic or para-aortic lymph node metastases. Bony anatomy rotations are shown around the left-right (LR), anterior-posterior (AP) and cranial-caudal (CC) axes, for patients treated with (N=20) and without vacuum cushion (N=20), for the three time intervals (mean time per interval reported).

Table S2. Literature overview of bony anatomy intrafraction motion with or without a vacuum cushion.

Study	Location motion analysis	Immobilization	N patients	N fractions	Mean time (min.)	Left-Right translation (mm)				
						Mean	SD	Abs. max	Σ	σ
Dahele 2012	Thoracic spine	None	30	109	10	0.0	0.6	2.0	<i>n.r.</i>	<i>n.r.</i>
Dahele 2016	Thoracic + lumbar spine + pelvic bone	None	18	83	6	-0.1	0.9	<i>n.r.</i>	<i>n.r.</i>	<i>n.r.</i>
Foster 2013	Spine (location undefined)	SBF without abdominal compression	45	91	15-20	0.1	1.0	<i>n.r.</i>	<i>n.r.</i>	<i>n.r.</i>
Han 2016	Thoracic + lumbar spine + sacrum	SBF without abdominal compression	32	118	5	0.1	0.4	<i>n.r.</i>	<i>n.r.</i>	<i>n.r.</i>
Knybel 2019	Thoracic spine	None	58	<i>n.r.</i>	30	0.2	0.7	<i>n.r.</i>	<i>n.r.</i>	<i>n.r.</i>
	Lumbar spine + sacrum		29	<i>n.r.</i>		-0.3	0.7	2.8	<i>n.r.</i>	<i>n.r.</i>
Li 2012	Thoracic + lumbar spine	Vacuum cushion	24	45	13	0.0	1.1	2.2	<i>n.r.</i>	<i>n.r.</i>
		Bodyfix	60	160	15	-0.2	0.8	3.4	<i>n.r.</i>	<i>n.r.</i>
		Vacuum cushion	24	77	24	-0.1	1.3	4.5	<i>n.r.</i>	<i>n.r.</i>
		Bodyfix	60	150	30	-0.2	0.9	2.6	<i>n.r.</i>	<i>n.r.</i>
Sonke 2009	Thoracic spine	None	65	195	28	0.0	<i>n.r.</i>	<i>n.r.</i>	1.0	1.3
Worm 2010	Thoracic spine	SBF, most with abdominal compression	19	57	24	0.3	<i>n.r.</i>	<i>n.r.</i>	0.7	0.9
	Lumbar spine		15	45		0.2	<i>n.r.</i>	<i>n.r.</i>	0.9	0.7
This study	Pelvic bone + lumbar spine	Vacuum cushion	20	100	15	0.0	0.6	2.2	0.4	0.4
		None	20	100	17	-0.2	0.9	3.9	0.7	0.6
		Vacuum cushion	20	100	31	-0.1	0.8	3.9	0.6	0.5
		None	20	100	33	-0.2	1.2	4.6	1.0	0.8

Overview of bony anatomy intrafraction motion during SBRT treatments in studies reporting on immobilization using a vacuum cushion, the Elekta Bodyfix system (vacuum cushion + dual vacuum compression), a stereotactic body frame (SBF, includes a vacuum cushion) or SBRT without immobilization. Mean and standard deviation (SD) of translations in 3 directions are reported in mm, as well as maximum absolute translation (abs. max), systematic (Σ) and random (σ) errors. *N.r.* = not reported.

Table S2 (continued)

Anterior-Posterior translation (mm)					Cranial-Caudal translation (mm)					Comments
Mean	SD	Abs. max	Σ	σ	Mean	SD	Abs. max	Σ	σ	
0.0	0.4	1.2	<i>n.r.</i>	<i>n.r.</i>	0.0	0.6	2.8	<i>n.r.</i>	<i>n.r.</i>	Lung SBRT
-0.2	0.7	3.4	<i>n.r.</i>	<i>n.r.</i>	0.1	0.6	<i>n.r.</i>	<i>n.r.</i>	<i>n.r.</i>	
-0.1	1.0	<i>n.r.</i>	<i>n.r.</i>	<i>n.r.</i>	0.4	1.2	<i>n.r.</i>	<i>n.r.</i>	<i>n.r.</i>	
-0.1	0.5	<i>n.r.</i>	<i>n.r.</i>	<i>n.r.</i>	-0.1	0.5	<i>n.r.</i>	<i>n.r.</i>	<i>n.r.</i>	
0.2	0.5	5.6	<i>n.r.</i>	<i>n.r.</i>	-0.2	0.5	<i>n.r.</i>	<i>n.r.</i>	<i>n.r.</i>	
0.1	0.7	<i>n.r.</i>	<i>n.r.</i>	<i>n.r.</i>	-0.7	0.6	3.4	<i>n.r.</i>	<i>n.r.</i>	
0.0	0.7	2.4	<i>n.r.</i>	<i>n.r.</i>	-0.2	1.0	2.3	<i>n.r.</i>	<i>n.r.</i>	
0.0	0.8	2.7	<i>n.r.</i>	<i>n.r.</i>	0.4	0.7	2.1	<i>n.r.</i>	<i>n.r.</i>	
-0.1	1.0	3.6	<i>n.r.</i>	<i>n.r.</i>	0.0	1.2	2.5	<i>n.r.</i>	<i>n.r.</i>	
0.0	0.9	2.9	<i>n.r.</i>	<i>n.r.</i>	0.4	0.7	2.3	<i>n.r.</i>	<i>n.r.</i>	
-0.3	<i>n.r.</i>	<i>n.r.</i>	1.1	1.1	0.4	<i>n.r.</i>	<i>n.r.</i>	0.8	1.0	Lung SBRT
0.4	<i>n.r.</i>	<i>n.r.</i>	0.6	0.8	0.4	<i>n.r.</i>	<i>n.r.</i>	0.7	1.0	Lung SBRT
0.2	<i>n.r.</i>	<i>n.r.</i>	0.7	0.7	0.2	<i>n.r.</i>	<i>n.r.</i>	0.5	0.7	Liver SBRT
0.2	0.5	2.2	0.3	0.4	-0.3	0.9	5.7	0.7	0.5	Lymph node SBRT
0.6	0.9	5.3	0.7	0.5	-0.4	0.6	2.3	0.5	0.4	
0.3	0.5	2.1	0.3	0.4	-0.6	0.9	2.9	0.8	0.5	
0.9	1.0	5.7	0.9	0.5	-0.5	1.0	4.1	0.7	0.7	

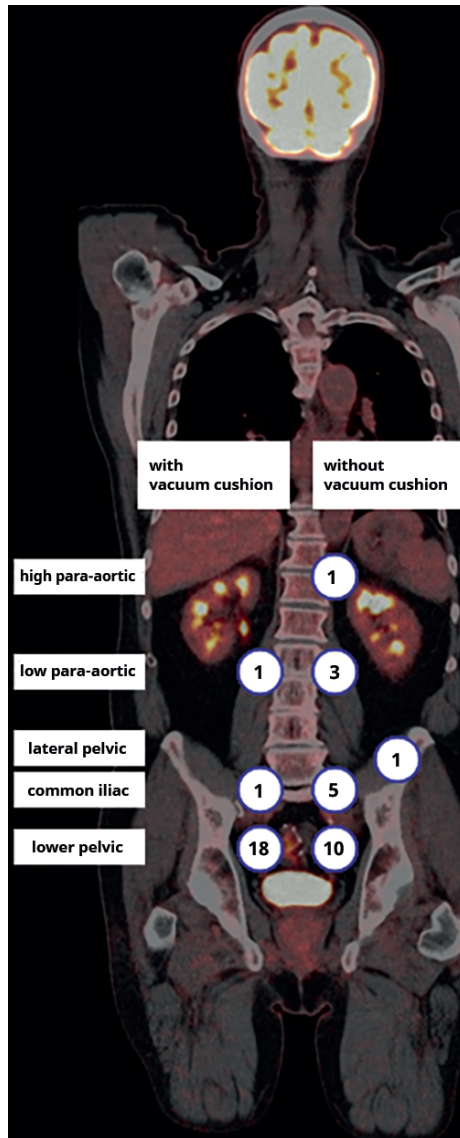


Figure S1. Anatomical locations of GTVs for patients treated with (N=20) and without vacuum cushion (N=20). The number of patients is plotted for each anatomical location. For patients with multiple GTVs, the situation was assigned to the location with the most GTVs. Anatomical levels were defined as high para-aortic (cranial of the level of insertion of renal veins into inferior vena cava), low para-aortic (caudal of the renal veins, cranial of aortic bifurcation), common iliac (caudal of aortic bifurcation, cranial of iliac artery bifurcation) and lower pelvic (caudal of iliac artery bifurcation). For one patient, the GTV was located lateral of the psoas major muscle, this situation is shown as 'lateral pelvic'.

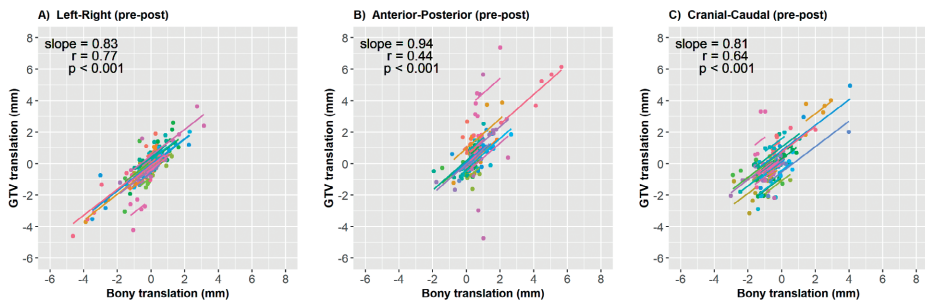
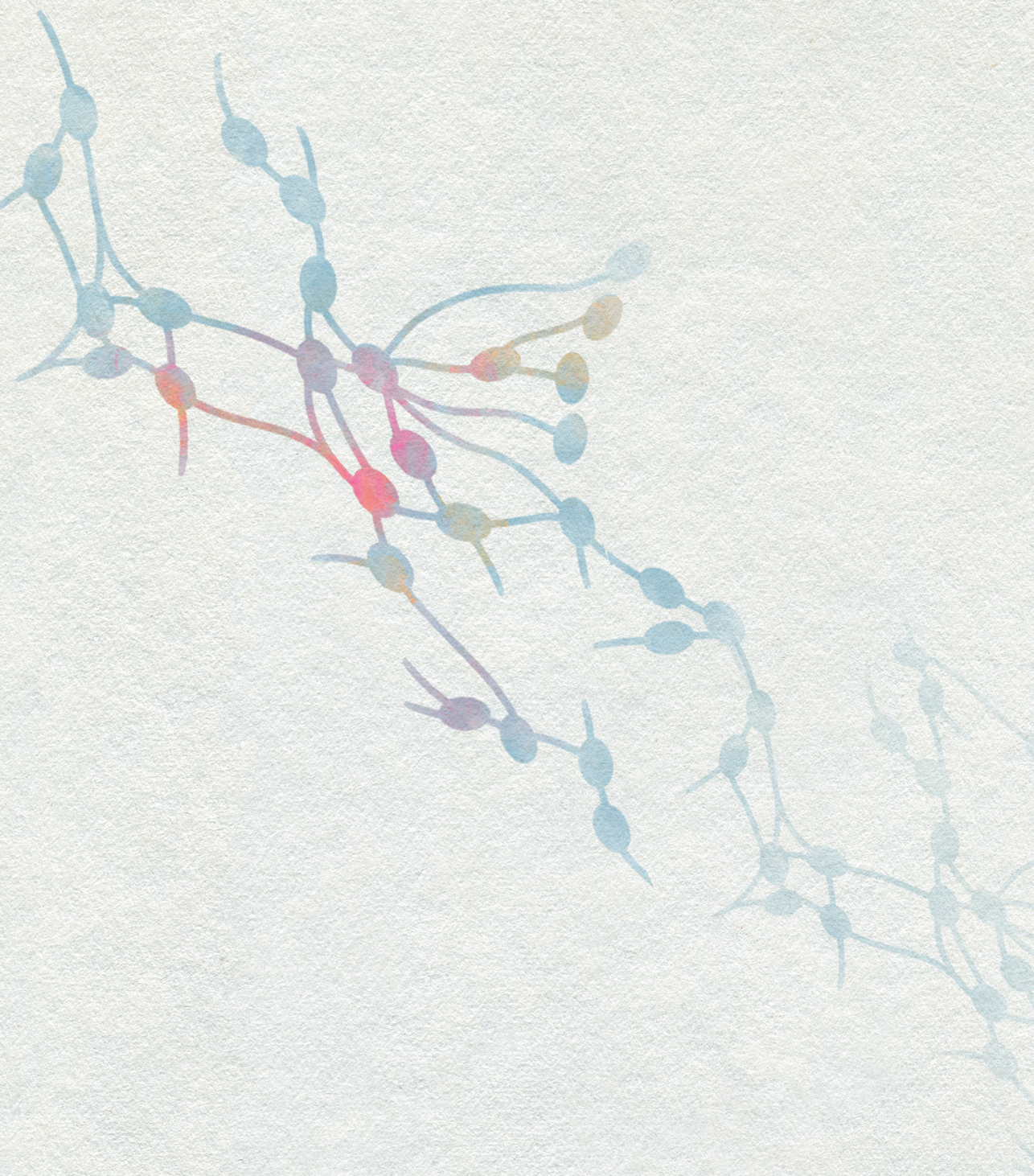


Figure S2. Repeated measures correlation between bony anatomy and GTV intrafraction motion. Intrafraction motion analysis of patients treated with MR-linac SBRT for pelvic or para-aortic lymph node metastases was performed for bony anatomy and GTV. The correlation between translations of bony anatomy and GTV was investigated. Each of the five SBRT fractions per patient was taken into account using repeated measures correlation [31]. Dots represent the individual fractions, colors represent the patients (N=40) and parallel lines have been fitted for each patient. Correlations are shown for pre-post interval (mean t=32 min), in left-right (LR, + towards left), anterior-posterior (AP, + towards posterior) and cranial-caudal (CC, + towards cranial) directions. No distinction was made regarding cushion use. Regression slope, repeated measures correlation coefficient r and corresponding p -value are shown.



Chapter 5

Target coverage and dose criteria based evaluation of the first clinical 1.5T MR-linac SBRT treatments of lymph node oligometastases compared with conventional CBCT-linac treatment

Dennis Winkel, Gijsbert H. Bol, Anita M. Werensteijn-Honingh, Martijn P.W. Intven, Wietse S.C. Eppinga, Jochem Hes, Louk M.W. Snoeren, Gonda G. Sikkes, Christa G.M. Gadellaa-van Hooijdonk, Bas W. Raaymakers, Ina M. Jürgenliemk-Schulz, Petra S. Kroon.

Radiother Oncol 2020;146:118-25.
<https://doi.org/10.1016/j.radonc.2020.02.011>.

Abstract

Background and purpose: Patients were treated at our institute for single and multiple lymph node oligometastases on the 1.5T MR-linac since August 2018. The superior soft-tissue contrast and additional software features of the MR-linac compared to CBCT-linacs allow for online adaptive treatment planning. The purpose of this study was to perform a target coverage and dose criteria based evaluation of the clinically delivered online adaptive radiotherapy treatment compared with conventional CBCT-linac treatment.

Materials and methods: Patient data was used from 14 patients with single lymph node oligometastases and 6 patients with multiple (2–3) metastases. All patients were treated on the 1.5T MR-linac with a prescribed dose of 5 x 7 Gy to 95% of the PTV and a CBCT-linac plan was created for each patient. The difference in target coverage between these plans was compared and plans were evaluated based on dose criteria for each fraction after calculating the CBCT-plan on the daily anatomy. The GTV coverage was evaluated based on the online planning and the post-delivery MRI.

Results: For both single and multiple lymph node oligometastases the GTV V_{35Gy} had a median value of 100% for both the MR-linac plans and CBCT-plans pre- and post-delivery and did not significantly differ. The percentage of plans that met all dose constraints was improved from 19% to 84% and 20% to 67% for single and multiple lymph node cases, respectively.

Conclusion: Target coverage and dose criteria based evaluation of the first clinical 1.5T MR-linac SBRT treatments of lymph node oligometastases compared with conventional CBCT-linac treatment shows a smaller amount of unplanned violations of high dose criteria. The GTV coverage was comparable. Benefit is primarily gained in patients treated for multiple lymph node oligometastases: geometrical deformations are accounted for, dose can be delivered in one plan and margins can be reduced.

Introduction

In recent years stereotactic body radiation therapy (SBRT) has become the standard treatment option for the treatment of patients with lymph node oligometastases in many centers [1,2]. SBRT allows for the delivery of a relatively high amount of dose in few fractions with a very steep dose gradient [3] and is often given to postpone the start of systematic therapy and improve progression-free or overall survival without compromising the quality of life [4,5]. In the majority of the patients treated for lymph node oligometastases the affected nodes originate from prostate cancer and have a low α/β ratio [6]. This means that, through SBRT, a high biologically effective dose (>100 Gy) can be given which is associated with high local control [7].

For accurate dose delivery, image-guided radiotherapy (IGRT) has become increasingly important for target visualization [8]. This reduces the effect of possible setup errors, caused by anatomical changes in the location of the target and organs at risk (OAR). Most modern radiotherapy systems are nowadays equipped with cone-beam computed tomography (CBCT) to visualize the tumor [9]. This has led to increased precision of radiotherapy treatment for tumors which are well visible on CBCT. However, compared to magnetic resonance imaging (MRI), CBCT yields relatively poor soft tissue contrast [10]. This makes it difficult to accurately identify soft tissue targets, based on CBCT imaging alone. For this reason, position verification may be performed on nearby bony anatomy or other surrogate structures. This is generally less accurate and could provide erroneous results for both localization and verification [11]. As an alternative, artificial markers may be implanted in the patient. While this may provide good target visualization, the procedure is invasive for the patient [12,13].

During SBRT of lymph node oligometastases on CBCT-linacs, inter-fraction motion is accounted for by couch translations and sometimes also for rotations. These translations and rotations can compensate for rigid target motion, but not for non-rigid changes of the target such as changes in size or shape or, for multiple lymph nodes, independent motion of the targets [14,15]. Additionally, it is not possible to account for anatomical changes in the location of the target and OARs, as well as path length changes and tissue attenuation. This can cause differences between the planned dose and delivered dose after position correction [16]. Therefore using position verification and correction procedures, but not optimally taking the new patient anatomy into account, may still result in unplanned violations of dose constraints [17,18]. Additionally, it may result in underdosage of the PTV prior to delivery, which in turn can cause underdosage of the GTV due to intra-fraction motion.

Inter-fraction variations of soft tissue targets can be more optimally dealt with using MR-guided radiotherapy systems such as the 1.5T MR-linac (combined 1.5T MR scanner and linear accelerator, Unity, Elekta AB, Stockholm, Sweden) [19,20]. This system provides diagnostic quality imaging of the patient anatomy before and during treatment, which allows for MR-guided online adaptive workflows [21]. In August 2018, SBRT of lymph node oligometastases on the 1.5T MR-linac has commenced within our institute using online MRI-based delineation of the target and OARs, full- online replanning and MRI based position verification [22].

A R-IDEAL [23] stage 0 study simulating the dosimetric impact of online replanning for SBRT of lymph node oligometastases on the 1.5T MR-linac compared to online position correction showed beneficial dosimetric outcomes and a reduction of unplanned violations of dose constraints [18]. The purpose of this study was to perform a target coverage and dose criteria based evaluation of the clinically delivered online adaptive radiotherapy treatment compared with simulated conventional CBCT-linac treatment.

Material and methods

Patient characteristics

Patients were treated at our institute for single and multiple lymph node oligometastases on the 1.5T MR-linac (Unity, Elekta AB, Stockholm, Sweden) since August 2018. For this study, patient data was used from 14 patients with single lymph node oligometastases and 6 patients with multiple (2–3) metastases located in the pelvic and para-aortic region (Table 1).

Clinical treatment

Pre-treatment CT and MR imaging were acquired for each patient and registered. To provide reproducibility of the patient position along the length of the couch between the pre-treatment CT scan and each MRI based treatment session, the pre-treatment CT was acquired using a special table overlay to enable patient set-up using specific couch index points [22]. To reduce potential intra-fraction motion, patients with lymph node metastases in the pelvic and low para-aortic region were initially immobilized using a vacuum mattress (BlueBAG, Elekta AB, Stockholm, Sweden) with both hands on the chest and the elbows along the body [20]. The patients with affected nodes in the high para-aortic region (above the renal veins) were treated whilst wearing an abdominal corset with the arms along the body [24].

Table 1
Patient data characteristics

Single lymph node oligometastases patients (N = 14)		
	CBCT-linac	MR-linac
GTV [cc]		0.53 [range, 0.15 – 6.83]
Δ GTV Pretreatment - Rx [cc]		0.01 [range, -2.25 – 0.82]
PTV margin [mm]	3 (N = 10), 8 (N = 4)	3 (N = 14)
Multiple lymph node oligometastases patients (N = 6)		
	CBCT-linac	MR-linac
GTV per patient [-]		2 (N = 3), 3 (N = 3)
GTV [cc]		0.36 [range, 0.08 – 1.49]
Δ GTV Pretreatment - Rx [cc]		0.01 [range, -1.04 – 0.29]
PTV per patient [-]	1 (N = 1), 2 (N = 4), 3 (N = 1)	2 (N = 3), 3 (N = 3)
PTV margin [mm]	3 (N = 8), 5 (N = 2), 8 (N = 3)	3 (N = 6)
PTV margin [mm]	1 (N = 4), 2 (N = 2)	1 (N = 6)

All patients were treated on the 1.5T MR-linac with a prescribed dose of 5 x 7 Gy to 95% of the PTV. For each patient, a six-, seven- or ten-beam MR-linac IMRT pre-treatment plan was created with a GTV-PTV margin of 3 mm using Monaco TPS (Elekta AB, Stockholm, Sweden), taking into account the presence of the 1.5T magnetic field. One patient was treated with adapted margins for fractions 2–5 (2 mm in inferior, left and anterior direction and 6 mm in superior, right and posterior direction). For patients treated with the arms along the body, beam angles were selected such that the beams would not traverse the arms. Additionally a CBCT-linac VMAT back-up plan was created for each patient. A radiation oncologist determined whether the lymph node oligometastases were well visible or not on CBCT. A PTV margin of 8 mm was used for poorly visible lymph nodes and 3 mm for visible lymph nodes [18]. For patients with multiple lymph node oligometastases, the plans consisted of one, two or three PTV's. For the CBCT-linac plans, a medical physicist and radiation oncologist decided on one or two separate plans, placement of the isocenter, depending on the specific anatomical situation of the patient and PTV margins (Table 1). OAR dose was lowered as much as possible, while maintaining a sufficient PTV coverage of $V_{35\text{Gy}} > 95\%$ and a D_{max} between 120–135%. Clinical dose criteria for the OARs were based on the UK SABR consortium guidelines (2016) (Table 2).

During each online treatment session the adapt to shape (ATS) workflow was followed to allow for adaptive treatment planning [21]. A daily MRI was acquired onto which the pre-treatment contours were automatically deformed. If necessary, the contours of the target lymph node(s) and OARs within 2 cm of the PTV(s) were manually adapted by a

radiation oncologist [22]. Based on the daily MRI and adapted contours, a new plan was created [25]. Radiation delivery according to the new plan was performed after MRI based position verification. After each treatment session offline assessment of the intra-fraction motion was performed by recalculating the GTV coverage on the actual anatomy as seen on the post-delivery MRI. Contouring of the GTV on the post-delivery MRI was performed by multiple observers. Inter-observer contouring variation on MRI is considered negligible for these small and well visible lesions.

Table 2
Clinical dose criteria

Structure	Offline constraints (pre-treatment plan)	Online constraints
PTV	$V_{35\text{Gy}} > 95\%$ $D_{0.1\text{ cm}^3} < 47.25\text{ Gy}$	$V_{35\text{Gy}} > 95\%$ $D_{0.1\text{ cm}^3} < 47.25\text{ Gy}$
Aorta	$V_{53\text{Gy}} < 0.5\text{ cm}^3$	$V_{53\text{Gy}} < 0.5\text{ cm}^3$
Bladder	$V_{38\text{Gy}} < 0.5\text{ cm}^3$ $V_{18.3\text{Gy}} < 15\text{ cm}^3$	$V_{38\text{Gy}} < 0.5\text{ cm}^3$
Bowel bag + colon	$V_{32\text{Gy}} < 0.5\text{ cm}^3$ $V_{25\text{Gy}} < 10\text{ cm}^3$	$V_{32\text{Gy}} < 0.5\text{ cm}^3$
Duodenum + stomach	$V_{35\text{Gy}} < 0.5\text{ cm}^3$ $V_{25\text{Gy}} < 10\text{ cm}^3$	$V_{35\text{Gy}} < 0.5\text{ cm}^3$
Esophagus	$V_{34\text{Gy}} < 0.5\text{ cm}^3$ $V_{27.5\text{Gy}} < 5\text{ cm}^3$	$V_{34\text{Gy}} < 0.5\text{ cm}^3$
Kidney	$V_{16.8\text{Gy}} < 67\%$	$V_{16.8\text{Gy}} < 67\%$
Nerve root + sacral plexus	$V_{32\text{Gy}} < 0.1\text{ cm}^3$	$V_{32\text{Gy}} < 0.1\text{ cm}^3$
Rectum + sigmoid	$D_{\text{max}} < 40\text{ Gy}$ $V_{32\text{Gy}} < 0.5\text{ cm}^3$	$V_{32\text{Gy}} < 0.5\text{ cm}^3$
Spinal cord	$D_{\text{max}} < 28\text{ Gy}$	$D_{\text{max}} < 28\text{ Gy}$
Ureter	$D_{\text{max}} < 40\text{ Gy}$	$D_{\text{max}} < 40\text{ Gy}$

Retrospective analyses

Dosimetric comparison of MR-linac and CBCT-linac treatment

The differences in target coverage between the clinically delivered MR-linac and the CBCT-linac plans were compared for each treatment session. Additionally, the plans were evaluated based on the clinical dose criteria for the target coverage and OAR dose. The CBCT-linac plan was recalculated on the daily MRI and using the contours from the online treatment. The electron density information was retained by matching and deforming the initial planning CT to the daily MRI data. During treatment on a CBCT-linac online

translation correction is performed by matching using a 0.5 cm mask around the GTV or a clipbox with nearby structures for lymph nodes with good or poor visibility, respectively. To simulate a best-case outcome of the online translation correction protocol, as performed in our current clinical practice for CBCT-linac treatment of these targets, we assumed that the correction reference point for single lymph nodes was equal to the isocenter and placed at the center of the daily contoured GTV. Modern CBCT- linac treatment systems could also have the possibility to compensate for rotational errors using six degrees of freedom (6DOF) couches. For this purpose, the lesions were automatically matched to each other making use of a clipbox around the lesions. For lesions adjacent to bony anatomy, this information was minimally included. The result of the match was manually inspected and verified. If the lesions were well visible, the plans were also recalculated after performing 6DOF rotational correction. For multiple PTV's, the isocenter was placed manually at the same location as was done in the pre-treatment planning of the CBCT-linac plans. This choice was made by the physician and was either in the middle of one of the targets or in-between the targets. If CBCT-linac treatment would be performed with two plans, the doses were summed. Additionally, the distances between the center of gravities between the targets was calculated to investigate the relative intra-fraction motion for each fraction compared to the pre- treatment data. The plans were evaluated using the clinical dose constraints and compared based on PTV and GTV coverage.

Intra-fraction GTV coverage analysis

To determine whether dose coverage was sufficient during treatment and if PTV margins were adequate, the GTV coverage for the clinically delivered (ATS) plans and the CBCT-linac plan were evaluated over all five fractions. This was done by evaluating the dose on both the online planning MRI, acquired at the start of the treatment fraction, as well as the post-delivery MRI, acquired after dose delivery.

Results

For single lymph node oligometastases the clinically delivered MR-linac plans had a median GTV $V_{35\text{Gy}}$ value of 100% [99.7– 100%] compared to 100% [98.7–100%] for the CBCT-linac plans recalculated on the daily anatomy after translation correction. The PTV $V_{35\text{Gy}}$ was significantly higher (p-value <0.01) with a median of 100% [90.7–100%] compared to 94.9% [47.7–100%] for the CBCT-linac plans (Figure 1). All dose criteria (PTV coverage and OAR constraints) were met for the MR-linac plans in 59/70 (84%) fractions. Violations of OAR criteria occurred with a maximum of 3 Gy above the set threshold. For the CBCT-plans recalculated on the daily anatomy all dose criteria were met in 13/70 (19%) fractions. Violations of OAR criteria occurred with a maximum of 2.5 Gy or 0.1 cc above the set threshold.

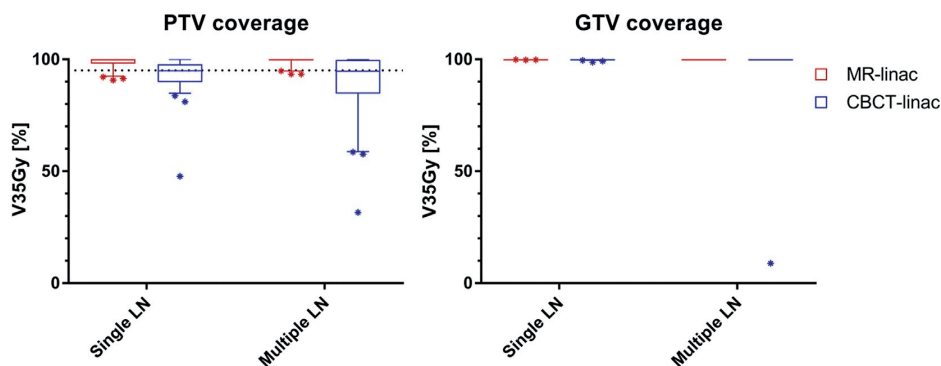


Figure 1. Boxplot of the target dose coverage described as planning target volume (PTV) and gross target volume (GTV) $V_{35\text{Gy}}$ in % for the adapted treatment plans and CBCT-linac plan recalculated on the daily anatomy after translation correction ($N = 14$ single and 6 multiple lymph node patients). The bars show the upper and lower quartiles. The whiskers show the 5–95 percentiles. Outliers are denoted with an asterisk. The dotted line for the PTV graph (left) denotes the minimal required coverage according to the dose constraints.

For multiple lymph node oligometastases the clinically delivered MR-linac plans had a median GTV $V_{35\text{Gy}}$ value of 100% [100–100%] compared to 100% [8.9–100%] for the CBCT-linac plans recalculated on the daily anatomy after translation correction. Also here the PTV $V_{35\text{Gy}}$ was significantly higher (p-value <0.01) with a median of 100% [93.4–100%] for the MR-linac compared to 94.7% [31.6–100%] for the CBCT-linac (Figure 1). All dose criteria were met for the MR-linac plans in 20/30 (67%) fractions. Violations of OAR criteria occurred with a maximum of 0.5 Gy or 0.1 cc above the set threshold. For the CBCT-plans all dose criteria were met in 6/30 (20%) fractions. Violations of OAR criteria occurred with a maximum of 0.5 Gy or 0.7 cc above the set threshold. For the clinically delivered single lymph node oligometastases plans the median GTV $V_{35\text{Gy}}$ was 100% [99.7–100%] and the median GTV D_{mean} was 43.0 Gy [37.6–46.1 Gy] on the online planning MRI. On the post-radiation delivery MRI the median GTV $V_{35\text{Gy}}$ was 100% [98.0–100%] and the median GTV D_{mean} was 42.9 Gy [37.9–45.8 Gy]. For 62 of the 70 fractions (89%) the GTV $V_{35\text{Gy}}$ on the post-delivery MRI remained 100%. For one patient, a slight reduction of the GTV coverage was necessary during online treatment planning for 3 fractions due to the dose constraint for the sacral plexus in the vicinity of the target. For the CBCT-linac plans the median GTV $V_{35\text{Gy}}$ was 100% [98.7–100%] and the median GTV D_{mean} was 44.5 Gy [41.6–46.8 Gy] on the online planning contours. On the post-radiation delivery contours the median GTV $V_{35\text{Gy}}$ was 100% [72.4–100%] and the median GTV D_{mean} was 44.5 Gy [37.2–46.2 Gy]. For 56 of the 70 fractions (80%) the GTV $V_{35\text{Gy}}$ was 100% on the post-delivery contours (Figure 2).

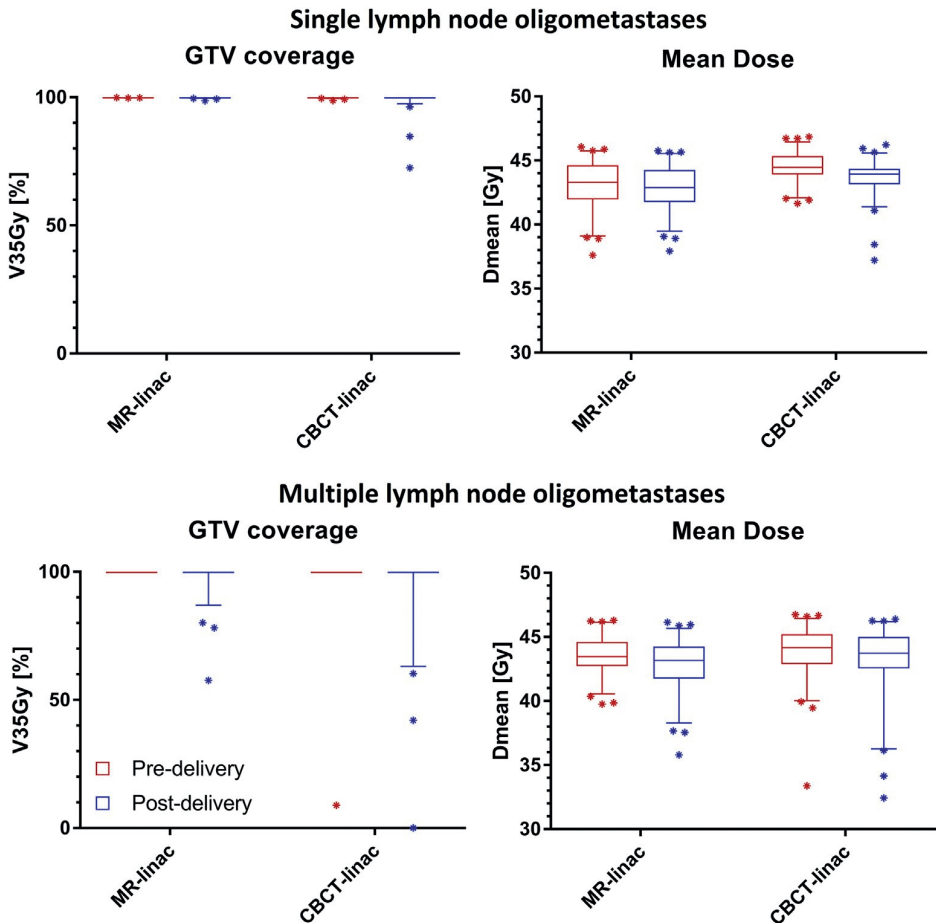


Figure 2. Boxplot graph of the GTV coverage and mean GTV dose of single ($N = 14$ patients) and multiple ($N = 6$ patients) lymph node oligometastases described as $V_{35\text{Gy}}$ in % and D_{mean} in Gy for the clinically delivered MR-linac plans and the CBCT-linac evaluated on pre- and post-delivery contours after translation correction. The bars show the upper and lower quartiles. The whiskers show the 5–95 percentiles. Outliers are denoted with an asterisk.

The clinically delivered multiple lymph node plans showed a median GTV $V_{35\text{Gy}}$ of 100% [100–100%] and the median GTV D_{mean} was 43.5 Gy [39.8–46.3 Gy] on the online planning MRI. On the post-radiation delivery MRI the median GTV $V_{35\text{Gy}}$ was 100% [57.7–100%] and the median GTV D_{mean} was 43.2 Gy [35.8–46.1 Gy]. For 63 of the 75 targets (84%) the GTV $V_{35\text{Gy}}$ on the post-delivery MRI remained 100%. For the CBCT-linac plans the median GTV $V_{35\text{Gy}}$ was 100% [8.9–100%] and the median GTV D_{mean} was 44.2 Gy [33.4–46.7 Gy] on the online planning contours. On the post-radiation delivery contours the median GTV $V_{35\text{Gy}}$ was 100% [0–100%] and the median GTV D_{mean} was 43.7 Gy [32.4–46.4 Gy]. For 61 of the 75 targets (81%) the GTV $V_{35\text{Gy}}$ was 100% on the post-delivery contours (Figure 2).

In total 11 of the single and 6 of the multiple lymph node oligometastases cases were eligible for rotational correction using a 6DOF-couch. For single lymph node oligometastases the CBCT-linac plans with 6DOF correction had a median GTV $V_{35\text{Gy}}$ value of 100% [98.9–100%] and a median PTV $V_{35\text{Gy}}$ value of 96.4% [85.6–100%] compared to 100% [98.7–100%] and 95.4% [86.1–100%] for the CBCT-linac plans with only translational correction. For the multiple lymph node oligometastases the CBCT-plans with 6DOF correction had a median GTV $V_{35\text{Gy}}$ value of 100% [7.9–100%] and a median PTV $V_{35\text{Gy}}$ value of 94.5% [33.1–100%] compared to 100% [8.9–100%] and 91.1% [31.6–100%] for the CBCT-linac plans with only translational correction. The clinically delivered MR-linac plans for this subset had a median GTV $V_{35\text{Gy}}$ value of 100% [99.7–100%] and a median PTV $V_{35\text{Gy}}$ value of 100% [90.7–100%] for single lymph nodes and a median GTV $V_{35\text{Gy}}$ value of 100% [100–100%] and a median PTV $V_{35\text{Gy}}$ value of 100% [93.4–100%] for multiple lymph nodes (Figure 3). There was a median difference of 0.8 mm [0.1–6.0 mm] in intra-target distance between the pre-treatment situation and the five treatment fractions. An example of large inter-fraction target motion can be seen in Figure 4.

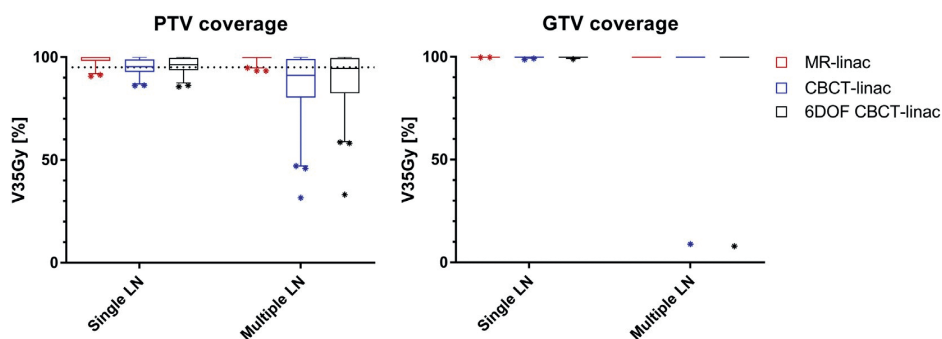


Figure 3. Boxplot of the target dose coverage described as planning target volume (PTV) and gross target volume (GTV) $V_{35\text{Gy}}$ in % for the adapted treatment plans and CBCT-linac plan recalculated on the daily anatomy, which were eligible for rotation correcting through a 6DOF-couch ($N = 11$ single and 6 multiple lymph node patients). The bars show the upper and lower quartiles. The whiskers show the 5–95 percentiles. Outliers are denoted with an asterisk. The dotted line for the PTV graph (left) denotes the minimal required coverage according to the dose constraints.

Independent target inter-fraction motion in a patient with multiple lymph node targets.

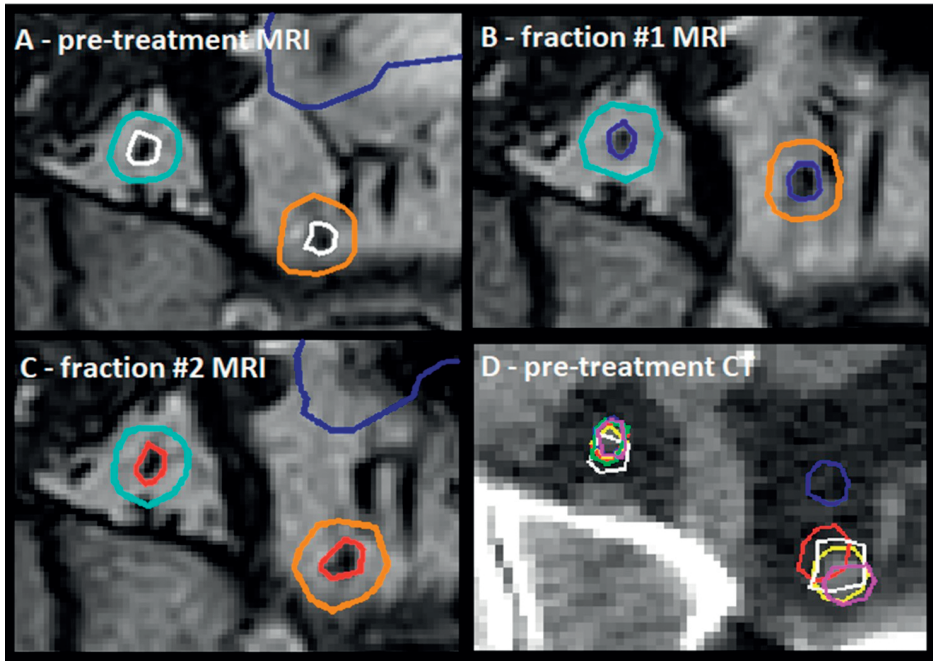


Figure 4. A depicts the pre-treatment situation on MRI and B and C show the online MRI and GTV and PTV contours of two targets (CBCT backup plan with PTV margins of 8 mm for these two targets, due to distance from isocenter/third target) in a multiple lymph node case for fraction one and two, respectively. In fraction one a large variation can be observed in the Euclidean distance between the center of gravities of both targets which decreased from 34.8 mm to 30.6 mm for this particular case because of bowel (dark-blue) influence. D depicts the pre-treatment CT with the online GTV contours for each fraction. The white contour shows the target in pre-treatment situation and the colored contours each represent the contours used in one of the five online fractions and correspond to those in the MRI images.

Discussion

In this study we have compared the target coverage of the clinically delivered online adaptive radiotherapy treatment with CBCT-linac treatment for patients with both single or multiple lymph node oligometastases and evaluated the plans based on the clinical dose criteria. Our results show no significant difference between the GTV coverage and mean GTV dose between the MR-linac and the simulated CBCT-linac treatment. Even though the PTV coverage was significantly higher for the MR-linac treatment, which corresponded to earlier findings [18], the GTV remained adequately covered for most fractions with both treatments. Because the post-delivery GTV coverage for the CBCT-linac plans was also evaluated on the post MR-linac delivery MRI, this potentially shows a worst-case scenario.

The CBCT-linac plans are VMAT plans which have shorter delivery times and so less intra-fraction motion might be expected. In addition to the longer delivery times, the entire workflow for MR-linac treatment is longer than the clinical used workflow of our CBCT-linac treatment. For targets which are poorly visible on CBCT, margins can be reduced, but this is not always the case. This means that the benefit with regards to improved GTV coverage for the group of single lymph node oligometastases for this particular patient group seems limited as with the necessary experience and expertise, manual positioning on CBCT can be adequately performed. Therefore, from an economic perspective, the justification of online MR-guided radiotherapy for these patients with a five fraction fractionation scheme is questionable at present. However, the performed treatments contributed greatly towards gaining clinical experience with MRI-guided treatment using the MR-linac and can be used as a step towards further hypo-fractionation and possibly even single fraction treatments. In these cases, target coverage and OAR constraints are more demanding for which benefit could be obtained through MR-guided treatment.

A benefit for treatment of multiple lymph node oligometastases is present in cases with large deformation of the patient anatomy and can additionally be explained by independent inter-fraction motion of the targets, which may occur [26]. Position correction through couch translations may therefore not always be sufficient. This can be seen in particular for one fraction in a patient receiving simultaneous treatment of three lymph node metastases. While GTV coverage was adequate in four fractions with a $V_{35\text{Gy}}$ of 100% for all targets, one target would receive only a GTV $V_{35\text{Gy}}$ of 8.9% and 0% in one fraction in the pre- and post-delivery situation, respectively (Figure 5). This is caused by independent motion of the targets due to deformation of the patient anatomy. In clinical practice each treatment is manually checked. If thresholds were exceeded, a physician and medical physicist would be called and appropriate action would be determined. Roper et al. [27] have shown that in general, the risk of compromised coverage increased with decreasing target volume, increasing rotational error and increasing distance between targets. This also corresponds with the relatively large distance and distal position of this particular target to the other two targets for this particular case. Although in general excellent plan quality and clinical efficiency can be reached with single-isocenter treatment of multiple targets [28], rotational errors cannot be ignored for high precision treatment, especially when the distance between a target and the isocenter is large [29]. Treating patients with multiple lymph node oligometastases on the 1.5T MR-linac means that the use of multiple plans and larger margins to account for inter-fraction rotational uncertainties are no longer required.

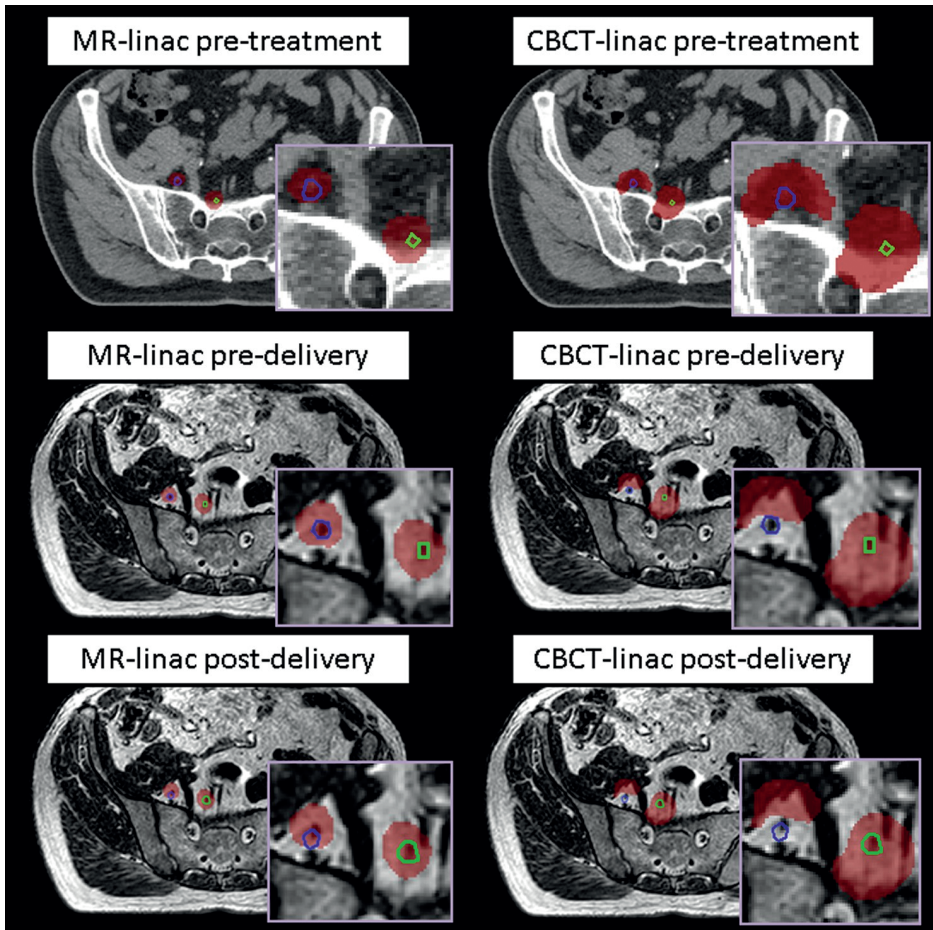


Figure 5. Pre-treatment, pre-delivery and post-delivery example of a multiple lymph node oligometastases case with three targets. Visible are the two most distal GTVs (blue and green) the 35 Gy dose level (red). Geometrical variations, causing independent motion of the targets, would have led to under-dosage ($V_{35\text{Gy}}$ of 8.9%) of the distal GTV (blue) when using the CBCT-linac plan in the pre-delivery situation and under-dosage ($V_{35\text{Gy}}$ of 0%) in the post-delivery situation, regardless of the use of a 8 mm PTV margin. GTV coverage remained adequate with a $V_{35\text{Gy}}$ of 100% for the MR-linac plans, using 3 mm PTV margins.

The 1.5T MR-linac allows for plan adaptation based on the new patient position (Adapt to Position, ATP) or based on the actual patient anatomy (Adapt to Shape, ATS) [21]. The CBCT-linac workflow is essentially comparable to the ATP workflow, as potential changes in target position are accounted for. Using the ATP workflow for poorly visible targets, in which no large deformations are expected, can also give direct benefit by taking advantage of improved target visibility through MR-guidance and could eliminate the need for larger margins. The possibility for accurate dose delivery using the ATS workflow in which the patient anatomy

is fully taken into account to mitigate for inter-fraction motion of target and OAR opens up further opportunities. One of such opportunities is improved patient comfort through hypo-fractionation and potentially single fraction treatment of lymph node oligometastases. While at this moment different hypo-fractionated schemes are already being applied [7], this is sometimes done using fiducial marker implantation which is invasive for the patient [30,31]. The superior soft-tissue contrast provided by MR-guidance might eliminate the need for such fiducial markers. Other opportunities for dosimetric improvements are expected in other tumor sites with the potential for large inter-fraction motion and anatomical deformations such as cervix [32], prostate [33] and rectum [34].

With online MR-guided adaptive radiotherapy being a relatively new technique, its distinct features already show to be able to effectively deal with day-to-day geometrical deformations of the target and surrounding OARs. Further research and technical improvements are expected to make this technique even more versatile and allow for various methods of dose delivery, intra-fraction plan adaptation [35] and adequate tissue tracking. Increased delivery speed will reduce the window of intra-fraction motion and may therefore also lead to further margin reduction. While it is currently possible to perform full online replanning in approximately one minute [36], computer power is also expected to grow over the years, decreasing computational time for some of these techniques. Additionally, it is important to have reliable quality assurance and contour propagation [37]. These developments may further contribute towards precise and patient-specific treatments.

Our results also show that with the use of MR-linac online plan adaptation, the amount of unplanned violations of online dose criteria (PTV coverage and OAR constraints) can be reduced, which corresponds to earlier studies [17,18,38]. A limitation of this study is that OARs were only evaluated based on high OAR dose constraints. Further research should be conducted to investigate the impact of daily online adaptive replanning on the OAR dose more thoroughly.

In conclusion, target coverage and OAR constraint based evaluation of the first clinical 1.5T MR-linac SBRT treatments of lymph node oligometastases compared with conventional CBCT-linac treatment shows a smaller amount of unplanned violations of these dose criteria. The GTV coverage was comparable. Benefit is primarily gained in patients treated for multiple lymph node oligometastases: geometrical deformations are then accounted for, dose can be delivered in one plan and margins are reduced.

Acknowledgement

The authors wish to thank the Dutch Cancer Society for their financial support (grant 2015-0848).

Conflict of interest statement

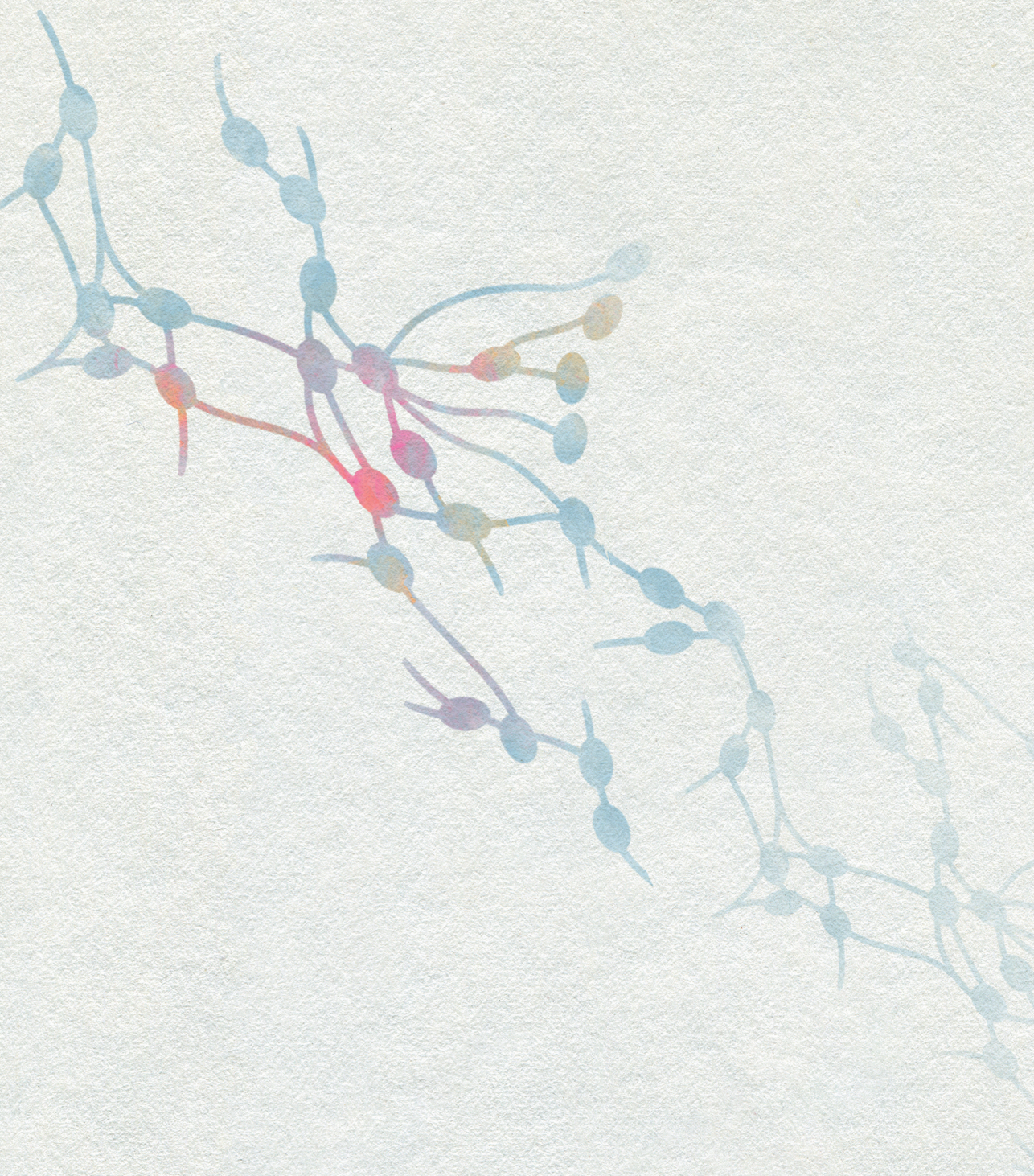
The University Medical Center Utrecht MR-linac scientific project, including employment of multiple authors, has been partly funded by Elekta AB (Stockholm, Sweden).

References

1. Tree AC, Khoo VS, Eeles RA, Ahmed M, Dearnaley DP, Hawkins MA, et al. Stereotactic body radiotherapy for oligometastases. *Lancet Oncol* 2013;14: e28–37. [https://doi.org/10.1016/s1470-2045\(12\)70510-7](https://doi.org/10.1016/s1470-2045(12)70510-7).
2. De Bleser E, Tran PT, Ost P. Radiotherapy as metastasis-directed therapy for oligometastatic prostate cancer. *Curr Opin Urol* 2017;27:587–95. <https://doi.org/10.1097/mou.0000000000000441>.
3. Park HJ, Chang AR, Seo Y, Cho CK, Jang WI, Kim MS, et al. Stereotactic body radiotherapy for recurrent or oligometastatic uterine cervix cancer: a cooperative study of the Korean Radiation Oncology Group (KROG 14–11). *Anti-cancer Res* 2015;35:5103–10.
4. Bouman-Wammes EW, van Dodewaard-De Jong JM, Dahele M, Cysouw MCF, Hoekstra OS, van Moorselaar RJA, et al. Benefits of using stereotactic body radiotherapy in patients with metachronous oligometastases of hormone-sensitive prostate cancer detected by [18F]fluoromethylcholine PET/CT. *Clin Genitourinary Cancer* 2017;15:e773–82. <https://doi.org/10.1016/j.clgc.2017.03.009>.
5. Ost P, Reynders D, Decaestecker K, Fonteyne V, Lumen N, De Bruycker A, et al. Surveillance or metastasis-directed therapy for oligometastatic prostate cancer recurrence: a prospective, randomized, multicenter phase II trial. *J Clin Oncol* 2017;36:446–53. <https://doi.org/10.1200/JCO.2017.75.4853>.
6. Fowler J, Chappell R, Ritter M. Is α/β for prostate tumors really low?. *Int J Radiat Oncol Biol Phys* 2001;50:1021–31. [https://doi.org/10.1016/S0360-3016\(01\)01607-8](https://doi.org/10.1016/S0360-3016(01)01607-8).
7. Ponti E, Lancia A, Ost P, Trippa F, Triggiani L, Detti B, et al. Exploring all avenues for radiotherapy in oligorecurrent prostate cancer disease limited to lymph nodes: a systematic review of the role of stereotactic body radiotherapy. *Eur Urol Focus* 2017;3:538–44. <https://doi.org/10.1016/j.euf.2017.07.006>.
8. Verellen D, De Ridder M, Linthout N, Tournel K, Soete G, Storme G. Innovations in image-guided radiotherapy. *Nat Rev Cancer* 2007;7:949–60. <https://doi.org/10.1038/nrc2288>.
9. Jaffray DA, Siewerdsen JH, Wong JW, Martinez AA. Flat-panel cone-beam computed tomography for image-guided radiation therapy. *Int J Radiat Oncol Biol Phys* 2002;53:1337–49. [https://doi.org/10.1016/S0360-3016\(02\)02884-5](https://doi.org/10.1016/S0360-3016(02)02884-5).
10. Noel CE, Parikh PJ, Spencer CR, Green OL, Hu Y, Mutic S, et al. Comparison of onboard low-field magnetic resonance imaging versus onboard computed tomography for anatomy visualization in radiotherapy. *Acta Oncol* 2015;54:1474–82. <https://doi.org/10.3109/0284186X.2015.1062541>.
11. Purdie TG, Bissonnette JP, Franks K, Bezjak A, Payne D, Sie F, et al. Cone-beam computed tomography for on-line image guidance of lung stereotactic radiotherapy: localization, verification, and intrafraction tumor position. *Int J Radiat Oncol Biol Phys* 2007;68:243–52. <https://doi.org/10.1016/j.ijrobp.2006.12.022>.
12. Litzenberg D, Dawson LA, Sandler H, Sanda MG, McShan DL, Ten Haken RK, et al. Daily prostate targeting using implanted radiopaque markers. *Int J Radiat Oncol Biol Phys* 2002;52:699–703. [https://doi.org/10.1016/S0360-3016\(01\)02654-2](https://doi.org/10.1016/S0360-3016(01)02654-2).
13. Dehnad H, Nederveen AJ, Heide UAvd, van Moorselaar RJA, Hofman P, Lagendijk JJW. Clinical feasibility study for the use of implanted gold seeds in the prostate as reliable positioning markers during megavoltage irradiation. *Radiother Oncol* 2003;67:295–302. [https://doi.org/10.1016/S0167-8140\(03\)00078-1](https://doi.org/10.1016/S0167-8140(03)00078-1).
14. Bjoreland U, Jonsson J, Alm M, Beckman L, Nyholm T, Thellenberg-Karlsson C. Inter-fraction movements of the prostate and pelvic lymph nodes during IGRT. *J Radiat Oncol* 2018;7:357–66. <https://doi.org/10.1007/s13566-018-0366-3>.

15. Schippers MG, Bol GH, de Leeuw AA, van der Heide UA, Raaymakers BW, Verkooijen HM, et al. Position shifts and volume changes of pelvic and para-aortic nodes during IMRT for patients with cervical cancer. *Radiother Oncol* 2014;111:442–5. <https://doi.org/10.1016/j.radonc.2014.05.013>.
16. Kerkhof EM, Balter JM, Vineberg K, Raaymakers BW. Treatment plan adaptation for MRI-guided radiotherapy using solely MRI data: a CT-based simulation study. *Phys Med Biol* 2010;55:N433–40. <https://doi.org/10.1088/0031-9155/55/16/n01>.
17. Henke L, Kashani R, Yang D, Zhao T, Green O, Olsen L, et al. Simulated online adaptive magnetic resonance-guided stereotactic body radiation therapy for the treatment of oligometastatic disease of the abdomen and central thorax: characterization of potential advantages. *Int J Radiat Oncol Biol Phys* 2016;96:1078–86. <https://doi.org/10.1016/j.ijrobp.2016.08.036>.
18. Winkel D, Kroon PS, Werensteijn-Honingh AM, Bol GH, Raaymakers BW, Jürgenliemk-Schulz IM. Simulated dosimetric impact of online replanning for stereotactic body radiation therapy of lymph node oligometastases on the 1.5T MR-linac. *Acta Oncol* 2018;1–8. <https://doi.org/10.1080/0284186X.2018.1512152>.
19. Raaymakers BW, Jürgenliemk-Schulz IM, Bol GH, Glitznier M, Kotte A, van Asselen B, et al. First patients treated with a 1.5 T MRI-Linac: clinical proof of concept of a high-precision, high-field MRI guided radiotherapy treatment. *Phys Med Biol* 2017;62:L41–50. <https://doi.org/10.1088/1361-6560/aa9517>.
20. Lagendijk JJW, Raaymakers BW, Raaijmakers AJE, Overweg J, Brown KJ, Kerkhof EM, et al. MRI/linac integration. *Radiother Oncol* 2008;86:25–9. <https://doi.org/10.1016/j.radonc.2007.10.034>.
21. Winkel D, Bol GH, Kroon PS, van Asselen B, Hackett SS, Werensteijn-Honingh AM, et al. Adaptive radiotherapy: The Elekta Unity MR-linac concept. *Clin Transl Radiat Oncol*. <https://doi.org/10.1016/j.ctro.2019.04.001>
22. Werensteijn-Honingh AM, Kroon PS, Winkel D, Aalbers EM, van Asselen B, Bol GH, et al. Feasibility of stereotactic radiotherapy using a 1.5 T MR-linac: multi-fraction treatment of pelvic lymph node oligometastases. *Radiother Oncol* 2019;134:50–4. <https://doi.org/10.1016/j.radonc.2019.01.024>.
23. Verkooijen HM, Kerkmeijer LGW, Fuller CD, Huddart R, Faivre-Finn C, Verheij M, et al. R-IDEAL: a framework for systematic clinical evaluation of technical innovations in radiation oncology. *Front Oncol* 2017;7:59. <https://doi.org/10.3389/fonc.2017.00059>.
24. Heerkens HD, Reerink O, Intven MPW, Hiensch RR, van den Berg CAT, Crijns SPM, et al. Pancreatic tumor motion reduction by use of a custom abdominal corset. *Phys Imag Radiat Oncol* 2017;2:7–10. <https://doi.org/10.1016/j.phro.2017.02.003>.
25. Winkel D, Werensteijn-Honingh AM, Kroon PS, Eppinga WSC, Bol GH, Intven MPW, et al. Individual lymph nodes: “See it and Zap it”. *Clin Transl Radiat Oncol* 2019. <https://doi.org/10.1016/j.ctro.2019.03.004>.
26. Chen G, Wang K, Li X. Independent interfraction motion of regional lymph nodes and breast targets in image-guided radiotherapy of breast cancer. *Int J Radiat Oncol Biol Phys* 2009;75:S208. <https://doi.org/10.1016/j.ijrobp.2009.07.482>.
27. Roper J, Chanyavanich V, Betzel G, Switchenko J, Dhabaan A. Single-isocenter multiple-target stereotactic radiosurgery: risk of compromised coverage. *Int J Radiat Oncol Biol Phys* 2015;93:540–6. <https://doi.org/10.1016/j.ijrobp.2015.07.2262>.

28. Quan K, Xu KM, Lalonde R, Horne ZD, Bernard ME, McCoy C, et al. Treatment plan technique and quality for single-isocenter stereotactic ablative radiotherapy of multiple lung lesions with volumetric-modulated arc therapy or intensity-modulated radiosurgery. *Front Oncol* 2015;5:213. <https://doi.org/10.3389/fonc.2015.00213>.
29. Chang J. A statistical model for analyzing the rotational error of single isocenter for multiple targets technique. *Med Phys* 2017;44:2115–23. <https://doi.org/10.1002/mp.12262>.
30. Jereczek-Fossa BA, Beltramo G, Fariselli L, Fodor C, Santoro L, Vavassori A, et al. Robotic image-guided stereotactic radiotherapy, for isolated recurrent primary, lymph node or metastatic prostate cancer. *Int J Radiat Oncol Biol Phys* 2012;82:889–97. <https://doi.org/10.1016/j.ijrobp.2010.11.031>.
31. Detti B, Bonomo P, Masi L, Doro R, Cipressi S, Iermano C, et al. Stereotactic radiotherapy for isolated nodal recurrence of prostate cancer. *World J Urol* 2015;33:1197–203. <https://doi.org/10.1007/s00345-014-1427-x>.
32. Kerkhof EM, van der Put RW, Raaymakers BW, van der Heide UA, Jürgenliemk-Schulz IM, Lagendijk JJW. Intrafraction motion in patients with cervical cancer: The benefit of soft tissue registration using MRI. *Radiother Oncol* 2009;93:115–21. <https://doi.org/10.1016/j.radonc.2009.07.010>.
33. McPartlin AJ, Li XA, Kershaw LE, Heide U, Kerkmeijer L, Lawton C, et al. MRI-guided prostate adaptive radiotherapy – a systematic review. *Radiother Oncol* 2016;119:371–80. <https://doi.org/10.1016/j.radonc.2016.04.014>.
34. Nijkamp J, Swellengrebel M, Hollmann B, de Jong R, Marijnen C, van Vliet-Vroegindeweij C, et al. Repeat CT assessed CTV variation and PTV margins for short- and long-course pre-operative RT of rectal cancer. *Radiother Oncol* 2012;102:399–405. <https://doi.org/10.1016/j.radonc.2011.11.011>.
35. Kontaxis C, Bol GH, Stemkens B, Glitzner M, Prins FM, Kerkmeijer LGW, et al. Towards fast online intrafraction replanning for free-breathing stereotactic body radiation therapy with the MR-linac. *Phys Med Biol* 2017;62:7233–48. <https://doi.org/10.1088/1361-6560/aa82ae>.
36. Kontaxis C, Bol GH, Kerkmeijer LGW, Lagendijk JJW, Raaymakers BW. Fast online replanning for interfraction rotation correction in prostate radiotherapy. *Med Phys* 2017;44:5034–42. <https://doi.org/10.1002/mp.12467>.
37. Zachiu C, de Senneville BD, Moonen CTW, Raaymakers BW, Ries M. Anatomically plausible models and quality assurance criteria for online mono- and multi-modal medical image registration. *Phys Med Biol* 2018;63. <https://doi.org/10.1088/1361-6560/aad109155016>.
38. Henke L, Kashani R, Robinson C, Curcuru A, DeWees T, Bradley J, et al. Phase I trial of stereotactic MR-guided online adaptive radiation therapy (SMART) for the treatment of oligometastatic or unresectable primary malignancies of the abdomen. *Radiother Oncol* 2018;126:519–26. <https://doi.org/10.1016/j.radonc.2017.11.032>.



Chapter 6

Impact of MR-guided versus conventional radiotherapy workflows on organ at risk doses in SBRT for lymph node oligometastases

Anita M. Werensteijn-Honingh, Petra S. Kroon, Dennis Winkel, J. Carlijn van Gaal, Jochem Hes, Louk M.W. Snoeren, Jaleesa K. Timmer, Christiaan C.P. Mout, Gijsbert H. Bol, Alexis N. Kotte, Wietse S.C. Eppinga, Martijn Intven, Bas W. Raaymakers, Ina M. Jürgenliemk-Schulz.

Submitted.

Abstract

Background and Purpose: Organ at risk (OAR) doses were compared for daily online adaptive MR-linac treatments and conventional CBCT-linac radiotherapy, taking into account differences in the current clinical workflows, especially the longer session times for MR-linac delivery with daily OAR re-contouring and plan optimization.

Materials and Methods: For 25 patients with pelvic/abdominal lymph node oligometastases, OAR doses were calculated for clinical pre-treatment and daily optimized 1.5 T MR-linac treatment plans (5x 7 Gy) and compared with simulated CBCT-linac plans for the pre-treatment and online anatomical situation. Bowelbag and duodenum were re-contoured on MRI scans acquired before, during and after each treatment session. OAR hard constraint violations, $D_{0.5cc}$ and D_{10cc} values were evaluated, focusing on bowelbag and duodenum.

Results: Overall, hard constraints for all OAR were violated less often in the daily online MR-linac treatment plans compared with CBCT-linac, in 5% versus 22% of fractions, respectively. $D_{0.5cc}$ and D_{10cc} values did not differ significantly. When taking treatment duration and intrafraction motion into account, the estimated delivered dose to bowelbag and duodenum was lower with CBCT-linac if identical PTV margins were used for both modalities. In case reduced PTV margins were achievable with MR-linac treatment, bowelbag doses were lower compared with CBCT-linac.

Conclusion: Compared with CBCT-linac treatments, the online adaptive MR-linac approach resulted in fewer hard planning constraint violations compared with single-plan CBCT-linac delivery. With respect to other dose-volume parameters for bowelbag and duodenum, the longer duration of MR-linac treatment sessions negatively impacts the potential dosimetric benefit of daily adaptive treatment planning.

Introduction

Clinical implementation of magnetic resonance (MR)-guided radiotherapy is rapidly increasing [1]. The superior soft-tissue contrast of MR imaging (MRI) compared with cone beam computed tomography (CBCT) allows improved visualization of target volumes and nearby organs at risk (OAR) [2]. With an MR-linac, MRI scans acquired before, during and after radiation dose delivery are used to optimize the treatment plan for each session [3,4]. As a result of daily contour adaptation, online plan optimization and longer dose delivery times, treatment sessions using MR-linac take roughly 20-40 minutes longer compared with CBCT-linac [1]. The longer session duration with MR-linac puts time pressure on all of these steps and as such imply a trade-off between plan optimization time and overall session time [4].

Dosimetric comparisons from two 'in silico' studies and from treatment plans for actual online MR-guided delivery indicate an advantage of MR-guided online adaptive radiotherapy for SBRT treatment of patients with (lymph node) oligometastases [5-8]. Fewer OAR constraint violations and lower mean OAR doses were reported using MR-guided online adaptive delivery compared with non-adaptive or CBCT-linac delivery [5-7]. Target coverage was also improved with MR-guided delivery, for patients with multiple targets or in the general population of abdominal/thoracic targets [5,7,8]. However, not all dosimetric evaluations of clinically delivered MR-guided radiotherapy showed a benefit compared with non-adaptive delivery: for prostate radiotherapy, both MR-linac and CBCT-linac delivery were estimated to achieve 98% of the OAR planning constraints, and better dosimetric outcomes on MR-linac were only seen for patients with an OAR close to the target [9]. For liver SBRT, online adaptive treatment with an MR-linac improved PTV coverage and OAR sparing only in case of OAR within 2 cm of the PTV, which comprised 53% of the population. On the contrary, 47% of the patients included in the study did not benefit from daily MR-guided plan optimization [10]. PTV coverage during treatment of patients with single lymph node oligometastases was excellent with both MR-linac and single-plan CBCT-linac delivery [8]. Furthermore, the longer duration of MR-linac treatment sessions has not been taken into account in most of the above-mentioned studies, which may have resulted in an overestimation of the dosimetric improvements using MR-guided radiotherapy because of a potential increase in intrafraction motion on an MR-linac [11].

The purpose of this study was to evaluate OAR doses during the first 19 months of online adaptive 1.5 T MR-linac treatment for patients with lymph node oligometastases and compare with data from simulated CBCT-linac delivery. Differences in the currently available clinical workflows for MR-linac and CBCT-linac delivery were taken into account, such as session duration and the associated target and OAR intrafraction motion.

Materials and Methods

Patients and MR-linac treatment

For this study we selected 25 patients: the first 15 and 10 patients with pelvic and abdominal lymph node targets, respectively, for whom specific OAR had been used for daily online plan optimization on a 1.5 T MR-linac (Unity, Elekta AB, Stockholm, Sweden) [12]. For patients with pelvic targets, either bowelbag, rectum or bladder had to have been taken into account, and duodenum for patients with abdominal targets. All patients gave written informed consent for use of their clinical and technical data as part of an IRB-approved observational study (www.trialregister.nl/trial/9252).

All patients were treated with a prescribed dose of 5 times 7 Gy to 95% of the PTV(s) in a single treatment plan. An offline pre-treatment intensity modulated radiotherapy (IMRT) plan with 6-10 beam angles was created after image fusion of MRI and PET/CT scans with the planning CT scan. GTVs consisted of target lymph nodes; 3 mm PTV margins were applied. OAR planning constraints are shown in Supplementary material: Table S1. Patients were immobilized using a vacuum cushion (BlueBAG BodyFIX, Elekta AB), with the exception of 4 patients with pelvic targets [13]. Patients with mesenteric or high para-aortic targets (above the renal veins) were treated whilst wearing an abdominal corset [14]. For each fraction, MRI scans were acquired before, during and after radiation delivery. MRI scans used for this study included a transverse 3D T1-weighted FFE scan and a transverse 3D T2-weighted TSE scan [13]. The adapt to shape workflow was used, with daily contour adaptation and plan optimization using a predefined template for treatment planning [8,12]. Contours of target lymph nodes (GTVs) and OAR within 2 cm of PTVs were deformed and manually adapted. An optimized treatment plan was created for each fraction, beam angles were identical to the offline pre-treatment plan. OAR planning constraints were prioritized above PTV coverage [8,12]. The average 'on couch time' (time between the start of the session (first MRI scan) and the end of radiation delivery) of the complete workflow is 32 minutes [12,13].

Simulation of CBCT-linac treatment

CBCT-linac SBRT was simulated by creating Volumetric-Modulated Arc Therapy (VMAT) plans for each patient and recalculating them on daily anatomy [8]. A radiation oncologist determined target visibility on CBCT. According to our clinical practice, PTV margin was 3 mm but larger PTV margins (5-8 mm) were used in case of poor target visibility on CBCT or in some cases with multiple targets to compensate for interfraction motion and rotations [15]. These treatment plans will be referred to as 'CBCT-linac with individualized margin'. To investigate the influence of PTV margin reduction, another set of CBCT-linac plans was created with 3 mm PTV margins for all cases: 'CBCT-linac with 3 mm margin'. CBCT-linac

treatment plans were recalculated using daily MR-linac contours, with deformed CT scans for electron density information as described previously [8].

Offline contouring of OAR of interest

For all MR-linac treatment fractions, we performed offline re-contouring of specific OAR: bowelbag, rectum and bladder for patients with pelvic targets and duodenum for patients with abdominal targets. OAR were contoured on transversal slices within a cranial-caudal extent of PTV(s) + 2 cm, on MRI scans that were obtained at the start of each fraction, at the time of position verification (PV) and directly after radiation delivery. For this study the bowelbag was defined as the outer contours of small and large bowel loops and included the sigmoid colon, starting at the recto-sigmoid junction. Multiple observers contributed to OAR contouring under supervision of radiation oncologists.

Time points for dosimetric comparison of MR-linac and CBCT-linac treatment

Radiation doses received by OAR were investigated at three time points. First, the 'offline pre-treatment' plans were compared, using clinical target and OAR contours from the offline pre-treatment imaging. Secondly, the 'daily plan' time point was based on the MRI scans acquired at the start of each treatment session with the (adapted) online contours. Finally, the 'estimated delivered' dose was calculated at the time point roughly halfway through radiation delivery, taking into account approximated session durations with MR-linac and CBCT-linac delivery based on previous experience [13]. For MR-linac, linear interpolation was used between dosimetric results based on PV and post-delivery scans. For CBCT-linac, dosimetric results were interpolated between daily plan and PV scans.

Dose-volume histogram parameters

Dose received by the OAR was investigated with two main dose-volume histogram (DVH) parameters: maximum dose received by 0.5 and 10 cc (1 cc = 1 cm³) of the OAR ($D_{0.5cc}$ and D_{10cc}). D_{1cc} , D_{2cc} , D_{5cc} , D_{9cc} , and OAR volumes that received 15-35 Gy (V_{15Gy} , V_{20Gy} , V_{25Gy} , V_{30Gy} , V_{35Gy}) were also calculated. DVH parameters were averaged over the five treatment sessions for each patient. Violations of OAR planning constraints (Supplementary material: Table S1) were calculated for individual treatment fractions.

SBRT plan quality metrics

To investigate differences in SBRT plan quality between MR-linac and CBCT-linac plans, offline pre-treatment plans were compared using four dedicated metrics from the NRG-BR001 phase 1 trial [16,17]:

- (1) Homogeneity index (HI) = PD^* / D_{\max} , acceptable if $60\% \leq HI \leq 90\%$,
with actual prescription dose (PD*) defined as the dose received by 95% of the PTV(s)
- (2) Volume ratio of PD* isodose to PTV ($R_{100\%}$) = V_{PD^*} / V_{PTV} , acceptable if $R_{100\%} \leq 1.5$,
preferred $R_{100\%} < 1.2$,
- (3) Volume ratio of 50% PD* isodose to PTV ($R_{50\%}$) = $V_{(PD^*/2)} / V_{PTV}$,
- (4) D_{2cm} = max. dose at 2 cm from PTV / PD*,

with limits for acceptable/preferred values for $R_{50\%}$ and D_{2cm} that depend on PTV (Supplementary material: Table S2).

Statistics

The open source R software package (v 4.1.0) was used (R Foundation for Statistical Computing, Vienna, Austria; <http://www.R-project.org/>). Two-sided Wilcoxon signed-rank tests were used to test for statistically significant differences in $D_{0.5cc}$, D_{1cc} , D_{2cc} , D_{5cc} , D_{9cc} and D_{10cc} between the MR-linac plan and both CBCT-linac plans; $p < 0.05$ was considered significant. V_{15Gy} , V_{20Gy} , V_{25Gy} , V_{30Gy} and V_{35Gy} were reported without statistical testing to limit the number of comparisons.

Results

A total of 25 patients with 1-3 pelvic and/or abdominal lymph node oligometastases who were treated between August 2018 and February 2020 were included in this study. Patient characteristics are shown in Table 1; for GTV locations see Supplementary material: Figure S1.

Anatomical locations of the GTV(s) are specified as pelvic (caudal of aortic bifurcation) or para-aortic/mesenteric (cranial of aortic bifurcation), this is shown in more detail in Supplementary Material: Figure S1. N: number; GTV: gross tumor volume; PTV: planning target volume; ECOG: Eastern Cooperative Oncology Group. PTV margins are shown for the simulated CBCT-linac treatment, in case of multiple PTV margins for a patient the largest margin is reported; 3 mm PTV margins were used for the clinical MR-linac treatment for all patients.

OAR doses in the pre-treatment plans were similar when comparing MR-linac plans with the CBCT-linac plans with individualized PTV margins, dosimetric outcomes are shown for bowelbag and duodenum (Figure 1, Supplementary material: Figure S2). Bowelbag doses were significantly lower for CBCT-linac plans with 3 mm margins, differences were smaller and mostly non-significant for duodenum (Figure 1, Supplementary material: Figure S2). SBRT plan quality metrics indicated that CBCT-linac plans with 3 mm PTV margins were more conformal than MR-linac plans (Supplementary material: Figure S3). (Supplementary material: Figure S3).

Table 1
Patient characteristics (N=25).

Characteristic		N patients
Location	Pelvic	15
	Para-aortic/mesenteric	10
N GTVs	1	17
	2	4
	3	4
N PTVs	1	18
	2	6
	3	1
GTV in cc (mean (sd))	Mean of GTVs per patient	6.6 (11.6)
	Sum of GTVs per patient	7.8 (14.3)
PTV margin for CBCT-linac treatment in mm	3	11
	5	8
	8	6
Treatment plans per patient for CBCT-linac treatment	1	23
	2	2
Primary tumor	Prostate	16
	Colorectal	6
	Esophageal	1
	Lung	1
	Hepatocellular carcinoma	1
ECOG performance status	0	16
	1	8
	2	1

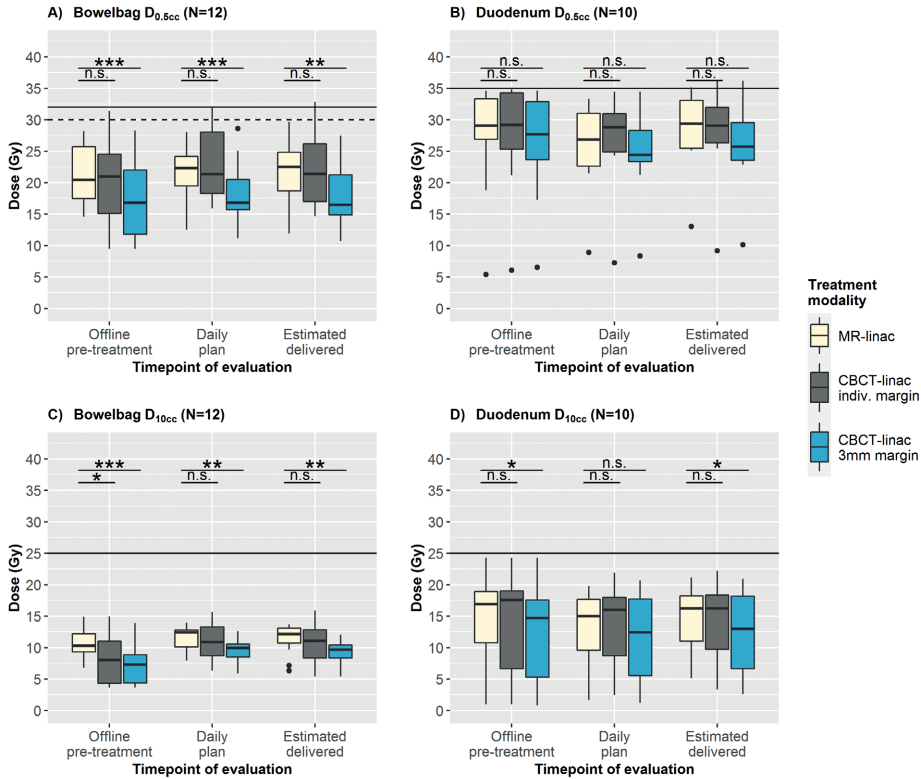


Figure 1. Comparison of bowelbag and duodenum dose using MR-linac and CBCT-linac SBRT for lymph node oligometastases. $D_{0.5cc}$ and D_{10cc} were calculated for three time points: offline pretreatment anatomy (offline pretreatment), anatomy at the start of each treatment fraction (daily plan) and estimated anatomy at the moment of radiation delivery for each fraction (estimated delivered, average of pre/PV scans for CBCT-linac and average of PV/post scans for MR-linac). Averages per patient are shown for MR-linac (3 mm PTV margin), CBCT-linac with the individualized PTV margin and CBCT-linac with 3 mm PTV margin. Center line indicates median, hinges depict 25th and 75th percentiles (inter-quartile range, IQR) and whiskers extend from the hinge to the largest/smallest value at maximally 1.5*IQR. Outlying data points (beyond end of the whiskers) are plotted individually. Hard constraints are plotted as solid lines, soft constraints as dashed lines. Asterisks depict significant differences in DVH parameters between MR-linac and both CBCT-linac plans (Mann-Whitney U-test (two-sided), * $p < 0.05$, ** $p < 0.01$, *** $p < 0.001$).

For the actual treatment sessions, the daily optimized MR-linac plans were compared with CBCT-linac plans. When considering all applicable OAR constraints (Supplementary material: Table S1), hard constraints were violated in 6/125 treatment fractions (5%) of the daily optimized MR-linac treatment plans ('daily plan' time point). For CBCT-linac plans with individualized and 3 mm margins, OAR constraints were violated in 28/125 sessions (22%) and in 16/125 (13%), respectively. Bowelbag and duodenum constraint violations are shown in Figure 2; rectum and bladder constraint violations were not observed (data not shown). The largest constraint violation was observed for CBCT-linac

with bowelbag $D_{0.5cc}$ being 40.4 Gy for a single fraction (hard constraint <32 Gy). Bowelbag and duodenum $D_{0.5cc}$ and D_{10cc} were not significantly different between MR-linac and CBCT-linac with individualized margins (Figure 1). When comparing MR-linac and CBCT-linac treatment plans with 3 mm PTV margins, bowelbag doses were significantly lower for the CBCT-linac plans; no significant differences were observed for duodenum (Figure 1, Supplementary material: Figure S2). Differences in bowelbag $D_{0.5cc}$ between MR-linac and CBCT-linac appeared to be related to the PTV margins: when a larger PTV margin was used for CBCT-linac, bowelbag doses were lower using MR-linac in 6 out of 7 cases. In case of identical PTV margins were used for both modalities, bowelbag doses were lower using CBCT-linac in 7 out of 8 cases (Figure 3).

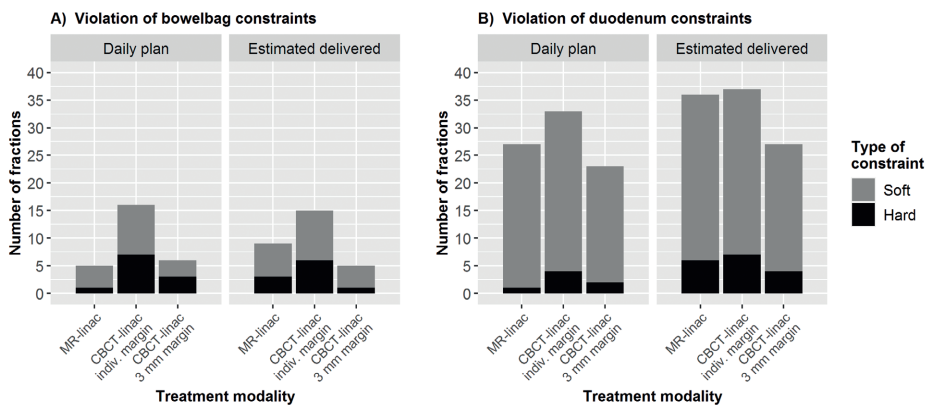


Figure 2. Violation of planning constraints using MR-linac and CBCT-linac SBRT for lymph node oligometastases. Number of individual treatment fractions for which soft and hard constraints were violated are shown for bowelbag (A) and duodenum (B). Results were calculated for MR-linac (3 mm PTV margin), CBCT-linac with the individualized PTV margin and CBCT-linac with 3 mm PTV margin. Constraint violations are shown at two time points: anatomy at the start of the treatment fraction (daily plan) and estimated anatomy at the moment of radiation delivery (estimated delivered, average of pre/PV scans for CBCT-linac and average of PV/post scans for MR-linac). Applicable planning constraints are shown in Supplementary Material: Table S1.

Furthermore, we estimated the doses that were actually delivered to the OAR, taking intrafraction motion into account ('estimated delivered' time point). Bowelbag or duodenum hard constraints would have been violated in 9, 13 and 5 treatment sessions using MR-linac, CBCT-linac with individualized margins and CBCT-linac with 3 mm margins, respectively (Figure 2). When averaged (per case) over the five treatment sessions, maximum violations of hard constraints were 0.8 and 1.2 Gy for bowelbag and duodenum, respectively (Figure 1). Rectum and bladder constraint adherence was 100% with both modalities (data not shown). No significant differences were observed for bowelbag and duodenum $D_{0.5cc}$ and D_{10cc} when comparing MR-linac and CBCT-linac with the individualized PTV margin (Figure 1). When comparing MR-linac with CBCT-linac with 3 mm PTV margins, all tested DVH

parameters for bowelbag and duodenum were significantly lower using CBCT-linac delivery except for duodenum $D_{0.5cc}$ (Figure 1).

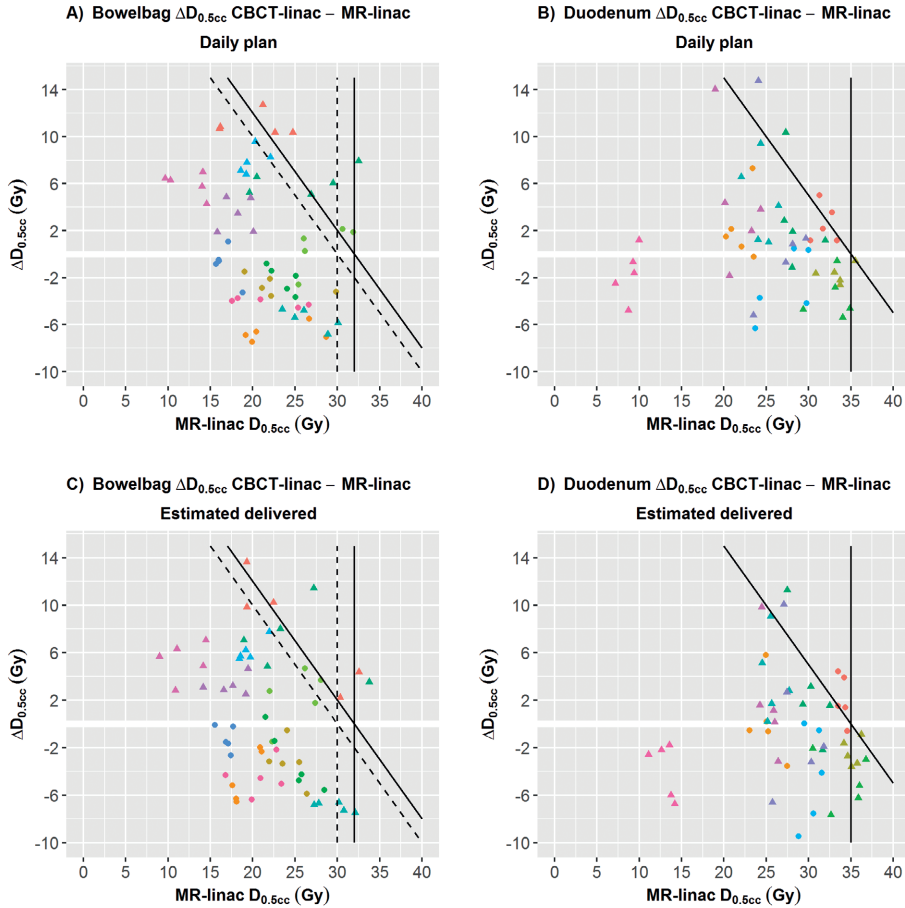
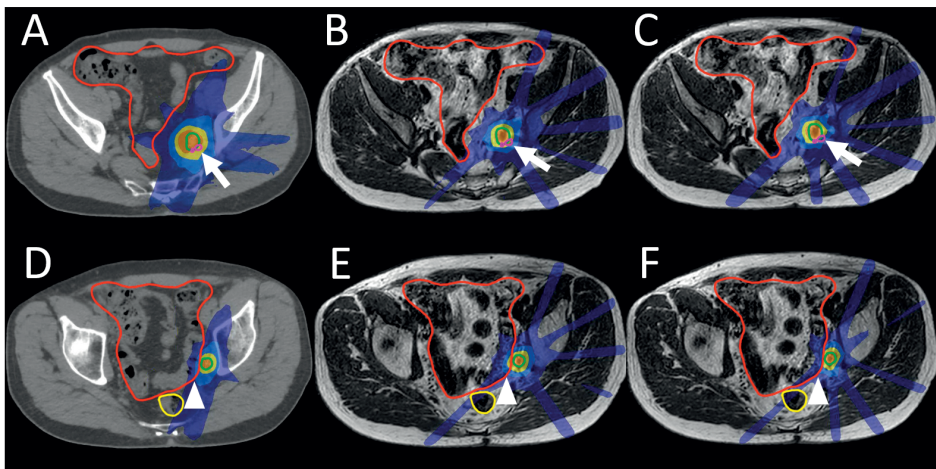


Figure 3. Differences in bowelbag and duodenum dose using MR-linac and CBCT-linac SBRT for lymph node oligometastases. Differences in $D_{0.5cc}$ between MR-linac and CBCT-linac, both with 3 mm PTV margins, are shown for bowelbag (A+C) and duodenum (B+D), at daily plan time point (A+B) or estimated delivered time point (C+D). Differences are plotted for each individual fraction, colors represent the patients (N=12 for bowelbag and N=10 for duodenum). Dots represent patients with a 3 mm PTV margin for CBCT-linac, triangles indicate patients with a CBCT-linac PTV margin of 5 mm or larger. MR-linac PTV margin was always 3 mm. A negative $\Delta D_{0.5cc}$ indicates a lower $D_{0.5cc}$ using CBCT-linac compared with MR-linac. Hard constraints are plotted as solid lines, soft constraints as dashed lines. Constraints are plotted both vertically and diagonally: dots to the right of a vertical line indicate fractions for which the constraint was violated with MR-linac, dots to the upper-right of a diagonal line indicate fractions with a constraint violation using CBCT-linac.

In Figure 4, treatment plans are shown for a case in which the distance between the target and the sacral plexus was less in the online treatment situation compared with the pre-treatment anatomy. In this situation the $D_{0.5cc}$ of bowelbag was lower using the CBCT-linac plan, despite larger PTV margins. However, the CBCT-linac plan would have violated the sacral plexus $D_{0.1cc}$ with 1 Gy (hard constraint <32 Gy). The MR-linac plan complied with all target and hard OAR constraints, but the bowelbag $D_{0.5cc}$ was 5.8 Gy higher than on the CBCT-linac plan. With some more attention on bowelbag sparing during online plan optimization, the bowelbag $D_{0.5cc}$ could have been reduced with 8.5 Gy without compromising PTV coverage or violating the sacral plexus constraint, as was shown with an offline-optimized plan (Figure 4).



Legend of dose levels

■ 47.25 Gy (135%) ■ 35.00 Gy (100%) ■ 26.25 Gy (75%) ■ 17.50 Gy (50%) ■ 8.75 Gy (25%)

Figure 4. Potential for improvement of the online plan optimization during MRgRT on a 1.5 T MR-linac. Treatment plans at the daily plan time point are shown for an illustrative case (patient 19, fraction 5): the CBCT-linac plan with individualized margins (A+D), the clinically delivered MR-linac plan (B+E) and an offline re-optimized MR-linac plan (C+F). This patient had three GTVs in two PTVs, with a 3 mm PTV margin for PTV1 and an 8 mm PTV margin for PTV2, with the isocenter placed in PTV1. The daily online MR-linac PTV2 contour (using 3 mm PTV margins used on MR-linac) is shown in green. PTV and OAR hard planning constraints were met for the MR-linac plans, whereas the sacral plexus (pink contour) constraint was violated on the CBCT-linac plan (A-C, arrows). Still, the bowelbag (red contour) $D_{0.5cc}$ was 5.8 Gy lower using CBCT-linac (D-F, arrowheads). The dose received by the bowelbag could have been further reduced for the clinically delivered MR-linac plan with adjustment of the bowelbag isoeffect settings during online plan optimization, resulting in a plan that met all planning goals, with a lower bowelbag dose (C+F).

Discussion

This is one of the first studies comparing OAR dose parameters of clinically used online MR-linac and simulated CBCT-linac plans. An important difference between MR-linac and CBCT-linac workflows is the duration of treatment sessions. For MR-linac, session duration is longer due to daily online plan optimization and longer dose delivery. Therefore, the impact of intrafraction motion on OAR doses should be considered. Our analysis demonstrates that hard OAR planning constraints were violated less frequently with the daily online adaptive MR-linac treatment plans. For other OAR dose-volume parameters, MR-linac treatment provided improved bowelbag sparing when smaller PTV margins were applied compared with CBCT-linac [6]. However, when applying 3 mm PTV margins for both modalities, the ‘estimated delivered’ doses to bowelbag and duodenum were significantly lower for the simulated CBCT-linac treatments. This effect may partially be due to our choices regarding the daily plan adaptation methodology for MR-linac treatments: first, due to time pressure on the daily plan optimization, currently only high-dose DVH parameters are being taken into account and re-contouring of OAR is limited to OAR within 2 cm of the PTV(s). Secondly, the individual pre-treatment plans for the 1.5 T MR-linac, which are used as templates for online plan adaptation, have to allow for fast online plan adaptation, must prevent unnecessary compromise for the target dose, and might therefore be somewhat less conformal than the CBCT pre-treatment plans [9]. Finally, intrafraction OAR motion is not corrected for in our current clinical MR-linac workflow despite longer time needed for dose delivery. Thus, specific aspects of the MR-guided online adaptive treatment workflow are likely to have contributed to our finding of fewer than anticipated benefits of current 1.5 T MR-linac delivery regarding OAR dosimetry.

A comparison between 1.5 T MR-linac and CBCT-linac dose delivery has previously been reported by Dunlop *et al.*, for prostate radiotherapy (20 times 3 Gy) [9]. They showed that target coverage could be improved using an MR-linac compared with CBCT-linac for patients with OAR close to the target volumes on offline pre-treatment imaging. Adherence to OAR planning constraints was excellent with both modalities. Higher rectum and bladder doses were described for particular cases using MR-linac, consistent with our findings. Henke *et al.* have reported on online adaptive MR-guided radiotherapy for oligometastatic or unresectable primary abdominal malignancies with a fractionation scheme of 5 times 10 Gy [7]. OAR planning constraint violations were observed for 63% of fractions, mainly for small bowel, duodenum and stomach. Target dose could be escalated in 21% of fractions. The benefits from online adaptive MR-guided radiotherapy seem to have been larger for this specific fractionation scheme. However, in both aforementioned studies the “estimated delivered doses” had not been calculated. With our current fractionation scheme of five SBRT fractions of 7 Gy, the estimated OAR constraint violations for individual treatment

fractions on CBCT-linac would have largely evened out over the course of treatment, with a maximum violation of bowelbag and duodenum $D_{0.5cc}$ constraints of 1.2 Gy. Stricter adherence to OAR planning constraints may be important when considering further hypofractionation [18].

In addition to daily plan adaptation, MR-linac treatment also enables offline reconstruction of OAR doses from previous treatment sessions using MRI scans acquired during and after radiation delivery. The planning goals for following fractions can thus be adapted based on the OAR dose estimated to have been delivered during previous fractions. Such a process of dose reconstruction is labor-intensive, but it can be of additional value for patients with an OAR located close to the GTV and for patients with a higher risk of toxicity because of previous radiotherapy or surgery in the target area [19]. Future developments are expected to improve the advantages of MR-linac treatments, such as fast intrafraction plan adaptation [20]. With intrafraction plan adaptation, changes in both target and OAR anatomy during radiation delivery could be incorporated. Finally, we observed a learning curve in our clinical experience regarding MR-linac treatments, with room for improving the workflow and the individual planning templates. As is shown in Figure 4, the dose received by the OAR can only be 'as low as reasonably achievable' (ALARA) with specific attention for reducing the OAR doses during the online plan optimization, rather than only examining OAR hard constraint adherence. Also, the templates for online plan optimization could be improved with addition of other dose-volume parameters, as long as the online plan optimization time remains acceptable [21,22].

The strength of this study is that OAR have been re-contoured on MRI scans acquired before, during and after each treatment session, which enabled us to estimate the delivered doses to bowelbag and duodenum at realistic time points. A limitation of this study is the application of 3-8 mm PTV margins for CBCT-linac simulations, with 5-8 mm margins in case of poor target visibility on CBCT. These margins reflect our clinical practice but are larger than the 3-5 mm margins that are also commonly used [23,24].

Compared with CBCT-linac treatments, the online adaptive MR-linac approach resulted in fewer hard planning constraint violations compared with single-plan CBCT-linac delivery. With respect to other dose-volume parameters for bowelbag and duodenum, differences in OAR sparing depended on the applicable treatment margins. MR-linac workflow aspects such as longer treatment sessions, limited time for online plan optimization and the absence of compensation for OAR intrafraction motion currently seem to decrease the potential advantages of online adaptive MR-guided delivery.

Funding

This work was supported by the Dutch Cancer Society under Grant 2015-0848.

Disclosure of interest

The overarching University Medical Center Utrecht MR-linac scientific project, including employment of multiple authors, has been partly funded by Elekta AB (Stockholm, Sweden). Elekta did not have any part in the design, execution or analysis of this study. The authors declared that there is no other conflict of interest.

References

- Hall WA, Paulson ES, van der Heide UA, Fuller CD, Raaymakers BW, Lagendijk JJW, et al. The transformation of radiation oncology using real-time magnetic resonance guidance: A review. *Eur J Cancer* 2019;122:42-52. <https://doi.org/10.1016/j.ejca.2019.07.021>.
- Noel CE, Parikh PJ, Spencer CR, Green OL, Hu Y, Mutic S, et al. Comparison of onboard low-field magnetic resonance imaging versus onboard computed tomography for anatomy visualization in radiotherapy. *Acta Oncol* 2015;54:1474-82. <https://doi.org/10.3109/0284186X.2015.1062541>.
- Klüter S. Technical design and concept of a 0.35 T MR-Linac. *Clin Transl Radiat Oncol* 2019;18:98-101. <https://doi.org/10.1016/j.ctro.2019.04.007>.
- Winkel D, Bol GH, Kroon PS, van Asselen B, Hackett SS, Werensteijn-Honingh AM, et al. Adaptive radiotherapy: The Elekta Unity MR-linac concept. *Clin Transl Radiat Oncol* 2019;18:54-9. <https://doi.org/10.1016/j.ctro.2019.04.001>.
- Henke L, Kashani R, Yang D, Zhao T, Green O, Olsen L, et al. Simulated Online Adaptive Magnetic Resonance-Guided Stereotactic Body Radiation Therapy for the Treatment of Oligometastatic Disease of the Abdomen and Central Thorax: Characterization of Potential Advantages. *Int J Radiat Oncol Biol Phys* 2016;96:1078-86. <https://doi.org/10.1016/j.ijrobp.2016.08.036>.
- Winkel D, Kroon PS, Werensteijn-Honingh AM, Bol GH, Raaymakers BW, Jürgenliemk-Schulz IM. Simulated dosimetric impact of online replanning for stereotactic body radiation therapy of lymph node oligometastases on the 1.5T MR-linac. *Acta Oncol* 2018;57:1705-12. <https://doi.org/10.1080/0284186X.2018.1512152>.
- Henke LE, Olsen JR, Contreras JA, Curcuru A, DeWees TA, Green OL, et al. Stereotactic MR-Guided Online Adaptive Radiation Therapy (SMART) for Ultracentral Thorax Malignancies: Results of a Phase 1 Trial. *Adv Radiat Oncol* 2018;4(1):201-9. <https://doi.org/10.1016/j.adro.2018.10.003>.
- Winkel D, Bol GH, Werensteijn-Honingh AM, Intven MPW, Eppinga WSC, Hes J, et al. Target coverage and dose criteria based evaluation of the first clinical 1.5T MR-linac SBRT treatments of lymph node oligometastases compared with conventional CBCT-linac treatment. *Radiother Oncol* 2020;146:118-25. <https://doi.org/10.1016/j.radonc.2020.02.011>.
- Dunlop A, Mitchell A, Tree A, Barnes H, Bower L, Chick J, et al. Daily adaptive radiotherapy for patients with prostate cancer using a high field MR-linac: Initial clinical experiences and assessment of delivered doses compared to a C-arm linac. *Clin Transl Radiat Oncol* 2020;23:35-42. <https://doi.org/10.1016/j.ctro.2020.04.011>.
- Mayinger M, Ludwig R, Christ SM, Dal Bello R, Ryu A, Weitkamp N, et al. Benefit of replanning in MR-guided online adaptive radiation therapy in the treatment of liver metastasis. *Radiat Oncol* 2021;16:84. <https://doi.org/10.1186/s13014-021-01813-6>.
- Kontaxis C, de Muinck Keizer DM, Kerkmeijer LGW, Willigenburg T, den Hartogh MD, et al. Delivered dose quantification in prostate radiotherapy using online 3D cine imaging and treatment log files on a combined 1.5T magnetic resonance imaging and linear accelerator system. *Phys Imaging Radiat Oncol* 2020;15:23-9. <https://doi.org/10.1016/j.phro.2020.06.005>.
- Werensteijn-Honingh AM, Kroon PS, Winkel D, Aalbers EM, van Asselen B, Bol GH, et al. Feasibility of stereotactic radiotherapy using a 1.5 T MR-linac: Multi-fraction treatment of pelvic lymph node oligometastases. *Radiother Oncol* 2019;134:50-4. <https://doi.org/10.1016/j.radonc.2019.01.024>.

13. Werensteijn-Honingh AM, Jürgenliemk-Schulz IM, Gadellaa-Van Hooijdonk CG, Sikkes GG, Vissers NGPM, Winkel D, et al. Impact of a vacuum cushion on intrafraction motion during online adaptive MR-guided SBRT for pelvic and para-aortic lymph node oligometastases. *Radiother Oncol* 2021;154:110-7. <https://doi.org/10.1016/j.radonc.2020.09.021>.
14. Heerkens HD, Reerink O, Intven MPW, Hiensch RR, van den Berg CAT, Crijns SPM, et al. Pancreatic tumor motion reduction by use of a custom abdominal corset. *Phys Imaging Radiat Oncol* 2017;2:7-10. <https://doi.org/10.1016/j.phro.2017.02.003.9>.
15. Roper J, Chanyavanich V, Betzel G, Switchenko J, Dhabaan A. Single-Isocenter Multiple-Target Stereotactic Radiosurgery: Risk of Compromised Coverage. *Int J Radiat Oncol Biol Phys* 2015;93:540-6. <https://doi.org/10.1016/j.ijrobp.2015.07.2262>.
16. Al-Hallaq HA, Chmura S, Salama JK, Winter KA, Robinson CG, Pisansky TM, et al. Rationale of technical requirements for NRG-BR001: The first NCI-sponsored trial of SBRT for the treatment of multiple metastases. *Pract Radiat Oncol* 2016;6:e291-8. <https://doi.org/10.1016/j.prro.2016.05.004>.
17. Chmura S, Winter KA, Robinson C, Pisansky TM, Borges V, Al-Hallaq H, et al. Evaluation of Safety of Stereotactic Body Radiotherapy for the Treatment of Patients With Multiple Metastases: Findings From the NRG-BR001 Phase 1 Trial. *JAMA Oncol* 2021;7:845-52. <https://doi.org/10.1001/jamaoncol.2021.0687>.
18. Winkel D, Werensteijn-Honingh AM, Eppinga WSC, Intven MPW, Hes J, Snoeren LMW, et al. Dosimetric feasibility of hypofractionation for SBRT treatment of lymph node oligometastases on the 1.5T MR-linac. *Radiother Oncol* 2021;154:243-8. <https://doi.org/10.1016/j.radonc.2020.09.020>.
19. Lee JJB, Choi SH, Im JH, Seong J. Clinical safety and efficacy of salvage reirradiation for upper abdominal malignancies. *Strahlenther Onkol* 2019;195:526-33. <https://doi.org/10.1007/s00066-018-01420-7>.
20. Kontaxis C, Bol GH, Stemkens B, Glitzner M, Prins FM, Kerkmeijer LGW, et al. Towards fast online intrafraction replanning for free-breathing stereotactic body radiation therapy with the MR-linac. *Phys Med Biol* 2017;62:7233-48. <https://doi.org/10.1088/1361-6560/aa82ae>.
21. Winkel D, Bol GH, Anita M Werensteijn-Honingh AM, Kiekebosch IH, van Asselen B, Intven MPW, et al. Evaluation of plan adaptation strategies for stereotactic radiotherapy of lymph node oligometastases using online magnetic resonance image guidance. *Phys Imaging Radiat Oncol* 2019;9:58-64. <https://doi.org/10.1016/j.phro.2019.02.003>.
22. van Timmeren JE, Chamberlain M, Krayenbuehl J, Wilke L, Ehrbar S, Bogowicz M, et al. Comparison of beam segment versus full plan re-optimization in daily magnetic resonance imaging-guided online-adaptive radiotherapy. *Phys Imaging Radiat Oncol* 2021;17:43-6. <https://doi.org/10.1016/j.phro.2021.01.001>.
23. Ost P, Reynders D, Decaestecker K, Fonteyne V, Lumen N, et al. Surveillance or Metastasis-Directed Therapy for Oligometastatic Prostate Cancer Recurrence: A Prospective, Randomized, Multicenter Phase II Trial. *J Clin Oncol* 2018;36:446-53. <https://doi.org/10.1200/JCO.2017.75.4853>.
24. Mazzola R, Francolini G, Triggiani L, Napoli G, Cuccia F, et al. Metastasis-directed Therapy (SBRT) Guided by PET-CT 18 F-CHOLINE Versus PET-CT 68 Ga-PSMA in Castration-sensitive Oligorecurrent Prostate Cancer: A Comparative Analysis of Effectiveness. *Clin Genitourin Cancer* 2021;19:230-6. <https://doi.org/10.1016/j.clgc.2020.08.002>.

Supplementary material

Table S1

Planning constraints for organs-at-risk in this study, for SBRT delivery in 5 fractions.

Organ at risk	Parameter	Hard constraint	Soft constraint
Bladder	$D_{0.5cc}$	< 42 Gy	
	D_{5cc}	< 37 Gy	
Bowelbag / Large bowel	$D_{0.5cc}$	< 32 Gy	< 30 Gy
	D_{5cc}		< 25 Gy
	D_{10cc}	< 25 Gy	
Duodenum	$D_{0.5cc}$	< 35 Gy	
	D_{1cc}		< 33 Gy
	D_{5cc}		< 25 Gy
	D_{9cc}		< 15 Gy
	D_{10cc}	< 25 Gy	
Rectum	$D_{0.5cc}$	< 40 Gy	
	D_{1cc}	< 38 Gy	< 35 Gy
Sacral plexus / Nerve roots / Cauda equina	$D_{0.1cc}$	< 32 Gy	
	D_{5cc}	< 30 Gy	
Stomach	$D_{0.5cc}$	< 35 Gy	< 33 Gy
	D_{5cc}		< 25 Gy
	D_{10cc}	< 25 Gy	
Ureter	$D_{0.5cc}$	< 42 Gy	

Table S2

Limits for SBRT plan quality/conformity metrics that depend on PTV volume. Recommended metric values are shown for maximum dose at 2 cm from PTV (D_{2cm}) relative to actual prescription dose (PD*) and for volume ratio of volume receiving 50% of PD* to PTV ($R_{50\%}$), as defined in the NRG-BR001 phase 1 trial [16,17]. Linear interpolation between table entries is required for PTV values not specified. Limits for D_{2cm} indicate acceptable values and for $R_{50\%}$ preferred values. Note that the $R_{50\%}$ was evaluated for summed doses in case of separate treatment plans for CBCT-linac, to allow for comparison with the MR-linac plan; for the NRG-BR001 trial $R_{50\%}$ would have been evaluated separately for each lesion/plan.

PTV (cc)	$R_{50\%}$ (-)	D_{2cm} (%)
< 1.8	< 7.5	< 57
< 3.8	< 6.5	< 57
< 7.4	< 6.0	< 58
< 13.2	< 5.8	< 58
< 22.0	< 5.5	< 63
< 34.0	< 5.3	< 68
< 50.0	< 5.0	< 77
< 70.0	< 4.8	< 86
< 95.0	< 4.4	< 89
< 126.0	< 4.0	< 91
<163.0	< 3.7	< 94

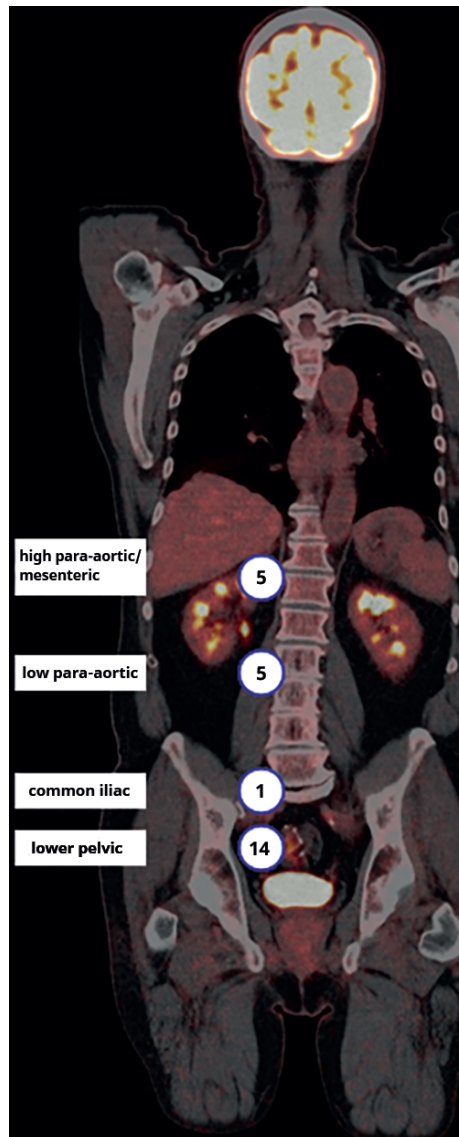


Figure S1. Anatomical locations of GTVs for patients in this study. The number of patients is plotted for each anatomical location. For patients with multiple GTVs, the situation was assigned to the location with the most GTVs. Anatomical levels were defined as high para-aortic/mesenteric (cranial of the level of insertion of renal veins into inferior vena cava), low para-aortic (caudal of the renal veins, cranial of aortic bifurcation), common iliac (caudal of aortic bifurcation, cranial of iliac artery bifurcation) and lower pelvic (caudal of iliac artery bifurcation).

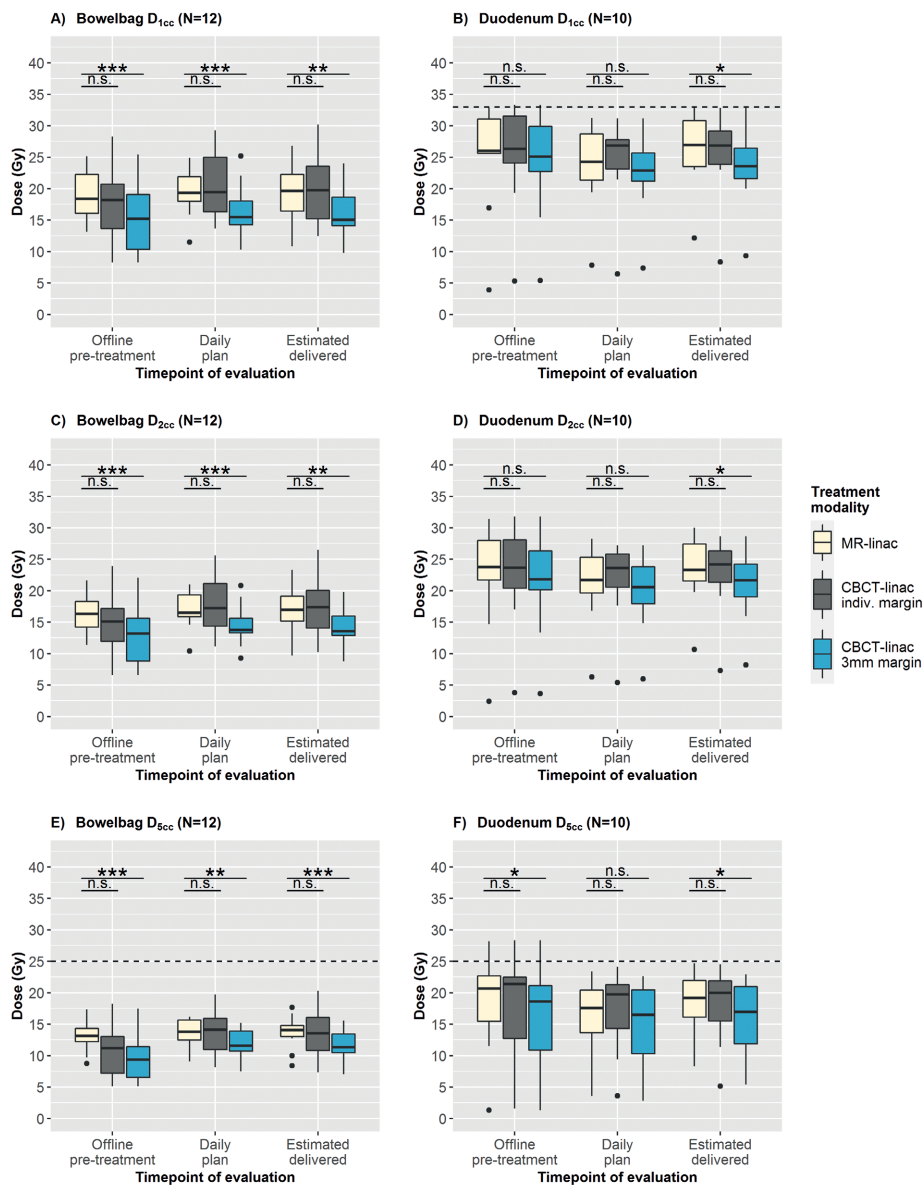


Figure S2

Comparison of bowelbag and duodenum dose using MR-linac and CBCT-linac SBRT for lymph node oligometastases. DVH parameters were calculated for three time points: offline pretreatment anatomy (offline pretreatment), anatomy at the start of each treatment fraction (daily plan) and anatomy at the moment of radiation delivery for each fraction (estimated delivered, average of pre/PV scans for CBCT-linac and average of PV/post scans for MR-linac). Averages per patient are shown for MR-linac (3 mm PTV margin), CBCT-linac with the individualized PTV margin and CBCT-linac with 3 mm PTV margin. Center line indicates median, hinges depict 25th and 75th percentiles (inter-quartile range, IQR) and whiskers extend from the hinge to the largest/smallest value at maximally 1.5*IQR. Outlying data points (beyond end of the whiskers) are

plotted individually. Hard constraints are plotted as solid horizontal lines, soft constraints as dashed lines. Asterisks depict significant differences in DVH parameters between MR-linac and both CBCT-linac plans (Mann-Whitney U-test (two-sided), * $p < 0.05$, ** $p < 0.01$, *** $p < 0.001$). Note the different y-axis ranges of bowelbag and duodenum plots in subfigures I-N.

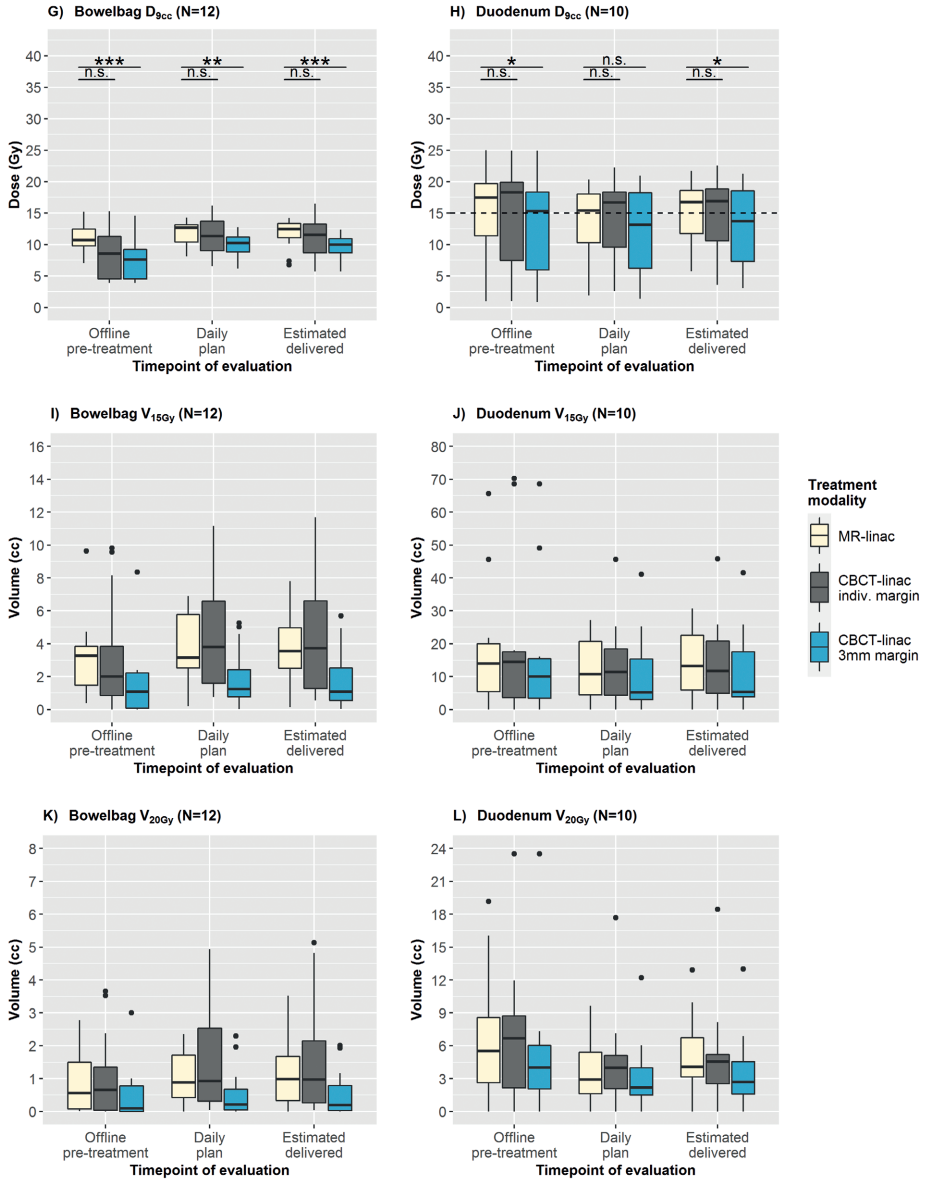


Figure S2

Comparison of bowelbag and duodenum dose using MR-linac and CBCT-linac SBRT for lymph node oligo-metastases. (continued)

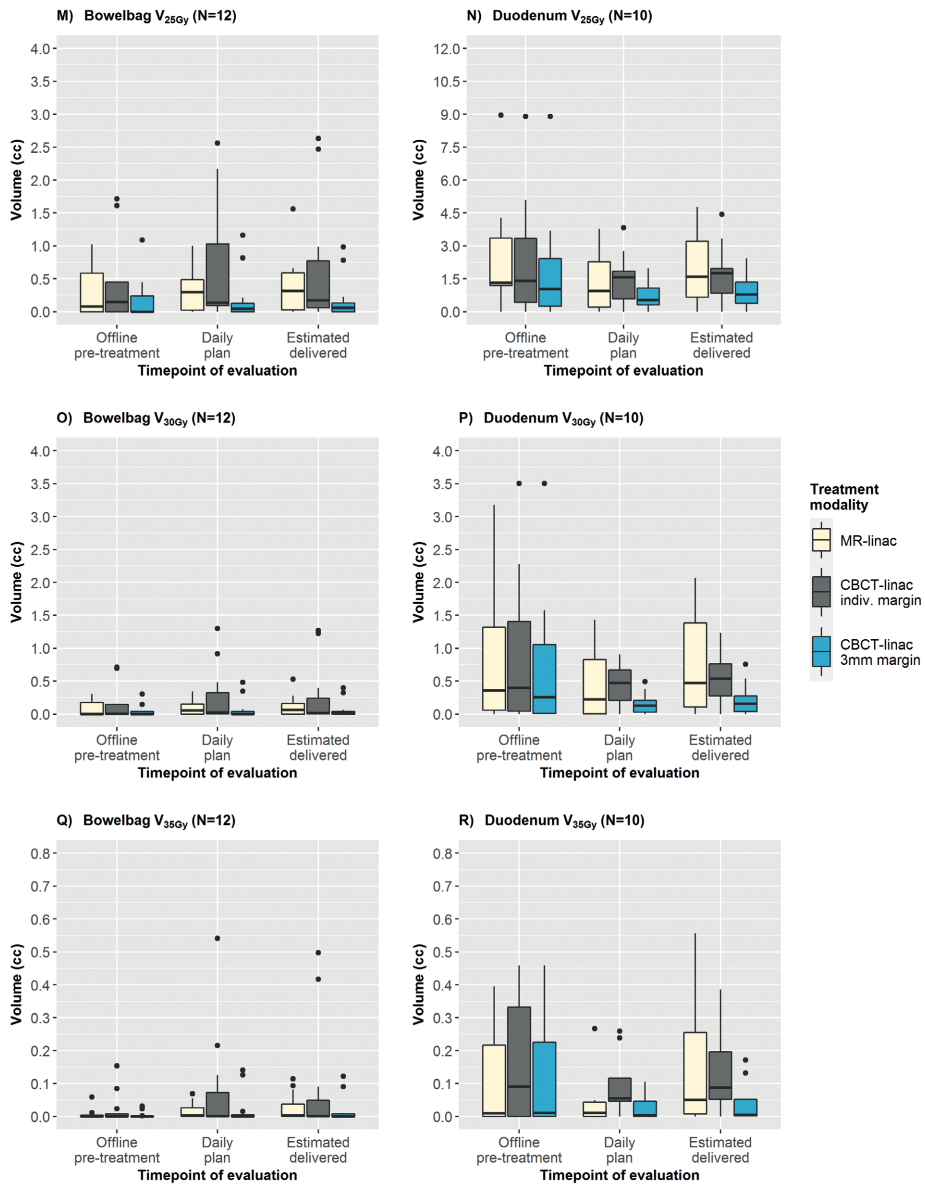


Figure S2
 Comparison of bowelbag and duodenum dose using MR-linac and CBCT-linac SBRT for lymph node oligo-metastases. *(continued)*

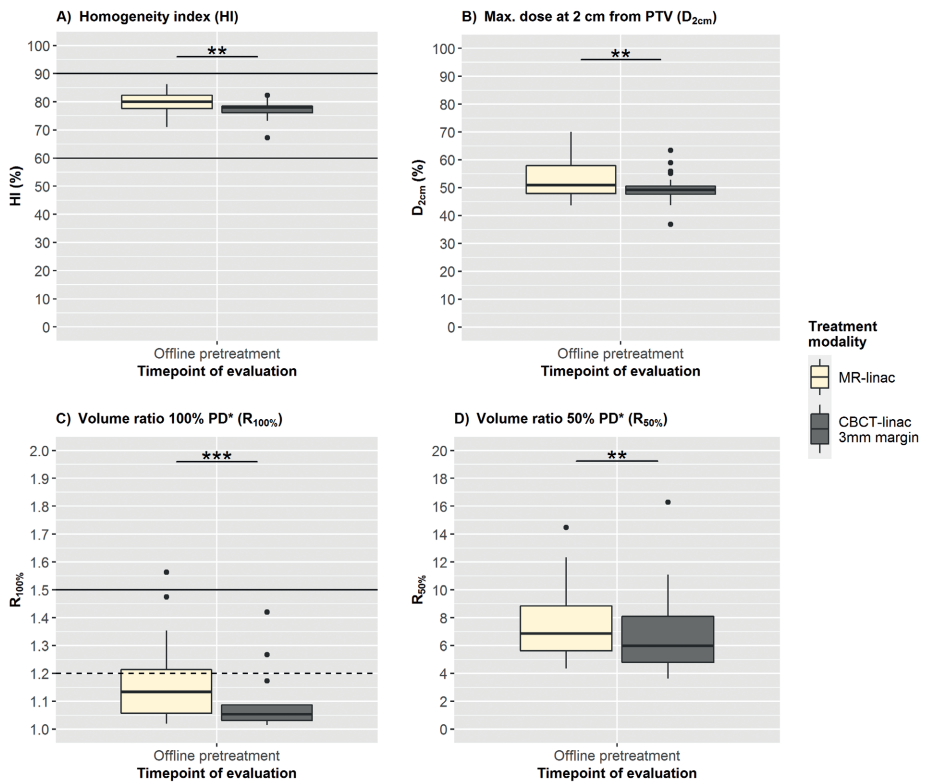
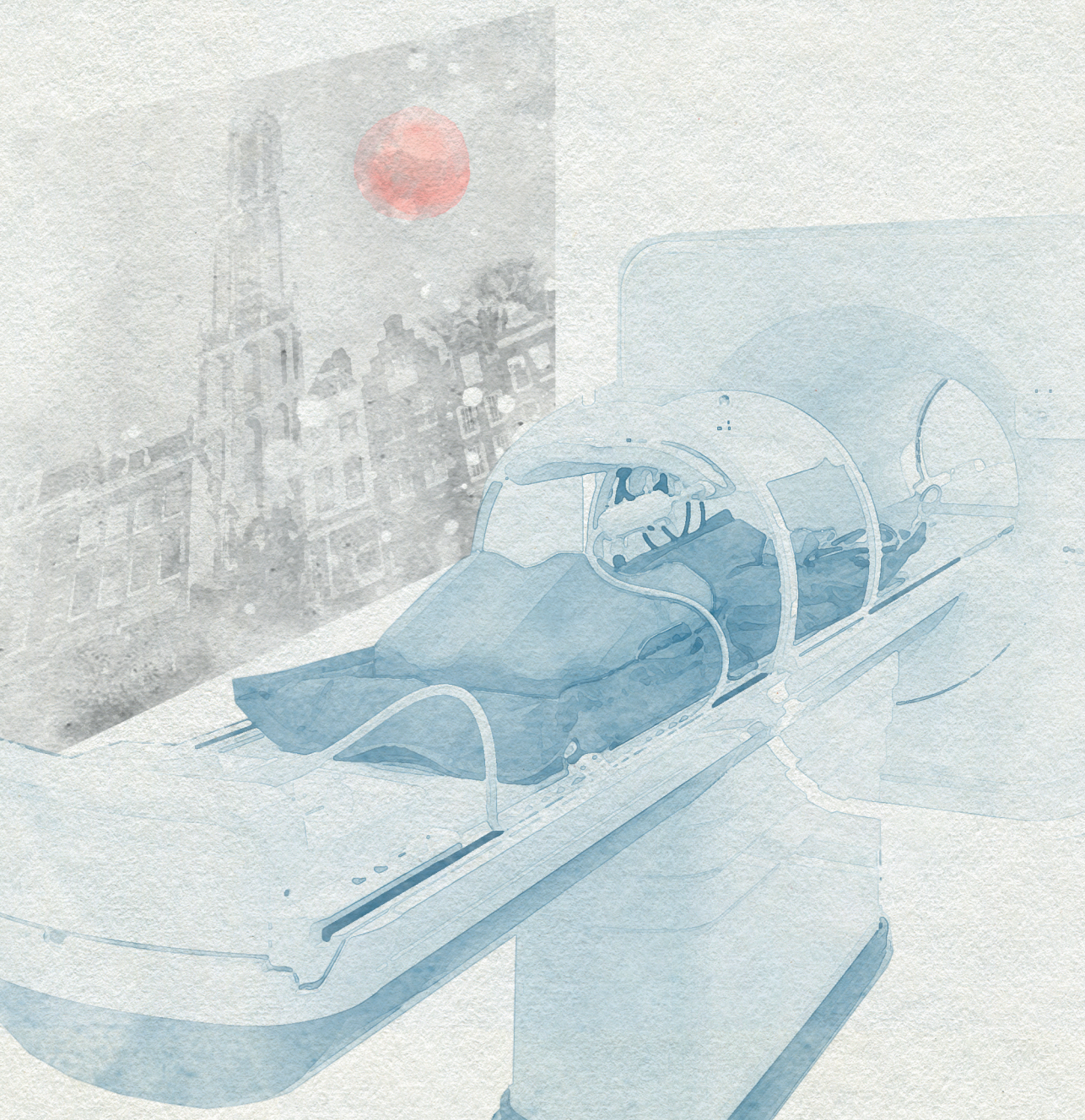


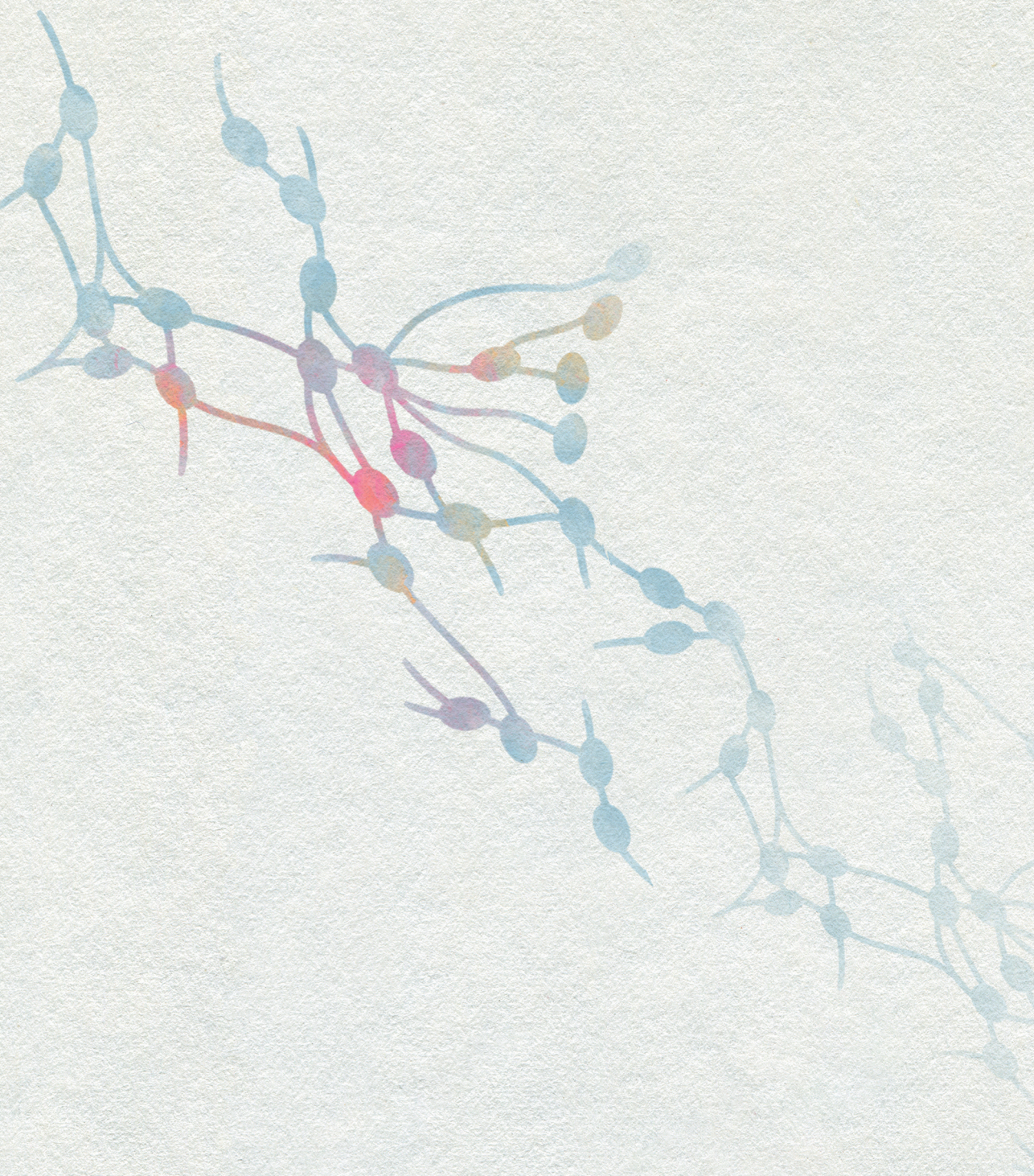
Figure S3

Plan conformity/quality evaluation of MR-linac and CBCT-linac SBRT for lymph node oligometastases. A) homogeneity index (HI), B) maximum dose at 2 cm from PTV (D_{2cm}) relative to actual prescription dose (PD*, calculated as dose received by 95% of PTV), C) volume ratio of volume receiving 100% of PD* to PTV ($R_{100\%}$) and D) volume ratio at 50% of PD* ($R_{50\%}$). Results for offline pretreatment plans are shown for MR-linac and CBCT-linac, both with 3 mm PTV margins. In subfigure A, the solid lines indicate the acceptable values of HI, all outcomes were in the acceptable range. In subfigure C, values below the solid line are acceptable values and values below the dashed line are preferred values. Acceptable and preferred values are not plotted for D_{2cm} and $R_{50\%}$ as they depend on PTV volume (the target values are supplied as Supplementary Material: Table S2). D_{2cm} values were acceptable for both modalities for all patients. Asterisks depict significant differences in parameters between MR-linac and CBCT-linac plans (Mann-Whitney U-test (two-sided), * $p < 0.05$, ** $p < 0.01$, *** $p < 0.001$).



Part II

**Treatment outcomes and
patient selection**



Chapter 7

Progression-free survival in patients with 68 Ga-PSMA-PET-directed SBRT for lymph node oligometastases

Anita M. Werensteijn-Honingh, Anne F.J. Wevers, Max Peters, Petra S. Kroon, Martijn Intven, Wietse S.C. Eppinga, Ina M. Jürgenliemk-Schulz.

Acta Oncol 2021;60:1342-51.

<https://doi.org/10.1080/0284186X.2021.1955970>.

Abstract

Background: Prostate cancer oligometastatic disease can be treated using stereotactic body radiotherapy (SBRT) in order to postpone start of systemic treatments such as androgen deprivation therapy (ADT). ^{68}Ga -PSMA-PET/CT imaging allows for diagnosis of oligometastases at lower PSA values. We analysed a cohort of patients with prostate cancer lymph node oligometastases detected on PSMA-PET/CT.

Material and Methods: Ninety patients with metachronous oligometastatic prostate cancer received SBRT for 1-3 lymph node metastases diagnosed on ^{68}Ga -PSMA-PET/CT. The primary end point was progression free survival (PFS), with disease progression defined as occurrence of either target lesion progression, new metastatic lesion or biochemical progression. Secondary outcomes were biochemical PFS (BPFS), ADT-free survival (ADT-FS), toxicity and quality of life (QoL). Baseline patient characteristics were tested for association with PFS and a preliminary risk score was created.

Results: Median follow-up was 21 months (interquartile range 10-31 months). Median PFS and BPFS were 16 and 21 months, respectively. Median ADT-FS was not reached (73% (95%-CI 62-86%) at 24 months). In multivariable analysis, younger age, higher PSA prior to SBRT and extrapelvic location were associated with shorter PFS. Grade 1 fatigue was the most predominant acute toxicity (34%). Highest grade toxicity was grade 2 for acute and late events. QoL analysis showed mild, transient increase in fatigue at 1-4 weeks after SBRT.

Conclusion: A median PFS of 16 months was attained after SBRT for patients with PSMA-PET positive oligometastatic lymph nodes from prostate cancer. Higher pre-SBRT PSA, younger age and extrapelvic location were found to be predictors of shorter PFS.

Introduction

Stereotactic body radiotherapy (SBRT) has gathered increasing interest as a local treatment option for patients with oligometastatic prostate cancer. It reduces the chance of disease progression after 6 months from 61% with observation alone, to 19% with SBRT, and can defer the start of androgen deprivation therapy (ADT) with a median period of 8 months [1,2]. Moreover, a survival benefit has been shown compared to palliative standard-of-care for patients with oligometastases from a range of primary tumour histologies [3].

With the advent of 68-gallium prostate-specific membrane antigen (PSMA) positron emission tomography (PET) imaging, prostate cancer oligometastases can be diagnosed with greater sensitivity compared with choline PET imaging, especially in patients with PSA <2 ng/mL [4-6]. In the ORIOLE trial, patients were treated on metastatic lesions diagnosed on conventional imaging, but also underwent PSMA-PET imaging prior to treatment. Patients who did not have any additional (untreated) lesions on PSMA-PET showed fewer new metastases at 6 months after SBRT (16% vs. 63%) [2].

However, even with PSMA-PET imaging, failure remains frequent after SBRT for oligometastases: recently reported progression-free survival (PFS) rates at 12 and 24 months were 46-73% and 16-73%, respectively [6-12]. To counteract undetected microscopic tumour spread, intermittent or continuous ADT can be added to metastasis-directed therapy (MDT), which can improve (biochemical) PFS [13-15]. ADT, however, influences quality of life (QoL) and seems counterintuitive to the application of MDT in trying to postpone systemic therapy [1,16]. Prediction of oncological outcomes could help physicians and patients in their shared decision making regarding SBRT with/without ADT [17]. Tumour biology shows great promise for oligometastatic patient selection but it is not ready to be used in a clinical setting [2,18-19]. Our aim was to report outcomes after PSMA-PET directed SBRT for lymph node oligometastases and find predictors of PFS to improve patient selection using baseline characteristics.

Material and Methods

Patients and treatment

We included patients with up to five metachronous ⁶⁸Ga-PSMA-PET/CT-detected prostate cancer lymph node oligometastases who were treated with SBRT and had >3 months of follow-up. All patients gave written informed consent for participation in a single centre, retrospective/prospective cohort study approved by the local medical ethics committee (www.trialregister.nl/trial/9252). Exclusion criteria were simultaneous local tumour

recurrence (including seminal vesicle recurrence), non-nodal metastases, previous polymetastatic disease or ADT up to 24 months before the current diagnosis.

Patients were treated between October 2016 and October 2020, with a prescribed dose of 5x 7 Gy or 3x 10 Gy to 95% of the planning target volume (PTV). ⁶⁸Ga-PSMA-PET/CT scans were acquired at multiple centres and were all assessed by nuclear medicine radiologists. Pre-treatment tumour delineation was based on PET/CT and MRI after image fusion with the planning CT scan. Gross Tumour Volume (GTV) consisted of the target lymph node(s) and GTVs were expanded with a 3-8 mm PTV margin, depending on nodal region, treatment machine, visibility of the target and distance between GTVs. Patients were treated on CBCT-linac (Agility, Elekta AB, Stockholm, Sweden) or on 1.5 T MR-linac (Unity, Elekta AB) [20]. Since the clinical introduction of the MR-linac at our department in August 2018, patients were treated on the MR-linac except for patients with exclusion criteria for MR-linac delivery, such as an inability to lie still for 60 minutes. Vacuum cushion immobilization was used for all patients until March 2019; we then investigated effect on target motion [21]. After March 2020, patients with single pelvic targets did not receive immobilization when treated on MR-linac, as the immobilization was found to offer no advantage during MR-linac treatment for these patients [21]. Follow-up after 3 months was at the discretion of the urologist for most patients; patients received a questionnaire every 6 months to register grade ≥ 3 late toxicities.

Patients undergoing SBRT from July 2018 onwards were included prospectively and were additionally monitored using QoL questionnaires (European Organization for Research and Treatment of Cancer (EORTC) C30, EuroQol EQ-5D-5L and Multidimensional Fatigue Inventory (MFI)) before start of treatment, at 1 and 4 weeks, at 3 and 6 months after SBRT and then every 6 months thereafter [22-24]. Completion of baseline QoL questionnaires was mandatory for further QoL questionnaire participation.

In case of repeat oligorecurrences after SBRT, patients were eligible to be treated with another cycle of SBRT, with a maximum of five metastatic lymph nodes per SBRT cycle. QoL questionnaires were restarted at each SBRT cycle.

Definition of baseline characteristics

Oligometastatic disease classification was according to the European Society for Radiotherapy and Oncology (ESTRO)-EORTC recommendation [25]. Pelvic region was defined as caudal of the aortic bifurcation. Primary therapy was categorized into robotic-assisted laparoscopic prostatectomy (RALP), with or without salvage radiotherapy; and radiotherapy, either external beam radiotherapy (EBRT) or brachytherapy (BT). Previous lymph node dissection was investigated as a combination of lymph node dissections at the

time of primary therapy and salvage lymph node dissections. Therapeutic free interval was time between the last treatment and current diagnosis. Time to first oligometastasis was measured from primary tumour diagnosis (date of biopsy, if available) to the first oligometastasis. PSA doubling time (PSADT) was calculated using the Memorial Sloan Kettering Cancer Center tool (www.mskcc.org/nomograms/prostate/psa-doubling-time), with ≥ 3 PSA measurements over a period of ≥ 3 months and individual measurements ≥ 4 weeks apart [26].

Oncological outcomes

The primary end point was progression free survival (PFS), defined as a composite endpoint as in the ORIOLE trial: either progression of a target lesion, a newly diagnosed metastasis or biochemical progression [2]. Progression of a target lesion was defined as an increase in short axis diameter $>20\%$ and >5 mm [1]. Secondary outcomes for this analysis were biochemical PFS (BPFS), ADT-FS, widespread PFS (WS-PFS), local control, acute and late toxicity and QoL. Biochemical progression was defined as a PSA rise >2 ng/ml above the lowest value after SBRT or the pre-SBRT value [2]. ADT-FS was measured from end of SBRT to the start of ADT. Widespread progression was investigated as metastatic disease that is no longer amenable to further local treatment [27]. For this study, widespread progression was defined as any progression that was not followed by another cycle of lymph node SBRT. Local control was defined as absence of progression of a target lesion. Physician-reported toxicity was according to the guidelines of the Common Terminology Criteria for Adverse Events v 5.0; acute toxicity was defined as toxicity within 3 months after SBRT.

Statistical analysis

The open source R software package (v 3.6.3) was used (R Foundation for Statistical Computing, Vienna, Austria; www.R-project.org). Data analysis and reporting was according to the TRIPOD statement [28]. Multiple imputation was used for missing baseline characteristics. The *mice* package was used to create 100 imputed datasets; both baseline characteristics and oncological outcomes were used for imputation (Supplementary material: Table S1). Pooled results from imputed baseline characteristics were used for subsequent analyses. Sensitivity analysis included complete case analysis. No imputation was performed for QoL data.

Oncological outcomes were analysed using Kaplan-Meier survival analysis, with *survival* and *survminer* packages, with log-rank tests to compare differences between subgroups. Model development and validation was done with the *rms* package. Cox proportional hazard regression was used to identify baseline characteristics that were associated with PFS. Hazard ratios and 95% confidence intervals (CI) were calculated. Continuous variables were kept at their original scale. Significant variables in univariable analysis ($p < 0.05$)

and age were compared with published literature to select variables for the multivariable model. Backward elimination of variables based on Akaike's information criterion (AIC) was used to construct the final multivariable model, retaining only the parameters that yielded the lowest AIC value when combined, allowing one variable per 10 events [29]. Correlation between variables was investigated. For continuous variables, proportional hazard assumption was assessed through Schoenfeld residuals and linearity through Martingale residuals. Proportional hazard assumption for categorical variables was checked using log-log curves.

We performed internal validation of the model using the *rms* package by creating 2000 bootstrap resamples of the imputed datasets and calculated the apparent and optimism-corrected C-statistic [30]. Due to the small sample size in this study, we did not create a nomogram for PFS. We constructed risk groups for PFS, based on the linear predictor of the final multivariable model.

Results

We included 90 patients, out of which data was prospectively collected for 68% (Supplementary material: Figure S1). Patients had metachronous (89%) or repeat (11%) oligorecurrences, with a median time to first oligometastasis of 59 months (Table 1). Most patients had RALP as primary treatment (73%). Thirty-nine percent of patients had a pelvic lymph node dissection prior to this study, either at the time of primary treatment or as a salvage lymph node dissection. Patients with T3-T4 stage tumours had a previous lymph node dissection in 58% of the cases; for patients with T1-T2 stage tumours this was 29%. For each group, the median of removed lymph nodes was 12. None of the patients in our study previously received whole pelvic radiotherapy.

Patients had up to three lymph node metastases for the first SBRT cycle in this study; metastatic disease was confined to the pelvis in 93% of patients. In total 116 SBRT cycles have been applied: 20 patients underwent a second SBRT cycle, five patients a third cycle and one patient a fourth cycle. A total of 177 lymph node metastases have been treated, of which 41 lymph nodes (23%) had a short axis diameter ≥ 10 mm on MRI, in 32 patients. Fifty patients have been treated using the MR-linac for at least one SBRT cycle.

Table 1

Baseline patient characteristics at the time of the first SBRT treatment for lymph node oligometastases at our center (N=90).

Baseline characteristics	N (%)	Median (IQR)	N missing (%)
Age (years)		71 (67-74)	0 (0)
Karnofsky performance score	39 (43)		51 (57)
90-100	36 (40)		
70-80	3 (3)		
Oligometastases classification	90 (100)		0 (0)
Metachronous oligorecurrence	80 (89)		
Repeat oligorecurrence	10 (11)		
Time to first oligometastasis (months)		59 (38-92)	0 (0)
Therapeutic free interval (months)		41 (18-61)	0 (0)
Primary T-stage	74 (82)		16 (18)
T1	20 (22)		
T2	35 (39)		
T3-4	19 (21)		
Primary Gleason score	89 (99)		1 (1)
<7	17 (19)		
7	51 (57)		
>7	21 (23)		
Primary treatment	90 (100)		0 (0)
RALP only	29 (32)		
RALP + salvage/adjvant EBRT	37 (41)		
Brachytherapy	9 (10)		
EBRT only	7 (8)		
EBRT + adjuvant ADT	8 (9)		
Previous lymph node dissection	90 (100)		0 (0)
Yes, combined with RALP	26 (29)		
Yes, combined with EBRT	2 (2)		
Yes, salvage lymph node dissection	7 (8)		
No	55 (61)		
Resection margin status RALP	66 (100)		0 (0)
R0	36 (55)		
R1	30 (45)		
Initial PSA before primary treatment (ng/mL)		10 (6-17)	4 (4)
PSA nadir after primary treatment (ng/mL)		0.0 (0.0-0.2)	2 (2)
Pre-SBRT PSA (ng/mL)		1.3 (0.6-2.7)	0 (0)

Table 1 (continued)

Baseline characteristics	N (%)	Median (IQR)	N missing (%)
Pre-SBRT PSA doubling time (months)		9 (6-15)	15 (17)
Highest nodal region			
Lower pelvic level	69 (77)		0 (0)
Common iliac level	13 (14)		
Extrapelvic	8 (9)		
Number of nodal targets	90 (100)		0 (0)
1	56 (62)		
2	27 (30)		
3	7 (8)		
Short axis diameter (mm)			
Mean of GTVs per patient		8.0 (6.7-9.7)	0 (0)
Sum of GTVs per patient		10.0 (7.5-16.4)	0 (0)
Nodal target volume (mL)			
Mean of GTVs per patient		0.8 (0.5-1.5)	0 (0)
Sum of GTVs per patient		1.1 (0.6-2.4)	0 (0)
Fractionation schedule	90 (100)		0 (0)
3 x 10 Gy	9 (10)		
5 x 7 Gy	80 (89)		
6 x 6 Gy	1 (1)		
Treatment machine	90 (100)		0 (0)
CBCT-linac	51 (57)		
MR-linac	39 (43)		

IQR: interquartile range; RALP: robot-assisted laparoscopic radical prostatectomy; EBRT: external beam radiotherapy; ADT: androgen deprivation therapy; R0/R1: positive/negative resection margins at RALP; PSA nadir: lowest PSA after primary treatment; GTV: gross tumor volume.

Median follow-up time was 21 months (interquartile range 10-31 months). One patient died during follow-up due to newly diagnosed lung cancer. Disease progression was observed in 54 patients. Median (95% CI) survival times were 16 (12-19), 21 (17-34) and 19 (16-37) months for PFS, BPFS and WS-PFS, respectively (Figure 1). Median ADT-FS was not reached, ADT-FS at 24 months was 73% (95% CI 62-86%). In univariable analysis, higher T-stage, RALP as primary treatment, lower PSA at current diagnosis and metastases limited to the pelvic nodal region were associated with longer PFS (Table 2). Patients with a PSA \leq 2 ng/mL before SBRT had longer PFS, especially when compared with PSA >4 ng/mL (median PFS 18 vs. 6 months); no difference was observed in PFS of patients with respect to PSADT or Gleason score (Table 2, Supplementary material: Figure S2).

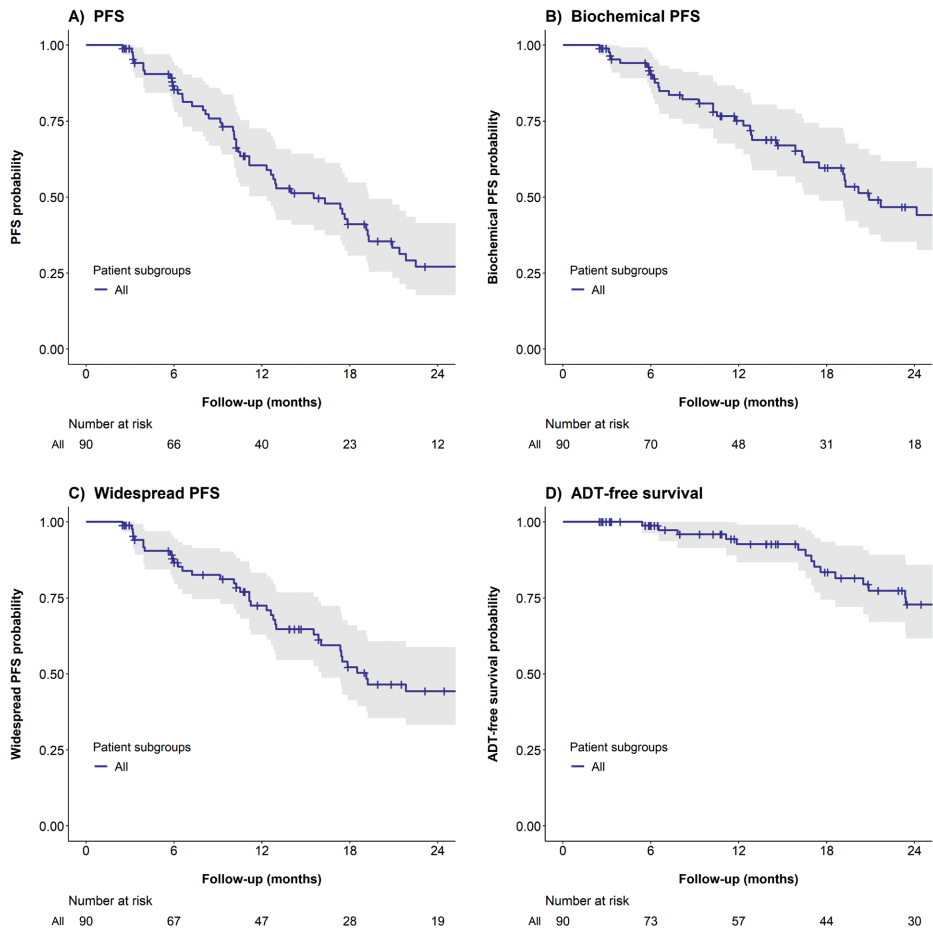


Figure 1. Kaplan-Meier survival estimates of four oncological outcomes after SBRT for prostate cancer lymph node oligometastases. PFS: progression free survival (composite endpoint including also biochemical progression, start of ADT and death due to disease progression); biochemical PFS: PSA rise $\geq 2 \mu\text{g/L}$ compared to lowest PSA value after SBRT (or baseline PSA); widespread PFS: disease progression not amenable to renewed SBRT treatment; ADT-free survival: survival until start of ADT. 95% confidence intervals were plotted as ribbons around the survival estimates.

Table 2

Univariable and multivariable analysis of factors associated with progression free survival.

Variable comparison	Univariable analysis			Multivariable analysis		
	HR	95% CI	p	HR	95% CI	p
Age	0.96	0.91-1.01	0.13	0.91	0.86-0.97	<0.01
KPS 70-80 vs 90-100	0.68	0.30-1.53	0.34			
Time to first oligometastasis	1.00	1.00-1.01	0.48			
Repeat vs metachronous oligorecurrence	1.45	0.64-3.29	0.37			
Therapeutic free interval	1.00	0.99-1.01	0.37			
T2 vs T1	0.44	0.23-0.85	0.02			
T3-T4 vs T1	0.27	0.12-0.61	<0.01			
Gleason <7 vs 7	0.51	0.21-1.20	0.12			
Gleason >7 vs 7	0.55	0.26-1.13	0.10			
Radiotherapy (EBRT/BT) vs RALP	2.00	1.05-3.79	0.04	1.99	0.91-4.34	0.08
Previous LND vs no LND	0.69	0.39-1.20	0.18			
R1 vs R0	1.47	0.77-2.80	0.24			
iPSA (initial PSA from primary diagnosis)	1.00	0.98-1.02	0.78			
PSA nadir (lowest after primary treatment)	1.08	0.74-1.56	0.69			
PSA at current diagnosis	1.39	1.21-1.60	<0.01	1.42	1.20-1.68	<0.01
PSADT at current diagnosis	0.98	0.94-1.01	0.20			
(Also) other nodal region vs pelvic only	5.43	2.17-13.62	<0.01	4.52	1.73-11.85	<0.01
3 vs 1-2 nodal target(s)	2.64	1.00-6.98	0.05			
Mean GTV short axis diameter	0.95	0.85-1.07	0.39			
Sum of GTV short axis diameters	1.02	0.98-1.07	0.33			
Mean GTV volume	1.00	0.85-1.18	0.95			
Sum of GTV volumes	1.06	0.93-1.21	0.36			

HR: hazard ratio; CI: confidence interval; EBRT: external beam radiotherapy; BT: brachytherapy; RALP: robot-assisted laparoscopic radical prostatectomy; LND: lymph node dissection; R1/R0: positive/negative resection margins at RALP; iPSA: initial PSA at time of primary tumor diagnosis; PSA nadir: lowest PSA after primary treatment; PSADT: PSA doubling time; GTV: gross tumor volume. Significant results ($p < 0.05$) are shown in bold.

We selected age, PSA at current diagnosis, nodal region and type of primary treatment as parameters for the final multivariable model. Higher age, lower PSA and pelvic nodal region remained significantly associated with longer PFS. Calibration plots at 12, 18 and 24 months showed good concordance of the observed and predicted PFS (Supplementary material: Figure S3). Based on the final multivariable model, we constructed 2 risk groups (Figure 2). The linear predictor L of the model can be calculated according to Eq. (1):

$$L = -0.09 \times A + 0.35 \times P + 1.51 \times R + 0.69 \times T + 5.63 \quad (1)$$

Where A is the patient age (years), P is the current PSA value (ng/mL), R is the nodal region (1 extrapelvic, 0 pelvic) and T is the treatment type (1 radiotherapy, 0 RALP).

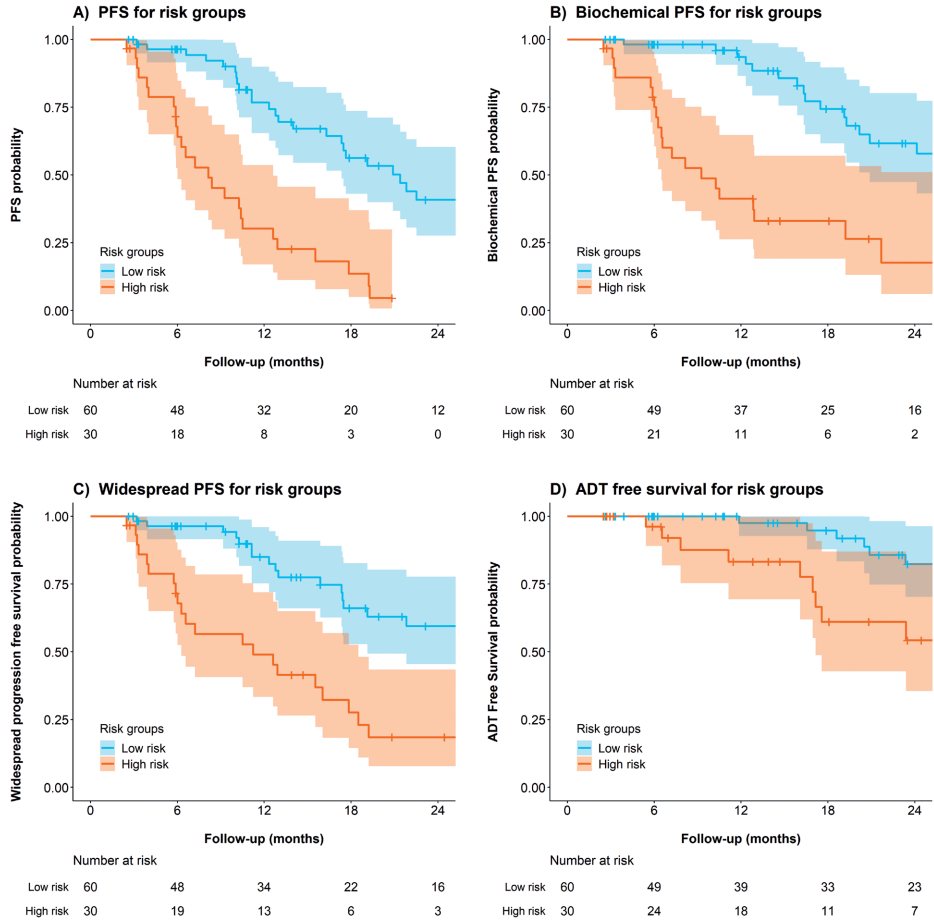


Figure 2. Progression free survival for the risk group based on quantiles of the linear predictor of the final multivariable model. The patients were divided into two risk groups (creating a 2:1 distribution) based on the multivariable model derived in this study. The observed progression free survival was then plotted for each risk group, with 95% confidence intervals displayed as ribbons.

The linear predictor L can be calculated using the following formula:

$$L = -0.09 \times A + 0.35 \times P + 1.51 \times R + 0.69 \times T + 5.63$$

Where A is the patient age (years), P is the current PSA value (ng/mL), R is the nodal region (1 extrapelvic, 0 pelvic) and T is the treatment type (1 radiotherapy, 0 RALP).

Low risk is depicted by $L < 0.19$, high risk is depicted by $L \geq 0.19$.

A 2:1 distribution of linear predictors was chosen after visual inspection, as it allowed the best stratification of observed PFS (compared with 1:2:1/1:1 distributions), with 60 patients classified as low risk and 30 as high risk. Low risk was depicted by score < 0.19 , high risk was depicted by score ≥ 0.19 . Median PFS (95% CI) was 21 (17-35) and 8 (6-13) months for low and high risk groups, respectively (Figure 2). Similar differences between the risk groups were also observed for BPFS, WS-PFS and ADT-FS. The apparent C-statistic for model performance was 0.71, after internal validation the mean optimism-corrected C-statistic was 0.69.

Progression of a target lesion was not observed. For five patients (6%), biochemical progression occurred without any further imaging available. After pelvic lymph node SBRT, 51% of patients with progression had metastases outside the pelvic lymph nodes. The number of patients with extrapelvic or non-nodal progression was similar for both risk groups and was also similar for patients with and without a previous lymph node dissection (data not shown). Twelve percent of patients had progression limited to lymph nodes in the same pelvic sub-region as before (classified as lower pelvic region left and right (comprised of internal and external iliac and obturator regions), presacral or mesorectal region and common iliac region left and right). A shorter PFS was observed after SBRT for repeat oligometastatic disease compared with newly diagnosed oligometastatic disease: median PFS (95% CI) was 9 (7-18) vs. 17 (13-21) months, respectively (Figure 3).

One patient had a PSA bounce after SBRT, with a PSA increase of 2.9 ng/mL. No suspect lesions were seen on PSMA-PET and PSA spontaneously declined afterwards.

Grade 1 and 2 acute toxicity were reported in 41% and 3% of the treatments, with grade 1 fatigue in 34% of treatments (Supplementary material: Table S2). Grade 2 acute toxicity comprised non-infective cystitis in two patients after previous salvage EBRT to the prostate bed, and grade 2 fatigue in one patient. Grade 1 and 2 late toxicity was reported for 15% and 7% of patients. Grade 2 late toxicity comprised non-infective cystitis for three patients, proctitis with bloody stools in two patients, an increase in urinary incontinence in two patients and lower back pain for one patient. All patients with late grade 2 toxicity had undergone previous salvage EBRT. No grade 3 or higher events were observed. No significant differences were observed in toxicity stratified by number of SBRT cycles (Supplementary material: Tables S3 and S4).

QoL data was available from 58 SBRT cycles of 49 patients. Patients reported an increase in fatigue at 1-4 weeks after SBRT which was resolved at 3-6 months (Supplementary material: Figure S4). Overall health status and physical functioning were unaffected. Investigation of fatigue subdomains showed mainly reduced activity after SBRT, which was resolved at 6 months (Supplementary material: Figure S5) [23].

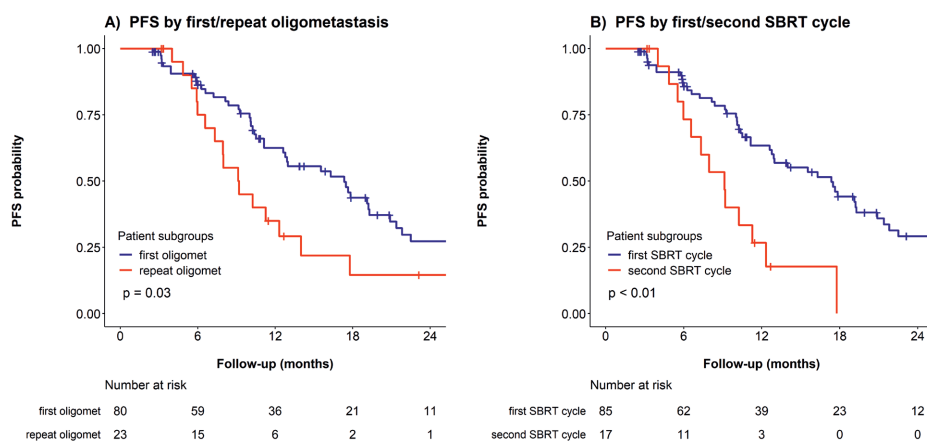


Figure 3. Kaplan-Meier survival estimates of progression free survival (PFS), stratified by oligometastatic disease characteristics: A) first vs. repeat oligometastases* and B) first vs. second SBRT cycle for oligometastases. In subfigure A, ‘first oligomet’ refers to patients with a first diagnosis of oligometastases (metachronous oligorecurrences, N=80) and ‘repeat oligomet’ refers to patients with repeat oligometastases (repeat oligorecurrences, N=23). PFS was recalculated from the end of the second SBRT cycle for 13 patients who underwent repeated SBRT. In subfigure B, data from four patients who had undergone a single SBRT cycle for previous oligometastatic disease in another center was combined with the data from the second SBRT cycle of the 13 patients who underwent two sequential SBRT cycles at our center. One patient was excluded from the graph in subfigure B as he had already undergone two previous SBRT cycles at another center. * Repeat oligometastases = previously treated oligometastases, regardless of treatment modality. Log-rank test p-values for comparisons between subgroups are included.

Discussion

With a PSMA-PET cohort of patients with prostate cancer lymph node oligometastases, we report median PFS and BPFS of 16 and 21 months after SBRT, with 73% of patients free of ADT at 24 months. Toxicity was limited to grade 1-2, with mild, transient fatigue reported in both toxicity and QoL. Our definition of PFS was comparable to the definition used in the ORIOLE trial, in which median PFS after SBRT was not reached with a median follow-up of 19 months [2]. In the ORIOLE trial, patients had 1-3 metastases diagnosed with conventional imaging (CT/MRI/bone scintigraphy). Patients in our study had lymph node metastases with a median short axis diameter of 8 mm, so most lesions would probably not have been identified with conventional imaging yet. The shorter PFS in our PSMA-PET diagnosed population shows that the risk of microscopic tumour spread beyond detectable (oligo)metastases may not have been reduced due to the use of PSMA-PET imaging. A wide range of median (B)PFS has been reported after PSMA-PET directed SBRT monotherapy, from 10 to 22 months [6,7]. These outcomes are very comparable to (B)PFS after choline-PET directed SBRT [1,6,32]. ADT-FS seems to be longer when using PSMA-PET to guide SBRT compared with choline-PET, but this may be an effect of stage migration with more

sensitive PSMA-PET imaging at lower PSA levels [6]. Thus, PSMA-PET imaging may have influenced the patient population treated for prostate cancer oligometastases but it has not increased the median period of PFS after SBRT.

To aid in patient selection, we have developed a preliminary risk classification that divides patients into low and high risk of progression after SBRT, with median PFS of 21 and 8 months, respectively. Higher age, lower PSA values and metastatic disease limited to the pelvic lymph nodes were associated with longer PFS after SBRT. Previous reports on predictors of PFS from literature were taken into account in building the model. We did not find an association between primary tumour Gleason score and PFS, which was consistent with previous studies [10,15,32]. Higher primary tumour T-stage was significantly associated with longer PFS based on univariable analysis in our cohort, whereas an opposite relation was found previously [10]. We excluded T-stage from our multivariable model for this reason. The association between number of target metastases (1-2 vs. 3) and PFS was borderline significant in univariable analysis ($p=0.05$), it was eliminated from the final multivariable model as it did not contribute to the model based on AIC value. Lower pre-SBRT PSA, especially PSA <2 ng/mL, was associated with longer PFS in our study (Supplementary material: Figure S3), which is consistent with other reports [7,33]. Patients with extrapelvic versus only-pelvic lymph node metastases had median PFS of 7 vs. 17 months, which coincides with median PFS of 6 vs. 15-18 months reported previously [32]. Finally, radiotherapy versus RALP as primary therapy for prostate cancer was included in our model as a predictor of shorter PFS; although it was not significantly associated with PFS in multivariable analysis, it did contribute to the model. Primary therapy as predictor of PFS is in line with results from a large retrospective analysis [34]. This finding could be related to general patient characteristics, such as age and comorbidity, that may have influenced the choice of therapy at the time of primary tumour diagnosis: an overall survival benefit of patients treated with RALP versus radiotherapy was found in a meta-analysis of non-randomized studies, but was not observed in the randomized PROTECT trial [35,36]. For prediction purposes, this potential bias associated with primary therapy can be incorporated in a risk score, a causal relationship is not necessary for this purpose. However, these results will need to be validated in an external cohort to ascertain the applicability in other clinical situations than the one on which the model was based. It seems from literature this bias is persistent, therefore it has been included in the prediction models.

An important limitation of the current study is the small sample size, which made it impossible to construct a nomogram to predict PFS for individual patients. Furthermore, we used univariable analysis to guide model development, which underlines the need for external validation of this model. Follow-up after SBRT was non-standardized; in

4% of the cases with biochemical progression no PSMA-PET scan was available during follow-up. Interpretation of ADT-FS is limited by the lack of uniform clinical management with regards to the start of ADT, usually ADT was started with a PSA doubling time of approximately 3 months, a PSA of approximately 20 or symptomatic progression. This limits the ability to compare our results with the ADT-FS of 21 months that was reported in the STOMP trial, in which stricter guidelines for start of ADT were used [1]. Finally, we did not investigate biological tumour characteristics in this study, which could further improve patient selection [2].

In our study, half of the patients with progression after SBRT had extrapelvic or non-nodal metastases at the time of first progression. This is concordant with previous reports, with 54% - 69% extrapelvic or non-nodal progressions after choline-PET directed SBRT [33,34]. Thus, the pattern of progression does not seem to have changed as a result of PSMA-PET guidance and our risk classification could not predict the pattern of progression. Thus the addition of an elective treatment field, such as whole pelvic radiotherapy (WPRT), thus remains a clinical debate in which prevention of pelvic nodal relapses should be weighed against the increased risk of toxicity [34]. The STORM/PEACE V trial (NCT0356924) may shed additional light on this: it randomizes patients between metastasis-directed therapy with 6 months of ADT with or without WPRT [37]. Furthermore, the POP-RT trial (NCT02302105) has recently shown a prolonged disease free survival after addition of WPRT to prostate EBRT in the primary treatment of patients with a high risk of pelvic lymph node involvement [38]. A large reduction of pelvic relapses and also a reduction in extrapelvic relapses was observed in the WPRT group as compared to prostate-only EBRT. An increased use of WPRT for patients with high risk of pelvic lymph node involvement in the future could impact the population of patients with prostate cancer oligometastases compared to our series, given the number of patients with pelvic-only disease in our study (91%). However, 73% of our study population consisted of patients that underwent RALP as primary treatment and we have estimated that only about 41% of our patients would have had a large enough risk of lymph node involvement to have been eligible for inclusion in the POP-RT trial.

Addition of 6-12 months of ADT to the SBRT has been shown to defer the onset of new metastases after SBRT and has even shown a survival benefit in the setting of salvage lymph node dissections [14,39]. ADT could suppress microscopically spread tumour cells that are likely present in many oligometastatic patients, even with PSMA-PET imaging. The addition of 6 months of ADT to SBRT is currently investigated in the ADOPT trial (NCT04302454) and will be mandatory in both arms of the STORM/PEACE V trial (NCT0356924) [37]. However, patients may still be reluctant to undergo temporary ADT due to the side effects [16]. After the first 6 months of intermittent ADT, recovery of serum testosterone levels

to non-castrate levels takes another 3-4 months and 6 months to recover to normal levels [40,41]. Especially for low risk patients, SBRT monotherapy might remain a valid treatment option for patients that are reluctant to receive (temporary) ADT.

In conclusion, we have shown that large differences exist in PFS after SBRT for prostate cancer lymph node oligometastases diagnosed with PSMA-PET. Patients with higher age, lower pre-SBRT PSA values and nodal metastases limited to the pelvis have longer PFS (median 21 months) after SBRT. Toxicity was limited to grade 1-2 and only mild, transient fatigue was reported by patients as influencing their quality of life.

Acknowledgements

The authors are grateful to Dr. Simon Woodings for comments on the manuscript.

Funding

This work was supported by the Dutch Cancer Society under Grant 2015-0848.

Disclosure of interest

The authors declare the following financial interests/personal relationships which may be considered as potential competing interests: The overarching University Medical Center Utrecht MR-linac scientific project, including employment of multiple authors, has been partly funded by Elekta AB (Stockholm, Sweden). Elekta did not have any part in the design, execution or analysis of this study. Max Peters declares a grant received in August 2017 from the Dutch Cancer Society for the phase 2 PRECISE study regarding focal salvage brachytherapy for radiorecurrent prostate cancer, outside the submitted work. The authors declared that there is no other conflict of interest.

References

- 1) Ost P, Reynnders D, Decaestecker K, Fonteyne V, Lumen N, De Bruycker A, et al. Surveillance or Metastasis-Directed Therapy for Oligometastatic Prostate Cancer Recurrence: A Prospective, Randomized, Multicenter Phase II Trial. *J Clin Oncol* 2018;36:446-53. <https://doi.org/10.1200/JCO.2017.75.4853>.
- 2) Phillips R, Yue Shi W, Deek M, Radwan N, Jin Lim S, Antonarakis ES, et al. Outcomes of Observation vs Stereotactic Ablative Radiation for Oligometastatic Prostate Cancer: The ORIOLE Phase 2 Randomized Clinical Trial. *JAMA Oncol* 2020;6:650-9. <https://doi.org/10.1001/jamaoncol.2020.0147>.
- 3) Palma DA, Olson R, Harrow S, Gaede S, Louie AV, Haasbeek C, et al. Stereotactic Ablative Radiotherapy for the Comprehensive Treatment of Oligometastatic Cancers: Long-Term Results of the SABR-COMET Phase II Randomized Trial. *J Clin Oncol* 2020;38:2830-8. <https://doi.org/10.1200/JCO.20.00818>.
- 4) Fodor A, Lancia A, Ceci F, Picchio M, Hoyer M, Jerezek-Fossa BA, et al. Oligorecurrent prostate cancer limited to lymph nodes: getting our ducks in a row : Nodal oligorecurrent prostate cancer. *World J Urol* 2019;37:2607-13. <https://doi.org/10.1007/s00345-018-2322-7>.
- 5) Moghul M, Somani B, Lane T, Vasdev N, Chaplin B, Peedell C, et al. Detection rates of recurrent prostate cancer: 68 Gallium (Ga)-labelled prostate-specific membrane antigen versus choline PET/CT scans. A systematic review. *Ther Adv Urol* 2019;11:1756287218815793. <https://doi.org/10.1177/1756287218815793>.
- 6) Mazzola R, Francolini G, Triggiani L, Napoli G, Cuccia F, Nicosia L, et al. Metastasis-directed Therapy (SBRT) Guided by PET-CT 18 F-CHOLINE Versus PET-CT 68 Ga-PSMA in Castration-sensitive Oligorecurrent Prostate Cancer: A Comparative Analysis of Effectiveness. *Clin Genitourin Cancer* 2021;19:230-6. <https://doi.org/10.1016/j.clgc.2020.08.002>.
- 7) Kneebone A, Hruba G, Ainsworth H, Byrne K, Brown C, Guo L, et al. Stereotactic Body Radiotherapy for Oligometastatic Prostate Cancer Detected via Prostate-specific Membrane Antigen Positron Emission Tomography. *Eur Urol Oncol* 2018;1:531-7. <https://doi.org/10.1016/j.euo.2018.04.017>.
- 8) Artigas C, Flamen P, Charlier F, Levillain H, Wimana Z, Diamand R, et al. ⁶⁸Ga-PSMA PET/CT-based metastasis-directed radiotherapy for oligometastatic prostate cancer recurrence after radical prostatectomy. *World J Urol* 2019;37:1535-42. <https://doi.org/10.1007/s00345-019-02701-1>.
- 9) Ong WL, Koh TL, Joon DL, Chao M, Farrugia B, Lau E, et al. Prostate-specific membrane antigen-positron emission tomography/computed tomography (PSMA-PET/CT)-guided stereotactic ablative body radiotherapy for oligometastatic prostate cancer: a single-institution experience and review of the published literature. *BJU Int* 2019;124 Suppl 1:19-30. <https://doi.org/10.1111/bju.14886>.
- 10) Hurmuz P, Onal C, Ozyigit G, Igdem S, Atalar B, Sayan H, et al. Treatment outcomes of metastasis-directed treatment using 68 Ga-PSMA-PET/CT for oligometastatic or oligorecurrent prostate cancer: Turkish Society for Radiation Oncology group study (TROD 09-002). *Strahlenther Onkol* 2020;196:1034-43. <https://doi.org/10.1007/s00066-020-01660-6>.
- 11) Kalinauskaite G, Senger C, Kluge A, Furth C, Kufeld M, Tinhofer I, et al. 68Ga-PSMA-PET/CT-based radiosurgery and stereotactic body radiotherapy for oligometastatic prostate cancer. *PLoS One* 2020;15:e0240892. <https://doi.org/10.1371/journal.pone.0240892>.
- 12) Marzec J, Becker J, Paulsen F, Wegener D, Olthof S-C, Pfannenbergs C, et al. ⁶⁸Ga-PSMA-PET/CT-directed IGRT/SBRT for oligometastases of recurrent prostate cancer after initial surgery. *Acta Oncol* 2020;59:149-56. <https://doi.org/10.1080/0284186X.2019.1669816>.

- 13) Deek MP, Yu C, Phillips R, Song DY, Deville C, Greco S, et al. Radiation Therapy in the Definitive Management of Oligometastatic Prostate Cancer: The Johns Hopkins Experience. *Int J Radiat Oncol Biol Phys* 2019;105:948-56. <https://doi.org/10.1016/j.ijrobp.2019.08.008>.
- 14) Chaw CL, deSouza NM, Khoo V, Suh YE, Van As N. Clinical Outcomes of Stereotactic Body Radiotherapy With Immediate Versus Delayed Hormone Therapy in Men With Oligometastatic Recurrence of Prostate Cancer. *Clin Oncol (R Coll Radiol)* 2020;32:509-17. <https://doi.org/10.1016/j.clon.2020.03.008>.
- 15) Kroeze SGC, Henkenberens C, Schmidt-Hegemann NS, Vogel MME, Kirste S, Becker J, et al. Prostate-specific Membrane Antigen Positron Emission Tomography-detected Oligorecurrent Prostate Cancer Treated with Metastases-directed Radiotherapy: Role of Addition and Duration of Androgen Deprivation. *Eur Urol Focus* 2021;7:309-16. <https://doi.org/10.1016/j.euf.2019.08.012>.
- 16) Nguyen PL, Alibhai SMH, Basaria S, D'Amico AV, Kantoff PW, Keating NL, et al. Adverse effects of androgen deprivation therapy and strategies to mitigate them. *Eur Urol* 2015;67:825-36. <https://doi.org/10.1016/j.eururo.2014.07.010>.
- 17) Fossati N, Suardi N, Gandaglia G, Bravi CA, Soligo M, Karnes RJ, et al. Identifying the Optimal Candidate for Salvage Lymph Node Dissection for Nodal Recurrence of Prostate Cancer: Results from a Large, Multi-institutional Analysis. *Eur Urol* 2019;75:176-83. <https://doi.org/10.1016/j.eururo.2018.09.009>.
- 18) Pitroda SP, Khodarev NN, Huang L, Uppal A, Wightman SC, Ganai S, et al. Integrated molecular subtyping defines a curable oligometastatic state in colorectal liver metastasis. *Nat Commun* 2018;9:1793. <https://doi.org/10.1038/s41467-018-04278-6>.
- 19) Dhondt B, De Bleser E, Claeys T, Buelens S, Lumen N, Vandesompele J, et al. Discovery and validation of a serum microRNA signature to characterize oligo- and polymetastatic prostate cancer: not ready for prime time. *World J Urol* 2019;37:2557-64. <https://doi.org/10.1007/s00345-018-2609-8>.
- 20) Werensteijn-Honingh AM, Kroon PS, Winkel D, Aalbers EM, van Asselen B, Bol GH, et al. Feasibility of stereotactic radiotherapy using a 1.5 T MR-linac: Multi-fraction treatment of pelvic lymph node oligometastases. *Radiother Oncol* 2019;134:50-4. <https://doi.org/10.1016/j.radonc.2019.01.024>.
- 21) Werensteijn-Honingh AM, Jürgenliemk-Schulz IM, Gadellaa-Van Hooijdonk CG, Sikkes GG, Vissers NGPM, Winkel D, et al. Impact of a vacuum cushion on intrafraction motion during online adaptive MR-guided SBRT for pelvic and para-aortic lymph node oligometastases. *Radiother Oncol* 2021;154:110-7. <https://doi.org/10.1016/j.radonc.2020.09.021>.
- 22) Aaronson NK, Ahmedzai S, Bergman B, Bullinger M, Cull A, Duez NJ, et al. The European Organisation for Research and Treatment of Cancer QLQ-C30: A quality-of-life instrument for use in international clinical trials in oncology. *J Natl Cancer Inst* 1993;85:365-76. <https://doi.org/10.1093/jnci/85.5.365>.
- 23) Smets EM, Garssen B, Bonke B, De Haes JC. The Multidimensional Fatigue Inventory (MFI): psychometric qualities of an instrument to assess fatigue. *J Psychosom Res* 1995;39:315-25. [https://doi.org/10.1016/0022-3999\(94\)00125-o](https://doi.org/10.1016/0022-3999(94)00125-o).
- 24) Herdman M, Gudex C, Lloyd A, Janssen MF, Kind P, Parkin D, et al. Development and preliminary testing of the new five-level version of EQ-5D (EQ-5D-5L). *Qual Life Res* 2011;20:1727-36. <https://doi.org/10.1007/s11136-011-9903-x>.

- 25) Guckenberger M, Lievens Y, Bouma AB, Collette L, Dekker A, deSouza NM, et al. Characterisation and classification of oligometastatic disease: a European Society for Radiotherapy and Oncology and European Organisation for Research and Treatment of Cancer consensus recommendation. *Lancet Oncol* 2020;21:e18-28. [https://doi.org/10.1016/S1470-2045\(19\)30718-1](https://doi.org/10.1016/S1470-2045(19)30718-1).
- 26) Arlen PM, Bianco F, Dahut WL, D'Amico A, Figg WD, Freedland SJ, et al. Prostate Specific Antigen Working Group guidelines on prostate specific antigen doubling time. *J Urol* 2008;179:2181-6. <https://doi.org/10.1016/j.juro.2008.01.099>.
- 27) Poon I, Erler D, Dagan R, Redmond KJ, Foote M, Badellino S, et al. Evaluation of Definitive Stereotactic Body Radiotherapy and Outcomes in Adults With Extracranial Oligometastasis. *JAMA Netw Open* 2020;3:e2026312. <https://doi.org/10.1001/jamanetworkopen.2020.26312>.
- 28) Collins GS, Reitsma JB, DG, Moons KGM. Transparent reporting of a multivariable prediction model for individual prognosis or diagnosis (TRIPOD): the TRIPOD statement. *BMJ* 2015;350:g7594. <https://doi.org/10.1136/bmj.g7594>.
- 29) Heinze G, Wallisch C, Dunkler D. Variable selection – A review and recommendations for the practicing statistician. *Biom J* 2018;60:431–49. <https://doi.org/10.1002/bimj.201700067>.
- 30) Harrell Jr FE, Lee KL, Mark DB. Multivariable prognostic models: issues in developing models, evaluating assumptions and adequacy, and measuring and reducing errors. *Stat Med* 1996;15:361-87. [https://doi.org/10.1002/\(SICI\)1097-0258\(19960229\)15:4<361::AID-SIM168>3.0.CO;2-4](https://doi.org/10.1002/(SICI)1097-0258(19960229)15:4<361::AID-SIM168>3.0.CO;2-4).
- 31) Jereczek-Fossa BA, Fanetti G, Fodor C, Ciardo D, Santoro L, Francia CM, et al. Salvage Stereotactic Body Radiotherapy for Isolated Lymph Node Recurrent Prostate Cancer: Single Institution Series of 94 Consecutive Patients and 124 Lymph Nodes. *Clin Genitourin Cancer* 2017;15:e623-32. <https://doi.org/10.1016/j.clgc.2017.01.004>.
- 32) Nicosia L, Franzese C, Mazzola R, Franceschini D, Rigo M, D'agostino G, et al. Recurrence pattern of stereotactic body radiotherapy in oligometastatic prostate cancer: a multi-institutional analysis. *Strahlenther Onkol* 2020;196:213-21. <https://doi.org/10.1007/s00066-019-01523-9>.
- 33) De Bleser E, Jereczek-Fossa BA, Pasquier D, Zilli T, Van As N, Siva S, et al. Metastasis-directed Therapy in Treating Nodal Oligorecurrent Prostate Cancer: A Multi-institutional Analysis Comparing the Outcome and Toxicity of Stereotactic Body Radiotherapy and Elective Nodal Radiotherapy. *Eur Urol* 2019;76:732-9. <https://doi.org/10.1016/j.eururo.2019.07.009>.
- 34) Wallis CJD, Saskin R, Choo R, Herschorn S, Kodama RT, Satkunasivam R, et al. Surgery Versus Radiotherapy for Clinically-localized Prostate Cancer: A Systematic Review and Meta-analysis. *Eur Urol* 2016;70:21-30. <https://doi.org/10.1016/j.eururo.2015.11.010>.
- 35) Neal DE, Metcalfe C, Donovan JL, Lane JA, Davis M, Young GJ, et al. Ten-year Mortality, Disease Progression, and Treatment-related Side Effects in Men with Localised Prostate Cancer from the ProtecT Randomised Controlled Trial According to Treatment Received. *Eur Urol* 2020;77:320-30. <https://doi.org/10.1016/j.eururo.2019.10.030>.
- 36) De Bruycker A, Spiessens A, Dirix P, Koutsouvelis N, Semac I, Liefhooghe N, et al. PEACE V - Salvage Treatment of OligoRecurrent nodal prostate cancer Metastases (STORM): a study protocol for a randomized controlled phase II trial. *BMC Cancer* 2020;20:406. <https://doi.org/10.1186/s12885-020-06911-4>.

- 37) Murthy V, Maitre P, Kannan S, Panigrahi G, Krishnatry R, Bakshi G, et al. Prostate-Only Versus Whole-Pelvic Radiation Therapy in High-Risk and Very High-Risk Prostate Cancer (POP-RT): Outcomes From Phase III Randomized Controlled Trial. *J Clin Oncol* 2021;39:1234-42. <https://doi.org/10.1200/JCO.20.03282>.
- 38) Bravi CA, Fossati N, Gandaglia G, Suardi N, Mazzone E, Robesti D, et al. Long-term Outcomes of Salvage Lymph Node Dissection for Nodal Recurrence of Prostate Cancer After Radical Prostatectomy: Not as Good as Previously Thought. *Eur Urol* 2020;78:661-9. <https://doi.org/10.1016/j.eururo.2020.06.043>.
- 39) Tunn UW, Canepa G, Kochanowsky A, Kienle E. Testosterone recovery in the off-treatment time in prostate cancer patients undergoing intermittent androgen deprivation therapy. *Prostate Cancer Prostatic Dis* 2012;15:296-302. <https://doi.org/10.1038/pcan.2012.12>.
- 40) Langenhuijsen JF, Badhauser D, Schaaf B, Kiemeny LALM, Witjes JA, Mulders PFA. Continuous vs. intermittent androgen deprivation therapy for metastatic prostate cancer. *Urol Oncol* 2013;31:549-56. <https://doi.org/10.1016/j.urolonc.2011.03.008>.
- 41) Giesinger JM, Loth FLC, Aaronson NK, Arraras JI, Caocci G, Efficace F, et al. Thresholds for clinical importance were established to improve interpretation of the EORTC QLQ-C30 in clinical practice and research. *J Clin Epidemiol* 2020;118:1-8. <https://doi.org/10.1016/j.jclinepi.2019.10.003>.
- 42) Kuhnt S, Ernst J, Singer S, Rüffer JU, Kortmann R-D, Stolzenburg J-U, et al. Fatigue in cancer survivors--prevalence and correlates. *Onkologie* 2009;32:312-7. <https://doi.org/10.1159/000215943>.

Supplementary material

Table S1

Variables for multiple imputation of missing baseline characteristics.

Variable	Unit	% missing	Used for imputation	Options
Age	years	0	1	
Karnofsky score		57	0	70-80, 90-100
Time to first oligometastasis	months	0	1	
Classification of oligometastatic disease		0	0	metachronous oligorecurrence, repeat oligorecurrence
Therapeutic free interval	months	0	1	
T stage		18	0	1, 2, 3-4
Gleason score		1	0	<7, 7, >7
Primary therapy		0	1	RALP only, RALP + salvage/adjuvant EBRT, Brachytherapy, EBRT only, EBRT + adjuvant ADT
Previous lymph node dissection		0	1	0, 1
R1 resection		0	0	R0, R1, not applicable
IPSA	ng/mL	4	1	
PSA nadir	ng/mL	2	1	
PSA current diagnosis	ng/mL	0	1	
PSA doubling time	months	17	1	
Nodal region		0	1	only pelvic, (also) extrapelvic
Number of nodal targets		0	1	
Mean GTV diameter per patient	mm	0	1	
Sum of GTV diameters per patient	mm	0	1	
Mean GTV volume per patient	mL	0	1	
Sum of GTV volume per patient	mL	0	1	

Table S1 (continued)

Variable	Unit	% missing	Used for imputation	Options
Progression		0	1	0, 1
PFS	months	0	1	
Biochemical progression		0	1	0, 1
Biochemical PFS	months	0	0	
ADT during FU		0	1	0, 1
ADT Free Survival	months	0	1	
Widespread progression		0	1	0, 1
Widespread PFS	months	0	1	
Previous lymph node dissection		0	1	0, 1
Nelson-Aalen estimator of cumulative hazard rate		0	1	

PFS: Progression Free Survival. Missing baseline characteristics were imputed using the 'mice' package. All baseline characteristics and outcome variables were used for the multiple imputation except for variables that could not be reliably used in the imputation model. These variables were not used for imputation of other variables and are coded as '0' in the column 'Used for imputation'.

Settings for mice imputation: 100 imputations, 10 iterations per imputation, seed = 10846.

Table S2

Acute and late toxicity after SBRT for prostate cancer lymph node oligometastases.

Variable	Acute toxicity		Late toxicity	
	% treatments	N treatments	% patients	N patients
Grade 1 all toxicity	41.4	48	15.6	14
Grade 1 fatigue	33.6	39	3.3	3
Grade 1 genito-urinary	1.7	2	8.9	8
Grade 1 gastro-intestinal	13.8	16	6.7	6
Grade 1 other toxicity	4.3	5	1.1	1
Grade 2 all toxicity	2.6	3	6.7	6
Grade 2 fatigue	0.9	1	0	0
Grade 2 genito-urinary	1.7	2	5.6	5
Grade 2 gastro-intestinal	0	0	2.2	2
Grade 2 other toxicity	0	0	1.1	1

Acute toxicity (≤ 3 months after SBRT) is reported from all SBRT treatments (N=116); late toxicity is reported from all patients (N=90).

Table S3

Acute toxicity stratified by SBRT treatment cycle for prostate cancer lymph node oligometastases.

Variable	Acute toxicity first SBRT cycle		Acute toxicity following SBRT cycles		p value
	% treatments	N treatments	% treatments	N treatments	
Grade 1 all toxicity	42.2	38	38.5	10	0.82
Grade 1 fatigue	33.3	30	34.6	9	1
Grade 1 genito-urinary	2.2	2	0	0	1
Grade 1 gastro-intestinal	12.2	11	19.2	5	0.35
Grade 1 other toxicity	5.6	5	0	0	0.59
Grade 2 all toxicity	2.2	2	3.8	1	0.54
Grade 2 fatigue	1.1	1	0	0	1
Grade 2 genito-urinary	1.1	1	3.8	1	0.4
Grade 2 gastro-intestinal	0	0	0	0	1
Grade 2 other toxicity	0	0	0	0	1

Acute toxicity (≤ 3 months after SBRT) is reported for the first SBRT cycle of all patients (N=90) and for following SBRT cycles (N treatments = 26; N patients with repeated SBRT = 20). P-values are shown for Fisher's exact test between acute toxicity occurrence after first vs. following SBRT cycles (with $p < 0.05$ = significant difference).

Table S4

Late toxicity stratified by number of SBRT treatment cycles for prostate cancer lymph node oligometastases.

Variable	Late toxicity one SBRT cycle		Late toxicity multiple SBRT cycles		p value
	% patients	N patients	% patients	N patients	
Grade 1 all toxicity	12.9	9	25	5	0.29
Grade 1 fatigue	1.4	1	10	2	0.12
Grade 1 genito-urinary	8.6	6	10	2	1
Grade 1 gastro-intestinal	7.1	5	5	1	1
Grade 1 other toxicity	1.4	1	0	0	1
Grade 2 all toxicity	5.7	4	10	2	0.61
Grade 2 fatigue	0	0	0	0	1
Grade 2 genito-urinary	5.7	4	5	1	1
Grade 2 gastro-intestinal	2.9	2	0	0	1
Grade 2 other toxicity	0	0	5	1	0.22

Late toxicity (> 3 months after SBRT) is reported patients who have undergone only a single SBRT cycle (N=70) and for patients with repeated SBRT (N=20). P-values are shown for Fisher's exact test between late toxicity occurrence after one vs. multiple SBRT cycles (with $p < 0.05$ = significant difference).

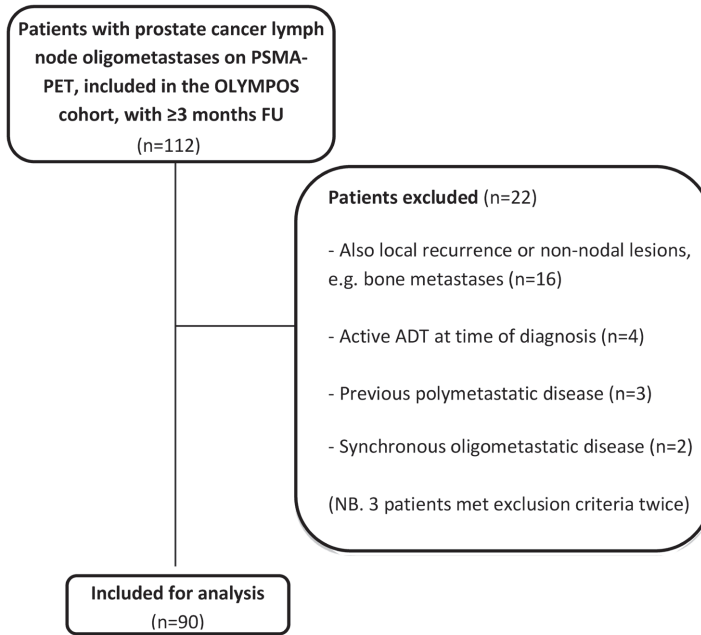


Figure S1
Flowchart of patient inclusion.

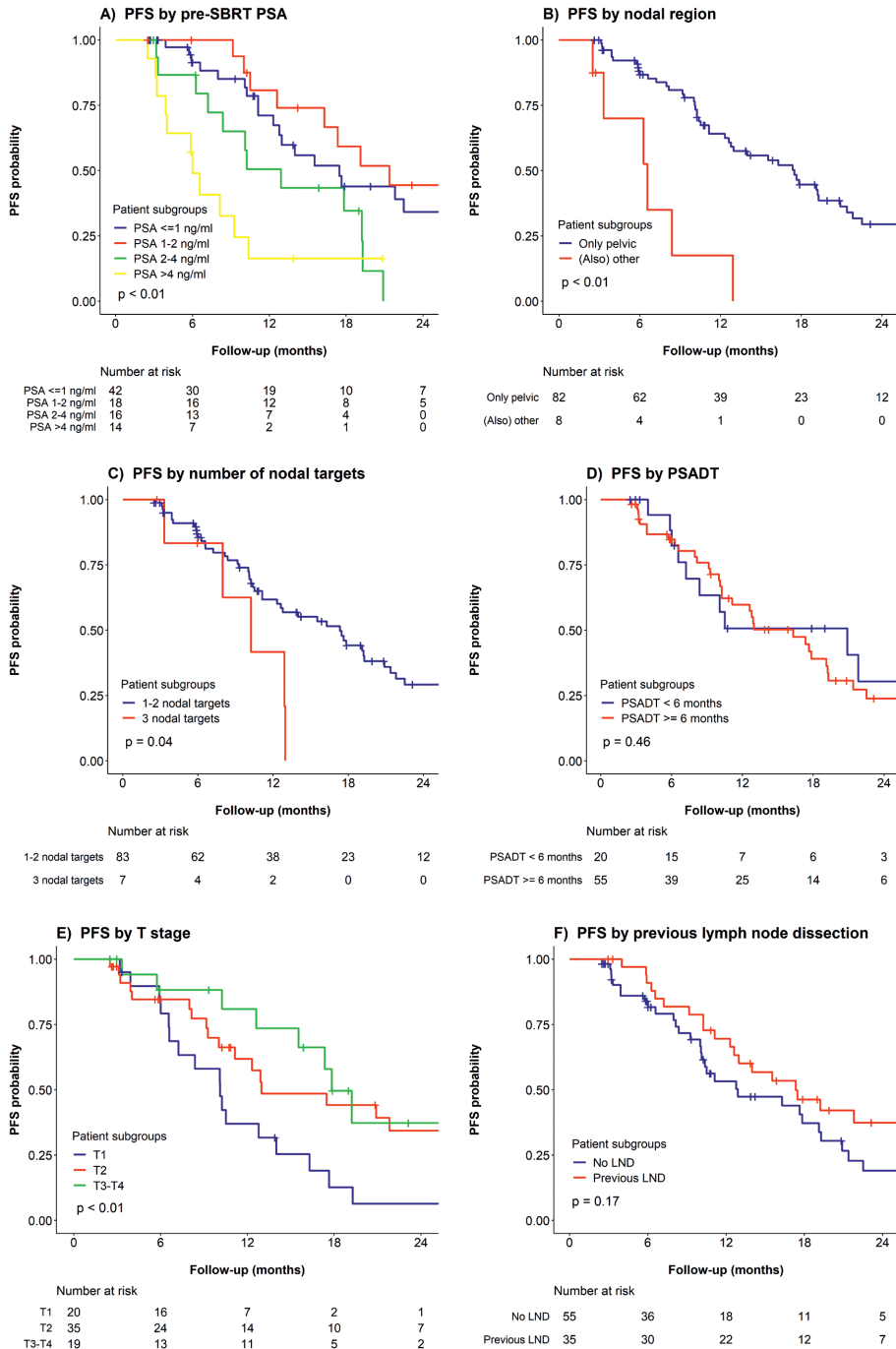


Figure S2

Kaplan-Meier survival estimates of progression free survival (PFS), stratified by baseline patient characteristics: A) pre-SBRT PSA (ng/mL), B) nodal region, C) number of nodal targets, D) PSA doubling time (PSADT), E)

Figure S2 (continued)

primary tumor T stage and F) previous lymph node dissection. In subfigures B-D and F, log-rank test p-values for comparisons between subgroups are included. In subfigures A and E, the log-rank test p-values for comparisons over all subgroups are included in the graphs. Log-rank test p-values for comparisons between subgroups are as follows: subfigure A) PSA ≤ 1 vs. PSA 1-2: $p=0.8$; PSA ≤ 1 vs. PSA 2-4: $p=0.04$; PSA ≤ 1 vs. PSA >4 : $p<0.01$; PSA 1-2 vs. PSA 2-4: $p=0.01$; PSA 1-2 vs. PSA >4 : $p<0.01$; PSA 2-4 vs. PSA >4 : $p=0.1$; subfigure E) T1 vs. T2: $p=0.01$; T1 vs. T3-T4: $p<0.01$; T2 vs. T3-T4: $p=0.4$.

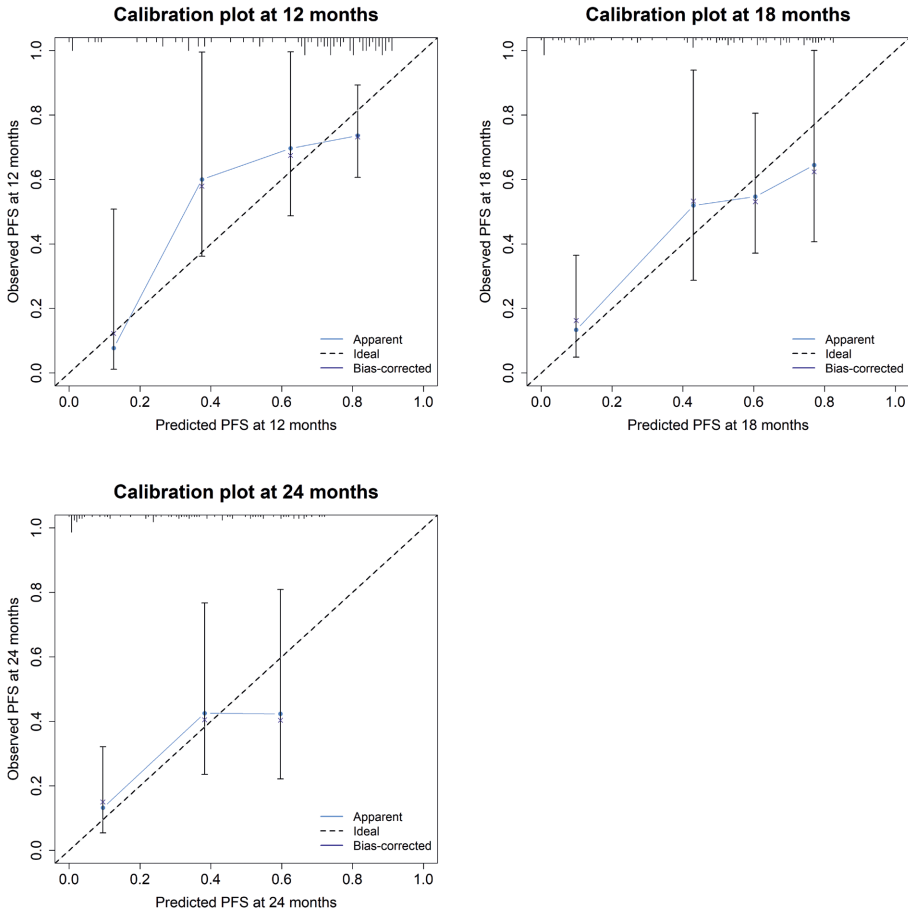


Figure S3

Calibration plots of the final multivariable model of progression free survival (PFS), after multiple imputation of baseline characteristics. Calibration plots were made of PFS at 12, 18 and 24 months.

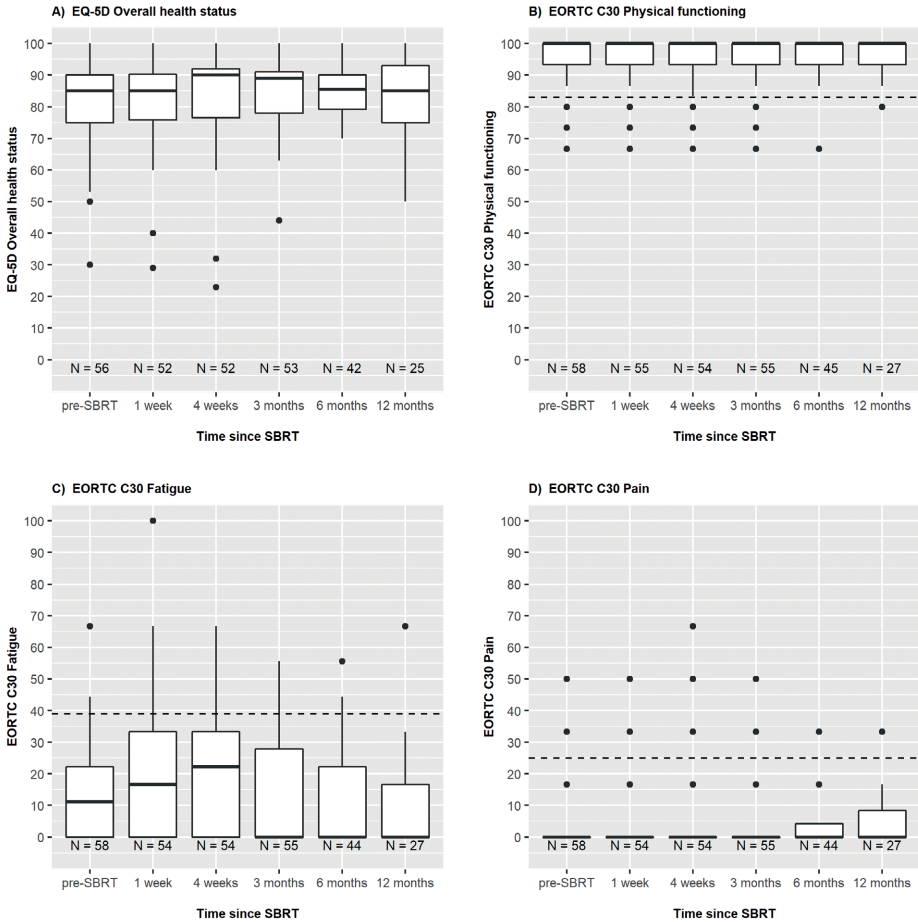


Figure S4

Quality of life after SBRT for prostate cancer lymph node oligometastases. A) EQ-5D overall health status, B) EORTC C30 physical functioning scale, C) EORTC C30 fatigue symptom scale, D) EORTC C30 pain symptom scale. The number of questionnaires that were filled in are shown per time point; questionnaires were restarted for patients who underwent sequential SBRT treatments and results were taken into account per treatment. Center line indicates median, hinges depict 25th and 75th percentiles (inter-quartile range, IQR) and whiskers extend from the hinge to the largest/smallest value at maximally 1.5*IQR. Outlying data points (beyond end of the whiskers) are plotted individually. For sub-figures B-D, a dashed line is plotted at the threshold of clinical importance from Giesinger *et al.*, 2020 [41].

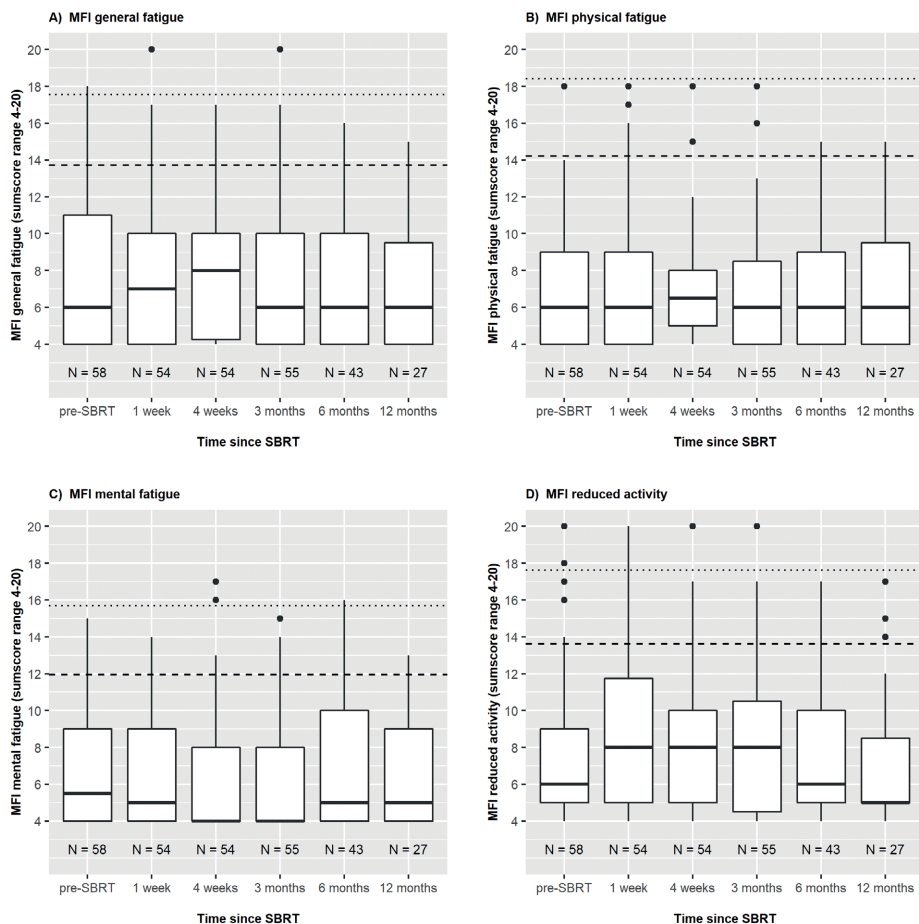
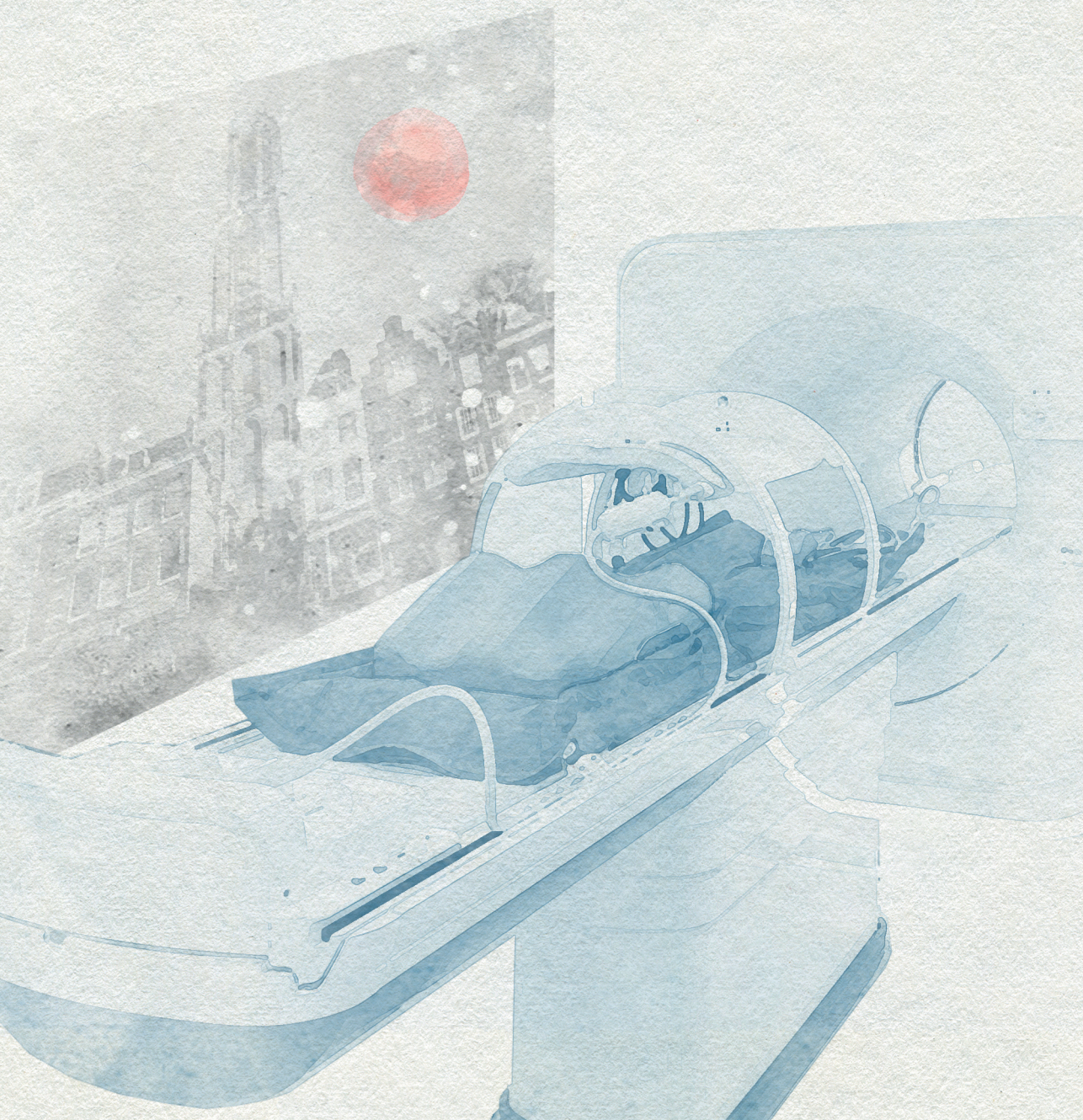
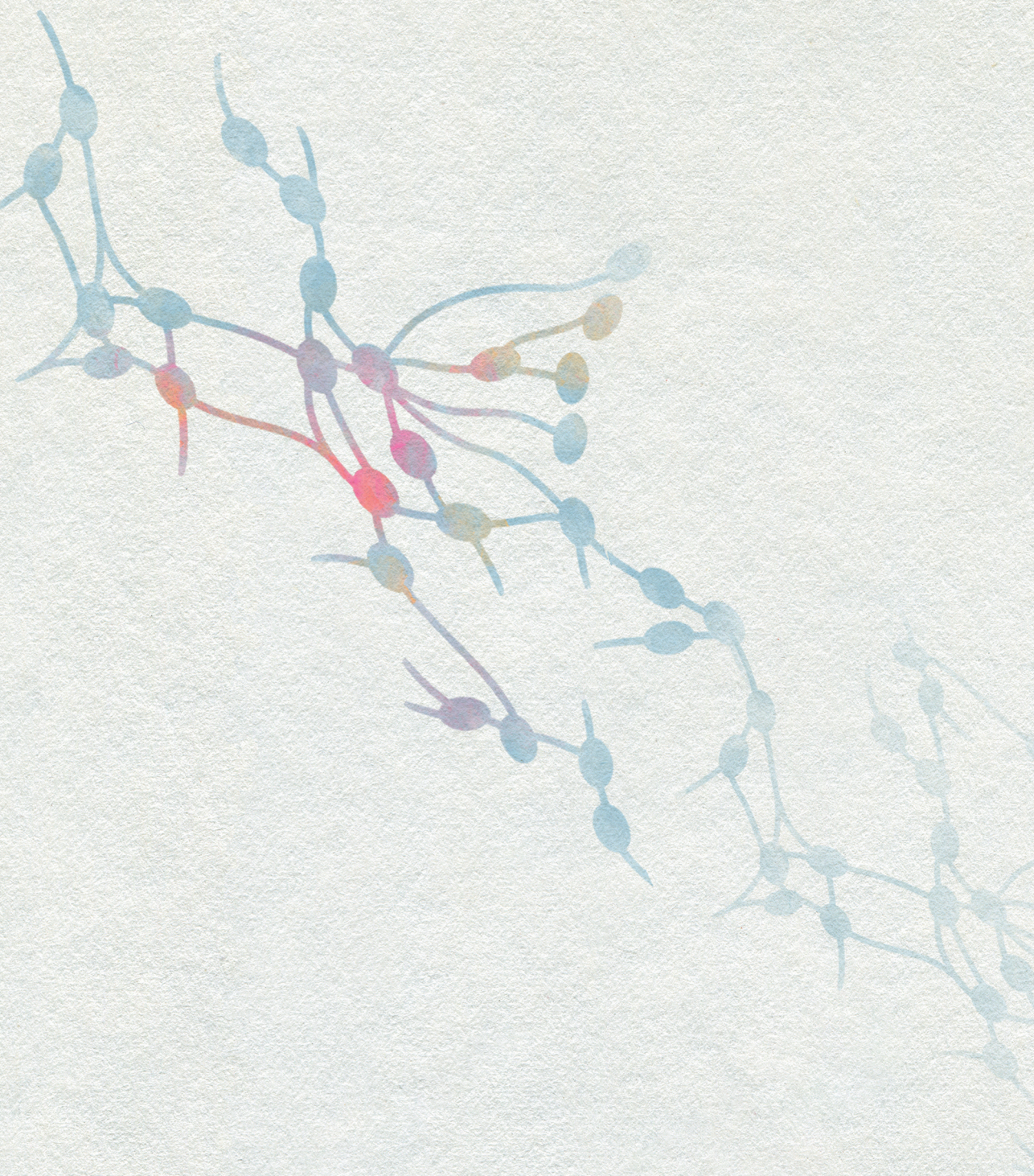


Figure S5

Fatigue after SBRT for prostate cancer lymph node oligometastases. Results from the multidimensional fatigue inventory (MFI) are plotted for the different domains [23]: A) general fatigue, B) physical fatigue, C) mental fatigue and D) reduced activity. Results for ‘reduced motivation’ domain are not shown. The number of questionnaires that were filled in are shown per time point; QoL questionnaires were restarted for patients who underwent sequential SBRT treatments and results were taken into account per treatment. Center line indicates median, hinges depict 25th and 75th percentiles (inter-quartile range, IQR) and whiskers extend from the hinge to the largest/smallest value at maximally 1.5*IQR. Outlying data points (>1.5*IQR from hinge) are plotted individually. Lines are plotted at reference levels of a population of cancer survivors from the study of Kuhnt et al., 2009: a dashed line is plotted at the level of mean+1SD and a dotted line is plotted at the level of mean+2SD [42].



Summary and discussion



Chapter 8

Summary

Part I: Online adaptive MR-guided lymph node SBRT

The first clinical use of the 1.5 T MR-linac after acquisition of the Conformité Européenne (CE)-certification was the radiotherapy treatment of patients with lymph node oligometastases, which took place in August 2018 at the University Medical Center Utrecht. At that time, only technical outcomes were available from the ‘first in mankind’ trial, in which painful bone metastases had been irradiated with a single, palliative radiation dose on a machine with a similar set-up. The clinical and technical feasibility of delivering stereotactic body radiotherapy (SBRT) with the 1.5 T MR-linac for soft tissue targets, in this case lymph node metastases, has been shown in *chapter 2*. Treatment details were reported for the first five patients, which indicated that all treatment sessions (five per patient) had been delivered using the MR-linac, new treatment plans were generated for each treatment session based on the daily anatomy, all treatment sessions were completed within 60 minutes and all quality assurance tests were passed, including independent 3D dose calculations and film measurements.

The treatments of the first ten patients with single lymph node oligometastases were dosimetrically evaluated in *chapter 3*. Two different methods for daily online plan adaptation were compared: Adapt To Shape (ATS), which had been used clinically, and Adapt To Position (ATP). ATS comprises daily contour adaptation of the target volumes and the nearby healthy organs, referred to as organs at risk (OAR). The treatment plan is optimized using this understanding of the anatomy of the day. When ATP is used, the pre-treatment contours are not adapted and the treatment plan is shifted to account for changes in the target volume location, which makes ATP treatment delivery faster but less adaptive to changes in target volume and OAR anatomy. Sufficient coverage of the target lymph nodes (gross tumor volume, GTV) with the prescribed amount of radiation dose had been obtained throughout the treatment sessions in 90% of the clinically delivered ATS treatments, which would have been 70% when ATP would have been used. Still, the majority of patients would have received an adequate radiation dose on the entire target volume with both plan adaptation methods, with median target lymph node coverages of 100% for both methods. Treatment margins of 3 mm were found to be sufficient for SBRT delivery in the time frame of MR-linac treatments, taking into account the geometric uncertainties and GTV intrafraction motion.

In *chapter 4*, the impact of vacuum cushion immobilization on target motion during MR-linac treatment sessions was investigated. Vacuum cushions are used to immobilize the patients, which can reduce target intrafraction motion. Indeed, a significant reduction was observed in the anterior-posterior translations (median reduction 0.7 mm) of both target volumes and patient bony anatomy. However, part of the target intrafraction motion can

be compensated for during MR-linac treatments, especially for patients with single lymph node metastases. Most intrafraction motion of the target volumes was found to take place in the first ~16 minutes of the treatment session, before radiation delivery is started. This is motion that can be compensated for by performing an additional ATP procedure. When such an additional ATP procedure is applied even for limited intrafraction motion, vacuum cushion immobilization no longer reduces the intrafraction motion, so it may not be needed for MR-linac treatments.

In *chapter 5*, target volume coverage was compared between MR-linac and CBCT-linac treatments. For patients with single lymph node oligometastases, target coverage was similar between MR-linac and CBCT-linac treatment plans. An improved target coverage was observed for MR-linac treatment of patients with multiple targets. With an MR-linac, interfraction motion of one target relative to the other target(s) can be compensated for at the start of each treatment session, but this is impossible for CBCT-linac treatments if multiple targets are treated in a single treatment plan. Still, differences in target coverage were again observed only in a minority of patients; median coverage of the target lymph nodes was 100% with both modalities, both for patients with single and multiple targets.

Chapter 6 continued the comparison between MR-linac and CBCT-linac treatment plans with a focus on OAR dosimetry. Fewer OAR planning constraints were violated using MR-linac treatment. For patients with poorly visible targets on CBCT, the use of smaller treatment margins on an MR-linac resulted in improved sparing of the healthy nearby bowel. However, the time frame for online plan adaptation is short, treatment sessions take longer on an MR-linac and OAR anatomy can change during this time (intrafraction motion). All these factors decrease the potential benefit of online adaptive radiotherapy delivery using an MR-linac. Overall, the doses that would have been received by bowel and duodenum were similar between MR-linac and CBCT-linac; bowelbag doses would even have been significantly lower using CBCT-linac if identical PTV margins could have been used for all patients.

Part II: Treatment outcomes and patient selection

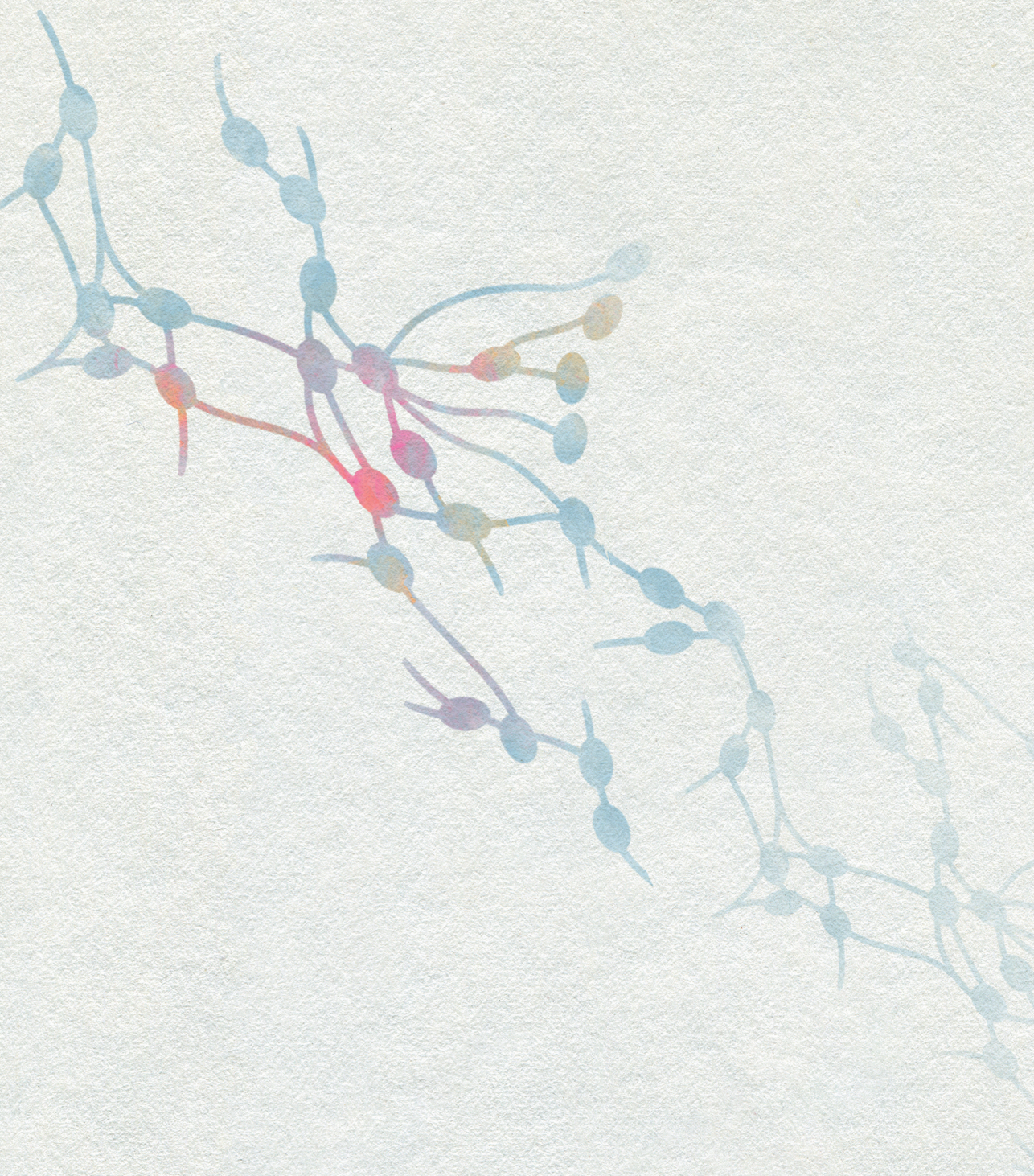
Clinical outcomes were evaluated in *chapter 7*, specifically for patients with prostate cancer lymph node oligometastases diagnosed using prostate-specific membrane antigen (PSMA)-PET scans. With a median follow-up of 21 months, the median progression-free survival (PFS), defined as time to occurrence of a new metastatic lesion or biochemical progression, was 16 months. Several baseline patient characteristics were found to be associated with shorter PFS: younger age, higher prostate specific antigen (PSA) before SBRT and extrapelvic target location. A preliminary risk score was created, yielding median PFS

of 8 and 21 months for high and low risk groups, respectively. The highest grade toxicity was grade 2 for acute and late toxicity events, and only a mild, transient fatigue around 1-4 weeks after SBRT was observed in the quality of life analysis.

General discussion

MR-guided online adaptive radiotherapy for patients with lymph node oligometastases is feasible, it even results in improved target volume coverage in case of multiple target lymph nodes. It allows for better adherence to OAR constraints and it provides an opportunity to monitor the dose delivered to nearby OAR at each session. However, with the current 1.5 T MR-linac set-up and the current workflow, limited benefit in terms of OAR sparing is obtained compared with CBCT-linac, due to the long session times and OAR intrafraction motion. Shorter session times and improved mitigation of target and OAR intrafraction motion are needed to reach the full potential of 1.5 T MR-linac delivery.

SBRT is a safe treatment for lymph node oligometastases, with only a mild and transient impact on quality of life, mainly fatigue. Local control can be obtained in almost all patients but disease progression is very common after local treatment for lymph node oligometastases. Improved outcome prediction could be helpful, as most patients might benefit from combined treatments consisting of SBRT and some form of systemic therapy. Such combined treatments might improve progression-free survival and potentially even overall survival for most patients with oligometastases and possibly even for patients with polymetastatic disease.



Chapter 9

General discussion

Part I: Online adaptive MR-guided lymph node SBRT

With recent advancements in the field of image-guided radiotherapy (IGRT), especially the advent of MR-guided online adaptive radiotherapy, the first part of this discussion is focused at the clinical rationale of MR-guided online adaptive radiotherapy, and in particular its application in SBRT delivery for patients with lymph node oligometastases.

Image-guided radiotherapy

IGRT is increasingly becoming the standard-of-care for EBRT delivery; it often relies on X-ray imaging techniques, such as cone beam CT (CBCT) and kilovolt x-ray imaging [1]. CBCT-linear accelerators (CBCT-linacs) allow for daily position verification before radiation delivery, and if needed delivery can be halted and intra-fraction position verification can be performed. Dedicated systems such as the Cyberknife (Accuray Inc., Sunnyvale, USA) use kilovoltage x-ray imaging throughout radiation delivery and allow for continuous tumor tracking and compensation for respiratory motion, although it often still requires fiducial marker implantation [2].

MR-guided online adaptive radiotherapy

MR imaging offers an improved soft tissue contrast compared to CT imaging, which allows for better visualization of target volumes and organs at risk (OAR) for radiotherapy treatment planning [3]. The advantages of an MR-guided workflow have been shown for cervical cancer brachytherapy, with smaller clinical target volumes after MRI-based contouring and with improved clinical outcomes such as local control and overall survival after MR-guided adaptive brachytherapy [4,5].

For MR-guided radiotherapy, no fiducial markers need to be implanted and OAR are also adequately visualized during each session, so inter-fraction changes in OAR anatomy can be accounted for [6]. Furthermore, the daily MR imaging also allows for the acquisition of diffusion-weighted MRI, facilitating response monitoring over the course of treatment [7]. The proof of principle for integration of a linear accelerator and an MRI scanner was reported in 2009, but the first patients were only treated with this 1.5 T MR-linac (Elekta AB, Stockholm, Sweden) in 2017 [8,9]. The first clinical treatment system for MR-guided online adaptive radiotherapy was the MRIdian (ViewRay Inc., Oakwood, USA), which combined 0.35 T MRI with three Co-60 heads for radiation delivery in the initial set-up (2014), but which now also has a linear accelerator set-up, since 2017 [10].

Currently, the 1.5 T MR-linac allows for daily online plan adaptation based on the actual patient anatomy on MRI, with MRI scans being acquired before, during and after radiation delivery [11]. A limitation of the current machine set-up is the inability to compensate

for intra-fraction motion such as breathing motion, although progress has been made regarding fast intrafraction motion compensation in a research setting [12,13]. In contrast, the MRIdian system already allows for gating of the radiation beam based on cine-MRI during radiation delivery [11]. Currently, both MR-linac systems are based on step-and-shoot intensity-modulated radiotherapy (IMRT). Recently, the feasibility of arc therapy delivery analogous to VMAT has been shown in a research set-up of the 1.5 T MR-linac [14]. On CBCT-linacs, volumetric modulated arc therapy (VMAT) has been known to significantly decrease the 'beam on' treatment delivery time and it has also been reported to result in more conformal treatment plans, with an improved sparing of OAR [15]. On an MR-linac, the gantry is rotating at a higher speed compared with a CBCT-linac and also the MLC speed is higher, whilst the dose rate is lower on MR-linac [14,16]. When combining these factors, we expect that the reduction in 'beam on' time from VMAT instead of IMRT may be smaller for an MR-linac compared with a CBCT-linac. Furthermore, VMAT could increase the time needed for online plan optimization due to a higher complexity of the online plan optimization. Besides a potential reduction in session time, VMAT delivery on MR-linac might also offer more degrees of freedom during online plan optimization, but it remains unknown whether this results in more conformal treatment plans as the time pressure on daily plan optimization remains a limiting factor [11,17]. Most benefit from VMAT delivery on an MR-linac is currently expected from its potential contribution to real-time, continuous online plan optimization, by exploring arc-by-arc re-optimization [12,14]. Another hurdle to overcome is the manual input required for correct contour propagation and the relatively long calculation times for plan optimization. In the future, these challenges might be overcome using improvements in image registration (for instance Zachiu *et al.*, 2020) and with the application of deep learning for improved contour propagation and for fast dose calculation [18-20]. Automated contour adaptation could speed up the workflow, which could reduce target and OAR intrafraction motion and improve patient comfort through shorter treatment sessions. In summary, 1.5 T MR-linac systems are now clinically available and allow for daily plan optimization and in some cases compensation for breathing motion based on online MR imaging before, during and after radiation delivery, but future improvements of the systems will be needed before the full potential of this treatment technique can be exploited.

Feasibility of MR-guided online adaptive radiotherapy for lymph node oligometastases

At the UMC Utrecht, clinical treatments with the Conformité Européenne (CE)-certified 1.5 T MR-linac were initiated for patients with lymph node oligometastases. This patient population was selected for the first R-IDEAL 1 study with the CE-certified 1.5 T MR-linac as the gross tumor volumes (GTVs) were small for most patients, with a median short axis diameter of 7 mm for the target lymph nodes [21,22]. Online contour adaptation of the target lesions and nearby OAR (within a ring of 2 cm around the PTV) could be performed

quickly. Furthermore, the treatment plans for these patients were relatively simple and experience with plan optimization for these treatment plans had already been gained in a research setting [23]. The limited amount of OAR re-contouring and the resulting strategy to optimize solely on absolute, high-dose OAR constraints was chosen in order to keep the session time within acceptable limits. With the steep dose gradients of SBRT, the hypothesis was that preventing high radiation doses in nearby OAR would lead to an adequate sparing of OAR further away from the target volume. In chapters 5 and 6 it was shown that the planning constraints were indeed met, both for target coverage and OAR constraints. Still, OAR turned out to receive slightly more radiation dose compared with CBCT-linac, which will be discussed in the section '*Comparison between MR-linac and CBCT-linac treatments*' below.

The 1.5 T MR-linac had already received the CE certification, which allowed the treatments to be delivered as standard clinical care, also because the radiotherapy fractionation schedules and target volume and OAR planning constraints were very similar to our standard clinical practice at that time. Still, care was taken to try to include almost all patients in observational studies such as the OLYMPOS study and later on also the MOMENTUM study, which focused specifically on 1.5 T MR-linac treatments, independently from the tumor site [24]. Up to July 1st 2021, 129 of 146 (88%) patients treated on the MR-linac for soft tissue oligometastases were included in the OLYMPOS study. This yielded a lot of research data on the first application of a 1.5 T MR-linac for soft tissue targets, as opposed to the bone metastases that were irradiated in 2017 [9]. As described in chapter 2, the feasibility of multi-fraction treatment for soft tissue targets was shown with five patients with lymph node oligometastases that were treated in 2018. All treatment fractions were successfully delivered with full online planning based on the daily anatomy, all sessions were completed within 60 minutes and all quality assurance tests were passed, including film measurements and independent 3D dose calculations, so multi-fraction treatment on the 1.5 T MR-linac was shown to be feasible [22].

Comparison between MR-linac and CBCT-linac treatments

From both R-IDEAL stage 0 (in silico comparison) and stage 2a (development and optimization of the workflow) dosimetric comparison studies we found that clinical dose criteria such as target coverage and OAR constraint adherence were improved using MR-linac compared with CBCT-linac [21,23,25]. Clinical outcomes have yet only been reported for single-arm studies, but the MIRAGE randomized clinical trial is now recruiting patients, in which prostate cancer patients are randomized between CBCT-linac and 0.35 T MR-linac SBRT delivery, which will be the first R-IDEAL stage 2b study investigating the advantage of MR-guided online adaptive delivery [26].

Most dosimetric comparisons between MR-linac and CBCT-linac delivery focused on the benefit of daily plan optimization, which was evaluated using the daily MRI-observed anatomy, without taking intrafraction motion into account [23,27-29]. Furthermore, dosimetric comparisons regarding soft tissue oligometastases compared online adaptive MR-guided radiotherapy with IMRT-based CBCT-linac delivery [23,30,31]. On CBCT-linac, VMAT delivery is faster and therefore it is less affected by intrafraction motion, and it may also be more conformal compared with IMRT delivery [15]. Therefore, comparing VMAT-based CBCT-linac delivery with (IMRT-based) MR-linac treatments, as we have done in chapters 5 and 6, may be considered a more suitable benchmark for dosimetric comparisons than comparing IMRT-based CBCT-linac and MR-linac delivery.

As has been described in chapters 5 and 6, differences in target coverage and OAR doses were compared for patients with lymph node oligometastases based on data from actual 1.5 T MR-linac treatments, taking intrafraction motion into account and comparing with VMAT delivery on CBCT-linac. For patients with a single target lymph node, GTV coverage was excellent for both CBCT-linac and MR-linac delivery [25]. For most patients with multiple target lymph nodes, GTV coverage was also excellent with both modalities, but incidentally, one of the GTVs would have received an inadequate dose because of independent interfraction motion of the targets [25,32]. GTV coverage at the post-delivery anatomy was significantly higher using MR-linac for patients with multiple targets and an adequate GTV coverage for all targets on the post-delivery anatomy was reached in 80 and 89% of sessions for CBCT-linac and MR-linac, respectively [25]. Similarly, PTV coverage on the daily anatomy was significantly higher using MR-linac, especially for patients with multiple targets. With this improvement in target coverage, MR-linac delivery may thus be beneficial for patients with multiple targets, but no clinically relevant improvement in target coverage was observed for patients with single targets.

In chapter 6 it was shown that 1.5 T MR-linac delivery reduced the number of OAR constraint violations, both at the start of the online sessions and at the moment of actual radiation delivery. However, OAR sparing considers adherence to the OAR constraints but also keeping the dose in OAR 'as low as reasonably achievable', ALARA. Because of the optimization on the daily anatomy, MR-linac delivery reduced the number of OAR constraint violations for evaluation on both the anatomy at the start of the treatment sessions and on the anatomy at the time point of radiation delivery [17]. Treatment sessions on an MR-linac take ~20-40 minutes longer than on a CBCT-linac, due to contour adaptation, plan optimization and longer delivery times [33]. With these longer treatment sessions, more intrafraction motion can occur between the daily MRI scan at the start of the session and the actual radiation delivery. Target intrafraction motion is mitigated by the use of a position verification scan directly before radiation delivery, but OAR intrafraction motion

is currently not taken into account on the 1.5 T MR-linac. The potential benefit of daily adaptive treatment planning on an MR-linac thus seems to be decreased as a result of the increased intrafraction motion: when investigating the 'estimated delivered doses' to bowelbag and duodenum, OAR doses were only lower using MR-linac when a substantial PTV margin reduction could be realized as compared with CBCT-linac [17]. For patients that could have been treated with 3 mm PTV margins on CBCT-linac, bowelbag doses would have been significantly lower using CBCT-linac delivery and duodenum doses would have been comparable between the two modalities.

The current workflows on the 1.5 T MR-linac constitute a trade-off between session time (amount of OAR contour adaptation and time spent on online plan optimization) and optimal OAR sparing. Currently, the speed of the online plan optimization procedure is maximized by focussing on absolute high-dose OAR constraints, which may have impacted OAR sparing at lower dose levels. With potential faster plan optimization possibilities in the future, this trade-off could be changed and 1.5 T MR-linac OAR sparing might be further improved. These results coincide with a recent dosimetric comparison between 1.5 T MR-linac and CBCT-linac delivery for prostate radiotherapy, in which excellent OAR constraint adherence was shown for both modalities but higher rectum and bladder doses were described for some patients using MR-linac delivery [34]. Furthermore, for liver SBRT, online adaptive treatment with a 0.35 T MR-linac improved PTV coverage and OAR sparing only for patients with an OAR close to the PTV; 47% of the patients included in the study did not benefit from daily MR-guided plan optimization [29]. For future dosimetric comparisons, our results indicate that it is important to take intrafraction motion into account, as comparisons that only take the daily anatomy into account might suffer from an overestimation of dosimetric benefits using an MR-linac, for both target coverage and OAR sparing. In conclusion, OAR constraint adherence was improved with our current 1.5 T MR-linac workflow compared with CBCT-linac, but OAR sparing at lower dose levels was not improved for most patients due to the longer session times on MR-linac and the associated intrafraction OAR motion.

Combining the results on target coverage and OAR sparing, treatment delivery with the current 1.5 T MR-linac for lymph node SBRT seems to give a dosimetric benefit in cases with a critical OAR in a high-dose region, or in cases with multiple targets. An example of a critical OAR in a high-dose region is a patient with a mesenteric or para-aortic lymph node metastasis very close to the duodenum. For abdominal (mesenteric/para-aortic) lymph nodes, target visibility on CBCT is often poor and it is likely that the PTV margin could be reduced with better visibility on an MR-linac. However, with the current 1.5 T MR-linac, and with our current online workflow, the focus is still mainly on adherence to the OAR constraints. In this case, reduction of the PTV margin can only be expected to result in

improved OAR sparing if an OAR is closeby and if the constraint of this OAR might be violated. As stated before, patients with multiple targets may be expected to benefit from an improved target coverage due to independent interfraction motion of the targets. There is a clear need to generate the daily treatment plan faster, and at the same time the ability to adapt the treatment on an intrafraction time scale. These are ongoing activities for future adaptations of the 1.5 T MR-linac treatment machine and associated workflow, such as fast intrafraction plan adaptation or even real-time MLC-tracking of the target volume. With these, PTV margins could be further reduced, which may increase the group of patients that could benefit from treatment delivery using an MR-linac [12].

Comparison between ‘adapt to position’ (ATP) and ‘adapt to shape’ (ATS) workflows

On the 1.5 T MR-linac, two main strategies for online plan optimization are available: ‘adapt to position’ (ATP) and ‘adapt to shape’ (ATS) [11,32]. ATP is essentially a way to rigidly adapt the treatment plan to the daily target location, in which the original target and OAR contours are translated to the new target location based on a rigid registration between the pre-treatment CT scan and the daily online MRI scan. The contours are not edited and therefore anatomical changes of targets and OAR, such as rotation of the target volume or different OAR position due to bladder and rectum filling, are not taken into account. This ATP workflow is quite similar to the workflow that is used on a CBCT-linac, although position correction is slightly different on an MR-linac, as the treatment table can only be moved in the patient cranial-caudal direction, whereas on a CBCT-linac the treatment table can be shifted in all directions and sometimes even allows for rotation corrections. On an MR-linac, the treatment plan is recalculated or re-optimized when the target has shifted in patient anterior-posterior or lateral direction [11]. Of course, ATP on an MR-linac also offers the advantage of improved soft tissue contrast, which may be useful for patients with targets that are poorly visible on CBCT imaging. ATS is a more time-consuming treatment strategy compared with ATP, as target and OAR contours need to be manually adapted: the contours are automatically propagated based on deformable image registration, but manual contour adaptation is still required. These contours can then be used to create a new, optimized treatment plan based on the ‘anatomy of the day’ [11,22].

As described in chapter 3, the GTVs had been adequately covered (planning aim GTV $V_{35Gy} = 100\%$) during the entire MR-linac treatment sessions in 70% and 90% of treatment sessions using ATP and ATS, respectively. PTV coverage at the start of the treatment sessions was slightly lower with ATP compared with ATS: median PTV V_{35Gy} values were 94 and 98%, respectively (planning aim >95%), with minimum PTV coverages of 76 and 91% [32]. For both methods, OAR constraints were well respected at the start of the treatment sessions, with maximum OAR constraint violations of 2 Gy or 0.2 cc. However, most of the potential benefits of MR-linac delivery, as compared to CBCT-linac, only hold for ATS-based

MR-linac workflows. The only potential benefit from an ATP-based MR-linac treatment over CBCT-linac delivery is improved target visibility. We have previously estimated that roughly 30% of patients had poorly visible lymph node oligometastases on CBCT-linac [23]. ATP could thus be applied in the situation that session duration is considered too long with ATS and only for patients with poor target visibility on CBCT-linac. In other situations, ATP-based delivery may lead to poorer dosimetrical outcomes: OAR are not recontoured to the daily anatomy, so OAR sparing is likely better using CBCT-linac (with more conformal treatment plans) or, in case of critical OAR, OAR sparing is expected to be better using ATS-based delivery on MR-linac. Furthermore, ATP-based workflows are not advisable and currently not even possible for patients with multiple targets. Another strategy can be to make the choice of workflow adaptive, based on the daily OAR anatomy: some institutes use ATP for sessions with only limited changes in the daily anatomy or when the OARs are further away from the target, and they switch to ATS if indicated based on the daily anatomy [35]. However, for patients with non-critical OAR, CBCT-linac approaches may still yield better OAR sparing at lower dose levels, so it would be advisable to use poor target visibility on CBCT as a prerequisite for MR-linac delivery in these situations. Also, when ATS-based workflows would be faster, session duration would no longer be a reason to use the MR-linac with ATP-based delivery, as ATP remains a less potent way to treat patients on an MR-linac. In conclusion, an ATP-based workflow has no potential advantage over CBCT-linac delivery with respect to OAR sparing (as the same OAR contours as defined on the pre-treatment CT are used in both approaches), except when a substantial PTV margin reduction and a lower chance of geographical miss could be realized in case of very poor target visibility on CBCT.

Vacuum cushion immobilization

Patient immobilization can help to improve reproducible patient positioning and can decrease inter- and intrafraction motion, so motion occurring between treatment sessions and during a treatment session respectively. As such, vacuum cushions are used to immobilize patients as part of the standard clinical care for lymph node SBRT on CBCT-linac. However, on an MR-linac, vacuum cushions are more inconvenient than on a CBCT-linac: some obese patients no longer fit inside the MR-linac bore when placed on a vacuum cushion and the vacuum cushions were also considered less convenient for emergency evacuation procedures on an MR-linac. Furthermore, interfraction motion reduction is not needed for MR-linac delivery, as the treatment plan is adapted to the daily target location. The impact of vacuum cushion immobilization on target intrafraction motion for pelvic and para-aortic lymph node SBRT investigated as chapter 4. We found that vacuum cushion immobilization was not necessary in case of MR-linac delivery for patients with single lymph node targets: the vacuum cushions mainly reduced the patient intrafraction motion occurring in the first ~16 minutes [36]. When using ATS, with an additional round of ATP

in case target intrafraction motion was observed on the position verification (PV) scan, vacuum cushion immobilization was no longer needed: the increase in intrafraction motion was sufficiently corrected with the additional ATP cycle. It remains important to stress that a low threshold should be used for target intrafraction motion as observed on the PV scan before an additional ATP procedure was used: even for target intrafraction motions of ~1 mm, an additional ATP procedure should be used before vacuum cushion immobilization is no longer needed. Also, for patients with multiple targets, vacuum cushion immobilization remains strongly advisable as intrafraction motion correction is more complex and usually more time-consuming for treatment sessions with multiple target volumes, with frequently observed independent intrafraction motion of the different targets. Finally, when using ATP instead of ATS for online plan adaptation, vacuum cushion immobilization might still be needed: with the shorter session duration using ATP instead of ATS, the excess intrafraction motion without a vacuum cushion cannot be adequately corrected before starting the radiation delivery. Thus, vacuum cushion immobilization is not necessary during MR-linac SBRT delivery for patients with single pelvic or para-aortic lymph node metastases, as long as a specific workflow (ATS with an additional ATP in case of target intrafraction motion) is employed.

Perspective on future research

A lot of research is ongoing related to the MR-linac treatment system, currently mainly focused on two aspects: first, to speed up the online workflow components such as contour adaptation and daily plan optimization. Secondly, to compensate for intrafraction motion using fast intrafraction plan optimization or using beam gating, MLC-tracking or real-time dose painting [12,37]. Such developments may bring substantial improvements in the dosimetric advantage of MR-guided online adaptive radiotherapy, especially for thoracic and upper-abdominal targets that exhibit large amounts of intrafraction motion. For the current machine set-up, results from chapter 6 show that it is necessary to take intrafraction motion into account when investigating the dosimetric benefits of MR-linac delivery for other tumor sites. Concluding, with a faster online workflow on the 1.5 T MR-linac, less intrafraction motion will occur and this motion could be mitigated using intrafraction plan optimization and using MLC tracking or real-time dose painting, which is likely to increase the dosimetric advantages of MR-linac delivery. Also, future motion mitigation strategies might allow for further hypofractionation to two-fraction schedules and it might further increase the number of (poly)metastases that can be safely treated simultaneously.

Part II: Treatment outcomes and patient selection

A smaller, but important part of this thesis has been focused on the clinical rationale of SBRT treatment for patients with lymph node oligometastases. It may be practically possible to deliver SBRT, even with innovative treatment systems as described above, but only a limited body of evidence currently contributes to the clinical rationale to treat these patients using SBRT as a monotherapy.

Local treatment for oligometastatic disease

Theoretically it may be beneficial to eradicate all macrometastatic disease in an oligometastatic setting and thereby prevent seeding of new metastases from the initial oligometastases [38,39]. Indeed, favorable outcomes have been reported in large series on metastasectomy of liver and lung (oligo)metastases from colorectal cancer, with an overall survival rate at 5 years after lung metastasectomy of 46% and an overall survival rate at 10 years after liver metastasectomy of 23% [40,41]. In the SABR-COMET randomized controlled trial, oligometastatic patients had a significantly improved overall survival when SBRT was applied compared with standard palliative radiotherapy to alleviate symptoms or prevent complications, with median overall survival of 28 and 50 months in the control and SBRT arms, respectively [42]. This suggests that (repeated) SBRT treatment could slow disease progression and thus improve overall survival in a long-term palliative setting. However, the patient population included in the SABR-COMET trial was very diverse, with a wide range of primary tumor types (mainly breast, colorectal, lung and prostate) and also different types of metastases that were treated (mainly bone, lung, liver and adrenal). Furthermore, the distribution of prostate cancer oligometastases was not well-balanced between the two study arms, constituting 21% of the SBRT arm and 6% of the control arm; which may be an important finding given the generally long overall survival of patients with (oligo)metastatic prostate cancer [43,44]. Given the small number of lymph node oligometastatic patients in the SABR-COMET trial, it remains difficult to draw conclusions for this specific patient group. The clinical scenario may be different for lymph node oligometastases, as they might be more prone to widespread micrometastatic spread, especially to other lymph nodes, as opposed to circulatory spreading oligometastases such as liver or lung metastases, for which there might be a better window of opportunity to intervene before the oligometastasis seeds new metastases, because further circulatory seeding may depend more on certain 'hallmarks of metastasis', such as motility and invasion, modulation of the microenvironment, plasticity and colonization [45].

An increasing body of evidence shows that SBRT is a safe and locally effective treatment for patients with oligometastases, with estimated grade ≥ 3 acute and late toxicity rates of 1.2% and 1.7%, respectively, and with an estimated 1-year local control rate of 94.7% [46].

Specifically for lymph node oligometastases, promising results with very low toxicity rates have been described for patients with primary gynecological, prostate and breast tumors, and also for colorectal cancer, although lesions with a colorectal origin likely require higher radiation doses due to relative radio-resistance [47]. In our OLYMPOS trial with patients treated for soft tissue oligometastases, 58% of the treated patients had lesions originating from prostate cancer and 20% originally had a colorectal tumor (*unpublished data*). The large amount of prostate cancer oligometastases in our patient population may be explained by the high sensitivity of 68-gallium prostate-specific membrane antigen (PSMA) positron emission tomography (PET) imaging. With ⁶⁸Ga-PSMA-PET, prostate cancer oligometastases can be diagnosed with greater sensitivity compared with choline PET imaging, especially for diagnostic imaging earlier in the natural disease history, with prostate specific antigen (PSA) levels below 2 ng/mL [48-50]. The ability to diagnose lesions early in the natural disease history has made it an attractive target population for metastasis-directed therapy (MDT), such as SBRT or surgery [51]. In chapter 7 the very limited effect of SBRT on the quality of life of these patients has been confirmed, indicating only a transient mild fatigue at 1-4 weeks after SBRT. Thus, SBRT is a safe treatment with an acceptable toxicity profile and only a very limited effect on the quality of life of patients.

Selecting the target population for SBRT treatment

Even with promising outcomes, one of the main challenges in oligometastatic SBRT remains patient selection. SBRT as monotherapy may be an attractive treatment option because it allows to postpone systemic therapies such as androgen deprivation therapy (ADT) by approximately 8 months and it has been shown to reduce the chance of disease progression within 6 months from 61% with observation alone, to 19% with SBRT [51,52]. The toxicity profile of SBRT monotherapy is favorable, especially when compared with the adverse effects of ADT such as erectile dysfunction, reduced libido, hot flashes and also effects on bone health, increased diabetic and cardiovascular risk [53]. Still, against expectations, progression-free survival has not been improved with the advent of PSMA-PET imaging: PFS rates at 12 and 24 months after SBRT were 46-73% and 16-73%, respectively [50,54-59]. In comparison, Ost *et al.*, reported PFS rates at 12 and 24 months of approximately 80% and 45%, respectively, in a population that was diagnosed with Choline-PET (75%) or FDG-PET (24%) [60]. In a comparative study by Mazzola *et al.*, PFS rates at 12 and 24 months were 63.6% and 44.1% in the choline-PET group and 62.8% and 33.9% in the PSMA-PET arm [50]. Mazzola *et al.* reported a longer ADT-free survival in the PSMA-PET group, so a longer time to polymetastatic disease diagnosis, but at least part of this difference might be explained by diagnosing and treating patients earlier in the natural disease course. Repeated courses of SBRT can be applied, but in chapter 7 it has been shown that the PFS after a second SBRT cycle is almost halved compared with the first SBRT cycle, with median PFS rates after a first and second SBRT cycle of 17 and 9 months, respectively [61]. The

relatively poor PFS rate observed after SBRT monotherapy for patients with lymph node oligometastases indicates the presence of further micrometastatic spread, especially in other lymph nodes, in most patients at the time of oligometastatic diagnosis.

It would be very helpful to be able to predict PFS after SBRT monotherapy for individual patients, especially when patients are reluctant towards (temporary) ADT because of side-effects such as erectile dysfunction. Recent results from the ORIOLE randomized controlled trial suggest that detection of high-risk mutations in circulating tumor DNA is a strong predictor for disease progression: when a high-risk mutation was present, disease progression occurred within 12 months for all patients treated with SBRT, whereas for the patients that did not have a high-risk mutation, no disease progression was found at median ~15 months after progression [52]. However, this analysis was limited to 41% of the patients in whom circulating tumor DNA was detectable or in whom a truncating/pathogenic germline mutation had been found. To be able to apply this prediction methodology for all patients, tumor cell biopsies would be needed, which is challenging for most lymph node oligometastases and which would make the entire oligometastatic treatment considerably more invasive than it currently is. Still, this screening methodology in its current form, as venipuncture-based high-risk mutation screening, might be a valuable addition already, especially when combined with other potential predictive factors, such as baseline patient characteristics. An important contribution to the predictive power of baseline characteristics is expected from the ESTRO-EORTC OligoCare cohort, which is part of the E²-RADIatE study (NCT03818503). In chapter 7 a preliminary risk score has been presented, which already indicates a relatively large difference in PFS between patients with a low and a high risk score: median PFS was 21 and 8 months, respectively [61]. Once confirmed, such a risk score would be readily available to be used in clinical practice: it could inform patients and physicians about the estimated PFS that is obtainable with PSMA-PET-directed SBRT. A small subset of patients may still exhibit long-term (>24 months) disease control after SBRT monotherapy, but for most patients SBRT monotherapy may not be enough and combined treatments such as SBRT and temporary ADT, or possibly other combinations such as SBRT and Radium-223, in the setting of bone metastases, or SBRT combined with 177-Lutetium-PSMA, could be more beneficial than SBRT monotherapy [62-64]. For patients with polymetastases, the possibility of PET/biology-guided radiotherapy delivery using the new RefleXion X1 system (RefleXion Medical, Hayward, USA) combined with a systemic therapy such as chemotherapy or immunotherapy may improve long-term palliative treatment options by combining the irradiation of all macroscopic lesions with some form of systemic therapy to eradicate microscopic disease [65].

In conclusion, more sensitive PET tracers such as PSMA are not likely to improve clinical outcomes after SBRT monotherapy, outcome prediction based on both baseline

patient characteristics and tumor biology will be needed to select patients with ‘true’ oligometastatic disease, for all other patients a combination of local and systemic therapies will be needed to adequately deal with microscopically spread disease.

Perspective on future research

The preliminary prediction model presented in chapter 7 requires external validation. Ideally it would be examined in a study that also takes biological tumor characteristics into account, such as high-risk gene mutations in circulating tumor DNA and possibly also immune phenotype [52]. The outcomes of such a study could inform future treatment choices but may also be used for subgroup analyses of ongoing randomized clinical trials examining combined treatment strategies such as SBRT and ADT, possibly even combined with additional whole-pelvic radiotherapy [62]. Furthermore, future studies will be needed to investigate the potential of other combination therapies such as SBRT with ¹⁷⁷Lutetium-PSMA for patients with prostate cancer oligometastases and PET/biology-guided radiotherapy with immunotherapy or chemotherapy for patients with polymetastatic disease. Another example is the upcoming SIRIUS trial (a multicenter phase II randomized trial to evaluate systemic therapy versus systemic therapy in combination with stereotactic radiotherapy in patients with metastatic colorectal cancer), in which the impact of SBRT is explored when combined with standard first line palliative systemic therapy for patients with ≤ 10 metastases from colorectal carcinoma. In general, improvement of PFS and potentially even OS may be obtainable using combination therapies for most patients that are currently treated with SBRT monotherapy for oligometastases, and potentially also for patients with polymetastatic disease.

Conclusion

The research presented in this thesis shows that MR-guided online adaptive radiotherapy for patients with lymph node oligometastases is feasible and can be used to deliver radiotherapy with a very high precision with respect to target volume coverage, even in case of multiple target lymph nodes. OAR constraint adherence is improved using MR-linac compared with CBCT-linac and the MR-linac provides an opportunity to monitor the dose delivered to nearby OAR at each session. However, with the current 1.5 T MR-linac set-up and the current workflow, limited clinical benefit is obtained with regards to OAR sparing due to the long session times and due to OAR intrafraction motion. Shorter session times and improved mitigation of target and OAR intrafraction motion are needed to reach the full potential of 1.5 T MR-linac delivery. Currently, CBCT-linac delivery may be just as suitable for most patients who present with a single lymph node oligometastases without a critical OAR nearby. For patients with multiple lymph node targets, or with a critical OAR nearby, MR-linac delivery might be preferable, but only with daily full online re-planning

(ATS workflow for online plan adaptation). Future technological advancements of the MR-linac system might also allow for further hypofractionation. Regardless of the treatment machine, SBRT is a safe treatment for lymph node oligometastases, with only a mild and transient impact on quality of life, mainly fatigue. Local control can be obtained in almost all patients but disease progression is very common after local treatment for lymph node oligometastases. Improved outcome prediction could help to inform patients and physicians in their shared decision making regarding SBRT monotherapy or combined treatments, consisting of SBRT and some form of systemic therapy. Such combined treatments might improve progression-free survival and potentially even overall survival for most patients with oligometastases and possibly even for patients with polymetastatic disease.

References

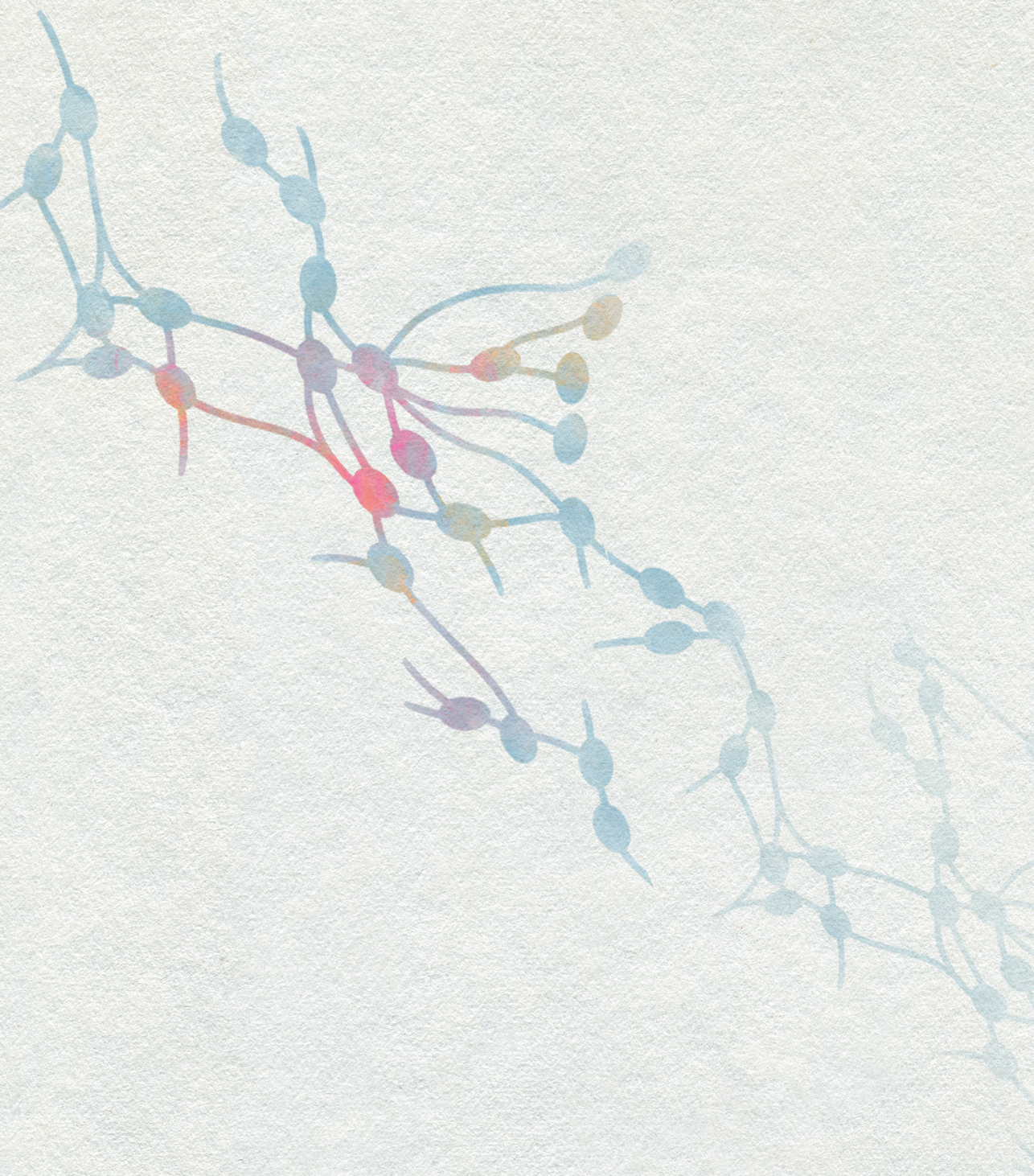
- Jaffray DA. Image-guided radiotherapy: from current concept to future perspectives. *Nat Rev Clin Oncol* 2012;9:688-99. <https://doi.org/10.1038/nrclinonc.2012.194>.
- Ding C, Saw CB, Timmerman RD. Cyberknife stereotactic radiosurgery and radiation therapy treatment planning system. *Med Dosim* 2018;43:129-40. <https://doi.org/10.1016/j.meddos.2018.02.006>.
- Noel CE, Parikh PJ, Spencer CR, Green OL, Hu Y, Mutic S, et al. Comparison of onboard low-field magnetic resonance imaging versus onboard computed tomography for anatomy visualization in radiotherapy. *Acta Oncol* 2015;54:1474-82. <https://doi.org/10.3109/0284186X.2015.1062541>.
- Viswanathan AN, Erickson B, Gaffney DK, Beriwal S, Bhatia SK, Lee Burnett 3rd O, et al. Comparison and consensus guidelines for delineation of clinical target volume for CT- and MR-based brachytherapy in locally advanced cervical cancer. *Int J Radiat Oncol Biol Phys* 2014;90:320-8. <https://doi.org/10.1016/j.ijrobp.2014.06.005>.
- Pötter R, Tanderup K, Schmid MP, Jürgenliemk-Schulz I, Haie-Meder C, Fokdal LU, et al. MRI-guided adaptive brachytherapy in locally advanced cervical cancer (EMBRACE-I): a multicentre prospective cohort study. *Lancet Oncol* 2021;22:538-47. [https://doi.org/10.1016/S1470-2045\(20\)30753-1](https://doi.org/10.1016/S1470-2045(20)30753-1).
- Legendijk JJ, van Vulpen M, Raaymakers BW. The development of the MRI linac system for online MRI-guided radiotherapy: a clinical update. *J Intern Med* 2016;280:203-8. <https://doi.org/10.1111/joim.12516>.
- Kooreman ES, van Houdt PJ, Keesman R, Pos FJ, van Pelt VWJ, Nowee ME, et al. ADC measurements on the Unity MR-linac - A recommendation on behalf of the Elekta Unity MR-linac consortium. *Radiother Oncol* 2020;153:106-13. <https://doi.org/10.1016/j.radonc.2020.09.046>.
- Raaymakers BW, Legendijk JJ, Overweg J, Kok JG, Raaijmakers AJ, Kerkhof EM, et al. Integrating a 1.5 T MRI scanner with a 6 MV accelerator: proof of concept. *Phys Med Biol* 2009;54:N229-37. <https://doi.org/10.1088/0031-9155/54/12/N01>.
- Raaymakers BW, Jürgenliemk-Schulz IM, Bol GH, Glitzner M, Kotte ANTJ, van Asselen B, et al. First patients treated with a 1.5 T MRI-Linac: clinical proof of concept of a high-precision, high-field MRI guided radiotherapy treatment. *Phys Med Biol* 2017;62:L41-50. <https://doi.org/10.1088/1361-6560/aa9517>.
- Klüter S. Technical design and concept of a 0.35 T MR-Linac. *Clin Transl Radiat Oncol* 2019;18:98-101. <https://doi.org/10.1016/j.ctro.2019.04.007>.
- Winkel D, Bol GH, Kroon PS, van Asselen B, Hackett SS, Werensteijn-Honingh AM, et al. Adaptive radiotherapy: The Elekta Unity MR-linac concept. *Clin Transl Radiat Oncol* 2019;18:54-9. <https://doi.org/10.1016/j.ctro.2019.04.001>.
- Kontaxis C, Bol GH, Stemkens B, Glitzner M, Prins FM, Kerkmeijer LGW, et al. Towards fast online intrafraction replanning for free-breathing stereotactic body radiation therapy with the MR-linac. *Phys Med Biol* 2017;62:7233-48. <https://doi.org/10.1088/1361-6560/aa82ae>.
- Prins FM, Stemkens B, Kerkmeijer LGW, Barendrecht MM, de Boer HJ, Vonken EPA, et al. Intrafraction Motion Management of Renal Cell Carcinoma With Magnetic Resonance Imaging-Guided Stereotactic Body Radiation Therapy. *Pract Radiat Oncol* 2019;9:e55-61. <https://doi.org/10.1016/j.prro.2018.09.002>.
- Kontaxis C, Woodhead PL, Bol GH, Legendijk JJW, Raaymakers BW. Proof-of-concept delivery of intensity modulated arc therapy on the Elekta Unity 1.5 T MR-linac. *Phys Med Biol* 2021;66:04LT01. <https://doi.org/10.1088/1361-6560/abd66d>.

15. Teoh M, Clark CH, Wood K, Whitaker S, Nisbet A. Volumetric modulated arc therapy: a review of current literature and clinical use in practice. *Br J Radiol* 2011;84:967-96. <https://doi.org/10.1259/bjr/22373346>.
16. Glitzner M, Woodhead PL, Borman PTS, Lagendijk JJW, Raaymakers BW. Technical note: MLC-tracking performance on the Elekta unity MRI-linac. *Phys Med Biol* 2019;64:15NT02. <https://doi.org/10.1088/1361-6560/ab2667>.
17. Werensteijn-Honingh AM, Kroon PS, Winkel D, van Gaal JC, Hes J, et al. Differences in the workflows of MR-linac and CBCT-linac impact organ at risk doses in SBRT treatments of lymph node oligometastases. *Submitted*.
18. Savenije MHF, Maspero M, Sikkes GG, van der Voort van Zyp JRN, Kotte ANTJ, Bol GH, et al. Clinical implementation of MRI-based organs-at-risk auto-segmentation with convolutional networks for prostate radiotherapy. *Radiat Oncol* 2020;15:104. <https://doi.org/10.1186/s13014-020-01528-0>.
19. Kontaxis C, Bol GH, Lagendijk JJW, Raaymakers BW. DeepDose: towards a fast dose calculation engine for radiation therapy using deep learning. *Phys Med Biol* 2020;65:075013. <https://doi.org/10.1088/1361-6560/ab7630>.
20. Zachiu C, Denis de Senneville B, Willigenburg T, Voort van Zyp JRN, de Boer JCJ, Raaymakers BW, et al. Anatomically-adaptive multi-modal image registration for image-guided external-beam radiotherapy. *Phys Med Biol* 2020;65:215028. <https://doi.org/10.1088/1361-6560/abad7d>.
21. Verkooijen HM, Kerkmeijer LGW, Fuller CD, Huddart R, Faivre-Finn C, Verheij M, et al. R-IDEAL: A Framework for Systematic Clinical Evaluation of Technical Innovations in Radiation Oncology. *Front Oncol* 2017;7:59. <https://doi.org/10.3389/fonc.2017.00059>.
22. Werensteijn-Honingh AM, Kroon PS, Winkel D, Aalbers EM, van Asselen B, Bol GH, et al. Feasibility of stereotactic radiotherapy using a 1.5 T MR-linac: Multi-fraction treatment of pelvic lymph node oligometastases. *Radiother Oncol* 2019;134:50-4. <https://doi.org/10.1016/j.radonc.2019.01.024>.
23. Winkel D, Kroon PS, Werensteijn-Honingh AM, Bol GH, Raaymakers BW, Jürgenliemk-Schulz IM. Simulated dosimetric impact of online re-planning for stereotactic body radiation therapy of lymph node oligometastases on the 1.5T MR-linac. *Acta Oncol* 2018;3:1-8. <https://doi.org/10.1080/0284186X.2018.1512152>.
24. de Mol van Otterloo SR, Christodouleas JP, Blezer ELA, Akhlat H, Brown K, Choudhury A, et al. The MOMENTUM Study: An International Registry for the Evidence-Based Introduction of MR-Guided Adaptive Therapy. *Front Oncol* 2020;10:1328. <https://doi.org/10.3389/fonc.2020.01328>.
25. Winkel D, Bol GH, Werensteijn-Honingh AM, Intven MPW, Eppinga WSC, Hes J, et al. Target coverage and dose criteria based evaluation of the first clinical 1.5T MR-linac SBRT treatments of lymph node oligometastases compared with conventional CBCT-linac treatment. *Radiother Oncol* 2020;146:118-25. <https://doi.org/10.1016/j.radonc.2020.02.011>.
26. Ma TM, Lamb JM, Casado M, Wang X, Basehart TV, Yang Y, et al. Magnetic resonance imaging-guided stereotactic body radiotherapy for prostate cancer (mirage): a phase iii randomized trial. *BMC Cancer* 2021;21:538. <https://doi.org/10.1186/s12885-021-08281-x>.
27. Da Silva Mendes V, Nierer L, Li M, Corradini S, Reiner M, Kamp F, et al. Dosimetric comparison of MR-linac-based IMRT and conventional VMAT treatment plans for prostate cancer. *Radiat Oncol* 2021;16:133. <https://doi.org/10.1186/s13014-021-01858-7>.

28. Ding S, Li Y, Liu H, Li R, Wang B, Zhang J, et al. Comparison of Intensity Modulated Radiotherapy Treatment Plans Between 1.5T MR-Linac and Conventional Linac. *Technol Cancer Res Treat* 2021;20:1533033820985871. <https://doi.org/10.1177/1533033820985871>.
29. Mayinger M, Ludwig R, Christ SM, Dal Bello R, Ryu A, Weitkamp N, et al. Benefit of replanning in MR-guided online adaptive radiation therapy in the treatment of liver metastasis. *Radiat Oncol* 2021;16:84. <https://doi.org/10.1186/s13014-021-01813-6>.
30. Henke L, Kashani R, Yang D, Zhao T, Green O, Olsen L, et al. Simulated Online Adaptive Magnetic Resonance-Guided Stereotactic Body Radiation Therapy for the Treatment of Oligometastatic Disease of the Abdomen and Central Thorax: Characterization of Potential Advantages. *Int J Radiat Oncol Biol Phys* 2016;96:1078-86. <https://doi.org/10.1016/j.ijrobp.2016.08.036>.
31. Henke LE, Olsen JR, Contreras JA, Curcuru A, DeWees TA, Green OL, et al. Stereotactic MR-Guided Online Adaptive Radiation Therapy (SMART) for Ultracentral Thorax Malignancies: Results of a Phase 1 Trial. *Adv Radiat Oncol* 2018;4:201-9. <https://doi.org/10.1016/j.adro.2018.10.003>.
32. Winkel D, Werensteijn-Honingh AM, Kroon PS, Eppinga WSC, Bol GH, Intven MPW, et al. Individual Lymph Nodes: "See It and Zap It". *Clin Transl Radiat Oncol* 2019;18:46-53. <https://doi.org/10.1016/j.ctro.2019.03.004>.
33. Hall WA, Paulson ES, van der Heide UA, Fuller CD, Raaymakers BW, Lagendijk JJW, et al. The transformation of radiation oncology using real-time magnetic resonance guidance: A review. *Eur J Cancer* 2019;122:42-52. <https://doi.org/10.1016/j.ejca.2019.07.021>.
34. Dunlop A, Mitchell A, Tree A, Barnes H, Bower L, Chick J, et al. Daily adaptive radiotherapy for patients with prostate cancer using a high field MR-linac: Initial clinical experiences and assessment of delivered doses compared to a C-arm linac. *Clin Transl Radiat Oncol* 2020;23:35-42. <https://doi.org/10.1016/j.ctro.2020.04.011>.
35. Bertelsen AS, Schytte T, Møller PK, Mahmood F, Riis HL, Gottlieb KL, et al. First clinical experiences with a high field 1.5 T MR linac. *Acta Oncol* 2019;58:1352-7. <https://doi.org/10.1080/0284186X.2019.1627417>.
36. Werensteijn-Honingh AM, Jürgenliemk-Schulz IM, Gadellaa-Van Hooijdonk CG, Sikkens GG, Vissers NGPM, Winkel D, et al. Impact of a vacuum cushion on intrafraction motion during online adaptive MR-guided SBRT for pelvic and para-aortic lymph node oligometastases. *Radiother Oncol* 2021;154:110-7. <https://doi.org/10.1016/j.radonc.2020.09.021>.
37. Thorwarth D, Low DA. Technical Challenges of Real-Time Adaptive MR-Guided Radiotherapy. *Front Oncol* 2021;11:634507. <https://doi.org/10.3389/fonc.2021.634507>.
38. Hellman S, Weichselbaum RR. Importance of local control in an era of systemic therapy. *Nat Clin Pract Oncol* 2005;2:60-1. <https://doi.org/10.1038/ncponc0075>.
39. Haffner MC, Mosbrugger T, Esopi DM, Fedor H, Heaphy CM, Walker DA, et al. Tracking the clonal origin of lethal prostate cancer. *J Clin Invest* 2013;123:4918-22. <https://doi.org/10.1172/JCI70354>.
40. Rees M, Tekkis PP, Welsh FKS, O'Rourke T, John TG. Evaluation of long-term survival after hepatic resection for metastatic colorectal cancer: a multifactorial model of 929 patients. *Ann Surg* 2008;247:125-35. <https://doi.org/10.1097/SLA.0b013e31815aa2c2>.

41. Casiraghi M, De Pas T, Maisonneuve P, Brambilla D, Ciprandi B, Galetta D, et al. A 10-year single-center experience on 708 lung metastasectomies: the evidence of the “international registry of lung metastases”. *J Thorac Oncol* 2011;6:1373-8. <https://doi.org/10.1097/JTO.0b013e3182208e58>.
42. Palma DA, Olson R, Harrow S, Gaede S, Louie AV, Haasbeek C, et al. Stereotactic Ablative Radiotherapy for the Comprehensive Treatment of Oligometastatic Cancers: Long-Term Results of the SABR-COMET Phase II Randomized Trial. *J Clin Oncol* 2020;38:2830-8. <https://doi.org/10.1200/JCO.20.00818>.
43. Wu JN, Fish KM, Evans CP, Devere White RW, Dall’Era MA. No improvement noted in overall or cause-specific survival for men presenting with metastatic prostate cancer over a 20-year period. *Cancer* 2014;120:818-23. <https://doi.org/10.1002/cncr.28485>.
44. Poon I, Erler D, Dagan R, Redmond KJ, Foote M, Badellino S, et al. Evaluation of Definitive Stereotactic Body Radiotherapy and Outcomes in Adults With Extracranial Oligometastasis. *JAMA Netw Open* 2020;3:e2026312. <https://doi.org/10.1001/jamanetworkopen.2020.26312>.
45. Welch DR, Hurst DR. Defining the Hallmarks of Metastasis. *Cancer Res* 2019;79:3011-27. <https://doi.org/10.1158/0008-5472.CAN-19-0458>.
46. Lehrer EJ, Singh R, Wang M, Chinchilli VM, Trifiletti DM, Ost P, et al. Safety and Survival Rates Associated With Ablative Stereotactic Radiotherapy for Patients With Oligometastatic Cancer: A Systematic Review and Meta-analysis. *JAMA Oncol* 2021;7:92-106. <https://doi.org/10.1001/jamaoncol.2020.6146>.
47. Matsushita H, Jingu K, Umezawa R, Yamamoto T, Ishikawa Y, Takahashi N, et al. Stereotactic Radiotherapy for Oligometastases in Lymph Nodes-A Review. *Technol Cancer Res Treat* 2018;17:1533033818803597. <https://doi.org/10.1177/1533033818803597>.
48. Fodor A, Lancia A, Ceci F, Picchio M, Hoyer M, Jereczek-Fossa BA, et al. Oligorecurrent prostate cancer limited to lymph nodes: getting our ducks in a row : Nodal oligorecurrent prostate cancer. *World J Urol* 2019;37:2607-13. <https://doi.org/10.1007/s00345-018-2322-7>.
49. Moghul M, Somani B, Lane T, Vasdev N, Chaplin B, Peedell C, et al. Detection rates of recurrent prostate cancer: 68 Gallium (Ga)-labelled prostate-specific membrane antigen versus choline PET/CT scans. A systematic review. *Ther Adv Urol* 2019;11:1756287218815793. <https://doi.org/10.1177/1756287218815793>.
50. Mazzola R, Francolini G, Triggiani L, Napoli G, Cuccia F, Nicosia L, et al. Metastasis-directed Therapy (SBRT) Guided by PET-CT 18 F-CHOLINE Versus PET-CT 68 Ga-PSMA in Castration-sensitive Oligorecurrent Prostate Cancer: A Comparative Analysis of Effectiveness. *Clin Genitourin Cancer* 2021;19:230-6. <https://doi.org/10.1016/j.clgc.2020.08.002>.
51. Ost P, Reynders D, Decaestecker K, Fonteyne V, Lumen N, De Bruycker A, et al. Surveillance or Metastasis-Directed Therapy for Oligometastatic Prostate Cancer Recurrence: A Prospective, Randomized, Multicenter Phase II Trial. *J Clin Oncol* 2018;36:446-53. <https://doi.org/10.1200/JCO.2017.75.4853>.
52. Phillips R, Yue Shi W, Deek M, Radwan N, Jin Lim S, Antonarakis ES, et al. Outcomes of Observation vs Stereotactic Ablative Radiation for Oligometastatic Prostate Cancer: The ORIOLE Phase 2 Randomized Clinical Trial. *JAMA Oncol* 2020;6:650-9. <https://doi.org/10.1001/jamaoncol.2020.0147>.
53. Nguyen PL, Alibhai SMH, Basaria S, D’Amico AV, Kantoff PW, Keating NL, et al. Adverse effects of androgen deprivation therapy and strategies to mitigate them. *Eur Urol* 2015;67:825-36. <https://doi.org/10.1016/j.eururo.2014.07.010>.

54. Kneebone A, Hruby G, Ainsworth H, Byrne K, Brown C, Guo L, et al. Stereotactic Body Radiotherapy for Oligometastatic Prostate Cancer Detected via Prostate-specific Membrane Antigen Positron Emission Tomography. *Eur Urol Oncol* 2018;1:531-7. <https://doi.org/10.1016/j.euo.2018.04.017>.
55. Artigas C, Flamen P, Charlier F, Levillain H, Wimana Z, Diamand R, et al. 68 Ga-PSMA PET/CT-based metastasis-directed radiotherapy for oligometastatic prostate cancer recurrence after radical prostatectomy. *World J Urol* 2019;37:1535-42. <https://doi.org/10.1007/s00345-019-02701-1>.
56. Ong WL, Koh TL, Joon DL, Chao M, Farrugia B, Lau E, et al. Prostate-specific membrane antigen-positron emission tomography/computed tomography (PSMA-PET/CT)-guided stereotactic ablative body radiotherapy for oligometastatic prostate cancer: a single-institution experience and review of the published literature. *BJU Int* 2019;124 Suppl 1:19-30. <https://doi.org/10.1111/bju.14886>.
57. Hurmuz P, Onal C, Ozyigit G, Igdem S, Atalar B, Sayan H, et al. Treatment outcomes of metastasis-directed treatment using 68 Ga-PSMA-PET/CT for oligometastatic or oligorecurrent prostate cancer: Turkish Society for Radiation Oncology group study (TROD 09-002). *Strahlenther Onkol* 2020;196:1034-43. <https://doi.org/10.1007/s00066-020-01660-6>.
58. Kalinauskaitė G, Senger C, Kluge A, Furth C, Kufeld M, Tinhofer I, et al. 68Ga-PSMA-PET/CT-based radiosurgery and stereotactic body radiotherapy for oligometastatic prostate cancer. *PLoS One* 2020;15:e0240892. <https://doi.org/10.1371/journal.pone.0240892>.
59. Marzec J, Becker J, Paulsen F, Wegener D, Olthof S-C, PfannenberG C, et al. 68 Ga-PSMA-PET/CT-directed IGRT/SBRT for oligometastases of recurrent prostate cancer after initial surgery. *Acta Oncol* 2020;59:149-56. <https://doi.org/10.1080/0284186X.2019.1669816>.
60. Ost P, Jereczek-Fossa BA, Van As N, Zilli T, Tree A, Henderson D, et al. Pattern of Progression after Stereotactic Body Radiotherapy for Oligometastatic Prostate Cancer Nodal Recurrences. *Clin Oncol (R Coll Radiol)* 2016;28:e115-20. <https://doi.org/10.1016/j.clon.2016.04.040>.
61. Werensteijn-Honingh AM, Wevers AFJ, Peters M, Kroon PS, Martijn Intven M, Eppinga WSC, et al. Progression-free survival in patients with 68 Ga-PSMA-PET-directed SBRT for lymph node oligometastases. *Acta Oncol* 2021;60:1342-51. <https://doi.org/10.1080/0284186X.2021.1955970>.
62. De Bruycker A, Spiessens A, Dirix P, Koutsouvelis N, Semac I, Liefhooghe N, et al. PEACE V - Salvage Treatment of OligoRecurrent nodal prostate cancer Metastases (STORM): a study protocol for a randomized controlled phase II trial. *BMC Cancer* 2020;20:406. <https://doi.org/10.1186/s12885-020-06911-4>.
63. Hasan H, Deek MP, Phillips R, Hobbs RF, Malek R, Radwan N, et al. A phase II randomized trial of Radium-223 dichloride and SABR Versus SABR for oligometastatic prostate cancer (RAVENS). *BMC Cancer* 2020;20:492. <https://doi.org/10.1186/s12885-020-07000-2>.
64. Sartor O, de Bono J, Chi KN, Fizazi K, Herrmann K, Rahbar K, et al. Lutetium-177-PSMA-617 for Metastatic Castration-Resistant Prostate Cancer. *N Engl J Med* 2021;385:1091-1103. <https://doi.org/10.1056/NEJMoa2107322>.
65. Shirvani SM, Huntzinger CJ, Melcher T, Olcott PD, Voronenko Y, Bartlett-Roberto J, et al. Biology-guided radiotherapy: redefining the role of radiotherapy in metastatic cancer. *Br J Radiol* 2021;94:20200873. <https://doi.org/10.1259/bjr.20200873>.



Chapter 10

Dutch summary

Algemene inleiding

Radiotherapie is een vorm van kankerbehandeling waarbij gebruik gemaakt wordt van bestraling, meestal met fotonen, om tumorcellen te doden. Een groot deel van dit proefschrift gaat over een nieuw bestralingsapparaat, de 1.5 T MR-linac. Dit is een combinatie tussen een MRI scanner met een veldsterkte van 1.5 T en een bestralingsapparaat (lineaire versneller). Het is een apparaat waarmee kankerpatiënten bestraald kunnen worden onder geleide van MRI beeldvorming. Op de meeste moderne bestralingsapparaten wordt elke dag een snelle CT scan gemaakt, een cone beam CT (CBCT) scan. Echter MRI beeldvorming geeft een betere visualisatie van zachte weefsels, waarmee de MR-linac meer en mogelijk betere mogelijkheden biedt om het bestralingsplan tijdens elke behandelsessie af te stemmen op de dagelijkse anatomie. Dit gaat bijvoorbeeld over de ligging van het doelgebied ten opzichte van nabijgelegen gezonde organen, waar zo min mogelijk stralingsdosis op dient te komen om de kans op bijwerkingen te minimaliseren.

Het onderzoek in dit proefschrift richt zich op één specifieke patiëntengroep, namelijk patiënten met heel beperkte uitzaaiingen, oligometastasen genoemd, in dit geval specifiek lymfeklier uitzaaiingen. Bij oligometastasen zijn er maximaal 3-5 metastasen aanwezig, afhankelijk van de gebruikte definitie, en vaak is de primaire tumor al eerder curatief behandeld. Op moment van behandeling zijn de oligometastasen meestal de enige plekken waar de kanker dan nog vastgesteld kan worden, ter plaatse van de primaire tumor is de kanker weg en er zijn ook nog geen verdere uitzaaiingen vastgesteld. Deze patiënten worden bestraald met een lange termijn palliatieve intentie, namelijk om de uitzaaiingen lokaal goed te behandelen zodat daar geen klachten van ontstaan en om systemische therapie te kunnen uitstellen, zoals chemo- of hormoontherapie. Vaak zijn er echter al wel micrometastasen aanwezig op andere plaatsen in het lichaam, daarom heeft de behandeling van deze patiënten meestal geen curatieve intentie meer. Het doel is dan vooral om de kwaliteit van leven zo lang mogelijk te behouden.

Deel I: Adaptieve MRI-gestuurde stereotactische bestraling van lymfeklieren

De eerste klinische toepassing van de 1.5 T MR-linac na Conformité Européenne (CE)-accreditatie betrof bestraling van patiënten met lymfeklier oligometastasen, in augustus 2018 in het Universitair Medisch Centrum Utrecht. Op dat moment waren er alleen nog technische uitkomsten beschikbaar uit een eerdere studie waarin patiënten een eenmalige palliatieve bestraling hadden ondergaan voor pijnlijke botmetastasen, op een eerdere versie van de 1.5 T MR-linac (nog zonder CE-markering). De klinische en technische uitvoerbaarheid van stereotactische radiotherapie behandeling voor weke delen doelgebieden met de 1.5 T MR-linac, in dit geval voor lymfekliermetastasen, is

aangetoond in *hoofdstuk 2*. Behandelingsgegevens zijn gerapporteerd voor de eerste vijf patiënten, waaruit bleek dat alle bestralings sessies (vijf per patiënt) waren voltooid met de MR-linac, dat er voor iedere sessie een nieuw bestralingsplan gemaakt was gebaseerd op de dagelijkse anatomie, dat alle behandelings sessies binnen 60 minuten waren afgerond en dat alle kwaliteitscontroles succesvol waren doorstaan, waaronder onafhankelijke 3D dosisberekeningen en filmmetingen.

De behandeling van de eerste tien patiënten met slechts één lymfeklieroligometastase is dosimetrisch geëvalueerd in *hoofdstuk 3*. Twee verschillende methodes voor het dagelijks aanpassen van de bestralingsplannen zijn vergeleken: Adapt To Shape (ATS), oftewel aanpassen aan vorm, welke klinisch gebruikt was voor de onderzochte behandelingen, en Adapt To Position (ATP), oftewel aanpassen aan positie. Bij ATS worden iedere sessie de intekeningen aangepast van het doelgebied en van de nabijgelegen gezonde organen. Het bestralingsplan wordt dan geoptimaliseerd met deze kennis van de dagelijkse anatomie. Bij het gebruik van ATP worden de eerdere intekeningen niet aangepast, maar het bestralingsplan wordt verplaatst om te corrigeren voor een andere ligging van het doelgebied. Hiermee is planadaptatie met ATP sneller maar men kan niet inspelen op veranderingen in volume van het doelgebied en veranderingen in de ligging en vulling van gezonde nabijgelegen organen. Voldoende dekking van het doelgebied met de voorgeschreven bestralingsdosis tijdens de gehele behandelings sessie werd bereikt in 90% van de klinisch toegepaste ATS behandelingen, dit zou 70% geweest zijn als ATP gebruikt zou zijn in plaats van ATS. Desalniettemin zou voor de meerderheid van de patiënten met beide planadaptatie methodes een voldoende dekking van de lymfekliermetastasen zijn bereikt, met een mediane dekking van 100% voor beide methodes. Marges van 3 mm om de lymfekliermetastasen bleken voldoende te zijn om te compenseren voor geometrische onzekerheden en de beweging van doelgebieden tijdens MR-linac bestralings sessies.

In *hoofdstuk 4* is onderzocht wat de invloed is van immobilisatie met een vacuüm matras op beweging van het doelgebied tijdens MR-linac bestralings sessies. Vacuüm matrassen worden gebruikt om patiënten te immobiliseren, onder meer om beweging van het doelgebied tijdens een behandelings sessie te verminderen. Er werd inderdaad een significante afname gevonden van anterieure-posterieure translaties (mediane afname 0,7 mm) van zowel de doelgebieden als van nabijgelegen botten, die een indicatie vormen van bewegingen van de gehele patiënt. Echter, een deel van de doelgebied bewegingen tijdens een sessie kunnen gecompenseerd worden tijdens MR-linac behandelingen, vooral voor patiënten met slechts één lymfekliermetastase. Het bleek dat de meeste beweging van de doelgebieden optrad in de eerste ~16 minuten van een behandelings sessie, dit is voordat de daadwerkelijke bestraling gestart wordt. Er kan dan gecorrigeerd worden voor deze beweging door een extra ATP procedure uit te voeren. Als zo'n extra ATP procedure zelfs

toegepast wordt bij beperkte beweging van het doelgebied, dan levert een vacuümmatras geen vermindering meer op van doelgebied beweging, dus dan is een vacuümmatras meestal niet meer nodig voor behandeling op een MR-linac.

In *hoofdstuk 5* is de dekking van de doelgebieden vergeleken tussen behandelingen op een MR-linac en op een regulier bestralingsapparaat waarbij CBCT scans gebruikt worden voor positieverificatie, een CBCT-linac. Voor patiënten met slechts één lymfeklier oligometastase bleek de dekking van het doelgebied vergelijkbaar te zijn tussen MR-linac en CBCT-linac behandelplannen. MR-linac bestraling gaf wel een verbeterde doelgebied dekking voor patiënten met meerdere doelgebieden. Met een MR-linac kan er namelijk bij de start van elke behandelssessie gecorrigeerd worden voor bewegingen van een doelgebied ten opzichte van een ander doelgebied, terwijl dit op een CBCT-linac niet mogelijk is als de verschillende doelgebieden in één bestralingsplan worden behandeld. Echter, verschillen in dekking van de doelgebieden werden wederom slechts in een klein deel van de patiënten geconstateerd; de mediane doelgebied dekking was 100% met beide modaliteiten, voor zowel patiënten met één als meerdere doelgebieden.

Hoofdstuk 6 vervolgt de vergelijking tussen MR-linac en CBCT-linac behandelplannen, nu gericht op de dosis die gezonde nabijgelegen organen ontvangen. Er werden minder dosislimieten voor gezonde nabijgelegen organen overschreden met MR-linac behandeling. Verder bood de MR-linac een voordeel voor patiënten bij wie de doelgebieden niet goed zichtbaar waren op een CBCT scan. Voor deze patiënten zou op een CBCT-linac een grotere marge om de lymfekliermetastasen meegenomen moeten worden in het doelgebied, terwijl dit niet hoeft met een MR-linac, waar zelfs kleine lymfeklieren adequaat gevisualiseerd konden worden. Door het verschil in marge om de lymfeklier, kregen deze patiënten een lagere stralingsdosis op nabijgelegen gezonde darmen als ze met MR-linac behandeld werden in plaats van CBCT-linac. Echter, de tijdsspanne waarin de dagelijkse planadaptatie moet plaatsvinden is kort, behandelssessies duren langer met een MR-linac en de gezonde nabijgelegen organen bewegen ook gedurende een behandelssessie. Deze factoren zorgen ervoor dat het aanpassen van het bestralingsplan aan het begin van iedere sessie minder effect heeft als het gaat om de dosis die daadwerkelijk door de gezonde nabijgelegen organen wordt ontvangen. Over het algemeen waren de stralingsdosissen die nabijgelegen darmen (voornamelijk colon en duodenum) zouden hebben ontvangen vergelijkbaar tussen CBCT-linac en MR-linac; als er vergelijkbare marges rondom de lymfeklieren gebruikt konden worden dan bleken darmen in het kleine bekken zelfs significant minder stralingsdosis te ontvangen met een CBCT-linac dan met een MR-linac.

Deel II: Behandeluitkomsten en patiëntselectie

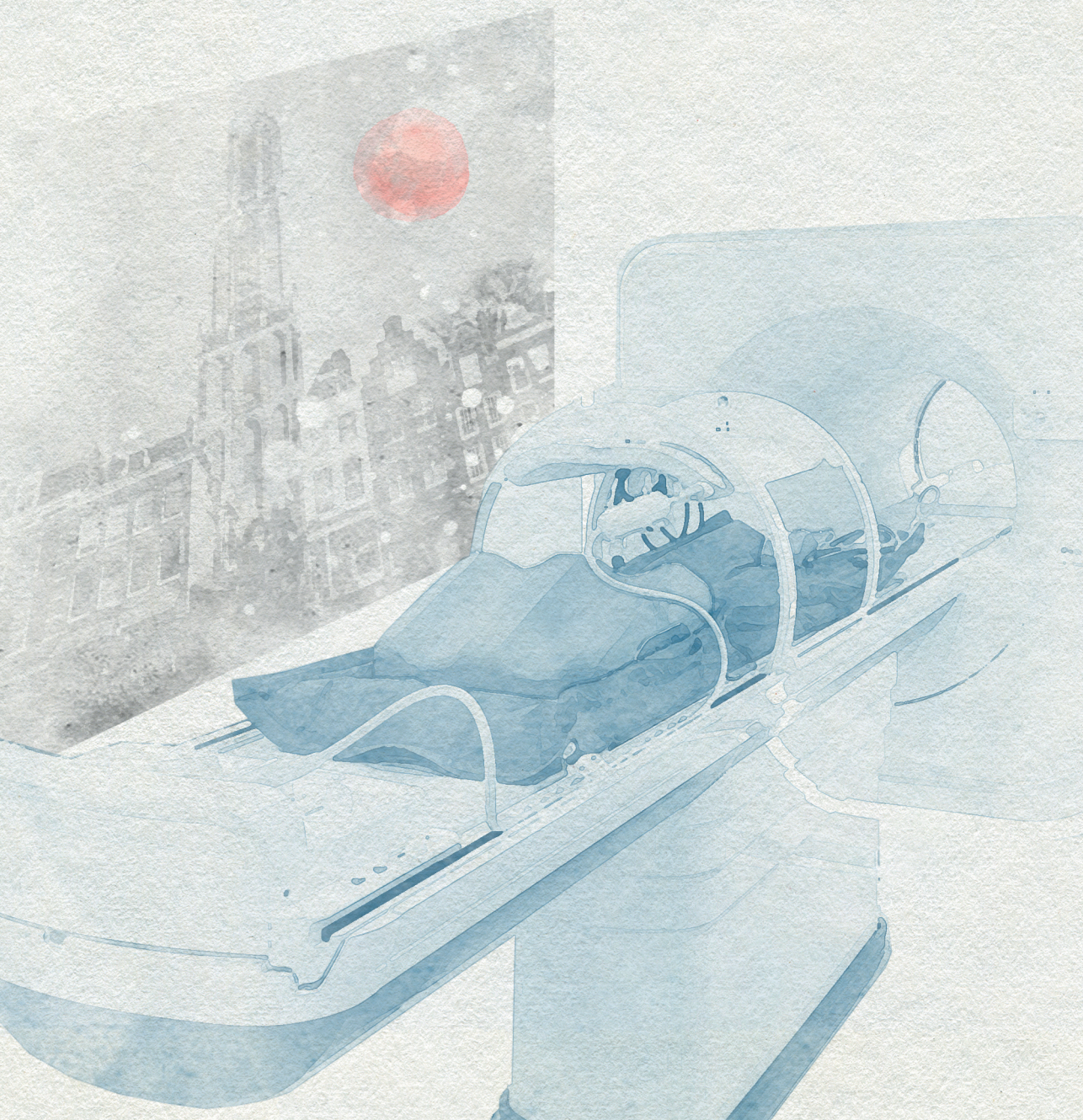
Klinische uitkomstmaten werden onderzocht in *hoofdstuk 7*. Dit onderzoek betrof een specifieke patiëntcategorie, namelijk patiënten met lymfeklier oligometastasen van prostaatkanker. Prostaatkanker tumorcellen kunnen met een hoge sensitiviteit opgespoord worden met Prostate-Specific Membrane Antigen (PSMA)-PET scans. Door deze sensitieve PSMA-PET scans, en mogelijk ook door het tragere beloop van prostaatkanker, worden er nu relatief veel prostaatkanker patiënten behandeld voor oligometastasen. De uitkomsten van CBCT-linac en MR-linac behandelingen werden gecombineerd geanalyseerd voor deze patiëntencategorie. Met een mediane volgperiode van 21 maanden bleek de progressie-vrije overleving, welke was gedefinieerd als tijd tot ontstaan van een nieuwe metastase of tot biochemische progressie, 16 maanden te zijn. Verschillende patiëntkarakteristieken bleken geassocieerd te zijn met een kortere progressie-vrije overleving: jongere leeftijd, hogere PSA (tumormarker) waarde voor de start van de behandeling en de aanwezigheid van lymfekliermetastasen buiten het kleine bekken. Met deze karakteristieken werd een voorlopig risicoscore model gemaakt, waarmee er een onderscheidend vermogen in progressie-vrije overleving leek te zijn met een mediane progressie-vrije overleving van respectievelijk 8 en 21 maanden voor patiënten in de hoog- en laagrisico groepen. Acute en late toxiciteit was hoogstens graad 2 en uit de analyse van kwaliteit van leven vragenlijsten werd vooral een tijdelijke, milde vermoeidheid gevonden rond de 1-4 weken na afloop van de bestralingen.

Algemene discussie

Adaptieve MRI-gestuurde stereotactische bestraling voor patiënten met lymfeklier oligometastasen is uitvoerbaar, meerdere lymfeklieren kunnen met grote nauwkeurigheid tegelijk bestraald worden. MRI-gestuurde bestraling heeft als voordeel dat er beter voldaan wordt aan de dosislimieten voor gezonde nabijgelegen organen en het biedt de mogelijkheid om per behandelingsessie na te gaan welke stralingsdosis er op deze gezonde organen is gekomen. Echter met de huidige 1.5 T MR-linac en met onze huidige workflow wordt er nog vrij weinig voordeel behaald in het sparen van gezonde nabijgelegen organen vergeleken met behandeling op een CBCT-linac. Dit komt vooral door de langere behandelingsessies en door beweging van de gezonde nabijgelegen organen tijdens zo'n sessie. Een kortere sessieduur en meer mogelijkheden om te corrigeren voor orgaanbeweging tijdens de sessies zijn nodig om optimaal te kunnen profiteren van behandeling met de 1.5 T MR-linac.

Stereotactische bestraling is een veilige behandeling voor lymfeklier oligometastasen, met vooral een tijdelijke, milde vermoeidheid als invloed op de kwaliteit van leven. Voor bijna alle patiënten kan lokale controle van de uitzaaingen bereikt worden maar bij een groot deel van de patiënten treedt ziekteprogressie op, regelmatig binnen 2 jaar,

na lokale behandeling voor lymfeklier oligometastasen. Betere voorspelling van de behandeluitkomsten zou nuttig kunnen zijn voor patiënt en behandelaar om een afweging te maken tussen alleen stereotactisch bestralen versus om bestraling te combineren met systemische therapie. Een groot deel van de patiënten met oligometastasen, en mogelijk zelfs patiënten met meer wijdverspreide ziekte, zouden kunnen profiteren van zulke gecombineerde behandelingen, door een langere progressie-vrije overleving en mogelijk zelfs door een langere algehele overleving.



Appendices

Review committee

Prof. dr. Miriam Koopman

Professor in Medical Oncology at the University Medical Center Utrecht, the Netherlands

Prof. dr. Lenny Verkooijen

Professor of Evaluation of Image-Guided Treatment at the University Medical Center Utrecht, the Netherlands

Prof. dr. Jorrit-Jan Verlaan

Professor in Orthopedics at the University Medical Center Utrecht, the Netherlands

Prof. dr. Marnix Lam

Professor in Nuclear Medicine at the University Medical Center Utrecht, the Netherlands

Prof. dr. Marcel Verheij

Professor in Radiotherapy at the Radboud University Medical Center, Nijmegen, the Netherlands

List of publications

Submitted:

Werensteijn-Honingh AM, Kroon PS, Winkel D, van Gaal JC, Hes J, Snoeren LMW, Timmer JK, Mout CCP, Bol GH, Kotte AN, Eppinga WSC, Intven M, Raaymakers BW, Jürgenliemk-Schulz IM. Differences in the workflows of MR-linac and CBCT-linac impact organ at risk doses in SBRT treatments of lymph node oligometastases. *Submitted*.

Published:

den Boer D, den Hartogh MD, Kotte ANTJ, van der Voort van Zyp JRN, Noteboom JL, Bol GH, Willigenburg T, **Werensteijn-Honingh AM**, Jürgenliemk-Schulz IM, van Lier ALHMW, Kroon PS. Comparison of Library of Plans with two daily adaptive strategies for whole bladder radiotherapy. *Phys Imaging Radiat Oncol* 2021;20:82-7. <https://doi.org/10.1016/j.phro.2021.11.002>.

Werensteijn-Honingh AM, Wevers AFJ, Peters M, Kroon PS, Martijn Intven M, Eppinga WSC, Jürgenliemk-Schulz IM. Progression-free survival in patients with 68 Ga-PSMA-PET-directed SBRT for lymph node oligometastases. *Acta Oncol* 2021;60:1342-51. <https://doi.org/10.1080/0284186X.2021.1955970>.

Winkel D, **Werensteijn-Honingh AM**, Eppinga WSC, Intven MPW, Hes J, Snoeren LMW, Visser SA, Bol GH, Raaymakers BW, Jürgenliemk-Schulz IM, Kroon PS. Dosimetric feasibility of hypofractionation for SBRT treatment of lymph node oligometastases on the 1.5T MR-linac. *Radiother Oncol* 2021;154:243-8. <https://doi.org/10.1016/j.radonc.2020.09.020>.

Werensteijn-Honingh AM, Jürgenliemk-Schulz IM, Gadellaa-Van Hooijdonk CG, Sikkes GG, Vissers NGPM, Winkel D, Eppinga WSC, Intven M, Raaymakers BW, Kroon PS. Impact of a vacuum cushion on intrafraction motion during online adaptive MR-guided SBRT for pelvic and para-aortic lymph node oligometastases. *Radiother Oncol* 2021;154:110-7. <https://doi.org/10.1016/j.radonc.2020.09.021>.

Winkel D, Bol GH, **Werensteijn-Honingh AM**, Intven MPW, Eppinga WSC, Hes J, Snoeren LMW, Sikkes GG, Gadellaa-van Hooijdonk CGM, Raaymakers BW, Jürgenliemk-Schulz IM, Kroon PS. Target coverage and dose criteria based evaluation of the first clinical 1.5T MR-linac SBRT treatments of lymph node oligometastases compared with conventional CBCT-linac treatment. *Radiother Oncol* 2020;146:118-25. <https://doi.org/10.1016/j.radonc.2020.02.011>.

Winkel D, Bol GH, Kroon PS, van Asselen B, Hackett SS, **Werensteijn-Honingh AM**, Intven MPW, Eppinga WSC, Tijssen RHN, Kerkmeijer LGW, de Boer HCJ, Mook S, Meijer GJ, Hes J, Willemsen-Bosman M, de Groot-van Breugel EN, Jürgenliemk-Schulz IM, Raaymakers BW. Adaptive radiotherapy: The Elekta Unity MR-linac concept. *Clin Transl Radiat Oncol* 2019;18:54-9. <https://doi.org/10.1016/j.ctro.2019.04.001>.

Winkel D, **Werensteijn-Honingh AM**, Kroon PS, Eppinga WSC, Bol GH, Intven MPW, de Boer HCJ, Snoeren LMW, Hes J, Raaymakers BW, Jürgenliemk-Schulz IM. Individual Lymph Nodes: "See It and Zap It". *Clin Transl Radiat Oncol* 2019;18:46-53. <https://doi.org/10.1016/j.ctro.2019.03.004>.

Werensteijn-Honingh AM, Kroon PS, Winkel D, Aalbers EM, van Asselen B, Bol GH, Brown KJ, Eppinga WSC, van Es CA, Glitzner M, de Groot-van Breugel EN, Hackett SL, Intven M, Kok JGM, Kontaxis C, Kotte AN, Lagendijk JJW, Philippens MEP, Tijssen RHN, Wolthaus JWH, Woodings SJ, Raaymakers BW, Jürgenliemk-Schulz IM. Feasibility of stereotactic radiotherapy using a 1.5 T MR-linac: Multi-fraction treatment of pelvic lymph node oligometastases. *Radiother Oncol* 2019;134:50-4. <https://doi.org/10.1016/j.radonc.2019.01.024>.

de Boer P, Mandija S, **Werensteijn-Honingh AM**, van den Berg CAT, de Leeuw AAC, Jürgenliemk-Schulz IM. Cervical cancer apparent diffusion coefficient values during external beam radiotherapy. *Phys Imaging Radiat Oncol* 2019;9:77-82. <https://doi.org/10.1016/j.phro.2019.03.001>.

Winkel D, Bol GH, **Werensteijn-Honingh AM**, Kiekebosch IH, van Asselen B, Intven MPW, Eppinga WSC, Raaymakers BW, Jürgenliemk-Schulz IM, Kroon PS. Evaluation of plan adaptation strategies for stereotactic radiotherapy of lymph node oligometastases using online magnetic resonance image guidance. *Phys Imaging Radiat Oncol* 2019;9:58-64. <https://doi.org/10.1016/j.phro.2019.02.003>.

Winkel D, Kroon PS, **Werensteijn-Honingh AM**, Bol GH, Raaymakers BW, Jürgenliemk-Schulz IM. Simulated dosimetric impact of online replanning for stereotactic body radiation therapy of lymph node oligometastases on the 1.5T MR-linac. *Acta Oncol* 2018;3:1-8. <https://doi.org/10.1080/0284186X.2018.1512152>.

Wisse LEM, Kuijf HJ, **Honingh AM**, Wang H, Pluta JB, Das SR, Wolk DA, Zwanenburg JJM, Yushkevich PA, Geerlings MI. Automated hippocampal subfield segmentation at 7T MRI. *AJNR Am J Neuroradiol* 2016;37:1050-7. <https://doi.org/10.3174/ajnr.A4659>.

Dankwoord

In een proefschrift komt het werk samen van velen, daarom wil ik iedereen bedanken die direct of indirect heeft bijgedragen aan de totstandkoming van dit proefschrift. Veel dank aan de **patiënten** die deel hebben genomen aan de **OLYMPOS studie**. Bedankt voor het delen van uw ervaringen middels de vragenlijsten en dat we uw MRI scans en bestralingsplannen mochten gebruiken voor dit onderzoek. Ook dank aan de **leden van de beoordelingscommissie**, voor het lezen en beoordelen van dit proefschrift en voor de gedachtewisseling tijdens de verdediging. Dank aan alle **collega's van de afdeling Radiotherapie**; het was een inspirerende omgeving voor een promotietraject.

Ina Schulz, al tijdens mijn bacheloropleiding wist jij jouw enthousiasme voor patiëntenzorg en wetenschappelijk onderzoek op mij over te brengen. Samen met **Astrid de Leeuw** heb je mij veel geleerd tijdens mijn bachelor- en masterscripties en daar heb ik sindsdien op verder kunnen bouwen. Jullie gezamenlijke inzet voor het verbeteren van de gyn-brachytherapie vind ik inspirerend. Ina, ik bewonder je omdat je wetenschappelijk onderzoek, ook rondom de lymfeklier oligometastasen, altijd benadert met een klinische blik. Dank voor de begeleiding en betrokkenheid vanaf dag één!

Petra Kroon, dank voor je enthousiaste en gemotiveerde begeleiding gedurende dit hele promotietraject, tot en met de laatste puntjes op de 'i' voor de verschillende artikelen. Gefocust op de 'gap of knowledge' hielp jij om mijn werk te verbeteren, zowel voor technische als meer epidemiologische artikelen. Ik vind het heel knap hoe jij werk en privé zo goed in balans weet te houden; dank dat je altijd tijd had voor mijn begeleiding!

Bas Raaymakers, dank voor je begeleiding als promotor. In het begin van het traject door mij te stimuleren om me wat minder formeel te gedragen, met een joviale en ontspannen houding als technische professor in een - tijdens mijn geneeskunde opleiding toch wat meer hiërarchisch overkomend - academisch ziekenhuis. Aan het einde van mijn promotietraject kwam je weer meer in beeld en hielp je mij met een technische blik om de discussie sterker te maken. Je leidt vanuit een bescheiden houding een heel indrukwekkende en inspirerende onderzoekslijn op de afdeling, dank voor de kansen die ik hierbinnen heb gekregen!

Andere collega's van de tumorwerkgroep oligometastasen: **Martijn Intven** en **Wietse Eppinga**, dank voor jullie bijdragen aan de verschillende artikelen. Met jullie erbij kreeg ik vanuit drie verschillende klinische invalshoeken suggesties om het onderzoek verder te verbeteren, dat vond ik heel waardevol. **Dennis Winkel**, jij was mijn maatje bij het onderzoek van de oligo-lymfeklieren. Onze promotietrajecten liepen vrij parallel en ik wil je bedanken voor de fijne samenwerking hierin. **Jochem Hes** en **Louk Snoeren**, dank voor

jullie bijdragen als specialistisch laboranten aan meerdere artikelen. **Gijs Bol** en **Alexis Kotte**, dank voor de tumorwerkgroep-overstijgende hulp rond Volumetool en voor de technische ‘multi-consulti’. **Max Peters**, dank voor je begeleiding bij het epidemiologische artikel; ik heb veel van je geleerd en ik bewonder je om al de verschillende onderzoeken die je al hebt gedaan in je carrière. **Anne Wevers**, **Jaleesa Timmer** en **Christiaan Mout**, dank voor jullie bijdragen en het werk dat jullie hebben verzet in het kader van jullie stages.

Alle **collega's van de innovatiepoli en van het trialbureau** van de divisie Beeld (en Oncologie), dank voor de fijne samenwerking. Met de innovatiepoli hebben we het onderzoek en de patiëntinclusies goed kunnen organiseren en ik ben jullie natuurlijk ook dankbaar voor alle OLYMPOS studie-inclusies. In het bijzonder wil ik **Shanta Kalaykhan** bedanken, je was onmisbaar bij het meermaals doorlopen van alle stappen rondom wetenschappelijke studies opzetten, uitvoeren en afronden.

Dank ook aan al mijn **mede-promovendi** en **collega's van de IGRT onderzoeksgroep**, voor de inspirerende overleggen en de gezelligheid tijdens de lunches en op andere momenten. Dank in het bijzonder aan mijn kamergenootjes **Eva van Grinsven** en **Charisma Hehakaya**, voor jullie betrokkenheid en de gezelligheid onder en na werktijd. Het was fijn om dit traject met jullie te kunnen delen!

Dank aan mijn nieuwe collega's bij het **UWV Utrecht** voor het warme onthaal, in het bijzonder **Erwin van Elsäcker**, **Lisa Menting**, **Katrien van den Brande**, **Jos Kuckelkorn**, **Anouk Kraft**, **Roland Burgers** en **Marinus van Kuijk**. Een nieuwe start die ondanks veel thuiswerken toch persoonlijk en fijn verliep. Dank ook voor de interesse in de afrondende fase van dit promotietraject.

Dan naar de persoonlijker kring. **Eef Keuken** en **George Kreeft**, bedankt dat jullie mij op een hartelijke wijze inspireerden en stimuleerden om een academische opleiding te volgen.

Daniëlle van Keulen en **Janneke Smeele**, dank voor jullie vriendschap. Daniëlle, jij hield de moed bij mij erin tijdens de afrondende fase, als ervaringsdeskundige wist je waar ik het over had. Janneke, jij hebt laten zien hoe je kunt doorzetten als het niet vanzelf gaat, en opleiding/traject daarmee toch af te ronden.

Papa en mama, dank voor jullie steun, jullie zijn er altijd voor mij geweest en ik ben zo dankbaar dat jullie dat nu nog steeds zijn. Jullie stimuleerden mij altijd om de uitdaging te zoeken, om door te zetten en om dromen en ambities te verwezenlijken! Dank ook voor jullie liefde en betrokkenheid bij Maurits en Evelien, ook daarmee hebben jullie natuurlijk bijgedragen aan dit proefschrift. **Susanne** en **Dorien**, wat bof ik met jullie als zussen. Ik

vind het heel fijn dat jullie mijn paranimfen willen zijn tijdens de verdediging, alweer 'getuigen' van een bijzonder moment in mijn leven. **Wout en Yvonne**, ook met jullie heb ik het enorm getroffen, wat is het fijn om ook op jullie te kunnen bouwen en vertrouwen. Ook jullie wil ik bedanken voor het oppassen en voor jullie betrokkenheid bij dit traject. **Christa**, ik wil je bedanken voor je steun, je interesse en de warmte die je altijd weet uit te stralen.

Maurits en Evelien, wat zorgen jullie elke dag weer voor een hoop blijdschap in mijn leven. **Niels**, dank voor je steun, je begrip en je liefde, tijdens zware en leuke momenten van dit promotietraject. Dank je wel ook voor de begeleiding bij het leren programmeren, voor het gezellige thuiswerken, omdat je heel betrokken en geïnteresseerd was, maar vooral omdat je mij steunde in deze ambitie.

Curriculum vitae

Anita Werensteijn-Honingh was born on October 14th, 1990 in Goirle, The Netherlands. She graduated secondary education (vwo) cum laude from Revius Lyceum Doorn in July 2009. In July 2013 she obtained a cum laude BSc degree in Biomedical Sciences at Utrecht University, with Physics minor (60 ECTS) and Descartes College honours programme participation. She wrote her bachelor thesis at the department of Radiotherapy of the University Medical Center Utrecht, on dosimetric evaluation of deformable image registration for cervical cancer external beam radiotherapy.

She continued her education with the Selective Utrecht Medical Master (MSc), with a technical specialization track, from which she graduated in August 2017. As part of this masters program she returned to the department of Radiotherapy, where she completed both a clinical and a research internship, under supervision of dr. Ina Jürgenliemk-Schulz and dr. Astrid de Leeuw. She wrote her master thesis about automatic contour propagation for MRI-linac treatment of pelvic lymph node oligometastases. After her graduation she continued to work at the department of Radiotherapy as a medical PhD candidate, under supervision of dr. Ina Jürgenliemk-Schulz, dr. ir. Petra Kroon and prof. dr. Bas Raaymakers. Her PhD project was focused on stereotactic radiotherapy delivery using a 1.5 T MR-linac for patients with lymph node oligometastases. The results of this PhD project are summarized in this thesis. In July 2021 she started working as a physician at Uitvoeringsinstituut Werknemersverzekeringen (UWV).

